Building Engineering

http://ojs.acad-pub.com/index.php/BE

2024 VOLUME 2 ISSUE 1
ISSN: 3029-2670 (Online)

1

Editorial Team

Editor-in-Chief

Co-Editor-in-Chief

Associate Editor

Editorial Board Members

Rosa Agliata
Universitas Mercatorum; Università della Campania
Italy

Parsa Ghannadi
Islamic Azad University
Iran

Jolanta Tamošaitienė
Vilnius Gediminas technical university - Vilnius TECH
Lithuania

Volume 2 Issue 1 • 2024

Building Engineering

ACADEMIC
ACADEMIC PUBLISHING PTE LTD

2024 | Volume 2 | Issue 1

Building Engineering

https://ojs.acad-pub.com/index.php/BE

Contents

Articles

Review

Building Engineering 2024, 2(1), 470.
https://doi.org/10.59400/be.v2i1.470

Article

Comprehensive seismic loss model of Tehran, Iran in the case of Mosha fault seismic scenario using stochastic finite-fault method

Nazila Kheirkhah[1], Reza Alikhanzadeh[2], Ozhan Musavi[2], Ali Aghajani[2], Erfan Firuzi[2,*]

[1] Institute of Geophysics, University of Tehran, Tehran 1435944411, Iran
[2] International Institute of Earthquake Engineering and Seismology (IIEES), Tehran 1953714453, Iran
*** Corresponding author:** Erfan Firuzi, e.firuzi@iiees.ac.ir

CITATION

Kheirkhah N, Alikhanzadeh R, Musavi O, et al. Comprehensive seismic loss model of Tehran, Iran in the case of Mosha fault seismic scenario using stochastic finite-fault method. Building Engineering. 2024; 2(1): 470. https://doi.org/10.59400/be.v2i1.470

ARTICLE INFO

Received: 9 January 2024
Accepted: 13 February 2024
Available online: 20 February 2024

Abstract: This paper presents the results of a study carried out to assess probable seismic loss in terms of damage to the residential buildings and the number of fatalities in the case of the Mosha Fault seismic scenario in Tehran, Iran. Accordingly, seismic risk components (including seismic hazards, exposure models, and fragility curves) are evaluated. The stochastic finite-fault method with dynamic corner frequency is applied for quantifying ground motion values. The results show that PGA on the soil surface could range between 0.1 g and 0.45 g. Then, a reliable model of building exposure by analyzing census data from Tehran is compiled. This model included 19 different classes of buildings and is used to evaluate the potential damage to buildings from seismic scenarios. The results indicate that the median damage ratio from 100,000 iterations for the whole of the city is about 6% ± 1.54%. The study found that the central and eastern parts of Tehran are the most vulnerable areas, with an estimated 15,952 residents at risk of losing their lives in this scenario. This is equivalent to 0.2 percent of the total population of Tehran. The findings from this study can be used by local authorities to provide appropriate emergency response and preparedness plans in the case of the Mosha Fault seismic scenario.

Keywords: stochastic finite-fault model; seismic risk; building damages; casualty; Tehran

1. Introduction

The Iranian plateau is a wide zone of compressional deformation along the active Alpine-Himalayan seismic belt, resulting from the convergence of the Eurasian and Arabian plates [1,2]. This region is considered one of the most seismically prone regions in the world. Buin-Zahra (7.1 Mw, 1962), Tabas (7.4 Mw, 1978), Manjil-Roudbar (7.4 Mw, 1990), Bam (6.6 Mw, 2003), and Sarpole-Zahab (7.3 Mw, 2017) are among the most catastrophic seismic events that have occurred in Iran during the last few decades. According to the global catalog of UTSU, more than 92,000 individuals lost their lives in these earthquakes. This demonstrates the country's high seismic risk and highlights the importance of implementing appropriate seismic risk reduction plans in major cities of the country.

Tehran, the capital of Iran, as the most populated city in Iran, is also exposed to high seismic risk. Based on the latest data from the Statistical Center of Iran (SCI), the population of the city was around 8,737,510 in 2016. Tehran also contributes more than 30% to the gross domestic product of the country [3]. In addition, the majority of economic, social, and political centers are located in Tehran. Consequently, its safety and security against natural and man-made hazards are crucial for the government.

Tectonically, Tehran is located on the southern edge of the central Alborz Mountain belt. This region is characterized by discontinuities, with many active faults

in or around the city [4]. The major active faults in or around Tehran are Mosha, North Tehran Fault (NTF), Ray, and Taleghan (**Figure 1**). These are the sources of several devastating historical earthquakes, as listed in **Table 1**. The Mosha fault, with an approximate length of 220 km, is the causative fault for most of the historical earthquakes in this region. By considering the time intervals of historical earthquakes that occurred along the Mosha fault, it can be inferred that the return period of major earthquakes is approximately 165 years. The last devastating earthquake in the Tehran region caused by Mosha fault occurred in 1830; thus, more than 190 years have passed since that event. Accordingly, the possibility of a similar strong earthquake occurring in the near future is quite high [5,6]. Such a strong earthquake is likely to cause numerous casualties and severe damage to buildings and infrastructure in Tehran. These issues have also been addressed in the studies of Berberian et al. [7], Firuzi et al. [8], Kalantari et al. [9], and Firuzi et al. [10].

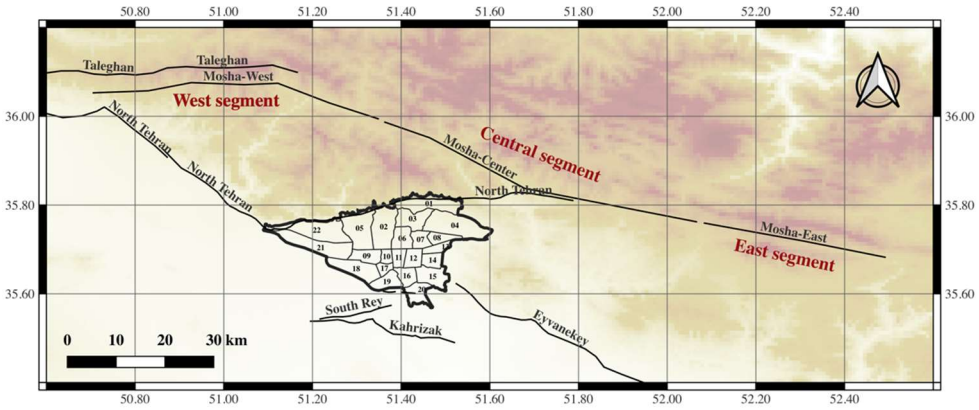

Figure 1. The location of Tehran with respect to the major active faults.

Table 1. List of devastating historical events occurred around Tehran.

Date	Ms	Longitude	Latitude	Causative fault	Reference
855/5/22	7.1	51.5	35.6	Kahrizak	[11]
958/2//23	7.7	51.1	36.0	Taleghan/Mosha	[12]
1177/5/-	7.2	50.7	35.7	North Tehran Fault	[13]
1665/6/15	6.5	52.1	35.7	Mosha	[14]
1815/6/-	7.1	52.2	35.9	Mosha	[14]
1830/3/27	7.1	52.5	35.7	Mosha	[15]

The above explanations show the importance of conducting detailed seismic hazards and risk assessments to address the impact of the Mosha fault scenario on the region. Such studies can play a fundamental role in developing appropriate risk reduction and emergency response plans to deal with the consequences of a potential earthquake.

In order to assess seismic risk, the seismic hazard must first be characterized. Then, an exposure model needs to be developed, and appropriate fragility/vulnerability curves should be employed. For seismic hazard assessment, most studies use Ground Motion Prediction Equations (GMPEs), which generally do not address parameters such as directivity or pulse waves. To the authors' knowledge,

no work in the literature assesses the seismic loss of Tehran for the Mosha fault seismic scenario using the finite-fault method. However, this is an appropriate approach for modeling the source, path, and near-surface effects properly. The finite-fault method is especially applicable in regions like Tehran, where the last destructive earthquake dates back to the pre-instrumental period, and there is a lack of recorded strong ground motions from earthquakes on the faults to develop empirical GMPEs. Some of the most recent seismic risk studies in Tehran are introduced as follows.

JICA [16] assessed the seismic risk of Tehran in terms of the number of casualties and economic losses by considering three seismic scenarios, including the rupture of Ray, Mosha, and North-Tehran faults. In that study, GMPEs were used to provide the ground motion shaking map. Their findings showed that the most and least destructive seismic scenarios are the Ray and Mosha fault events, respectively. Based on this study, the rupture of the Mosha fault may cause a damage ratio equal to 13% of total buildings with 20,000 deaths, which is equivalent to 0.3% of the total population. By using the stochastic approach proposed by Beresnev [17], Zafarani et al. [18] assessed the seismic hazard of Tehran based on the seismic scenarios of Ray, North Tehran, and Mosha faults. That study showed that the rupture of the Mosha fault will generate the highest PGAs, between 0.1 and 0.3 g. However, Zafarani et al. [18] did not perform the seismic risk analysis to identify the most destructive seismic scenarios. Saffari et al. [19] also evaluated the potential seismic hazard of Tehran by considering the rupture of Mosha fault using the stochastic finite-fault model. They performed their analysis using the EXSIM program. Their results depict that the PGA in Tehran may vary from 0.13 g to 0.55 g in the Mosha fault seismic scenario.

As discussed above, there is no comprehensive study in the literature that has employed the stochastic method for conducting a full seismic risk assessment in Tehran for the Mosha seismic scenario. Therefore, this study attempts to estimate seismic loss (in terms of the number of fatalities and damage to residential buildings) using the stochastic finite-fault method for the Mosha fault seismic scenario, which is widely regarded as the most likely seismic scenario in Tehran. In following, first, a description of the stochastic finite-fault approach is presented. Then the seismic hazard map of Tehran, developed based on the stochastic finite-fault method, is introduced, and the results are compared with GMPEs. Next, the exposure model is described, and employed fragility and vulnerability curves are introduced. Finally, an estimation of the possible losses in terms of building damages and fatalities is presented and discussed.

2. Stochastic finite-fault method

Estimating potential ground motion values of earthquakes in terms of engineering parameters (such as PGA, PGV, seismic intensity, or spectral acceleration) is a key step for seismic risk assessment. In practice, the common approach for seismic hazard analysis is GMPE; however, it has some deficiencies, including its dependence on the availability of data on ground motions. In fact, these equations are developed based on the regression of observed ground motions in past earthquakes. Clearly, the lack of sufficient data at different distance or magnitude ranges will affect their accuracy [20]. This is the case in many cities in Iran, such as Tehran, where an adequate number of

records (particularly near-source data) is not available. In addition, there are uncertainties in selecting appropriate functional forms of GMPEs. Moreover, GMPEs only provide strong ground motion parameters rather than the time history waveform required for dynamic analysis of important structures. To address these issues, using simulating tools attracts the attention of seismologists and earthquake engineers.

Several simulating methodologies have been proposed in the literature, which vary from simple approaches that replicate certain characteristics of ground motion records to sophisticated physic-based methods that mathematically model the earthquake phenomenon [21]. In the present study, an improved stochastic finite-fault approach developed by Motazedian [22] is employed. An open-source FORTRAN program named EXSIM with high calculation capabilities is also used. EXSIM is an extended version of stochastic point source simulation (stochastic method simulation, SMSIM), developed by Boore [23,24], and the finite-fault simulation (FINSIM) approach introduced by Beresnev [17]. The basic premise of EXSIM is dividing the rupture plane into an array of sub-faults treated as point sources, like FINSIM, by introducing the dynamic corner frequency. These improvements overcome two main shortcomings of the aforementioned approaches. The idea of dividing the rupture area into sub-faults provides the capability of EXSIM to simulate large earthquakes and eliminates the limitation to small or moderate magnitude events as SMSIM. In addition, introducing the dynamic corner frequency eliminates the dependence of the results on the sub-fault size as FINSIM. Based on the above explanations, EXSIM, by superimposing the motion from each sub-fault (as given in Equation (1)), provides the ground motion by considering the rupture and propagation delay.

$$a(t) = \sum_{i=1}^{nl} \sum_{j=1}^{nw} a_{ij}(t + \Delta_{ij}) \tag{1}$$

In the above equation, nl and nw are the number sub-faults along the strike and dip of the fault, respectively. Δ_{ij} is the relative delay time from ijth subfaults to the observed point and $a(t)$ represents the simulated ground motion values of the entire fault. The Fourier amplitude of each sub-fault is estimated using the w^2 shape, where w is angular frequency [25].

$$A_{ij}(f) = CH_{ij}M_{0ij}\frac{(2\pi f)^2}{1+\left(\frac{f}{f_{0ij}}\right)^2}e^{-\pi f k_0}\frac{e^{-\frac{\pi f R_{ij}}{Q(f)\beta}}}{R_{ij}}G(R_{ij}) \tag{2}$$

In the above equation, M_{0ij} (dyn.cm) denotes the seismic moment of sub-fault (by considering identical sub-fault, this is equal to $M_{0ij} = M_0/N$), f_{0ij} depicts the dynamic corner frequency of sub-fault, H_{ij} is a scaling factor to be applied to conserve the high frequency spectral level of sub-fault, term $e^{-\pi f k_0}$ is a high cut filter that take into account the near surface attenuation effect, where k_0 is the fast spectral decay at high frequency, $Q(f)$ (with general form of $Q(f) = Q_0 f^n$) is a quality factor represents anelastic and scattering attenuation, ρ (kg/m^3) is density, β (Km/s) is the shear-wave velocity in vicinity of the source, R_{ij} (Km) is the distance of the sub-fault from the observed point, $G(R_{ij})$ denotes the geometric spreading function, and C is a constant defined as:

$$C = \frac{R_{\theta\phi} V F}{(4\pi\rho\beta^3 R_0)} \tag{3}$$

where $R_{\theta\phi\sim}0.55$ is the radiation pattern (typically 0.55 for shear waves), $F = 2$ is the free surface amplification, $V = 1/\sqrt{2}$ is the partition of total shear-wave energy into two horizontal components, and $R_0 = 1$ km is the reference distance.

As mentioned, EXSIM uses dynamic frequency (f_{0ij}) as given in Equation (4) to remove the dependence of results to sub-fault size [22].

$$f_{oij} = N_R(t)^{-1/3} 4.9E + 6\beta(\frac{\Delta\sigma}{M_{0ave}})^{1/3} \tag{4}$$

In the above equation, $\Delta\sigma$ is the stress drop in bar, M_{0ave} is the average seismic moment of subfaults ($M_{0ij} = M_0/N$), and $N_R(t)$ is the cumulative number of ruptured sub-fault at time t. According to Equation (4), as the rupture area expands, $N_R(t)$ gradually increases; consequently, the corner frequency reaches the minimum value when the entire fault is ruptured. Thus, the radiated energy at high frequency will decrease ($A_{ij}(h)_{f \gg f_{oij}} \propto f_{oij}^2$). To overcome this issue, [22] proposed a scaling factor (H_{ij}) as given in Equation (5) to conserve the energy radiated from a sub-fault at high frequency. In this equation, f_0 is the static corner frequency is calculated by the seismic moment alongside the stress drop for the entire fault $f_0 = f_{oij}(end) = N^{-1/3} 4.9E + 6\beta(\frac{\Delta\sigma}{M_{oave}})^{1/3}$.

$$H_{ij} = \sqrt{\frac{N \sum f^2 / [1 + \left(\frac{f}{f_0}\right)^2]}{\sum f^2 / [1 + \left(\frac{f}{f_{0ij}}\right)^2]}} \tag{5}$$

It should be mentioned that the aforementioned explanations and formulation provide the Fourier spectrum (a_{ij}) of sub-fault, to take the stochastic characteristics into account, the Fourier spectrum multiplied into a windowed Gaussian white noise signal in the frequency domain. In the following section, a detailed application of this procedure for Mosha fault is described.

3. Application of finite-fault model for Mosha fault seismic scenario

Figure 2 shows the location of the Mosha fault with respect to the Tehran metropolitan area. As depicted, this fault has three main segments with slightly different orientations [26]. The western segment is located in the north of Tehran, parallel to the Taleghan fault. The relation between these two faults is not clear [27]. The central segment is a left-lateral strike-slip fault with an approximate length of 80 km, which intersects with the NTF. The eastern segment is located along the Mosha valley. Seismological evidence shows that the central part, which is the closest segment to Tehran, has the highest seismicity. Thus, this part has been considered the worst-case scenario in this study.

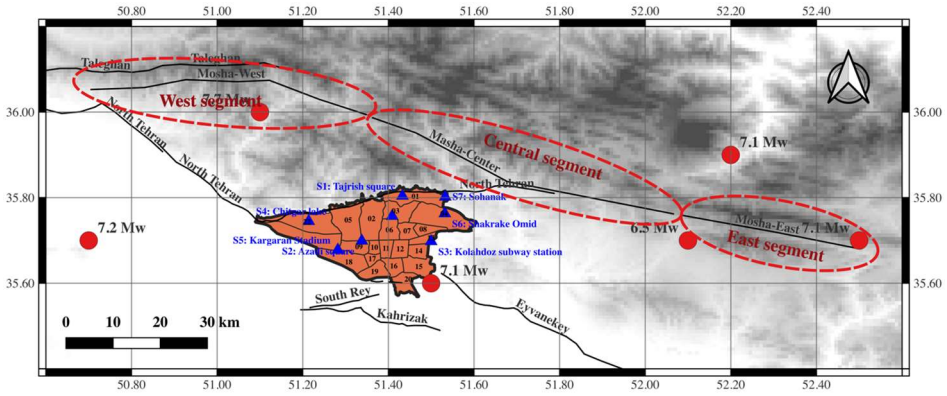

Figure 2. Tectonic map of the Mosha fault in relation to the Tehran Metropolitan; blue triangles are important locations in Tehran which their time history waveforms are depicted as sample (faults are from Solaymani Azad et al. [28]).

In stochastic finite-fault simulation, proper modelling of the plane, dimension of fault, and source parameters are important factors. A summary of the most important model parameters is listed in **Table 2**. According to historical data and the empirical relation of Wells and Coppersmith [29], the potential magnitude of the Mosha fault seismic scenario is estimated to be 7.4 (Mw). This moment magnitude is equivalent to a rupture plane with a length of 75 km and a width of 27 km along the strike and dip of the fault, respectively. The strike and dip of the fault are 283° and 75°, respectively, based on the study by Zafarani et al. [18]. Due to a lack of instrumental strong earthquake records on the Mosha Fault, providing an accurate estimation of stress drop is associated with uncertainties. In this study, a stress drop value of 50 bar is considered, which corresponds to the value proposed by Zafarani et al. [18]. The quality factor in the present study is also taken from the study of Zafarani et al., who proposed the value for earthquakes in the northern part of Iran. This value is extracted from the Manjil-Roudbar earthquake (7.4 Mw, 1990). Similarly, Motazedian [30], based on data from the Manjil-Roudbar earthquake, developed a trilinear geometric spreading function that is used in this study. The percentage of pulsing area is considered to be 50%, which means that during the rupture of sub-faults, at most 50% of all sub-faults could be active while the remaining are passive. This value is proposed by Motazedian [22] based on the concept of self-healing provided by Heaton [31]. It should be noted that due to a lack of information regarding slip distribution, a random normal distribution is considered for analysis.

Table 2. Summary of important model parameters for Mosh fault seismic scenario.

Parameter	Value	Reference
Strike, dip	283°, 75°	[18]
Magnitude	7.4 (Mw)	[18]
Fault dimension along strike and dip	75, 27 (Km)	[29]
Stress drop ($\Delta\sigma$)	50 (bar)	[18]
Sub-fault size	2 × 2 (Km)	-
Shear wave velocity (β)	3.5 (Km/s)	[18]
Density (ρ)	2.8 (kg/m^3)	[18]

Table 2. (*Continued*).

Parameter	Value	Reference
Kappa	0.05	[18]
Quality factor	$Q(f) = 87f^{1.47}$	[18]
Geometric spreading	R^{-1} $(R \leq 70)$ $R^{0.2}$ $(75 \leq R \leq 150)$ $R^{-0.1}$ $(R > 150)$	[30]
Pulsing area percentage	50%	[30]
Rupture velocity	0.8 Shear wave velocity	[30]
Window function	Saragoni-hart	-
Path duration	0.1R	-

Based on the aforementioned parameters, the time history waveform is simulated within a square grid cell with a 1 × 1 km dimension for the entire city of Tehran. The distribution of PGA on engineering bedrock within the 22 municipal districts of Tehran is shown in **Figure 3**. As depicted, the PGA values vary between 0.05 and 0.40 g, with maximum values in the northeast of Tehran, which has the closest distance to the Mosha fault. The result has good agreement with the study of Zafarani et al. [18], which used the stochastic approach proposed by Beresnev [17]. It should be noted that for seismic risk assessment, ground motion values on the soil surface are required. For this purpose, the amplification factor provided in the study by JICA [16] is used. In that study, based on information from 450 boreholes, the amplification factor for the entire city of Tehran is derived. **Figure 3** also shows the distribution of PGA on the soil surface. As shown, by employing the amplification factor, the ground motion values increase, especially in the southern regions of Tehran.

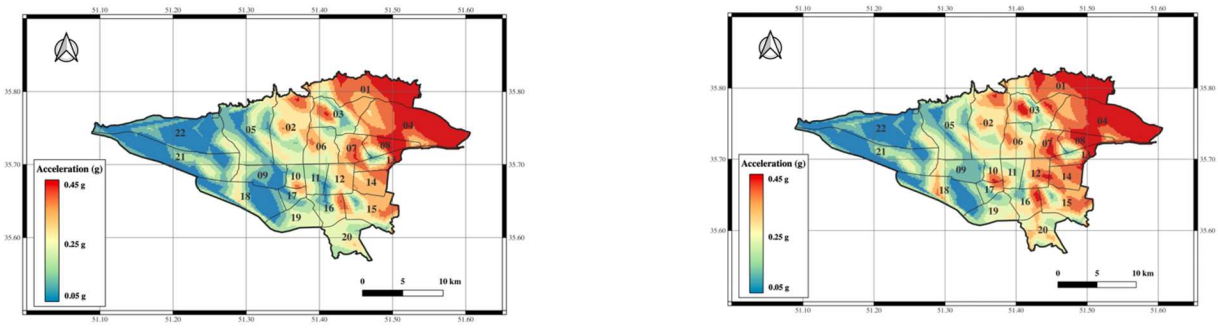

(a) **(b)**

Figure 3. Distribution of PGA within a grid cell of 1 × 1 km in Tehran based on assumed model parameters of Mosha fault seismic scenario. **(a)** on engineering bedrock; **(b)** on soil surface.

Since no strong earthquake has been instrumentally recorded on the Mosha fault, we compared our results with GMPEs. **Figure 4** shows the distribution of PGA derived from the stochastic finite-fault model and the NGA-west2 relations. The circles represent simulation results, while the black thick-dash line represents the fitted curve to simulated data. As depicted, there is appropriate consistency between the values of the stochastic finite-fault model and GMPEs, especially at short distances. It should be noted that there is some inter-event variability in the simulated data that should be considered in the analysis. This is discussed in detail in Section 5.

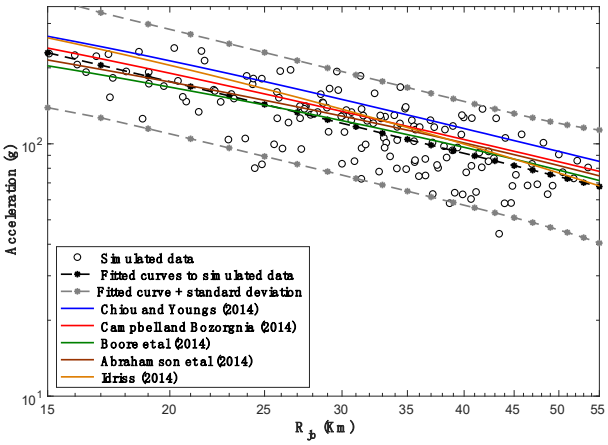

Figure 4. Comparison the PGA values derived from stochastic finite fault model (black circle) and NGA-west2 relations (black thick line is the mean of all GMPEs).

In **Figure 5**, the simulated time history waveform for the eight important locations in Tehran (represented by blue triangles in **Figure 2**) is presented. As shown, the time history waveform of points in the east of Tehran has a short duration with greater amplitude, while the time history waveform of points in the west of Tehran (which are far from the Mosha fault) has a longer duration with weaker amplitude. This is in accordance with our expectations. The pseudo-response acceleration for the same locations is also provided in **Figure 6**.

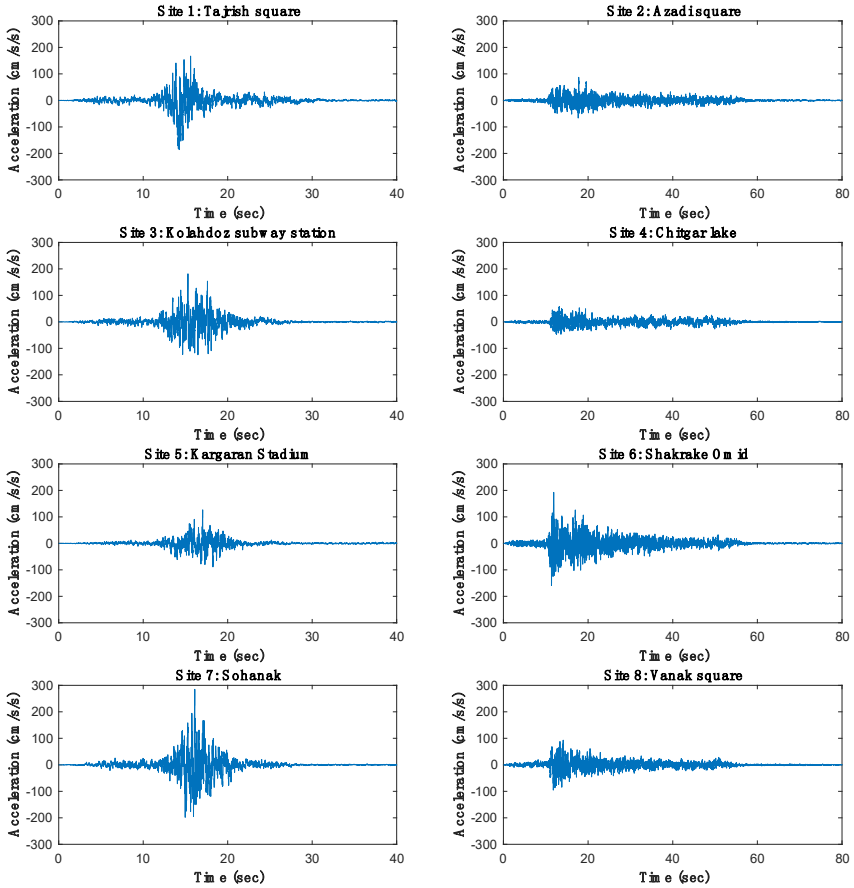

Figure 5. The time history waveform of 8 selected sites in Tehran.

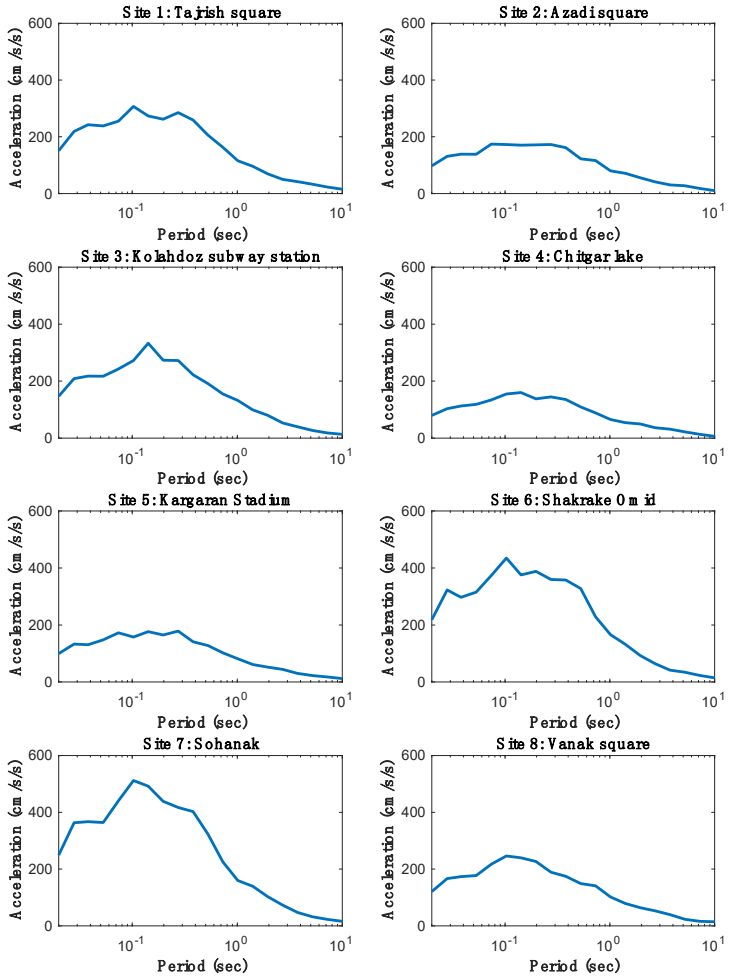

Figure 6. Pseudo response acceleration of the 8 selected sites in Tehran.

4. Compiling exposure model and selecting appropriate fragility curves

To assess the impact of earthquakes, it is necessary to compile a reliable database containing information about the building stock and population distribution in the area. In large-scale seismic risk assessment, buildings are generally categorized into different classes according to their likelihood of sustaining damage at different intensities. In the last few decades, several building taxonomies have been proposed, including ATC-13 [32], the European Macroseismic Scale (EMS-98) [33], HAZUS [34], PAGER-STR [35], Syner-G [36], and GEM [37] taxonomies. A comprehensive review of these classification methods can be found by Crowley et al. [36]. However, the application of these methods in regions like Iran is associated with uncertainties due to a lack of information about building characteristics. For instance, the HAZUS building classification focuses on the structural aspects of a building, while such detailed information about the seismic load resistance of buildings is not available in Iran. Therefore, in seismic loss assessment studies in Iran, most researchers consider a limited number of building taxonomies, considering available data such as construction material, age, and height of buildings. Certainly, considering such generic factors in building classification imposes uncertainties on results. On the other hand,

employing a set of unrealistic assumptions for building classification imposes greater uncertainty on the outcomes.

In the present study, information provided by the Statistical Center of Iran (SCI) is used to compile building taxonomies. SCI is the official authority for data collection on population and buildings in Iran. The latest data from SCI [3] is used, which is the most reliable and available information. SCI provides information on construction material and the age of buildings. Regarding construction material, SCI's information is limited to three groups: concrete (RC), steel (ST), and masonry (M). In this classification, adobe, masonry, rubble stone, and other types of structures are considered as masonry. By using the year of construction, the quality of buildings or the level of implementation of seismic regulations and codes can be estimated. The Iranian Code of Practice for Seismic Resistant Design of Buildings (Standard No. 2800) is the primary reference for seismic design of structures. To date, four versions of this standard have been developed and published by the Building and Housing Research Center (BHRC). The first edition was released in 1987, and buildings constructed based on this version are considered low-code. The second edition was published in 1996, and buildings designed according to this version are considered mid-code. The third and fourth versions were presented in 2005 and 2015, respectively. Buildings designed based on these versions are considered high-code.

Figure 7 shows the distribution of buildings in Tehran based on the quality and material of construction. As depicted, the majority of buildings are mid-quality steel and low-quality masonry, making them vulnerable to strong earthquakes. To improve the accuracy of building classification, the height of the building was also considered in this study. This factor was extracted from an additional database provided by Tehran Municipality. Based on the number of stories, buildings are classified into three groups: low-rise (less than 4 stories), mid-rise (between 4 and 6 stories), and high-rise (more than 7 stories). By considering the aforementioned factors (i.e., construction material, quality of construction, and height of the building), buildings are classified into 19 classes in this study. The number of different building categories within 22 municipal districts of Tehran is presented in **Table 3**.

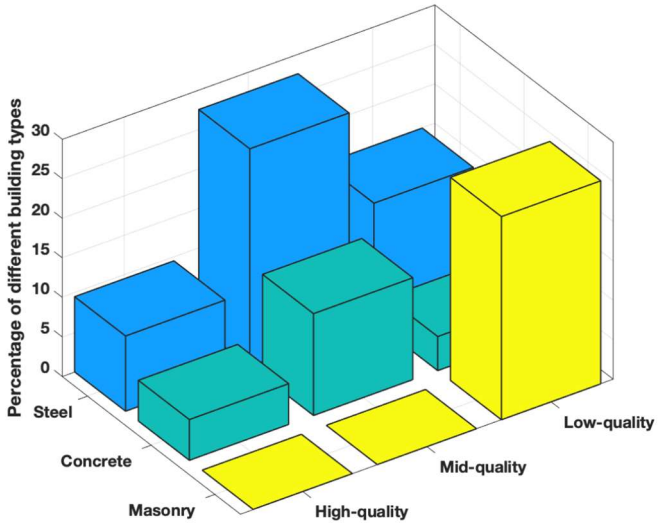

Figure 7. Distribution of buildings in Tehran based on the quality and construction material.

Figure 8 shows the spatial distribution of buildings within a grid cell of 1 × 1 km in Tehran. As illustrated, many buildings are located in the eastern and central parts of the city, which are closer to the Mosha fault. Thus, there is a higher seismic risk in these regions in the case of a Mosha fault seismic scenario.

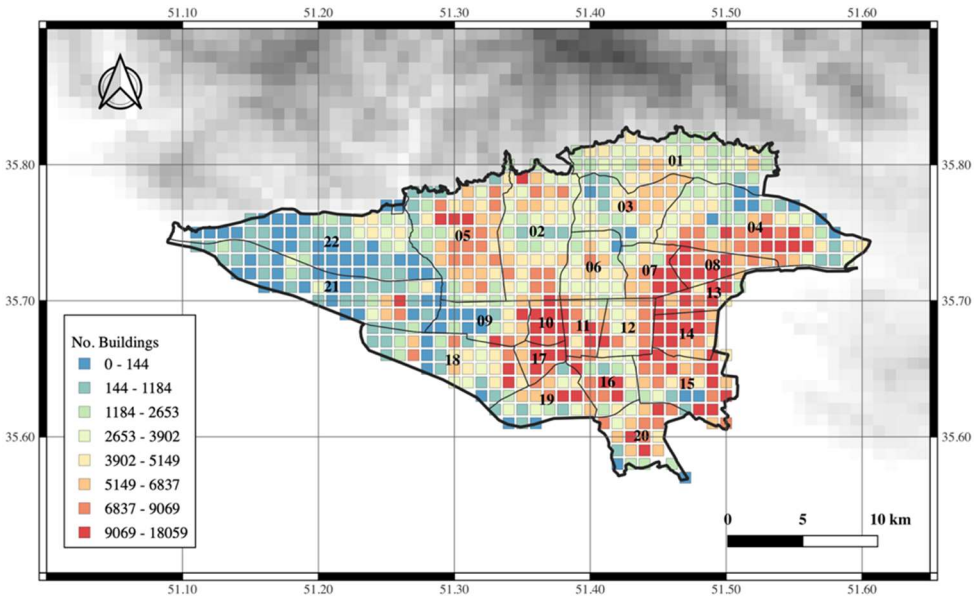

Figure 8. Distribution of buildings in a grid cell of 1 × 1 km within Tehran.

For seismic risk assessment, a set of fragility curves corresponding to the pre-defined building classes is required. Several fragility curves for typical residential buildings in Iran have been proposed by different scholars. In a study performed by the Japan International Cooperation Agency (JICA) [16], nine fragility curves were developed for seismic risk assessment in Tehran. JICA [16] classified the buildings according to their construction material and age. Omidvar et al. [38] developed empirical fragility curves for steel and concrete structures based on data from past earthquakes in Iran, mainly the 1990 Manjil-Roudbar (Mw: 7.4) and 2003 Bam (Mw: 6.6) earthquakes. Sadeghi et al. [39] developed vulnerability curves for 42 building types in Iran by compiling a set of local and global fragility/vulnerability curves and combining them based on engineering judgment. In that study, factors such as construction material, load resistance system, height, and quality of construction were considered in building classification. Motamed et al. [40] developed fragility curves for 23 building classes based on construction material, building height, lateral load resisting system, and year of construction for residential buildings in Iran. Fallah Tafti et al. [41] developed fragility curves for 19 building classes in Iran by compiling a set of existing fragility curves and merging them based on the Analytic Hierarchy Approach (AHP). They also validated their model based on records of some past earthquakes in Iran. Bastami et al. [42] provided a set of 26 vulnerability curves for residential buildings in Iran by considering construction material, age, and building height. In the present study, the fragility curves proposed by Fallah Tafti et al. [41] are used due to the compatibility of the building classes in the present study. These fragility curves provide the probability of damages at four levels, including slight, moderate, extensive, and collapse.

Table 3. Distribution of different building types in 22 municipal districts of Tehran (abbreviations are as follow: ST: steel, RC: concrete, MA: masonry, LR: low-rise, MR: mid-rise, HR: high-rise, LQ: low-quality, MQ: mid-quality, and HQ: high-quality).

District No	ST-LR-LQ	ST-LR-MQ	ST-LR-HQ	ST-MR-LQ	ST-MR-MQ	ST-MR-HQ	ST-HR-LQ	ST-HR-MQ	ST-HR-HQ	RC-LR-LQ	RC-LR-MQ	RC-LR-HQ	RC-MR-LQ	RC-MR-MQ	RC-MR-HQ	RC-HR-LQ	RC-HR-MQ	RC-HR-HQ	MA-LR-LQ	Sum
1	3393	6288	1628	8733	26405	8866	3003	9717	3328	2165	5144	1165	5850	22920	6616	1980	8928	2584	19069	147783
2	5702	9299	2289	14769	38052	11912	3265	9468	2817	3296	10421	1939	7939	40085	12931	2644	13483	3265	18945	212521
3	4323	6280	1271	11061	22820	5574	4072	8221	1959	1730	2736	708	4816	11457	3489	2005	4513	1321	10997	109350
4	10634	22505	6917	27179	77391	25716	2972	10160	3004	2036	5555	1987	5422	20283	9001	960	3779	1262	59311	296074
5	1070	9249	2262	3935	46641	14237	478	6830	2413	4791	16124	5161	9295	74915	30714	3905	11263	4743	7897	255922
6	5611	4113	1026	11928	12073	3346	3711	3251	812	1973	1671	432	4275	5156	1548	1368	1572	449	13254	77570
7	7992	9426	2531	16382	23030	6233	2303	2208	527	1161	1646	510	2542	4545	1596	316	439	260	40050	123695
8	8713	9259	4481	20495	28000	12735	1917	3042	1177	845	1180	528	2198	4009	1831	202	438	167	42860	144078
9	3727	1798	1119	6803	4305	2461	450	180	129	2250	929	758	3829	2157	1671	357	89	80	31113	64206
10	5820	9261	3787	11605	20000	7964	332	418	156	2038	3569	1687	3880	7735	3534	107	157	78	37302	119431
11	4661	8270	2744	11008	21126	7055	840	1165	376	1632	3542	1536	3915	9302	3941	245	454	225	27570	109606
12	4312	5451	2281	9479	15290	6472	927	1476	578	784	1164	796	1712	3016	2025	128	236	131	30101	86359
13	4692	9462	3519	12019	27190	10472	1077	2304	934	393	301	92	925	1126	412	82	99	26	23927	99053
14	12062	15610	6085	24259	39705	14904	2296	2526	834	293	708	175	592	1890	477	75	115	16	52317	174938
15	14821	19716	6180	25744	41606	12840	968	1331	554	1323	957	430	2607	3619	1211	21	385	45	103034	237389
16	7501	6062	2394	12800	12979	4825	670	600	199	1111	1349	359	1926	3455	834	92	39	21	57937	115151
17	5354	2877	2783	9783	6242	5959	508	220	252	2045	1122	1587	3179	2332	3073	176	105	158	49154	96908
18	4162	6850	3401	8754	15821	7973	281	388	187	2607	5277	4092	4997	11774	9039	141	333	238	47812	134127
19	3830	8342	2778	9452	21109	7504	452	878	305	356	805	543	753	1945	1447	77	63	34	16071	76747
20	6247	8144	3012	13865	21939	8706	754	1388	475	1077	2784	958	2293	6701	2545	61	262	65	37691	118966
21	1451	4489	843	2651	12385	2898	675	1394	242	685	2676	811	1145	6665	2640	178	866	183	13269	56149
22	768	2019	197	1434	8675	1590	214	1656	336	335	1397	440	535	7441	5179	158	1518	1320	3841	39053
Sum	126846	184770	63529	274137	542783	190243	32163	68823	21591	34924	71057	26695	74624	252531	105755	15278	49136	16670	743521	2895076

5. Estimating seismic loss based on Mosha fault seismic scenario

This section provides probable seismic losses in the case of the Mosha fault seismic scenario in terms of residential building damages and the number of fatalities. To provide a realistic estimation of damages in a distributed exposure model, spatial correlation due to coherent contributions from source, path, and site should be considered [43]. The impact of this factor on seismic loss assessment has been assessed in several studies. For example, Weatherill et al. [44] showed that disregarding spatial correlation in seismic risk assessment may underestimate the loss, especially in long return periods. In the present study, to consider spatial correlation in the analysis, random sampling from variability of ground motion values was performed, as shown in **Figure 4**. In general, variability from ground values can be categorized into two groups: inter-event variability and intra-event variability. The former represents variability from one earthquake to another, while the latter shows variability from one location to another [45,46]. While the variability of inter-event is sampled once for each synthetic event, intra-event uncertainty is sampled at each location. In the present study, we considered only one seismic scenario; thus, all variability in **Figure 4** can be considered as intra-event variability. Accordingly, the ground motion value at each location is determined based on Equation (6).

$$Ln\left(GMV_{ij}\right) = Ln(\overline{GMV_{ij}}) + \varepsilon_{ij}\sigma_{ij} \quad (6)$$

In the above equation, $\overline{GMV_{ij}}$ is the median ground motion value estimated by stochastic finite-fault model, σ_{ij} is intra-event variability, and ε is a random coefficient from a spatial correlation model. Several spatial correlation models have been proposed by now [47,48]. Here, the model proposed by Zafarani et al. [49] is used. By compiling a reliable database of three components records from 461 of Iran's earthquakes, they developed a spatial correlation for PGA and spectral acceleration. **Figure 9** shows the spatial correlation proposed by Zafarani et al. [49] in different spectral periods. As depicted, by increasing the separation distance, the spatial correlation is decreased, while the reduction in higher periods is lower than short periods.

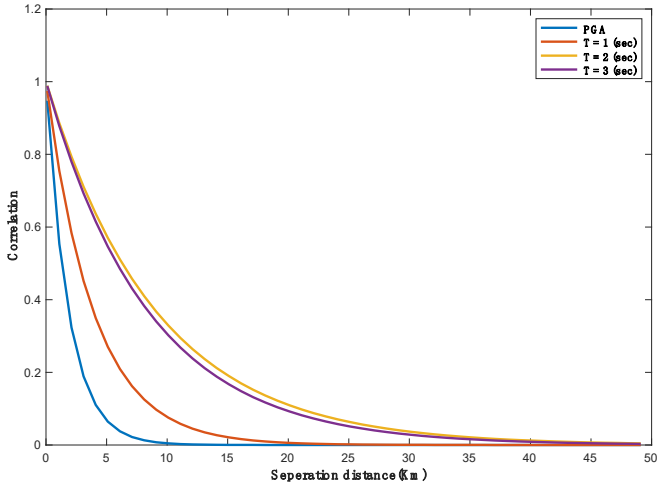

Figure 9. The spatial correlation proposed by Zafarani et al. [49] in different spectral periods.

The most important issue in the random sampling method is the number of iterations required to reach stable results. According to the law of large numbers, as the number of independent events increases, the distribution tends towards the normal distribution [50]. To this end, a sensitivity analysis was performed, and the results indicated that producing 100,000 iterations shows less than 5% variation in the median values of ground motion values. Thus, in the present study, the same number of repetitions was performed. The distribution of the mean damage ratio for Tehran (in a grid cell of 1 × 1 km) is shown in **Figure 10**. As depicted, the majority of damages occurred in the eastern and southern parts of Tehran, which experienced the highest acceleration. The high value of damages in the southern part of the city, which has a far distance from Mosha fault, is interesting. However, this could be mainly related to the concentration of many weak masonry structures in that region. The median mean damage ratio from 100,000 iterations for the whole of Tehran is 6% ± 1.54%. This value is significantly lower than the estimated damage in the study of JICA [16], which assessed the damage ratio of Tehran for the Mosha fault seismic scenario. This discrepancy can also be related to the years of studies and calculation methods. During recent years, many engineered structures have been constructed in Tehran based on the new seismic regulations. Thus, it is expected that the potential seismic loss in our study should be much lower than in the older one. In addition, JICA [16] used a deterministic approach based on the GMPEs for hazard estimation; however, in our study, the stochastic finite-fault method was employed for hazard evaluation.

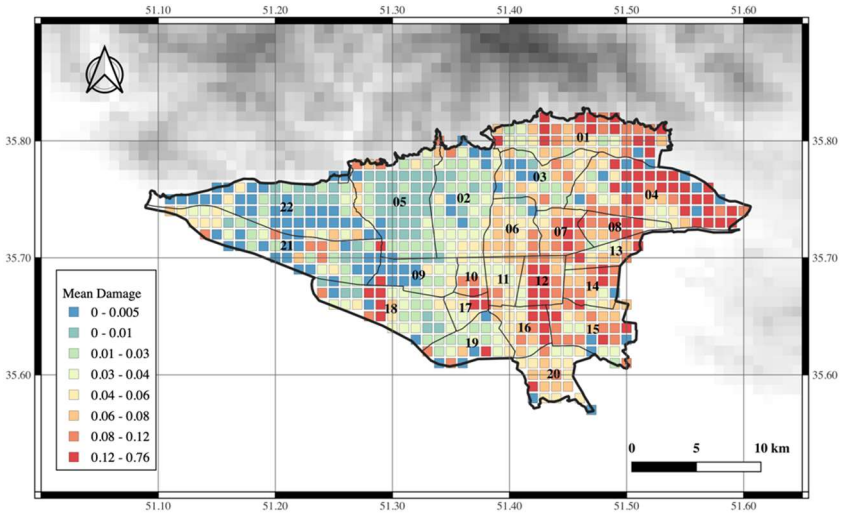

Figure 10. Distribution of mean damage ratio in Tehran.

Estimating the probable number of fatalities in the Mosha fault seismic scenario is another goal of this study. There are several approaches to estimate fatalities, which can be classified into two main groups: non-damage-based and damage-based approaches. In the non-damage-based approach, earthquake fatalities are directly correlated with ground shaking intensity and population. However, this method is based on several assumptions and eliminates many explanatory variables [51–53]. In the damage-based approach, an estimation of damages in different classes of buildings is derived, and then, based on fatality rates of different building classes, the number

of fatalities can be determined [35]. This approach allows for the effects of different types of buildings on fatalities to be taken into account.

In the present study, the damage-based approach is employed. The main challenging issue regarding the damage-based approach is providing a reliable fatality rate in different building classes. At present, there is no global agreement on applicable fatality rates to be used in loss estimation models, and there is certainly a lack of comprehensive data collection in the field following actual events [54]. Thus, in the present study, we used a judgment-based fatality rate for different building classes by considering information provided in peer-reviewed papers or guidelines (such as HAZUS). The fatality rate at different damage levels for the predefined building classes is presented in **Table 4**. As shown, it is assumed that there are no fatalities in the slight mode of damage in all building classes. In addition, due to a lack of data corresponding to different qualities of construction and heights of steel and concrete structures in past earthquakes, just one value of fatality rate was considered in this analysis. The highest fatality rate is also assigned to the masonry building classes. These buildings generally have no resistance to ground shaking and will completely collapse in strong earthquakes. Based on the aforementioned parameters, the total number of fatalities in the case of the Mosha fault seismic scenario for Tehran is estimated to be around 15,952. This is equivalent to 0.2 percent of the total population of the city. This is lower than the estimated value in the study of JICA [16], which proposed a value of 0.3 percent as the fatality ratio for Tehran. This is in accordance with our expectation because the damage ratio in the present study is lower than JICA [16]; consequently, it is expected that the fatality rate is also lower than JICA [16]. **Figure 11** shows the distribution of fatalities within grid cells. As depicted, again, the majority of victims are distributed in the eastern and central parts of the city, where they experience the highest damage (**Figure 10**).

Table 4. Fatality rate in different damage levels of pre-defined building classes.

Building classes	**Fatality rate in different damages level**			
	Slight	**Moderate**	**Extensive**	**Collapse**
ST-LR-LQ	-	-	5	15
ST-LR-MQ	-	-	5	15
ST-LR-HQ	-	-	5	15
ST-MR-LQ	-	-	5	15
ST-MR-MQ	-	-	5	15
ST-MR-HQ	-	-	5	15
ST-HR-LQ	-	-	5	15
ST-HR-MQ	-	-	5	15
ST-HR-HQ	-	-	5	15
RC-LR-LQ	-	-	5	15
RC-LR-MQ	-	-	5	15
RC-LR-HQ	-	-	5	15
RC-MR-LQ	-	-	5	15
RC-MR-MQ	-	-	5	15
RC-MR-HQ	-	-	5	15
RC-HR-LQ	-	-	5	15
RC-HR-MQ	-	-	5	15
RC-HR-HQ	-	-	5	15
MA-LR-LQ	-	5	10	35

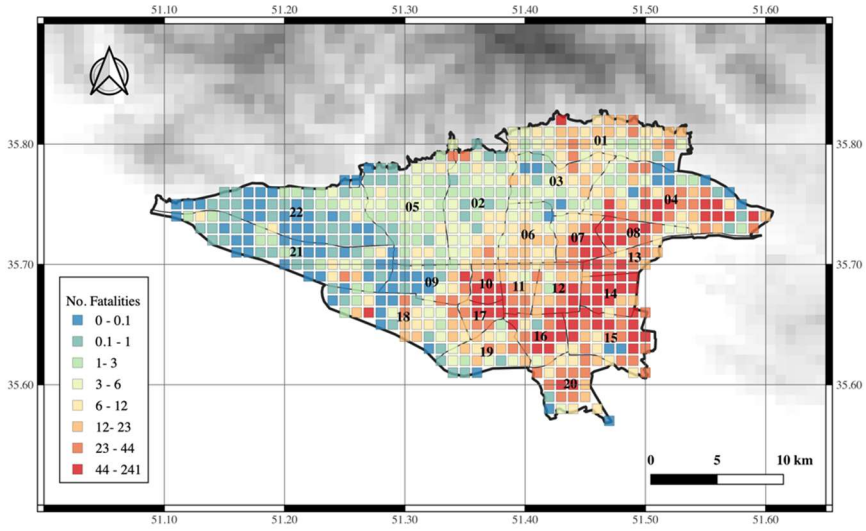

Figure 11. Distribution of fatalities in Tehran, in the case of Mosh seismic scenario.

It should be mentioned that due to contributing several factors in estimating the building damage and fatalities of an earthquake, the outcomes of this study are undoubtedly associated with uncertainties. However, these results can provide appropriate insight for emergency response authorities to develop appropriate action plans for the case of Mosha fault seismic scenario.

6. Conclusion

This paper presents an assessment of the probable seismic losses in Tehran, in terms of building damage and fatalities, that may result from a seismic event along the Mosha fault. To this end, the paper performs a comprehensive review of seismic risk components, which includes evaluating the seismic hazard, compiling an exposure model, and selecting appropriate fragility curves. The seismic hazard assessment employs the stochastic finite-fault method, an approach proposed by Motazedian [22], which is a robust tool considering source, path, and near-source effects. This method, treating earthquakes as a summation of point sources over a finite-fault plane, is well-suited for simulating time-history waveforms and estimating engineering parameters.

Given the absence of a recorded strong earthquake on the Mosha fault, model parameters such as stress drop, fault plane characteristics, and slip rate are inferred from geological, geotechnical, or data from similar historical earthquakes in Iran, like the Manjil-Roudbar earthquake in 1990. Although assumptions regarding model parameters introduce uncertainties into the results, this remains the only viable approach in the absence of real data from a significant seismic event in Tehran.

The study indicates that the Peak Ground Acceleration (PGA) in Tehran for a Mosha fault seismic scenario ranges from 0.05 g to 0.4 g. The highest accelerations are likely to be experienced in the eastern and central parts of the city, attributed to their proximity to the Mosha fault and the presence of soft soil in these areas. For validation, the simulated PGA values were compared with those from NGA-West2 Ground Motion Prediction Equations (GMPEs), showing reasonable agreement.

Building exposure models were compiled using data provided by the Statistical Center of Iran [3], which currently stands as the most comprehensive source of

information on building characteristics in Iran. In this research, buildings are categorized into 19 groups based on construction material, age, and height. Moreover, a set of fragility curves suggested by Fallah Tafti et al. [41] were employed to assess building damages. To account for intra-event variability in the analysis, a random sampling involving 100,000 iterations was conducted, each iteration generating a ground motion shaking map along with a randomly chosen value of intra-event uncertainty derived from a spatial correlation model. The median mean damage ratio derived from these iterations for Tehran is 6% ± 1.54%, with the highest damages predicted for the eastern and central parts of the city, which are also the areas most vulnerable to acceleration.

Fatality estimations were computed using a damage-based approach, wherein a judgment-based fatality rate was applied to different building classes to determine the likely number of victims from the Mosha fault seismic scenario. The estimations suggest that there could be 15,952 fatalities, which is approximately 0.2 percent of Tehran's total population. Furthermore, the distribution of fatalities across Tehran indicates that the most critical areas are the central and eastern parts, where many low-income residents live. It is imperative for local authorities to develop effective seismic risk mitigation strategies for these areas.

It is important to note that the study's conclusions, including both fatality and damage estimates, involve several explanatory parameters, which means they are subject to some degree of uncertainty. Despite this, the findings offer significant insights that can aid local disaster management authorities in devising necessary emergency response and preparedness plans.

Author contributions: Material preparation, data collection and analysis, NK and EF; the seismic hazard analysis, RA; the figures and material, OM; preparing the codes, AA; the first draft of the manuscript, EF; commented on manuscript, NK. All authors have read and agreed to the published version of the manuscript.

Acknowledgments: This paper presents some parts of the results of a project carried out in International Institute of Earthquake Engineering and Seismology (IIEES), Tehran. The financial and technical supports of this institute are highly appreciated. The authors also gratefully appreciate all individuals and organizations contributing to the compiling data sets used in the present study, particularly the Statistical Center of Iran (SCI) for providing the building inventories and population database.

Conflict of interest: The authors declare no conflict of interest.

References

1. Tchalenko JS, Braud J, Berberian M. Discovery of three earthquake faults in Iran. Nature. 1974; 248(5450): 661-663. doi: 10.1038/248661a0
2. Jackson J, McKenzie D. Active tectonics of the Alpine--Himalayan Belt between western Turkey and Pakistan. Geophysical Journal International. 1984; 77(1): 185-264. doi: 10.1111/j.1365-246x.1984.tb01931.x
3. Statistical Centre of Iran (SCI), Statistical Centre of Iran, Vice-Presidency for Strategic Planning and Supervision. National Census of Population and Housing Techical Reports, Sarshomāri 2016 (1395), 2011 (1390), 2006 (1385), 1996 (1375), 1986 (1365), and 1976 (1355): Tehran. formerly, the Plan & Budget Organization of the Imperial Government of Iran, Statistical Centre; 2016.

4. Berberian M. Contribution to the Seismotectonics of Iran II. Ministry of Industry and Mines; 1976.
5. Moinfar A, Mahdavian A, Maleki E. Historical and Instrumental Earthquake Data Collection of Iran. Publication Iranian Culture. Affairs Inst, Tehran; 1994. p. 446.
6. Jalalalhosseini SM, Zafarani H, Zare M. Time-dependent seismic hazard analysis for the Greater Tehran and surrounding areas. Journal of Seismology. 2017; 22(1): 187-215. doi: 10.1007/s10950-017-9699-4
7. Berberian M, Yeats RS. Tehran: An earthquake time bomb. In: Sorkhabi R (editor). Tectonic Evolution, Collision, and Seismicity of Southwest Asia: In Honor of Manuel Berberian's Forty-Five Years of Research Contributions. Geological Society of America; 2016. pp. 84.
8. Firuzi E, Ansari A, Amini Hosseini K, et al. Probabilistic earthquake loss model for residential buildings in Tehran, Iran to quantify annualized earthquake loss. Bulletin of Earthquake Engineering. 2019; 17(5): 2383-2406. doi: 10.1007/s10518-019-00561-z
9. Kalantari M, Firuzi E, Ahmadipour masoud, et al. Estimating Annualized Earthquake Loss for Residential Buildings in Tehran, Iran. Available online: https://assets-eu.researchsquare.com/files/rs-1685779/v1/3e963f1b-807a-4ae1-a30a-3d195a1db990.pdf?c=1697480440 (accessed on 2 January 2024).
10. Firuzi E, Ansari A, Amini Hosseini K, Kheirkhah N. Developing an earthquake damaged-based multi-severity casualty method by using Monte Carlo simulation and fuzzy logic; case study: Mosha fault seismic scenario, Tehran, Iran. Stochastic Environmental Research and Risk Assessment. 2024; 38: 2019-2039. doi: 10.1007/s00477-024-02667-6
11. De Martini PM, Hessami K, Pantosti D, et al. A geologic contribution to the evaluation of the seismic potential of the Kahrizak fault (Tehran, Iran). Tectonophysics. 1998; 287(1-4): 187-199. doi: 10.1016/s0040-1951(98)80068-1
12. Nazari H, Ritz JF, Salamati R, et al. Morphological and palaeoseismological analysis along the Taleghan fault (Central Alborz, Iran). Geophysical Journal International. 2009; 178(2): 1028-1041. doi: 10.1111/j.1365-246x.2009.04173.x
13. Ritz JF, Nazari H, Balescu S, et al. Paleoearthquakes of the past 30,000 years along the North Tehran Fault (Iran). Journal of Geophysical Research: Solid Earth. 2012; 117(B6). doi: 10.1029/2012jb009147
14. Ambraseys NN, Melville CP. A History of Persian Earthquakes. Cambridge University Press; 1982. p. 219.
15. Berberian M, Yeats RS. Patterns of historical earthquake rupture in the Iranian Plateau. Bulletin of the Seismological Society of America. 1999; 89(1): 120-139. doi: 10.1785/bssa0890010120
16. Japan International Cooperation Agency (JICA). The Study on Seismic Microzoning of the Greater Tehran Area in the Islamic Republic of Iran, Final Report, Japan International Cooperation Agency (JICA), Centre for Earthquake and Environmental Studies of Tehran (CEST) Tehran Municipality; 2000.
17. Beresnev IA. Source Parameters of Earthquakes in Eastern and Western North America Based on Finite-Fault Modeling. Bulletin of the Seismological Society of America. 2002; 92(2): 695-710. doi: 10.1785/0120010101
18. Zafarani H, Noorzad A, Ansari A, et al. Stochastic modeling of Iranian earthquakes and estimation of ground motion for future earthquakes in Greater Tehran. Soil Dynamics and Earthquake Engineering. 2009; 29(4): 722-741. doi: 10.1016/j.soildyn.2008.08.002
19. Saffari H, Roohafzayan A, Mahdavian A, Yari M. Stochastic Finite Fault Modeling and Simulation of Strong Ground Motion of Mosha Fault in Iran. Electronic Journal of Structural Engineering. 2020; 20: 63-71. doi: 10.56748/ejse.20247
20. Yu R, Song Y, Guo X, et al. Seismic hazard analysis for engineering sites based on the stochastic finite-fault method. Earthquake Science. 2022; 35(5): 314-328. doi: 10.1016/j.eqs.2022.05.007
21. Douglas J, Aochi H. A Survey of Techniques for Predicting Earthquake Ground Motions for Engineering Purposes. Surveys in Geophysics. 2008; 29(3): 187-220. doi: 10.1007/s10712-008-9046-y
22. Motazedian D. Stochastic Finite-Fault Modeling Based on a Dynamic Corner Frequency. Bulletin of the Seismological Society of America. 2005; 95(3): 995-1010. doi: 10.1785/0120030207
23. Boore DM. Stochastic simulation of high-frequency ground motions based on seismological models of the radiated spectra. Bulletin of the Seismological Society of America. 1983; 73: 1865-1894.
24. Boore DM. Simulation of Ground Motion Using the Stochastic Method. Pure and Applied Geophysics. 2003; 160(3): 635-676. doi: 10.1007/pl00012553
25. Aki K. Scaling law of seismic spectrum. Journal of Geophysical Research. 1967; 72(4): 1217-1231. doi: 10.1029/jz072i004p01217

26. Landgraf A, Ballato P, Strecker MR, et al. Fault-kinematic and geomorphic observations along the North Tehran Thrust and Mosha Fasham Fault, Alborz mountains Iran: implications for fault-system evolution and interaction in a changing tectonic regime. Geophysical Journal International. 2009; 177(2): 676-690. doi: 10.1111/j.1365-246x.2009.04089.x
27. Tatar M, Hatzfeld D, Abbassi A, et al. Microseismicity and seismotectonics around the Mosha fault (Central Alborz, Iran). Tectonophysics. 2012; 544-545: 50-59. doi: 10.1016/j.tecto.2012.03.033
28. Solaymani Azad S, Ritz JF, Abbassi MR. Left-lateral active deformation along the Mosha–North Tehran fault system (Iran): Morphotectonics and paleoseismological investigations. Tectonophysics. 2011; 497(1-4): 1-14. doi: 10.1016/j.tecto.2010.09.013
29. Wells DL, Coppersmith KJ. New empirical relationships among magnitude, rupture length, rupture width, rupture area, and surface displacement. Bulletin of the Seismological Society of America; 1994, 84(4): 974-1002. doi: 10.1785/bssa0840040974
30. Motazedian D. Region-Specific Key Seismic Parameters for Earthquakes in Northern Iran. Bulletin of the Seismological Society of America; 2006, 96(4A): 1383-1395. doi: 10.1785/0120050162
31. Heaton TH. Evidence for and implications of self-healing pulses of slip in earthquake rupture. Physics of the Earth and Planetary Interiors. 1990; 64(1): 1-20. doi: 10.1016/0031-9201(90)90002-f
32. ATC (Applied Technology Council). Earthquake damage evaluation data for California, ATC-13. Redwood City, CA; 1985.
33. Grunthal G. European macroseismic scale 1998 (EMS-98). Cahiers du Centre Europeen de Geodynamique et de Seismologie 15, Centre Europeen de Geodynamique et de Seismologie, Luxembourg; 1998.
34. FEMA (Federal Emergency Management Agency). HAZUS- MH MR4 technical manual. FEMA; 2003.
35. Jaiswal K, Wald DJ. Creating a Global Building Inventory for Earthquake Loss Assessment and Risk Management. Open-File Report; 2008. doi: 10.3133/ofr20081160
36. Crowley H, Colombi M, Silva V, et al. D3.1 Fragility functions for common RC building types in Europe. Available online: www.vce.at/SYNER-G/files/dissemination/deliverables.html (accessed on 2 January 2024).
37. Silva V, Brzev S, Scawthorn C, et al. A Building Classification System for Multi-hazard Risk Assessment. International Journal of Disaster Risk Science. 2022; 13(2): 161-177. doi: 10.1007/s13753-022-00400-x
38. Omidvar B, Gatmiri B, Derakhshan S. Experimental vulnerability curves for the residential buildings of Iran. Natural Hazards. 2011; 60(2): 345-365. doi: 10.1007/s11069-011-0019-y
39. Sadeghi M, Ghafory-Ashtiany M, Pakdel-Lahiji N. Developing seismic vulnerability curves for typical Iranian buildings. Proceedings of the Institution of Mechanical Engineers, Part O: Journal of Risk and Reliability. 2015; 229(6): 627-640. doi: 10.1177/1748006x15596085
40. Motamed H, Calderon A, Silva V, et al. Development of a probabilistic earthquake loss model for Iran. Bulletin of Earthquake Engineering. 2018; 17(4): 1795-1823. doi: 10.1007/s10518-018-0515-5
41. Fallah Tafti M, Amini Hosseini K, Mansouri B. Generation of new fragility curves for common types of buildings in Iran. Bulletin of Earthquake Engineering. 2020; 18: 3079-3099.
42. Bastami M, Abbasnejadfard M, Motamed H, et al. Development of hybrid earthquake vulnerability functions for typical residential buildings in Iran. International Journal of Disaster Risk Reduction. 2022; 77: 103087. doi: 10.1016/j.ijdrr.2022.103087
43. Verros SA, Wald DJ, Worden CB, et al. Computing spatial correlation of ground motion intensities for ShakeMap. Computers & Geosciences. 2017; 99: 145-154. doi: 10.1016/j.cageo.2016.11.004
44. Weatherill GA, Silva V, Crowley H, Bazzurro P. Exploring the impact of spatial correlations and uncertainties for portfolio analysis in probabilistic seismic loss estimation. Bulletin of Earthquake Engineering. 2015; 13: 957-981.
45. Silva V. Critical Issues on Probabilistic Earthquake Loss Assessment. Journal of Earthquake Engineering. 2017; 22(9): 1683-1709. doi: 10.1080/13632469.2017.1297264
46. Crowley H, Bommer JJ. Modelling Seismic Hazard in Earthquake Loss Models with Spatially Distributed Exposure. Bulletin of Earthquake Engineering. 2006; 4(3): 249-273. doi: 10.1007/s10518-006-9009-y
47. Goda K, Atkinson GM. Probabilistic Characterization of Spatially Correlated Response Spectra for Earthquakes in Japan. Bulletin of the Seismological Society of America. 2009; 99(5): 3003-3020. doi: 10.1785/0120090007
48. Jayaram N, Baker JW. Correlation model for spatially distributed ground-motion intensities. Earthquake Engineering & Structural Dynamics. 2009; 38(15): 1687-1708. doi: 10.1002/eqe.922

49. Zafarani H, Ghafoori SMM, Adlaparvar MR. Spatial Correlation of Peak Ground Motions and Pseudo Spectral Acceleration Based on the Iranian Multievent Datasets. Journal of Earthquake Engineering. 2021; 26(12): 6042-6062. doi: 10.1080/13632469.2021.1911882
50. Rohatgi VK, Saleh AKMdE. An Introduction to Probability and Statistics. John Wiley & Sons; 2015. doi: 10.1002/9781118799635
51. Badal J, Vazquez-Prada M, Gonzalez A. Preliminary Quantitative Assessment of Earthquake Casualties and Damages. Natural Hazards. 2005; 34(3): 353-374. doi: 10.1007/s11069-004-3656-6
52. Firuzi E, Amini Hosseini K, Ansari A, et al. An empirical model for fatality estimation of earthquakes in Iran. Natural Hazards. 2020; 103(1): 231-250. doi: 10.1007/s11069-020-03985-y
53. Firuzi E, Amini Hosseini K, Ansari A, et al. Developing a new fatality model for Iran's earthquakes using fuzzy regression analysis. International Journal of Disaster Risk Reduction. 2022; 80: 103231. doi: 10.1016/j.ijdrr.2022.103231
54. So E. Estimating Fatality Rates for Earthquake Loss Models. Springer International Publishing; 2016. doi: 10.1007/978-3-319-26838-5

Building Engineering 2024, 2(1), 561.
https://doi.org/10.59400/be.v2i1.561

Article

Roles of stakeholders for adopting sustainable design in buildings

Nor Aqilah Haji Juffle*, Md Motiar Rahman, Rajul Adli Asli

Civil Engineering Programme Area, Faculty of Engineering, Universiti Teknologi Brunei, Gadong BE1410, Brunei Darussalam
*** Corresponding author:** Nor Aqilah Haji Juffle, p20210002@student.utb.edu.bn

CITATION

Juffle NAH, Rahman MM, Asli RA. Roles of stakeholders for adopting sustainable design in buildings. Building Engineering. 2024; 2(1): 561. https://doi.org/10.59400/be.v2i1.561

ARTICLE INFO

Received: 21 February 2024
Accepted: 19 March 2024
Available online: 27 March 2024

Abstract: Buildings account for the highest carbon dioxide emissions during their operation stage, primarily due to high energy use for heating, cooling, and lighting, which in turn contribute to global warming and climate change. Such impact can be considerably reduced through crafting sustainable design (SusD) in buildings. So, availability of relevant information, professional guidance to clients, and appropriate decision-making are crucial. A study summarized the findings from a questionnaire survey conducted in Brunei with 122 responses. The results revealed that architects, consultants, and government are more important stakeholders to assist with SusD adoption, while clients and developers are important stakeholders in decision-making. The results appreciate the roles of clients and architects to a higher degree, despite a comparatively higher number of private projects in Brunei with relatively more influence of contractors. This was interpreted as having a good degree of awareness of the survey participants towards the role of SusD and who actually can better contribute to SusD adoption. However, the outcome also revealed inconsistent perception among the respondents, both within and between different groups based on their affiliations and nature of job. This inconsistency implies the need for appropriate training or education to enhance awareness of SusD, make pertinent information available, and develop appropriate skills.

Keywords: buildings; carbon dioxide emissions; energy consumption; sustainable design

1. Introduction

The construction industry is blamed for its adverse impact on the natural environment [1], owing to high energy consumption and environmental pollution [2]. Buildings account for a large proportion of these, which are rapidly increasing due to the increase in population, extended building use, and demand for comfort and satisfaction. As a result, global greenhouse gas (GHG)/ carbon dioxide (CO_2) emissions throughout the building life cycle are also increasing, which has been estimated to reach 42.4 billion tonnes/year by 2035, 43% more than the 2007 level [3]. This is considered one of the key reasons for global warming and climate change. It is reported that 80%–90% of such emissions occur during the building operation stage, mainly due to energy use for space heating and cooling, lighting, and other applications. Such energy use and relevant GHG emissions can be considerably reduced by adopting various energy efficiency measures and sustainable design approaches at the design stage [4–6].

Sustainable design (SusD) uses two natural elements (i.e., the sun and wind) and focuses mainly on reducing energy consumption and CO_2 emissions. Other benefits include reducing water and material use and improving indoor air quality and occupant comfort [7]. This is achieved by applying 'passive' principles in various architectural and structural design methodologies that exploit the design and properties of the

building envelope to reduce energy demand and maximize or minimize heat losses and heat gains [8]. Such passive design is associated with longer life spans or durability, lower life cycle costs, and higher benefits in energy saving [9,10] that can reduce energy consumption of up to 50%–60% [11–13]. Despite such benefits, the knowledge and awareness of construction stakeholders about SusD appears to be limited.

A crucial condition for the adoption of SusD is the availability of relevant information, knowledge, and interest among construction professionals and/or stakeholders [14], since a lack of adequate knowledge of SusD applications and their benefits may hinder the professional guidance, which can negatively influence the building owners to adopt SusD [15]. Lack of awareness and relevant knowledge plays a critical role in decision-making on adopting SusD. Prior knowledge, information, and understanding could make better decisions whether to adopt SusD, but their absence makes it impossible, as they do not know who to take the decision of adopting SusD [16,17]. Admittedly, effective adoption of SusD requires the knowledge, understanding, consciousness, and commitment of all stakeholders in their individual actions [18], especially potential building owners, to know who (i.e., which stakeholder or party) can help them with proper information and guidance on SusD so that they can select that party for their buildings and who actually should influence or take the decision of adopting SusD.

Unfortunately, hot and humid developing countries like Indonesia, Malaysia, and Brunei are facing these issues, which prevent them from adopting SusD. For example, the low level of awareness and knowledge of SusD is one of the challenges to early adoption of SusD practices in Malaysia [19]. The situation in Brunei Darussalam is not different. As such, in an attempt to assess the awareness of the local industry, the present study focused on identifying the suitable stakeholders who can help potential building owners to consider SusD by providing relevant information and who can guide them to adopt SusD. In addition to generating some degree of awareness among the industry participants, the findings of the study are expected to help the stakeholders in understanding and making decisions about, and selecting the right party for helping with, adopting SusD. The following sections present the relevant literature review, the methodology adopted, results and discussions, and finally, the conclusions.

2. Literature review

The study was undertaken in two stages: a structured literature review focusing on relevant past empirical studies and the practice of SusD. This review is exclusively based on relevant papers published in academic journals. A systematic literature search was performed using three academic listings, namely Science Direct, Taylor & Francis, and Emerald Insight. In order to collect relevant papers for this study, the following five keywords were used: ‘residential building’, ‘energy efficiency’, ‘low carbon building’, ‘passive design’, and ‘optimization’. These were searched within the title, abstract, and contents of the initially identified articles [20,21]. A total of 156 relevant papers were considered valid for further analysis. Each of the selected papers was analyzed for a wider study, in terms of identifying SusD features, motivators, challenges, and strategies for SusD adoption [20–22]. This also covered stakeholders/parties or roles who could help potential building owners/clients with

relevant knowledge and information to adopt SusD and who can guide to make decision to adopt SusD, which are being dealt with in this paper.

It was observed that the adoption of SusD in buildings by construction stakeholders is hampered by a number of challenges, including unfamiliarity with SusD technology [23], lack of relevant information [24], and insufficient professional knowledge and expertise [25]. In this regard, the following subsections provide a review of relevant segments of literature on the influence/ability of various stakeholders in terms of providing appropriate information and guidance to potential building owners and helping them to decide if to adopt SusD.

2.1. Assistance to building owners

Many stakeholders or parties can help potential building owners adopt different types and degrees of SusD. According to their roles or skills, they include the project team members like architects, design engineers, contractors, owners or clients, and project managers, as well as building occupants, financial experts, cost consultants, and government agents [26–28]. These project team members deploy their expertise and knowledge to ensure effective collaboration and decision-making and provide owners with relevant information. Their involvement also promotes communication and coordination among different stakeholders, eventually enhancing the overall project outcomes [29]. They are responsible for identifying and implementing SusD, monitoring and evaluating the project's environmental impact, and advocating for sustainable practices [30]. They also contribute to the development of SusD building codes and regulations, ensuring compliance with sustainability standards [29]. Additionally, they actively participate in educating and raising awareness about sustainable practices within the construction industry and society as a whole [26]. Their involvement is crucial in driving the adoption of sustainable practices and achieving long-term environmental goals in construction projects [27]. However, the design team (i.e., architect and/or engineer) and the construction team (i.e., contractor or builder/constructor) are the key stakeholders for SusD adoption because they can help the owner to oversee all phases of construction [28]. On the other hand, local governments and contractors are particularly powerful in several key phases of the construction process [29]. In the design and build system, cooperation between contractor and designer starts early, even during the invitation to tender phase. The involvement of financial experts in this phase helps settle disputes and prevent potential problems [30]. Local governments and contractors are crucial for ensuring that construction projects adhere to environmental and social standards. Their collaboration can lead to innovative solutions to minimize the project's impact on the surrounding community and ecosystem [30–32].

Marichova [33] mentioned that the government plays a major role, along with the contractor and design team in the construction market, in order to ensure the efficient use of technology, which in turn accelerates its adoption. Moreover, the government and client generally have a major role to play both at the project and industry level [34]. Furthermore, consultants also play a role in the SusD adoption, along with the design team and on behalf of the client. The consultants play a greater role with the government in incorporating green or sustainable components early in the design stage

so that a more holistic SusD is achieved [35]. Additionally, consultants play a crucial role in determining project success and technical aspects of performance. It is also argued that clients and architects are the most important stakeholders to be involved during the pre-feasibility phase, whereas government, contractors, and consultants are the least important during the pre-construction stage [30,34]. However, these stakeholders bring expertise in environmental regulations, energy efficiency, and SusD practices, making their roles essential [31]. Structural designers/consultants collaborate closely with architects and clients to ensure that sustainable goals are achieved, providing guidance on material selection, energy systems, and SusD strategies [34]. Their involvement throughout the project lifecycle ensures that SusD principles are seamlessly integrated into the construction process [35].

2.2. Decision-making

A "group" of individuals and groups is typically involved in the decision-making of a building project, including clients, users, building professionals, and external parties [36,37]. It is reported that the decision of whether to build green (that is, to use SusD) is made early in a project's development process by stakeholders like developers, investors, and the client. Early participation of key project stakeholders (i.e., client, designer, and contractor) leads to earlier completion of the project and more savings. These stakeholder groups have the highest influence on the decision-making of a project [38,39].

Menassa and Baer [40] argued that stakeholders' involvement in sustainable building construction is increasingly important for their cooperation and end-users' requirements. Tran [41] observed that developers are the key stakeholders in the decision-making process of adopting green building technologies in Vietnam. However, such a decision is likely to be dependent on the readiness level of other project partners, such as the government, designers, and contractors. Nevertheless, the decisions to adopt green buildings are typically taken internally by the developer, client, and investor and rarely include outside consultants [42], although the level of investors' participation in the decision to adopt sustainable features may be insignificant [43]. In addition to their decision-making role, stakeholders are also responsible for setting goals, implementing sustainable development practices, monitoring progress, and engaging with other stakeholders [33]. Moreover, stakeholders contribute substantially to the overall success of sustainable development adoption by providing support, resources, and expertise [34]. Therefore, it is crucial for developers to actively involve key stakeholders throughout the decision-making process to ensure a collaborative and comprehensive approach to sustainability [37].

On the other hand, it was observed in Malaysia that clients and developers are the core parties in construction to make decisions, followed by contractors and investors [44]. However, in a design and build contract, the developer and contractor are key parties in the final decision-making [45]. This is because the complete development of the project belongs to the client or developer, so it is important that they are the ultimate decision-makers [46]. If the client's decision-making process is delayed, it has an impact on the project and the contractor's job. Therefore, although various studies observed different outcomes, every stakeholder is important, with the

changing order of importance according to the stage and needs of the project. Thus, construction practitioners may have different perspectives about risks depending on their particular role in the projects [47].

2.3. Roles in focus

The above literature review identified nine stakeholders, namely consultants, financial experts, engineers, architects, government, contractors, clients, developers, and investors. The first seven parties appear to help/assist, and guide potential building owners by providing knowledge and information on SusD, and the last four parties help in decision-making for adopting SusD.

3. Methodology

3.1. Questionnaire development

The information gathered from the literature review guided the design of a questionnaire [48], which was divided into distinct sections. Section A explained the purpose and objectives of the questionnaire. Section B asked for ethical consent and anonymous details of the respondents for the sample composition. Section C listed various stakeholders/parties and asked potential respondents to prioritize who could help the building owner (with information and knowledge) in considering SusD and making the decision to adopt it. Respondents were asked to rank their priorities on a scale from 1 to 5, where 1 = most important, 2 = more important, 3 = average, 4 = less important, and 5 = least important. This means that the lower the eventual score of a party, the higher the importance of that party. The respondents were also requested to add any other relevant party/parties that is/are not listed. In addition, potential respondents were asked to provide any further comments or suggestions relating to the need/priority of the stakeholders and the role they play.

3.2. Data collection and potential respondents

The target population for this study was construction professionals from contractors, consultants, and clients (within the design and development phase of a building project). They were identified from the lists of professionals in Brunei Darussalam issued by the Ministry of Development (MoD) and Public Works Department (PWD) and via the purposive random sampling method. Initially, 399 invitations were sent to construction professionals via email, which included 133 each for clients, contractors, and consultants. The invitation contained a description of the research and its aim. It was also made clear where and how the outcomes of the study will be used. A Microsoft Word file containing a web link was added in the invitations for the respondents to respond using the Word file or online. However, some invitations were bounced back, and the actual distribution was reduced to 381. In order to increase the number of responses and develop interest, potential respondents were offered summary results of the survey. They were reminded each week from the first contact to increase the chance of responding. A total of 142 responses were received, but 20 were excluded due to incomplete or repetitive responses. The remaining 122 responsive responses (as seen in **Table 1**) were used for analysis. This registered a

32% rate of response (122/381), which is more than the average of 30% in most construction management studies [49,50]. So, the rate of response was regarded as acceptable.

Table 1. Demographic profile of respondents.

Variables	Category	Client	Consultant	Contractor	Total	%
ProfessionGroup	Architectural	0	27	0	27	22.1
	Engineering	15	35	8	58	47.5
	Management	14	8	15	37	30.3
	Total	29	70	23	122	100.0
Experience in SusD projects	< 5 projects	19	41	15	75	61.5
	6–10 projects	7	17	2	26	21.3
	11–15 projects	2	6	1	9	7.4
	> 15 projects	1	6	5	12	9.8

3.3. Data analysis

3.3.1. Testing for reliability

Data were analyzed using the SPSS (Statistical Package for Social Sciences, version 27) software. The analysis started with determining the Cronbach's alpha coefficient to measure the reliability or internal consistency of the survey items or factors used in the questionnaire [51]. The Cronbach's alpha coefficient ranges in number from 0 to 1, and the higher the score, the more reliable the survey items or factors/options are, and they consistently measure the same characteristic. To be acceptable, Taber [52] suggested that the Cronbach's alpha value should be higher than the threshold of 0.70, which was found for this study in the range of 0.793 to 0.965, indicating that the data collected was reliable and consistent and therefore suitable for further analysis, as presented in the following subsections.

3.3.2. Testing for normality

There are several methods to assess normality assumptions, including the Shapiro-Wilk test, the Kolmogorov-Smirnov test, and the skewness and kurtosis tests. Kim [53] argued that there is no current gold standard method to assess the normality of data. Shapiro-Wilk test and Kolmogorov-Smirnov test are unreliable for large samples (more than 100), while Skewness and kurtosis test may be relatively correct in both small and large samples [54]. So, for this study, skewness and kurtosis tests were used. It is widely argued that the normality assumption is fulfilled when the skewness and kurtosis coefficient are within the range of −2 to +2 [55–57]. The relevant values obtained from the collected sample were found between −0.053 and +1.071, indicating that respondents agreed on their opinions, which also reduced the occurrence of outliers, so the collected data may be considered as normally distributed. Therefore, the parametric test was employed, as presented in this paper.

3.3.3. Mean score ranking (M)

This study used the mean score ranking technique to prioritize the roles of different parties who can help potential building owners with relevant information and assist in making the decision to adopt SusD. Such an approach is widely used in construction management research, i.e., to rank the relative importance of specific

survey items or 'factors' [58]. The mean scores of individual parties were calculated and prioritized with ranks for the total sample and different respondent groups according to their affiliation (i.e., clients, contractors, and contractors) and nature of job (i.e., architectural, engineering, and managerial).

3.3.4. One sample T-test and analysis of variance (ANOVA)

The one-sample T-test compares the mean of sample data to a known value to determine whether a population mean is significantly different from a hypothesized value [59]. This is done by comparing the mean score found in an observed sample to some predetermined or hypothetical value. Typically, this hypothetical value is the population mean or some other theoretically derived value, such as the middle of the measuring scale. The study therefore considered one sample T-test to measure the statistical significance of the mean values for the whole sample and the groups based on affiliation and nature of job. The one-sample t-test was conducted at a 95% confidence interval with the corresponding p-value of 0.05.

One-way ANOVA is a suitable method for comparing the mean scores of more than two groups. In this study, ANOVA was used to check the significant differences in means between the groups based on affiliation and nature of job of the respondents, as explained above.

4. Results and discussions

4.1. Survey demographics

Table 1 shows the respondents' information in two-way groupings: (i) in terms of their affiliation (i.e., 29 clients, 70 consultants, and 23 contractors), and (ii) profession/nature of job (27 architectural, 58 engineering, and 37 management), totaling to 122. The table also shows respondents' experience/involvement in terms of the number of projects considered SusD.

It is seen that respondents' involvement in practicing SusD is much less, with 61.5% in <5 projects and 82.8% (i.e., 61.5 + 21.3) in <10 projects. Only 17.2% of them had involvement in >10 projects. This indicated that the respondents are aware of SusD, but the concept may be relatively new to them, or there is no sufficient demand for SusD from the clients. Nevertheless, all the respondents have some degree of experience on SusD, hence the relevance, quality, and acceptability of their responses to various survey items (i.e., factors and options).

4.2. Client demand

Tables 2 and **3** compare the respondents' opinions on clients' demand for providing SusD in their buildings, based on different groups of affiliation and nature of job, respectively. It is seen that clients have demand of either 'always' or 'often' for SusD only in 30.0% (12.3 + 18.0 ≈ 30.0) cases, in both way groupings based on affiliation and nature of job. The demand in the remaining 70% cases ranges from 'never' to 'sometimes'. This was considered an overall poor or less demand for SusD in Brunei Darussalam, which is also indicated in **Table 1** with relative less experience of the respondents. This situation could be blamed on the existence of numerous challenges in the industry, like justified/additional fees for architects and/or

consultants, a higher initial cost of construction, a lack of expertise, and many more [60–62]. This may also be indicative that some clients are still having difficulty transitioning from traditional to new methods of design. In addition, this may also relate to a general lack of interest in undertaking relevant education and technical trainings, which in turn might have resulted from a poor/low awareness of SusD.

Table 2. Demand for sustainable design based on affiliation.

Category	Client	Consultant	Contractor	Total	%
Always	3	6	6	15	12.3
Often	8	12	2	22	18.0
Sometimes	14	30	6	50	41.0
Rarely	2	20	7	29	23.8
Never	2	2	2	6	4.9

Table 3. Demand for sustainable design based on professional groups.

Category	Architectural	Engineering	Management	Total	%
Always	2	8	5	15	12.3
Often	3	11	8	22	18.0
Sometimes	13	22	15	50	41.0
Rarely	8	14	7	29	23.8
Never	1	3	2	6	4.9

4.3. Assistance to building owners

In terms of which party can best help the building owners with relevant information and knowledge and guide to adopt SusD, **Tables 4** and **5** present the mean values, ranks, and significances obtained from the one-sample t-tests within the total sample and different groups of respondents based on affiliation and nature of job, respectively, along with their relevant ANOVA results. All such results (**Tables 4–7**) have been arranged in order of the ranks in the total sample.

Table 4. Assisting SusD adoption: opinion of different groups based on affiliation.

Parties	Total			Client			Contractor			Consultant			A
	M	R	Sig.	M	R	Sig.	M	R	Sig.	M	R	Sig.	
Architects	2.01	1	0.000	1.83	1	0.000	1.70	2	0.000	2.20	2	0.000	0.16
Consultant	2.09	2	0.000	2.70	3	0.496	1.52	1	0.000	1.96	1	0.000	0.00
Government	2.36	3	0.000	2.46	2	0.170	2.67	5	0.260	2.23	3	0.000	0.46
Client	2.61	4	0.014	2.92	5	0.775	2.47	3	0.154	2.51	4	0.031	0.51
Engineer	2.67	5	0.005	3.07	6	0.712	2.59	4	0.143	2.52	5	0.004	0.13
Financial experts	2.86	6	0.377	2.89	4	0.670	2.92	6	0.820	2.88	6	0.537	0.91
Contractor	3.42	7	0.002	4.00	7	0.000	3.61	7	0.064	3.06	7	0.739	0.01

Table 5. Assisting SusD adoption: opinion of different professional groups.

Parties	Architectural			Engineering			Management			A
	M	R	Sig.	M	R	Sig.	M	R	Sig.	
Architects	2.00	2	0.000	2.11	1	0.000	1.86	1	0.000	0.65
Consultant	1.80	1	0.000	2.18	2	0.000	2.17	2	0.001	0.39
Government	2.32	4	0.065	2.27	3	0.000	2.54	3	0.102	0.74
Client	2.19	3	0.028	2.82	5	0.455	2.63	4	0.161	0.30
Engineer	2.70	5	0.259	2.69	4	0.071	2.64	5	0.079	0.98
Financial experts	2.71	6	0.385	2.97	6	0.899	2.80	6	0.519	0.77
Contractor	3.14	7	0.589	3.35	7	0.107	3.69	7	0.004	0.29

Table 6. Deciding SusD adoption: opinion of different parties based on affiliation.

Parties	Total			Client			Contractor			Consultant			A
	M	R	Sig.	M	R	Sig.	M	R	Sig.	M	R	Sig.	
Client	1.52	1	<0.001	1.76	1	0.000	1.22	1	0.000	1.53	1	0.000	0.089
Developer	2.37	2	<0.001	2.76	3	0.129	2.35	2	0.001	2.21	2	0.000	0.016
General contractor	2.70	3	0.002	1.97	2	0.000	3.09	4	0.648	2.87	3	0.295	<0.001
Investors	3.11	4	0.301	3.45	4	0.030	3.04	3	0.862	2.99	4	0.916	0.174

Table 7. Deciding SusD adoption: opinion of different professional groups.

Parties	Architectural			Engineering			Management			A
	M	R	Sig.	M	R	Sig.	M	R	Sig.	
Client	1.41	1	0.000	1.55	1	0.000	1.57	1	0.000	0.738
Developer	2.15	2	0.000	2.36	2	0.000	2.54	2	0.005	0.201
General contractor	3.19	4	0.284	2.47	3	0.000	2.70	3	0.110	0.011
Investors	2.74	3	0.283	3.17	4	0.255	3.27	4	0.115	0.152

It is seen that six out of seven parties have relatively low scores with mean values of less than 3.0 (i.e., the middle of the measuring scale, or average), implying their higher importance. The highest importance has been placed on architects with the least score of 2.01/5.00, indicating they are the most important party in assisting the owners by supplying the relevant information and knowledge and guiding them to adopt SusD. This is followed by consultant (score 2.09, rank 2), government (score 2.36, rank 3) and client (score 2.61, rank 4). This is simply the reflection of industry practice, as architects and consultants come first/earlier in the project environment to formally interact with and suggest the owners/clients on buildings' design and all other issues, based on clients' affordability and other choices, and in compliance with government regulations or initiatives [63]. They are also considered the 'home' of knowledge and expertise of SusD [64].

Such industry response may be reflecting their good sense of awareness towards SusD, despite the fact that Brunei has been recently experiencing building construction mostly in the private sector, where the roles of architects and consultants are minimal [65]. For the private buildings, they merely furnish the initial architectural and structural design/drawings, and then contractors become the most important party to

do the remaining works. Nevertheless, contractors cannot change the design, and therefore their role in crafting sustainability aspects in the design is minimal. This is seen to have been clearly expressed by the respondents, as the role of the contractor is seen as the lowest among all the parties with a score of 3.42/5.00, which is also the only party with a score of more than 3.0 (i.e., the average for the measuring scale). Significance levels obtained from the t-tests show that the mean values of all parties in the total sample are significantly important, except for financial experts, indicating the respondents' opinion that financial experts cannot help with the required information and knowledge on SusD, despite their 'more than average' importance with a score of 3.42/5.00.

Table 5 also shows that the scores for individual parties within the three groups of respondents based on 'nature of job' are clearly different, with different highest and lowest scores. However, their relative ranks are somewhat similar to those in the total sample. Expectedly, contractor and 'financial experts' occupy the bottom of the list, and 'consultant' and 'architecture' occupy the top of the table in all three groups. The only slight exception is seen in the 'client' group, in terms of the relative importance of 'financial experts' (rank 3) and 'consultant' (rank 5). This might be due to the reason that clients (as investors) may value the business aspect of their investment more than the technical aspects suggested by the consultants [66]. Significance levels obtained from the t-tests show that the scores of most of the parties are insignificant in general. For example, only the scores of 'contractor' and 'architect' are significant in the client group. Similarly, only the scores of 'consultant' and 'architect' are significant in the contractor group. On the other hand, scores for 'contractor' and 'financial experts' are insignificant only in the consultant group. Thus, contrary to that in the total sample, the levels of importance of SusD attributed to different parties by the three groups of respondents (based on affiliation) are broadly insignificant or inconsistent. However, amidst such conflicting agreement on the mean scores, ANOVA results show that the three groups agree on the relative importance of all the parties, except for 'contractor' and 'consultant'. This might be due to the differential degree of importance expressed by the parties. For example, contractors scored consultants with 1.52, compared to 2.93 by clients, a difference of $[(2.93 - 1.52)/4 \approx 35.25\%]$. Similarly, consultants scored contractors with 3.06, compared to 4.00 by clients, a difference of $[(4.00 - 3.06/4) \approx 23.5\%]$.

As seen in **Table 5**, the scores by the three groups according to 'nature of job' are different, but their ranks are similar to those in the total sample. Significance levels obtained from the t-tests show that the scores of only three parties are significant and the other four parties are insignificant in all three groups. It is also seen that only the scores of 'architects' and 'consultants' are significant in all three groups, indicating agreement or consistency. The scores of the other five parties are insignificant, at least in two groups. Despite such conflicting agreement of the mean scores, the ANOVA results indicate agreement of the three groups on the relative importance of all the parties. This may be indicative of some degree of consistency or overall awareness at the industry level, but lack of clear knowledge or awareness on specific roles by different parties within different 'professional' groups, as seen in the case of different groups based on affiliation.

The overall results appear to suggest that the Brunei construction industry participants need to be re-trained in terms of specific roles and contributions of various construction project stakeholders. For example, architects and consultants come first in the project scenario. They are knowledgeable and 'home' of relevant expertise, so it is invaluable to provide suitable information and suggest the owners/clients to adopt SusD [67]. However, contractors execute the job, so they need to interact with architects and consultants during the design stage to ensure issues like constructability and reduce the occurrence of conflicts and misunderstandings [68]. Roles and responsibilities of other parties should also be appreciated, since SusD is expected to be practiced under a supportive policy by the government and the willingness of the owners/clients, for example. Also, the role of government may vary depending on its effectiveness; in particular, since the government (or local government) is also the client in public buildings, there may be different regulations or support than in private projects. In fact, contractors, designers (i.e., consultants, architects, and engineers), and clients are directly involved in the execution of a project [69], and they are also the major participants who have a great deal of power that can influence and shape the progress of any project [70].

4.4. Decision-making

In terms of which party can best help in decision-making to adopt SusD, **Table 6** presents the mean values, ranks, and significances obtained from the one-sample t-tests within the total sample and three respondent groups of client, contractor, and consultant, along with their ANOVA results. It is seen in the total sample that 'client' plays the most important role in deciding if to adopt SusD, followed by 'developer' (rank 2), 'general contractor' (rank 3), and 'investor' (rank 4). The preference of the 'consultant' group is the same with the total sample. However, client group considers 'general contractors' (rank 2) are more important than 'developers' (rank 3), while contractor group considers 'investors' (rank 3) are more important than 'general contractors'.

Nevertheless, the scores of the parties both in the total sample and in different groups are mostly less than the average of the measuring scale (i.e., 3.00), and only a very few are slightly more than the average. This may be indicative of the general importance of all the parties in decision-making towards adopting SusD, both within the total sample and individual groups. It therefore conforms to the industry norm that clients are the most important party for any relevant decision-making on building design during the early project stage, while other parties can help with their supporting roles [71].

Significance levels obtained from the t-tests in the total sample show that the scores of three parties are significant and one party (i.e., investor) is insignificant, implying 'investors' are not relevant to decision-making for SusD adoption. This is contrary to Brunei's recent experience with building construction, which has largely occurred in the private sector, where the role of investors is important [72]. Developers of private sector projects often borrow funds from financial institutions, so the investor may appraise the project and see what is included in the project. In any case, investors have taken the bottom of the table with a score of 3.11/5.00, which is also the only

role with a score of more than 3.0 (i.e., the middle of the measuring scale), with a relevant importance level of 'less than average'. Moreover, the score of 'developer' in the client group is insignificant, while that for 'general contractor' and 'investors' in the contractor and consultant groups is insignificant. Moreover, ANOVA results show that the three groups agree on the relative importance of 'client' and 'investors' and disagree for 'developer' and 'general contractor'.

Such partial consistencies within the total sample (or, in other words, at the industry level) and both within and between different groups may be indicative of partial awareness both at the industry and group levels. The comparisons between different professional groups are also similar (see **Table 7**). The ranks of different parties in different groups are broadly similar to those in the total sample. Results from one-sample t-tests and ANOVA also show partial consistency within the industry and both between and within different groups of respondents. Interestingly, the three groups agree on the consistency of the scores of 'client', and disagree on the scores of investors.

The overall outcome appears to suggest that the practitioners in Brunei need to undertake suitable training or education in order to develop an appropriate level of awareness on SusD in general and decision-making for SusD adoption in particular. This is expected to allow industry participants to consistently assess the importance levels of various parties and their relative ranks, e.g., on deciding SusD adoption and when to include which party in the SusD process [73]. Usually, clients considerably contribute to the project's original decision-making process regarding design [74], more commonly appoint and engage architects and consultants for incorporating SusD, and typically allow contractors to enter the construction phase [73], after significant decisions have been made [74]. However, contractor involvement in the decision-making from the early design stage improves project performance, which is why they are influential stakeholders along with investors and clients [75].

4.5. Discussions and implications

The study revealed relatively less demand for SusD from clients (**Tables 2** and **3**), some disparity on the role of different parties to provide information and guide the potential building owners (**Tables 4** and **5**), as well as to help decision-making towards SusD adoption (**Tables 6** and **7**). All these together may be indicating many potential reasons, like lack of interest [4], cultural inertia [17], lack of training and education [76], lack of suitable fee [77], and lack of information and guidance [17,78]. This may help relevant authorities to look into the issues and design suitable policies to generate a higher level of awareness, information dissemination, create healthy demand for SusD, appropriate training and education, and may result in increased pay/fee for the consultants, as SusD requires more work from the consultants. A common platform may be suitable for such activities.

The findings suggest that construction professionals in Brunei, in particular, would benefit from training on the roles and responsibilities of stakeholders involved in the implementation of SusD. This training would improve communication and collaboration among stakeholders, leading to more successful implementation of SusD in construction projects. Stakeholders also need a clear understanding of the

advantages and potential challenges of SusD to effectively advocate for its adoption. By promoting knowledge sharing and continuous learning, stakeholders can collaborate to develop more environmentally friendly and efficient buildings in Brunei. Incorporating SusD in building projects will help reduce the environmental impact of construction activities, including carbon emissions, waste generation, and resource depletion. This will contribute to a more sustainable future for Brunei. Embracing SusD can also help construction professionals attract environmentally conscious clients, creating new business opportunities and enhancing competitiveness in the industry. Therefore, prioritizing ongoing education and training in SusD is crucial for establishing an environmentally responsible and economically viable construction sector in Brunei.

5. Conclusions

Sustainable design (SusD) is a global strategy for building design that aims to reduce energy consumption and carbon dioxide emissions in buildings. However, it is not gaining momentum in developing countries, particularly in hot and humid regions. One potential reason for this is the inadequate knowledge and awareness of the main stakeholders of building construction projects. As such, the present study attempted to address this issue by investigating the level of awareness of SusD within the local industry and identifying the most suitable parties to guide potential building owners in considering SusD and relevant decision-making to its adoption. It was revealed that the respondents consistently agree on the importance of architect and consultant roles in providing support and guidance on SusD, while the client role is the most important to decision-making for adopting SusD. This is in compliance with the existing industry practice.

However, different groups of respondents appear to lack the clear perception of the degree of importance of other roles, both within and between specific groups. This needs to be addressed through carefully designed actions/programmes by the regulatory bodies, namely the government departments, as they develop relevant rules and regulations. They are also the largest clients in developing countries. So, other parties (like architects and consultants) will comply with cliental requirements if to do business and remain in business in the industry. As such, the outcomes of this study will assist the appropriate authorities in comprehending the actions that must be taken to adopt SusD, such as raising awareness to the appropriate degree, making essential information available, and setting appropriate training/education schemes for each interest group of parties to facilitate its implementation and move towards a more carbon-responsive construction industry. The study outcomes and relevant discussions/suggestions are specific to Brunei construction industry, so those may not be applicable elsewhere. However, the methodology developed can be repeated for similar issues elsewhere, with much-needed country- or region-specific adjustments.

Author contributions: Conceptualization, NAHJ and MMR; methodology, NAHJ; software, NAHJ; validation, NAHJ, MMR and RAA; formal analysis, NAHJ; investigation, NAHJ; resources, NAHJ, MMR and RAA; data curation, NAHJ; writing—original draft preparation, NAHJ; writing—review and editing, MMR and

RAA; visualization, NAHJ and MMR; supervision, MMR and RAA; project administration, NAHJ; funding acquisition, MMR. All authors have read and agreed to the published version of the manuscript.

Conflict of interest: The authors declare no conflict of interest.

References

1. Susorova I. Green facades and living walls: Vertical vegetation as a construction material to reduce building cooling loads. In: Pacheco-Torgal F, Labrincha JA, Cabeza LF, Granqvist CG (editors). Eco-Efficient Materials for Mitigating Building Cooling Needs: Design, Properties and Applications. Woodhead Publishing; 2015. pp. 127-153. doi: 10.1016/b978-1-78242-380-5.00005-4
2. Zhou C, Wang Z, Chen Q, et al. Design optimization and field demonstration of natural ventilation for high-rise residential buildings. Energy and Buildings. 2014; 82: 457-465. doi: 10.1016/j.enbuild.2014.06.036
3. Zuo J, Read B, Pullen S, et al. Achieving carbon neutrality in commercial building developments – Perceptions of the construction industry. Habitat International. 2012; 36(2): 278-286. doi: 10.1016/j.habitatint.2011.10.010
4. Zainul Abidin N, Yusof N, Othman AAE. Enablers and challenges of a sustainable housing industry in Malaysia. Construction Innovation. 2013; 13(1): 10-25. doi: 10.1108/14714171311296039
5. Saridaki M, Haugbølle K. Towards sustainable design: Integrating data from operation of buildings in design practices. IOP Conference Series: Earth and Environmental Science. 2020; 588(5): 052051. doi: 10.1088/1755-1315/588/5/052051
6. Elbeltagi E, Wefki H, Khallaf R. Sustainable Building Optimization Model for Early-Stage Design. Buildings. 2022; 13(1): 74. doi: 10.3390/buildings13010074
7. Ma C, Liu Y, Wang D. Analysis of thermal performance and energy saving strategy of rural residential buildings in Northwest China.Architecture and Technology. 2015; 47: 427-432.
8. Shi F, Wang S, Huang J, et al. Design strategies and energy performance of a net-zero energy house based on natural philosophy. Journal of Asian Architecture and Building Engineering. 2019; 19(1): 1-15. doi: 10.1080/13467581.2019.1696206
9. Dahlstrøm O, Sørnes K, Eriksen ST, et al. Life cycle assessment of a single-family residence built to either conventional- or passive house standard. Energy and Buildings. 2012; 54: 470-479. doi: 10.1016/j.enbuild.2012.07.029
10. Zhang N, Bi Y. The development and application of passive architecture in China. E3S Web of Conferences. 2020; 165: 04019. doi: 10.1051/e3sconf/202016504019
11. Rana K. Towards Passive Design Strategies for Improving Thermal Comfort Performance in a Naturally Ventilated Residence. Journal of Sustainable Architecture and Civil Engineering. 2021; 29(2): 150-174. doi: 10.5755/j01.sace.29.2.29256
12. Moret Rodrigues A, Santos M, Gomes MG, et al. Impact of Natural Ventilation on the Thermal and Energy Performance of Buildings in a Mediterranean Climate. Buildings. 2019; 9(5): 123. doi: 10.3390/buildings9050123
13. Sharma L, Kishan Lal K, Rakshit D. Evaluation of impact of passive design measures with energy saving potential through estimation of shading control for visual comfort. Journal of Building Physics. 2017; 42(3): 220-238. doi: 10.1177/1744259117742989
14. Amos-Abanyie S, Akuffo FO, Kutin-Sanwu V. Effects of Thermal Mass, Window Size, and Night-Time Ventilation on Peak Indoor Air Temperature in the Warm-Humid Climate of Ghana. The Scientific World Journal. 2013; 2013: 1-9. doi: 10.1155/2013/621095
15. Berardi U. Stakeholders' influence on the adoption of energy-saving technologies in Italian homes. Energy Policy. 2013; 60: 520-530. doi: 10.1016/j.enpol.2013.04.074
16. Shen W, Tang W, Siripanan A, et al. Critical Success Factors in Thailand′s Green Building Industry. Journal of Asian Architecture and Building Engineering. 2017; 16(2): 317-324. doi: 10.3130/jaabe.16.317
17. Mohamad Bohari AA, Skitmore M, Xia B, et al. Insights into the adoption of green construction in Malaysia: The drivers and challenges. Environment-Behaviour Proceedings Journal. 2016; 1(4): 37. doi: 10.21834/e-bpj.v1i4.165
18. Loosemore M, Lim BTH. Linking corporate social responsibility and organizational performance in the construction industry. Construction Management and Economics. 2016; 35(3): 90-105. doi: 10.1080/01446193.2016.1242762

19. Rais SLA, Bidin ZA, Bohari AAM, et al. The Possible Challenges of Green Procurement Implementation. IOP Conference Series: Materials Science and Engineering. 2018; 429: 012023. doi: 10.1088/1757-899x/429/1/012023
20. Juffle NAH, Rahman MM. An overview of motivators and challenges of passive design strategies. IOP Conference Series: Earth and Environmental Science. 2023; 1195(1): 012039. doi: 10.1088/1755-1315/1195/1/012039
21. Juffle NAH, Rahman MM, Asli RA. Adopting Passive Design Strategies: A Brief Review. In: Proceedings of the 8th Brunei International Conference on Engineering and Technology 2021; 8–10 November 2021; Bandar Seri Begawan, Brunei Darussalam.
22. Juffle NA, Rahman MM. Sustainable Building Design Strategies: A Review Summary. UniMAP; 2022.
23. Ayarkwa J, Joe Opoku DG, Antwi-Afari P, et al. Sustainable building processes' challenges and strategies: The relative important index approach. Cleaner Engineering and Technology. 2022; 7: 100455. doi: 10.1016/j.clet.2022.100455
24. Häkkinen T, Belloni K. Barriers and drivers for sustainable building. Building Research & Information. 2011; 39(3): 239-255. doi: 10.1080/09613218.2011.561948
25. Toriola-Coker LO, Alaka H, Bello WA, et al. Sustainability Barriers in Nigeria Construction Practice. IOP Conference Series: Materials Science and Engineering. 2021; 1036(1): 012023. doi: 10.1088/1757-899x/1036/1/012023
26. Jin X, Zhang G, Liu J, et al. Major Participants in the Construction Industry and Their Approaches to Risks: A Theoretical Framework. Procedia Engineering. 2017; 182: 314-320. doi: 10.1016/j.proeng.2017.03.100
27. Saleh RM, Al-Swidi A. The adoption of green building practices in construction projects in Qatar: a preliminary study. Management of Environmental Quality: An International Journal. 2019; 30(6): 1238-1255. doi: 10.1108/meq-12-2018-0208
28. Aapaoja A, Haapasalo H. A Framework for Stakeholder Identification and Classification in Construction Projects. Open Journal of Business and Management. 2014; 02(01): 43-55. doi: 10.4236/ojbm.2014.21007
29. Ahmed N, Hussain A, Ahmed S. Sustainable Structural Design. IJREAS. 2012; 2(10).
30. Kubba S. Components of Sustainable Design and Construction in Handbook of Green Building Design and Construction. Elsevier; 2017.
31. Albino V, Berardi U. Green Buildings and Organizational Changes in Italian Case Studies. Business Strategy and the Environment. 2012; 21(6): 387-400. doi: 10.1002/bse.1728
32. Svenfelt Å, Engström R, Svane Ö. Decreasing energy use in buildings by 50% by 2050 — A backcasting study using stakeholder groups. Technological Forecasting and Social Change. 2011; 78(5): 785-796. doi: 10.1016/j.techfore.2010.09.005
33. Marichova A. Role of the Government for Development of Sustainable Construction. Ovidius University Annals of Constanta-Series Civil Engineering. 2020; 22(1): 53-62. doi: 10.2478/ouacsce-2020-0006
34. Lenard D, Abbott C. The Role of Government in Supporting the Construction Industry in the United Kingdom. Available online: https://www.researchgate.net/publication/265537156_THE_ROLE_OF_GOVERNMENT_IN_SUPPORTING_THE_CONSTRUCTION_INDUSTRY_IN_THE_UNITED_KINGDOM (accessed on 2 January 2024).
35. Farivar S, Agharabi A. Impact of Atrium and Glazed balcony on residential building energy consumption in cold semi-arid climate: case study in Mashhad, Iran. Journal of Solar Energy Research. 2021; 6(2): 726-739.
36. Akinshipe O, Oluleye IB, Aigbavboa C. Adopting sustainable construction in Nigeria: Major constraints. IOP Conference Series: Materials Science and Engineering. 2019; 640(1): 012020. doi: 10.1088/1757-899x/640/1/012020
37. Mok KY, Shen GQ, Yang R. Stakeholder complexity in large scale green building projects. Engineering, Construction and Architectural Management. 2018; 25(11): 1454-1474. doi: 10.1108/ecam-09-2016-0205
38. Hwang BG, Lim ESJ. Critical Success Factors for Key Project Players and Objectives: Case Study of Singapore. Journal of Construction Engineering and Management. 2013; 139(2): 204-215. doi: 10.1061/(ASCE)CO.1943-7862.0000597
39. Delgado-Hernandez DJ, Aspinwall E. A framework for building quality into construction projects – Part II. Total Quality Management & Business Excellence. 2010; 21(7): 725-736. doi: 10.1080/14783363.2010.483089
40. Menassa CC, Baer B. A framework to assess the role of stakeholders in sustainable building retrofit decisions. Sustainable Cities and Society. 2014; 10: 207-221. doi: 10.1016/j.scs.2013.09.002
41. Tran Q. Challenges in managing green building projects from the view of the contractors: An exploratory study in Vietnam. IOP Conference Series: Materials Science and Engineering. 2020; 869(6): 062030. doi: 10.1088/1757-899x/869/6/062030
42. Wen S, Qiang G. Managing Stakeholder Concerns in Green Building Projects with a View Towards Achieving Social Sustainability: A Bayesian-Network Model. Frontiers in Environmental Science. 2022; 10. doi: 10.3389/fenvs.2022.874367

43. Oyewole MO, Komolafe MO, Gbadegesin JT. Understanding stakeholders' opinion and willingness on the adoption of sustainable residential property features in a developing property market. International Journal of Construction Management. 2021; 23(2): 358-370. doi: 10.1080/15623599.2021.1874676
44. Alqadami AT, Zakaria R, Abdullah R, et al. Challenges of Stakeholders' Expectations to Develop Residential High-Rise Green Buildings in Malaysia. Advanced Science Letters. 2018; 24(6): 4496-4501. doi: 10.1166/asl.2018.11633
45. Badawy UI, Alastal AI, Jawabrah MQ, et al. Adoption of, the Palestine Green Building Design Approach, with the Help of Checklist Tools. Journal of Environmental Protection. 2021; 12(01): 49-74. doi: 10.4236/jep.2021.121005
46. Chigozie Osuizugbo I, Oyeyipo O, Lahanmi A, et al. Barriers to the Adoption of Sustainable Construction. European Journal of Sustainable Development. 2020; 9(2): 150. doi: 10.14207/ejsd.2020.v9n2p150
47. Feng W, Zhang Q, Ji H, et al. A review of net zero energy buildings in hot and humid climates: Experience learned from 34 case study buildings. Renewable and Sustainable Energy Reviews. 2019; 114: 109303. doi: 10.1016/j.rser.2019.109303
48. Saunders M, Lewis P, Thornhill A. Research Mehtods for Business Students, 5th ed. Pearson Education Limited; 2009.
49. Dosumu O, Iyagba R. An Analysis of the Factors Responsible for Errors in Nigerian Construction Documents. Ethiopian Journal of Environmental Studies and Management. 2013; 6(1). doi: 10.4314/ejesm.v6i1.6
50. Julayhe N, Rahman MM. Dwellers' perception on challenges and motivators of greening existing buildings in Brunei Darussalam. Built Environment Project and Asset Management. 2021; 11(5): 870-887. doi: 10.1108/bepam-08-2020-0147
51. Tavakol M, Dennick R. Making sense of Cronbach's alpha. International Journal of Medical Education. 2011; 2: 53-55. doi: 10.5116/ijme.4dfb.8dfd
52. Taber KS. The Use of Cronbach's Alpha When Developing and Reporting Research Instruments in Science Education. Research in Science Education. 2017; 48(6): 1273-1296. doi: 10.1007/s11165-016-9602-2
53. Kim HY. Statistical notes for clinical researchers: assessing normal distribution (2) using skewness and kurtosis. Restorative Dentistry & Endodontics. 2013; 38(1): 52. doi: 10.5395/rde.2013.38.1.52
54. Wulandari D, Sutrisno S, Nirwana MB. Mardia's Skewness and Kurtosis for Assessing Normality Assumption in Multivariate Regression. Enthusiastic: International Journal of Applied Statistics and Data Science. Published online April 21, 2021: 1-6. doi: 10.20885/enthusiastic.vol1.iss1.art1
55. Memon MA, Ting H, Cheah JH, et al. Sample Size for Survey Research: Review and Recommendations. Journal of Applied Structural Equation Modeling. 2020; 4(2). doi: 10.47263/JASEM.4(2)01
56. George D, Mallery P. IBM SPSS Statistics 26 Step by Step, 7th ed. Routledge; 2019.
57. Sarstedt M, Ringle CM, Hair JF. Partial Least Squares Structural Equation Modeling. In: Handbook of Market Research. Springer International Publishing; 2022.
58. Tebeje Zewdu Z. Causes of Contractor Cost Overrun in Construction Projects: The Case of Ethiopian Construction Sector. International Journal of Business and Economics Research. 2015; 4(4): 180. doi: 10.11648/j.ijber.20150404.11
59. Sekaran U, Bougie R. Research Methods for Business: A Skill-Building Approach, 7th ed. John Wiley & Sons Ltd; 2016.
60. Sorgato MJ, Melo AP, Lamberts R. The effect of window opening ventilation control on residential building energy consumption. Energy and Buildings. 2016; 133: 1-13. doi: 10.1016/j.enbuild.2016.09.059
61. Mahar WA, Verbeeck G, Reiter S, et al. Sensitivity Analysis of Passive Design Strategies for Residential Buildings in Cold Semi-Arid Climates. Sustainability. 2020; 12(3): 1091. doi: 10.3390/su12031091
62. Omrani S, Garcia-Hansen V, Capra BR, et al. On the effect of provision of balconies on natural ventilation and thermal comfort in high-rise residential buildings. Building and Environment. 2017; 123: 504-516. doi: 10.1016/j.buildenv.2017.07.016
63. Siva J, London K. Architects and their Clients: Relationship Analysis using Habitus Theory. The International Journal of Interdisciplinary Social Sciences: Annual Review. 2009; 4(3): 131-146. doi: 10.18848/1833-1882/cgp/v04i03/52874
64. Dansoh A, Frimpong S. Client perspectives on relationships with architects on private house projects. International Journal of Qualitative Research in Services. 2016; 2(3): 155. doi: 10.1504/ijqrs.2016.082643
65. Hj Abu Bakar R. Government construction projects expected to slow down', The Scoop, 20 March. Available online: https://thescoop.co/2023/03/20/government-construction-projects-expected-to-slow-down/ (accessed on 21 December 2023).
66. Bizon-Górecka J, Górecki J. Influence of Selected Stakeholders of Construction Investment Projects on the Course of Project. IOP Conference Series: Materials Science and Engineering. 2017; 245: 072018. doi: 10.1088/1757-899x/245/7/072018

67. Lee ZP, Rahman RA, Doh SI. Success Factors of Design-Build Public Sector Projects in Malaysia. IOP Conference Series: Materials Science and Engineering. 2020; 712(1): 012045. doi: 10.1088/1757-899x/712/1/012045
68. Masengesho E, Wei J, Niyirora R, et al. Relationship between Project Consultants' Performance and Project Success in the Rwandan Construction Industry. World Journal of Engineering and Technology. 2021; 9(1): 138-154. doi: 10.4236/wjet.2021.91011
69. Octaviani DS, Susanto D, Suganda E. The performance of the building envelope in high-rise residential related to occupant's comfort. IOP Conference Series: Earth and Environmental Science. 2020; 452(1): 012028. doi: 10.1088/1755-1315/452/1/012028
70. Hussin JM, Abdul Rahman I, Memon AH. The Way Forward in Sustainable Construction: Issues and Challenges. International Journal of Advances in Applied Sciences. 2013; 2(1). doi: 10.11591/ijaas.v2i1.1321
71. Ramabodu MS, Verster JJP. Factors that influence cost overruns in South African public sector mega-projects. International Journal of Project Organisation and Management. 2013; 5(1/2): 48. doi: 10.1504/ijpom.2013.053153
72. Bolomope M, Amidu AR, Ajayi S, et al. Decision-Making Framework for Construction Clients in Selecting Appropriate Procurement Route. Buildings. 2022; 12(12): 2192. doi: 10.3390/buildings12122192
73. Maudet N, Leiva G, Beaudouin-Lafon M, et al. Design Breakdowns. In: Proceedings of the 2017 ACM Conference on Computer Supported Cooperative Work and Social Computing; 25 February-1 March 2017; Portland, Oregon, USA. pp. 630-641. doi: 10.1145/2998181.2998190
74. Saferi MM, Mohamad Bohari AA, Bidin ZA, et al. Green Procurement for Construction Project: The Roles of Stakeholder Values. IOP Conference Series: Materials Science and Engineering. 2018; 429: 012024. doi: 10.1088/1757-899x/429/1/012024
75. Glass J, Haroglu H, Thorpe T, et al. Contractors' influence within the design process of design-build projects. In: Ghafoori N (editor). Challenges, Opportunities and Solutions in Structural Engineering and Construction, 1st ed. CRC Press; 2009. doi: 10.1201/9780203859926.ch113
76. Zainul Abidin N. Investigating the awareness and application of sustainable construction concept by Malaysian developers. Habitat International. 2010; 34(4): 421-426. doi: 10.1016/j.habitatint.2009.11.011
77. Nasereddin M, Price A. Addressing the capital cost barrier to sustainable construction. Developments in the Built Environment. 2021; 7: 100049. doi: 10.1016/j.dibe.2021.100049
78. Ipsen KL, Pizzol M, Birkved M, et al. How Lack of Knowledge and Tools Hinders the Eco-Design of Buildings—A Systematic Review. Urban Science. 2021; 5(1): 20. doi: 10.3390/urbansci5010020

Building Engineering 2024, 2(1), 1132.
https://doi.org/10.59400/be.v2i1.1132

Article

Digital transformation of quality management in the construction industry during the execution phase by integration of building information modeling (BIM) and cloud computing

Mohamed Shaban[1,*], Bassel Al-Hassan[2], Alaa Shekh Mohamad[1]

[1] Department of Engineering and Construction Management, Faculty of Civil Engineering, Al-Baath University, Homs 96331, Syria
[2] Department of Engineering and Construction Management, Faculty of Civil Engineering, University of Hama, Hama 96333, Syria
*** Corresponding author:** Mohamed Shaban, mshaaban@albaath-univ.edu.sy, shabanm85@gmail.com

CITATION

Shaban M, Al-Hassan B, Mohamad AS. Digital transformation of quality management in the construction industry during the execution phase by integration of building information modeling (BIM) and cloud computing. Building Engineering. 2024; 2(1): 1132. https://doi.org/10.59400/be.v2i1.1132

ARTICLE INFO

Received: 28 February 2024
Accepted: 25 March 2024
Available online: 17 April 2024

Abstract: The quality of construction projects significantly impacts social and economic development. However, low quality and project failure often result from factors such as lack of quality procedures, poor communication, task coordination, and inefficient progress monitoring. This research aims to improve the efficiency of the construction phase by creating quality control checklists for processes and enhancing quality management through a collaborative digital environment integrating building information modeling (BIM) and cloud computing. Expert constructive interviews were first conducted to define a construction process quality control procedure to be linked to the 3DBIM model and then transition to a collaborative cloud environment (Autodesk Construction Cloud). An actual instance in Latakia City (Syria) demonstrated that the proposed methodology improves the efficiency and effectiveness of quality management during the implementation phase. It does so by offering a robust database, enhancing on-site quality information extraction from BIM models using smartphones, documenting defects and entering inspection data directly into a shared digital environment, and making it easier to track corrective actions and feedback. This facilitates constant and organized access to current data, reducing errors and rework, saving money and time, and enhancing decision-making speed and effectiveness. The search recommends the necessity of strict laws to adhere to quality procedures and the importance of providing infrastructure for digital transformation in quality management.

Keywords: construction projects; quality management; digital quality management; quality control; building information modeling (BIM); cloud computing

1. Introduction

Construction project success is largely dependent on quality management since timely and cost-effective project execution depends on an effective and efficient management procedure. All phases of the project lifecycle should incorporate quality management [1]. However, the execution process is thought to be the most complex because it accounts for the majority of project costs (70%–80%), making quality control and management during this phase one of the most difficult tasks [2]. Accurate and consistent information gathering, processing, and stakeholder engagement are necessary for high-quality project management.

Engineering facilities in Syria suffer from quality deficiencies, often failing to achieve the desired results and incurring high rework costs. The main reasons for this include the absence of quality procedures during the execution phase, lack of cooperation and communication between project participants, poor task coordination between team members, inefficient progress monitoring, limited ability to track

changes, lack of strict supervision, and the inability to document problems and track their resolution. This is attributed to the limited sharing of information through traditional paper-based methods in conventional construction quality management approaches. The current practice of quality management in the construction industry involves issuing quality inspection checklists, conducting site inspections and testing, documenting non-conformity reports, and implementing corrective actions. However, there is no systematic method for recording the data that has been inspected, making it impossible to determine the quality status of the construction [3]. The revolution in computer systems and information technology has had a significant impact on the global community, as the construction sector or industry is now linked to information technology to increase construction efficiency. The construction industry has undergone a tremendous transformation thanks to building information modeling (BIM) technology, which covers all project phases and improves efficiency [4]. As BIM aims to change the way facilities and infrastructure are viewed and managed, it is seen as a gateway to technical innovation and helps to deliver projects successfully at a lower cost and higher quality [5]. According to Saad et al. [6], its benefits include increasing efficiency, facilitating competitive advantage, enhancing sustainability, streamlining complicated operations, and improving performance.

The rapid adoption of building information modeling (BIM) in the fields of architecture, engineering, and construction (AEC) has brought new and emerging challenges for collaborative practices related to the significant amount of BIM data that must be managed and controlled [7]. Because remote collaboration is not allowed and real-time construction information cannot be reported, participants must meet in person around a computer to discuss a particular building program using BIM files [8].

Cloud-based building information modelling, or cloud BIM, is a growing area of investigation for the architecture, engineering, and construction (AEC) sector [9]. The problem of storing too much BIM data can be solved by increasing the capacity of cloud storage. Because cloud storage services make cloud-based BIM easily accessible to users in many locations, organizations can quickly expand the system without having to purchase expensive servers. This allows project team members to collaborate and coordinate more effectively in real time [8].

On building sites, mobile devices like iPads, tablets, and smartphones are now often used because cloud-based BIM systems like BIMXtra, A360, and others improve communication between office personnel and site workers. Through wireless networks, site teams may now view and address issues immediately from their mobile or cloud devices [10]. This has a direct and positive impact on the quality management of the site.

2. Research objective

Enhancing the efficiency of the construction phase in construction projects by:

1) Conducting constructive interviews with experts to develop checklists for quality control of construction processes.
2) Developing a methodology to enhance quality management by providing a collaborative and shared digital environment through integrating BIM and cloud

computing.

3. Literature review

Hartmann and Fischer [11] described how the project team of the Fulton Street Transit Center project in New York City utilized 3D/4D models for knowledge communication and generation during the constructability review process. The management team effectively communicated generated knowledge to non-engineers, suggesting an integrated process for efficient 3D/4D model usage in construction projects.

According to Sears et al. [12], an essential procedure in construction project management is a constructability review, which assesses design and construction plans to find possible problems or difficulties. Within the limitations of time and money, it seeks to guarantee that the design is workable, efficient, and practical. In order to reduce risks and improve the quality and efficiency of projects, stakeholders such as contractors, engineers, and architects work together to evaluate design documents.

According to Love et al. [13], BIM can boost full life-cycle asset management, lower construction costs, lessen the likelihood of modified orders, integrate project systems, data, and teams, and improve the quality of design information and interoperability.

Wang et al. [14] discussed an integrated system of BIM and Light Detection and Ranging (LiDAR) to obtain real-time quality information on-site and process it for construction quality monitoring. The results show that the system is capable of efficiently identifying potential construction defects and supporting real-time quality control.

Lin et al. [15] introduced a BIM-based defect management (BIMDM) system for on-site quality managers in Taiwan during construction. The system integrates web and BIM technologies, enabling real-time visualization and analysis of defect information. The study shows its effectiveness in improving defect management efficiency and facilitating easy quality inspection in a 3D BIM environment.

Ma et al. [16] proposed a system that integrates BIM and indoor positioning technology, allowing inspectors to easily link the actual targeted element they are inspecting on the construction site with the corresponding BIM element by simply clicking on it to input inspection data on a mobile device. The inspection data is then uploaded to the server, and checklist forms are printed and signed.

Cheng [17] developed a preliminary model for a quality control system in the construction phase using the Autodesk Revit API, which can record quality defects on-site immediately and display the three-dimensional elements, including the defects. This quality control model can be uploaded to the cloud and provide real-time information. Users can also print quality control reports using this system.

Alhassan et al. [18] proposed a methodology for knowledge acquisition during public building maintenance using BIM and DYNAMO applications. Parametric models store information centrally, while visual programming enables processing, extraction, classification, and data export from the BIM model to enhance knowledge management.

In another study [4], a comprehensive approach to quality management through

the integration of BIM and augmented reality (AR) technologies was proposed. The results emphasize that objectives such as reducing delays, improving quality, and lowering costs can be achieved through the proposed quality management system, as the web-based checklist facilitates access to updated information by enhancing communication among stakeholders.

In a study by AA and Varghese [3], a 4D model was developed for project quality management using Revit software to link foundation elements with their quality parameters. The researcher concluded several benefits of using BIM in quality management: better visualization of construction activities, improved communication among project stakeholders, a robust database, better understanding of quality requirements, continuous flow of information, time savings, and cost savings.

Using a point cloud and as-designed BIM features, Bassier et al. [19] introduced an innovative way to quickly assess built objects on building sites. Periodic remote sensing opens up new opportunities for comprehensive evaluations. This technique computes positioning errors, detects building flaws early on, and reduces failure costs dramatically. The program offers a user-friendly positioning accuracy meter and is integrated into native BIM software.

The research of Dahbi et al. [20] aims to integrate AR, BIM, and cloud computing technologies into a mobile application called "CollaBIM" to improve construction sector practices. This open-source solution aids in digital transition, providing visualization of models on 2D plans and 3D virtual models, enabling better building analysis throughout their life cycle. Collaboration is central to the research.

Qinghe et al. [21] developed a BIM management platform that improves visualization, data integration, safety, quality, collaboration, and emergency response in bridge projects by utilizing cloud computing, the internet of things, and BIM technologies. The way these technologies work together for intelligent project management is demonstrated by this integration.

Irene [22] examined how a collaborative Cloud-BIM tool was used on the North Vancouver LGH ACF project, emphasizing how it improved interdisciplinary cooperation, design visualization, and project comprehension. Change management, file upload problems, and inadequate training are among the challenges that have been discovered.

In the research of Omran and Shaban [23], an integrated system for managing change orders electronically was developed that aligns with the expectations and ambitions of the construction industry through the integration of building information modeling (BIM) technology and cloud computing technology.

4. Methodology

1) Creating quality checklists: In this study, quality control checklists for construction execution processes were developed by conducting constructive interviews with 23 experienced engineers working in the construction industry in Syria for at least 20 years, in addition to relying on observation by reviewing work procedures.
2) Creating a quality-loaded BIM model: A 3D model of the case study building was created using the Revit software, as shown in **Figure 1**, and then quality

control procedures obtained from field surveys were added and linked to the corresponding elements in the model.

Figure 1. The BIM model (The Youth Housing Project).

3) Transition to a collaborative cloud-based environment: The transition was made to the Autodesk Construction Cloud (ACC) platform, a cloud-based platform designed by Autodesk for effective integrated management of construction projects. This platform includes a suite of BIM-based tools and project management capabilities designed to centralize all building information and related processes, improving communication, collaboration, and coordination between stakeholders through a single online platform.
4) Verification through a case study: The Youth Housing Project in the city of Latakia (Syria) was chosen as a case study. It is a residential building consisting of a ground floor and nine repetitive floors with an area of 350 square meters, where each floor contains four identical apartments. On-site, the PlanGrid application, which is part of the ACC platform, was used. Users can upload, organize, and share project documents through this application. The teams can view high-resolution drawings and 3D models (BIM) on smartphones and tablets smoothly. Team members can collaborate on drawings and provide comments and feedback directly within the application. Changes to drawings and documents can be tracked, and version history is maintained to ensure the use of the correct versions.

   It allows for documenting quality issues, safety concerns, and other problems at the worksite with the ability to attach photos and notes. In addition, the notification feature ensures real-time communication between the field team and the office team, significantly reducing the need for team feedback on unexpected problems. **Figure 2** shows the research approach chart.

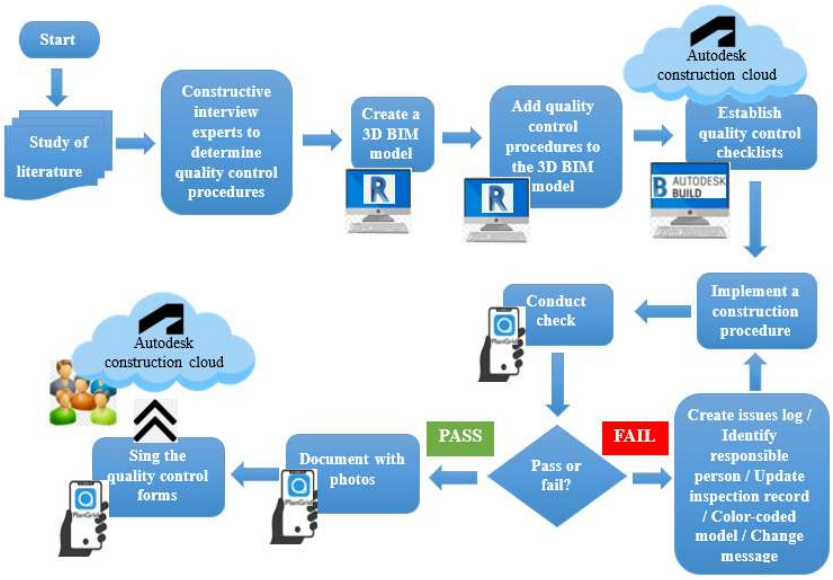

Figure 2. Research approach chart.

5. Results and discussion

1) After conducting constructive field interviews with experts, quality control checklists for executing earthworks and construction operations for structural elements (formwork, reinforcement, and pouring) were developed. As indicated in Appendix.
2) Through the digitization of quality management by integration of (BIM) and cloud computing, researchers have been able to address the most common issues in traditional quality management approaches by:

5.1. Collaboration and communication

The digitization of quality management helps to share information transparently and centrally between project members. As project participants are added to the platform, companies can invite their employees to join and define permissions for each member. This allows them to determine what they can see and do on the platform based on their responsibilities and project needs, as shown in **Figure 3**. This approach helps to organize and coordinate work more effectively, ensuring that participants are committed to the tasks assigned to them and that appropriate access to data and information is granted to each individual.

Figure 3. Add members to the platform with their company identification, their job roles and their permissions.

To facilitate access and organization of project information, the platform centrally stores crucial documents and files. These include blueprints, digital models, schedules, photos, and other project-related files. The stored data encompasses change orders, backups, and various document versions. This centralized repository allows for efficient comparison of different document versions, tracking change dates, and identifying responsible parties. As a result, companies can respond promptly and effectively to changes, ensuring the quality execution of their processes. **Figure 4** illustrates the centralized file storage within the platform.

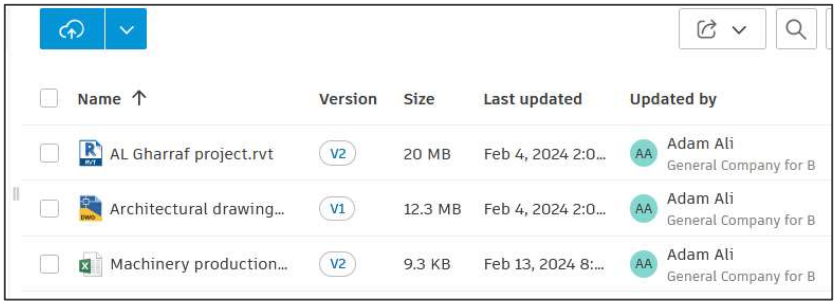

Figure 4. Centralized file storage.

5.2. Providing a repository for quality data

The proposed methodology establishes a highly centralized repository for quality data. This data is seamlessly integrated into the building information modeling (BIM) model using REVIT software. By incorporating a set of special parameters, REVIT allows for the inclusion of quality-related information. Specifically, each 3D element within the model is linked to these parameters, ensuring that alongside the geometric details, process-specific quality data is associated with each element. Refer to **Figure 5** for a visual representation of this integration.

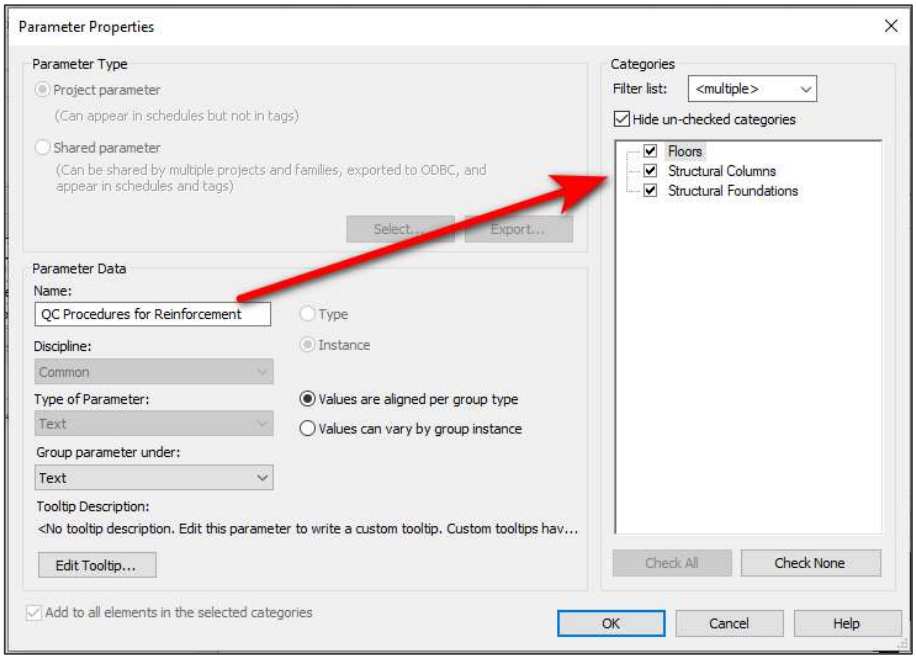

Figure 5. Adding parameters for reinforcing work quality control procedures.

5.3. On-site acquisition of quality data

In the proposed methodology, the BIM model loaded with quality data is viewed on site using a tablet or mobile phone to obtain all the necessary information about the elements on site, as shown in **Figure 6**. **Figure 7** illustrates a virtual tour inside the building to facilitate the process of obtaining information about the internal elements. The site official can find the required elements in the BIM model using a smartphone or tablet by performing a filtering process for the elements through selecting the level, category, and disciplines of the element as shown in **Figure 8**. The site official can also perform measurements directly on the model, as shown in **Figure 9**.

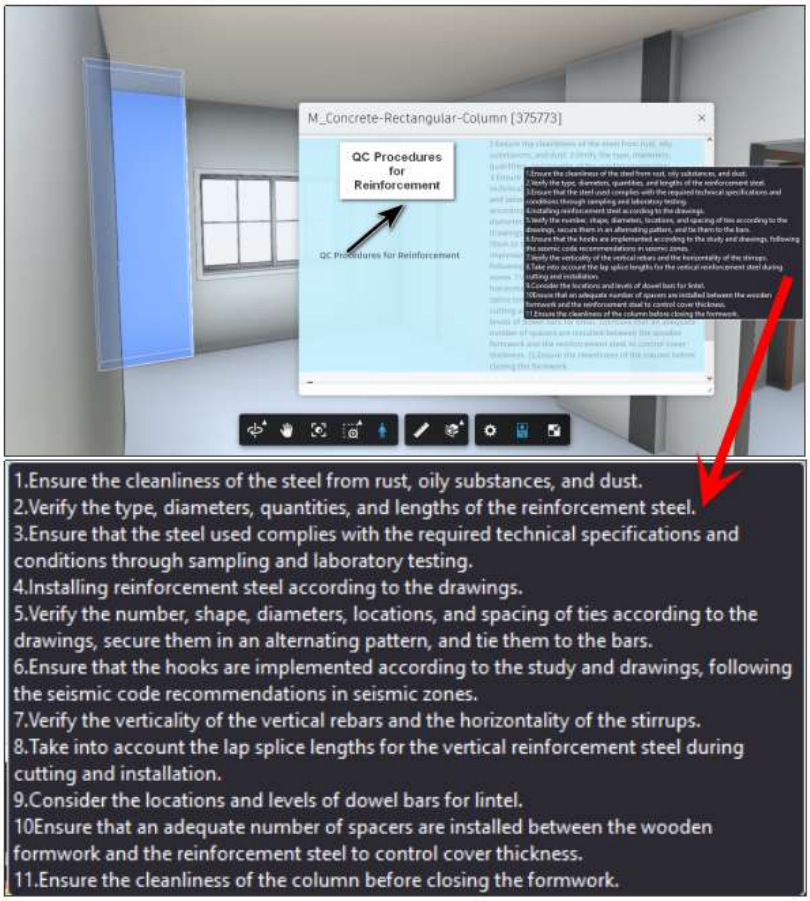

Figure 6. Quality control procedures for column reinforcement.

Figure 7. Virtual tour inside the building (The Youth Housing Project).

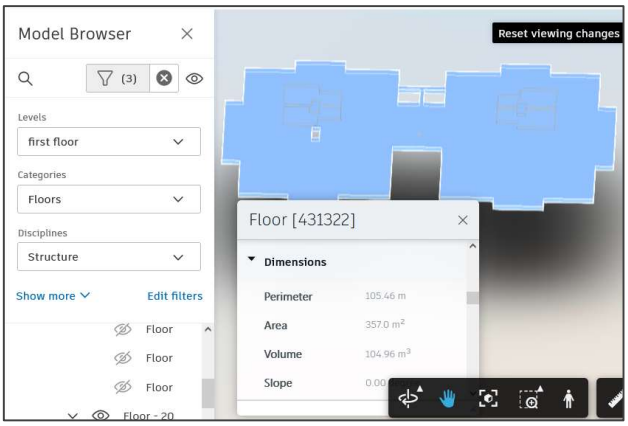

Figure 8. Filter elements.

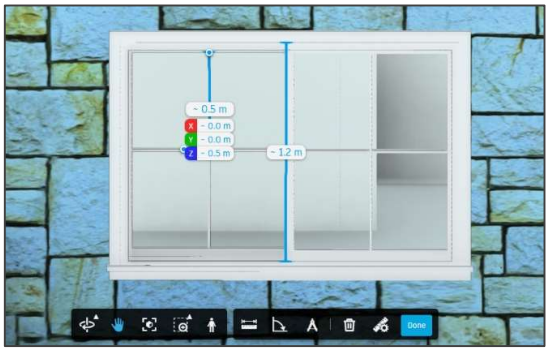

Figure 9. Taking measurements.

5.4. Track implementation and document quality issues

Digitizing quality management facilitates real-time monitoring of project progress by providing up-to-date data. This tracking and monitoring process offers a comprehensive view of process and quality performance through the analysis of data and key performance indicators. Companies can pinpoint areas that require improvement and development. Regular tracking enables effective data collection and analysis, allowing for the early identification of potential quality issues. Strategic decision-making can then address these challenges.

To streamline data collection, customized forms have been designed. These templates encompass various fields, including text, geographic location, weather conditions, electronic signatures, images, and dates. On-site personnel complete these forms using smart devices. The collected data serves as the foundation for customized reports, such as daily reports, progress updates, quality assessments, safety reports, and inspections (as depicted in **Figure 10**).

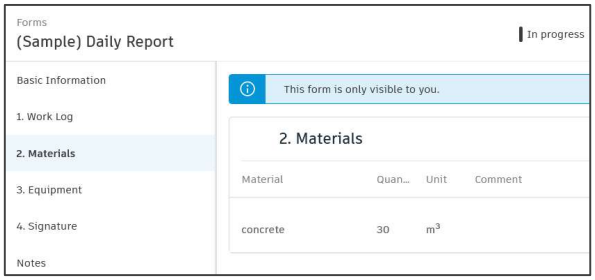

Figure 10. Daily report.

Digitizing quality management also facilitates the inspection process on-site through electronic checklists that are created as shown in **Figure 11**. The inspector fills out the checklists during the inspection process using a mobile phone and documents compliance cases with photos. In case of a violation, it is described and its location is identified on the 3D BIM model, and the responsible person is automatically notified through the platform and email with a message indicating the need for correction or rework. After completing the inspection process, the report is signed by the inspector and shared via the platform with relevant parties.

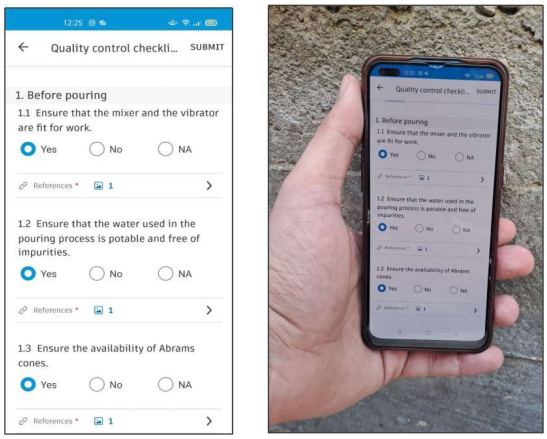

Figure 11. On-site form of quality control.

Quality issues that have arisen during the construction process have been visually documented in the BIM model, as have safety issues and the necessary accident prevention measures as shown in **Figure 12**. Cases of defects in materials or equipment used in the project are recorded with the responsible parties, and attachments of images, documents, notes, and rework messages are included as shown in **Figure 13**. The colored markings on the three-dimensional elements indicate a defect in the element, making it easier for responsible parties to note the location of defects and problems, helping to improve communication, simplify problem management, improve project quality, and manage it effectively.

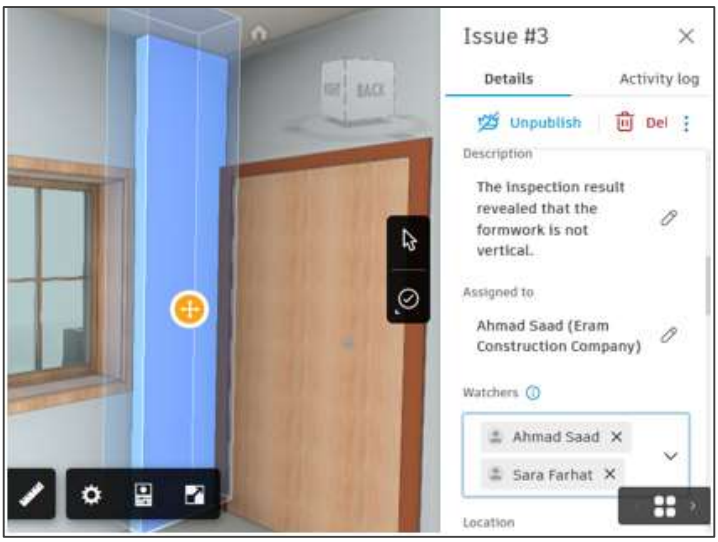

Figure 12. Documentation of a column issue in BIM model.

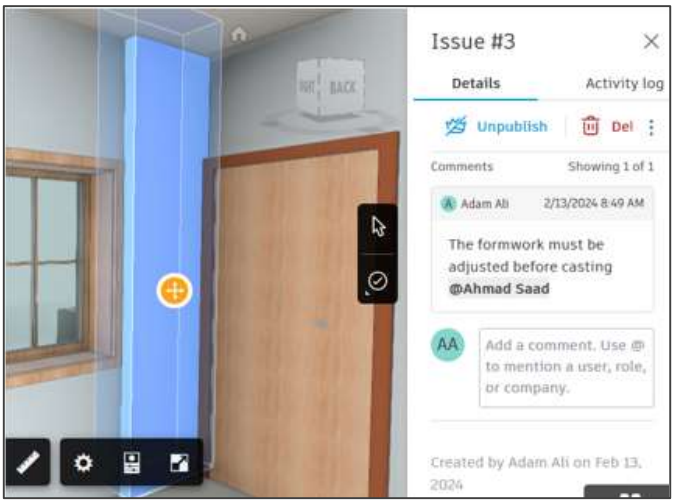

Figure 13. Fixing and reworking message from supervisor.

5.5. Corrective action tracking

Corrective action tracking plays a pivotal role in quality management. It serves several critical purposes. During the construction process, errors and issues inevitably arise. Corrective actions help identify these anomalies promptly. By addressing them, companies ensure the quality of operations, meet customer expectations, and safeguard their reputation.

Our proposed methodology establishes a detailed historical record of observed issues and non-compliances. Each issue is meticulously documented, including references to the responsible individuals. To streamline corrective actions, we employ a color-coded system within the 3D BIM model as shown in **Figure 14**. Each color corresponds to a specific stage of the corrective action process:

- Draft: Initial identification (Black).
- Open: Acknowledged and under review (Orange).
- Pending: Awaiting resolution (Blue).
- In review: Assessment by relevant parties (Purple).
- Closed: Successfully resolved (Grey).

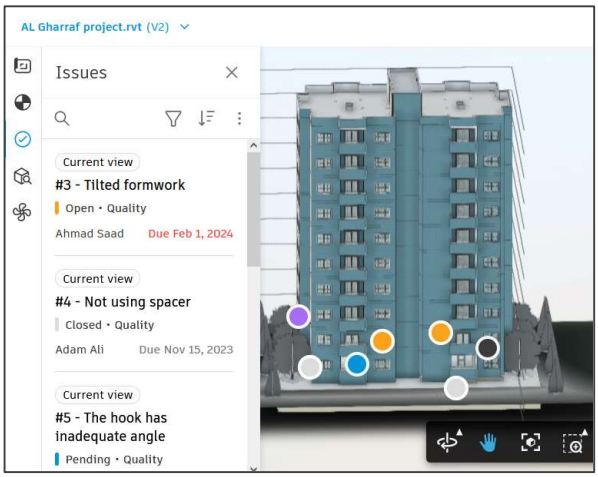

Figure 14. Visualization of the color-coded model, combined with historical record of the issues.

5.6. Feedback tracking

The proposed methodology serves as a comprehensive communication system for reporting, feedback tracking, review, and dissemination of lessons learned. It ensures a clear and consistent flow of information by providing feedback on documents, designs, and reports. Comments, notes, and direct changes are seamlessly incorporated into the documentation process.

Key components of this approach include feedback integration, detailed reports, team meetings, and efficiency enhancement. Stakeholders contribute feedback directly to documents, ensuring continuous improvement. The system generates detailed reports summarizing received feedback, serving as valuable insights for decision-making and process enhancement. Regular team meetings facilitate collaboration and knowledge sharing, identifying strengths and weaknesses in the construction process. Necessary actions are taken to improve work efficiency based on data analysis, ensuring adherence to quality standards and meeting customer needs.

6. Conclusions

This research aimed to improve the efficiency of the construction phase by creating quality control checklists for processes and enhancing quality management through a collaborative digital environment integrating building information modeling (BIM) and cloud computing. The effectiveness of the system was studied through a real-life case in Latakia City, Syria. The research found that the integrated use of BIM and cloud computing makes implementation phase quality management more efficient and effective by better understanding the design, providing a robust database, improving communication and collaboration between participants, enhancing on-site quality information extraction from BIM models using smartphones, documenting defects and entering inspection data directly into a shared digital environment, and facilitating the tracking of corrective actions and feedback. This enables continuous and structured access to up-to-date information and inspection results, thereby reducing defects, minimizing rework, saving time and cost, and improving the speed and efficiency of decision-making. Moreover, the color-coded model, combined with the historical record of the issues, gives an overview of the current quality status of the project both in qualitative and quantitative terms. The research recommended the need for strict regulations to adhere to quality control procedures, the need to provide technical infrastructure to move the construction industry to a collaborative digital environment, and the importance of conducting training courses for construction workers on the use of the new technology.

Author contributions: Conceptualization, MS, BAH and ASM; methodology, MS and BAH; software, ASM; validation, ASM; conducting interviews, ASM; data curation, MS, BAH and ASM; writing—original draft preparation, ASM; writing—review and editing, MS, BAH and ASM; supervision, MS and BAH. All authors have read and agreed to the published version of the manuscript.

Conflict of interest: The authors declare no conflict of interest.

References

1. Luo Y. Cooperative Design, Visualization, and Engineering. Springer Berlin Heidelberg; 2007. doi: 10.1007/978-3-540-74780-2
2. Nguyen P, Nguyen P, Nguyen Q, Huynh V. Project success evaluation using TOPSIS algorithm. Journal of Engineering and Applied Sciences. 2016; 11(8): 1876-1879.
3. AA AS, Varghese S. Application of BIM as a Model for Quality Management. International Research Journal of Engineering and Technology (IRJET). 2019; 6(6): 1197-1200.
4. Mirshokraei M, De Gaetani CI, Migliaccio F. A Web-Based BIM–AR Quality Management System for Structural Elements. Applied Sciences. 2019; 9(19): 3984. doi: 10.3390/app9193984
5. Abideen DK, Yunusa-Kaltungo A, Manu P, et al. A Systematic Review of the Extent to Which BIM Is Integrated into Operation and Maintenance. Sustainability. 2022; 14(14): 8692. doi: 10.3390/su14148692
6. Saad A, Ajayi SO, Alaka HA. Trends in BIM-based plugins development for construction activities: a systematic review. International Journal of Construction Management. 2022; 23(16): 2756-2768. doi: 10.1080/15623599.2022.2093815
7. Mutis I, Mehraj I. Cloud BIM governance framework for implementation in construction firms. Practice Periodical on Structural Design and Construction. 2022; 27(1): 04021074.
8. Ding L, Xu X. Application of Cloud Storage on BIM Life-Cycle Management. International Journal of Advanced Robotic Systems. 2014; 11(8): 129. doi: 10.5772/58443
9. Zhao Y, Taib N. Cloud-based Building Information Modelling (Cloud-BIM): Systematic literature review and Bibliometric-qualitative Analysis. Automation in Construction. 2022; 142: 104468. doi: 10.1016/j.autcon.2022.104468
10. Abanda FH, Mzyece D, Oti AH, et al. A Study of the Potential of Cloud/Mobile BIM for the Management of Construction Projects. Applied System Innovation. 2018; 1(2): 9. doi: 10.3390/asi1020009
11. Hartmann T, Fischer M. Supporting the constructability review with 3D/4D models. Building Research & Information. 2007; 35(1): 70-80. doi: 10.1080/09613210600942218
12. Sears SK, Clough RH, Sears GA. Construction Project Management: A Practical Guide to Field Construction Management. John Wiley & Sons; 2018.
13. Love PED, Matthews J, Simpson I, et al. A benefits realization management building information modeling framework for asset owners. Automation in Construction. 2014; 37: 1-10. doi: 10.1016/j.autcon.2013.09.007
14. Wang J, Sun W, Shou W, et al. Integrating BIM and LiDAR for Real-Time Construction Quality Control. Journal of Intelligent & Robotic Systems. 2014; 79(3-4): 417-432. doi: 10.1007/s10846-014-0116-8
15. Lin YC, Chang JX, Su YC. Developing construction defect management system using bim technology in quality inspection. Journal of Civil Engineering and Management. 2016; 22(7): 903-914. doi: 10.3846/13923730.2014.928362
16. Ma Z, Cai S, Mao N, et al. Construction quality management based on a collaborative system using BIM and indoor positioning. Automation in Construction. 2018; 92: 35-45. doi: 10.1016/j.autcon.2018.03.027
17. Cheng Y. Building Information Modeling for Quality Management. In: Proceedings of the 20th International Conference on Enterprise Information Systems; 21-24 March 2018; Funchal, Madeira, Portugal. pp. 351-358. doi: 10.5220/0006796703510358
18. Alhassan B, Omran JY, Jrad FA. Enhancing Public Buildings Maintenance Using Integration Between Knowledge Management and BIM. International Journal of Information Systems and Social Change. 2019; 10(3): 1-13. doi: 10.4018/ijissc.2019070101
19. Bassier M, Vincke S, de Winter H, et al. Drift Invariant Metric Quality Control of Construction Sites Using BIM and Point Cloud Data. ISPRS International Journal of Geo-Information. 2020; 9(9): 545. doi: 10.3390/ijgi9090545
20. Dahbi A, Laaouan I, Hajji R, et al. A Cloud-Based Mobile Augmented Reality Application for BIM Collaboration. In: Proceedings of the 2022 the 6th International Conference on Virtual and Augmented Reality Simulations; 25-27 March 2022; Brisbane, Australia. doi: 10.1145/3546607.3546612
21. Qinghe W, Ruixin L, Liye S, Yongchen Y. Applications of BIM, Cloud Computing and Internet of Things Technology in Full Life Cycle of Bridges. Railway Standard Design. 2022; 66(12).
22. Irene R. Investigating the Impact of a Cloud-Based BIM Tool on Design Coordination: A Case Study of the Lions Gate Hospital Acute Care Facility Project [Master's thesis]. University of British Columbia; 2023.
23. Omran A, Shaban M. Development of Methodology to Manage Change Orders in Construction Projects Using Cloud

Computing [Master's thesis]. Al-Baath Universiyt, Syria; 2023.

Appendix

Table A1. Quality control checklist for excavation.

Item number	Item description	Pass	Fail
1	Suitable excavation and relocation vehicles should be obtained after securing relocation sites.		
2	Accurately determine the drilling depth based on the soil mechanics report data.		
3	Identify the bench mark and fixed axes on the site.		
4	Determine the limits of the excavation based on accurate topographic surveys.		
5	Define of the outer boundaries of the buildings to be excavated.		
6	Check the groundwater level to ensure proper drainage if it is higher than the foundation level.		
7	Ensure that the land is free of gas pipes and electrical cables.		
8	Make sure that there are no materials or insects (some types of ants) that could damage the concrete.		
9	Check the type of soil.		
10	Random samples should be taken and tests carried out to observe changes in the classification and physical properties of the soil.		
11	Determine the type of temporary reinforcement for the sides of the trench where the ground is weak.		
12	The coefficient of swelling of the soil, which can be up to 20%, must be determined in order to determine the quantities of excavation and relocation.		
13	The soil settlement under the foundations must be leveled.		
14	Ensure that the excavated soil is not stored close to the pit to prevent the collapse of the sides.		

Table A2. Quality control checklist for backfilling.

Item number	Item description	Pass	Fail
1	Ensure that all types of insulation are completed.		
2	Ensure that the backfill material is a suitable soil, clean and free of organic residues, preferably sandy soils or rocky residues.		
3	Take into consideration the sieve analysis if the backfill material is gravel.		
4	Conduct laboratory and field density and moisture tests periodically and in random areas to achieve the physical requirements of the backfill material.		
5	Document the amount of aggregate to be used, taking into account the compaction coefficient, which may reach up to 20%.		
6	Ensure that the backfilling is done in layers according to the soil report, with an average thickness of no more than 20–25 cm.		
7	Ensure that the backfill layer is completely submerged in water for 24 h, in particular for sandy soils.		

Table A3. Quality control checklist for foundation formwork.

Item number	Item description	Pass	Fail
1	Ensure the proper installation of excavation sides (temporary shoring) and verify their completion in a correct and durable manner.		
2	Match the axes of the foundation with the correct survey axes.		
3	Matching the axes of the foundation with the correct survey axes.		
4	Check the dimensions and heights of the foundations.		
5	Ensure the perpendicularity of foundation angles by measuring the diagonals of each foundation to ensure that the foundation is square or rectangular and does not deviate.		
6	Ensure the stability of the formwork sides and their ability to withstand the force generated by pouring the concrete mass inside.		

Table A3. (*Continued*).

Item number	Item description	Pass	Fail
7	Properly close the sides of the foundations together and seal any gaps between the wooden panels.		
8	Verify the locations of openings and paths for plumbing and electrical installations, etc.		
9	Thoroughly wet the formwork with water before pouring if it is wooden to avoid absorbing concrete water.		
10	Check the horizontal level of the foundations pouring with each other and the rest of the foundations with a mercury scale.		

Table A4. Quality control checklist for foundation reinforcement.

Item number	Item description	Pass	Fail
1	Ensure that the steel is free from rust, oil, dust, or any material that will prevent good adhesion to the concrete.		
2	Check the type, number, and length of rebar diameters.		
3	Ensure that the steel used complies with the required technical and conditional specifications through sampling and laboratory testing.		
4	Ensure that the reinforcing steel is placed in the correct position according to the drawings.		
5	Ensure that the foundation rebars are horizontally leveled without any inclinations.		
6	Securely tie the steel and cut any excess binding wire.		
7	Install the rebar chairs to raise the top mesh steel according to the attached drawings.		
8	Ensure adequate cover thickness on all sides in accordance with code requirements, and place spacers on foundation sides and under bottom mesh steel.		
9	Check the diameter, number, and length of column dowel bars in accordance with code requirements.		
10	Check the position of the column dowel bars and connect them to the stirrups, ensuring that they do not move during the pouring process.		
11	Ensure that column dowel bars are properly anchored inside the foundation.		

Table A5. Quality control checklist for column formwork.

Item number	Item description	Pass	Fail
1	Ensure the dimensions of the column section are correct.		
2	Align the axes of the columns with the correct survey axes.		
3	Ensure the wood is clean from any debris.		
4	Ensure proper sealing of joints and openings (for pouring, etc.).		
5	Ensure horizontal and vertical bracing is securely in place to prevent any movement or tilting during pouring.		
6	Verify the verticality of the column before, during, and after pouring using available surveying equipment or traditional methods (plumb bob, mercury).		
7	Make sure that there is no deviation.		
8	Thoroughly wet the wooden formwork before pouring.		
9	Leave enough space between the wooden panels to prevent them from swelling when watering.		
10	Check the pouring level and determine the height of the column door.		
11	Leave a hole in the column formwork to check the pouring level.		

Table A6. Quality control checklist for column reinforcement.

Item number	Item description	Pass	Fail
1	Ensure the cleanliness of the steel from rust, oily substances, and dust.		
2	Verify the type, diameters, quantities, and lengths of the reinforcement steel.		
3	Ensure that the steel used complies with the required technical specifications and conditions through sampling and laboratory testing.		
4	Installing reinforcement steel according to the drawings.		
5	Verify the number, shape, diameters, locations, and spacing of ties according to the drawings, secure them in an alternating pattern, and tie them to the bars.		
6	Ensure that the hooks are implemented according to the study and drawings, following the seismic code recommendations in seismic zones.		
7	Verify the verticality of the vertical rebars and the horizontality of the ties.		
8	Take into account the lap splice lengths for the vertical reinforcement steel during cutting and installation.		
9	Consider the locations and levels of dowel bars for lintel.		
10	Ensure that an adequate number of spacers are installed between the wooden formwork and the reinforcement steel to control cover thickness.		
11	Ensure the cleanliness of the column before closing the formwork.		

Table A7. Quality control checklist for slab formwork.

Item number	Item description	Pass	Fail
1	Ensure the levelness of the slab before installing the formwork and take into consideration the thickness of the wood used.		
2	Ensure the dimensions of the structural elements to be poured and check for horizontal and vertical alignment.		
3	Verify the thickness of the slab in all areas.		
4	Use good quality wood without holes, protrusions, or defects.		
5	Ensure the safety of metal and wooden props and the distance between them and their height.		
6	Review the connection points of the props in case of high elevations and ensure the strength of the reinforcements at the joints.		
7	Ensure the installation of inclined props in both directions and secure them well with columns or walls.		
8	Ensure the stability of the slab under the props and its ability to bear the loads of the supports		
9	Avoid using blocks under the props and replace them with intersecting wooden battens.		
10	Ensure the presence of diagonal props.		
11	Ensure that the wooden formwork is flat and at a constant height.		
12	Ensure the adhesion of the wood panels to prevent concrete leakage during pouring.		
13	Ensure there are no protruding concrete pieces from columns due to poor execution.		
14	Verify the accuracy of the slab dimensions and the locations of any dropped beams if present.		
15	Review the dimensions and heights of any dropped beams.		
16	Review the vertical sides of the dropped beams.		
17	Check the accuracy of the angles of the slabs.		
18	Review the reinforcements when connecting application panels together and ensure proper jointing.		
19	Check that bathroom slabs drop below the level of other slabs.		
20	Review the locations and dimensions of electrical, plumbing, and HVAC openings.		

Table A8. Quality control checklist for slab reinforcement.

Item number	Item description	Pass	Fail
1	Ensure the cleanliness of the reinforcement steel and the absence of rust.		
2	Verify the type, diameters, quantities, and lengths of the reinforcement steel according to the design code.		
3	Ensure that the reinforcement steel is placed in its designated location as per the drawings, especially in the cantilever and the stair.		
4	Check the connections and lengths of the rebars according to the drawings.		
5	Place spacers beneath the bottom mesh steel and between the formwork and the beam sides.		
6	Ensure the dimensions of the beam's stirrups, their quantities, and their spacing are equal or as per the drawings.		
7	Ensure that the stirrups are interlocked alternately.		
8	Properly connect the upper and lower beam reinforcement steel with the stirrups.		
9	Ensure proper bending of beam reinforcement steel and ensure it is executed as per the drawings.		
10	Ensure the continuity of column ties within the beams (according to the plans and code instructions).		
11	Review the reinforcement steel of stairs and ensure dowel bars.		
12	Review the reinforcement steel of column capital.		
13	Review the lengths of column dowel bars and ensure their correct placement in case of reducing the column section.		
14	Ensure proper bending of column dowel bars in the last floor slab.		
15	Review the detailing of sanitary drop-downs.		

Table A9. Quality control checklist for hollow blocks distribution.

Item number	Item description	Pass	Fail
1	Review the dimensions and quality of the hollow block and avoid using broken blocks.		
2	Ensure that the hollow blocks meet the conditions and technical specifications by conducting fracture and loading tests.		
3	Ensure the distribution of the hollow blocks to guarantee the dimensions of the ribs and beams as shown in the drawings.		
4	Ensure that the ends of the hollow blocks row are completely closed to prevent concrete from leaking into the hollow blocks during the pouring process.		

Table A10. Quality control checklist for pouring.

Quality control checklist for pouring			
Before pouring			
Item number	**Item description**	**Pass**	**Fail**
1	Ensure that the mixer and the vibrator are fit for work.		
2	Ensure the quality of the concrete in accordance with project specifications: (mix temperature does not exceed 35 Celsius, fineness of cement, setting time not exceeding 45 min, mix consistency or water content in concrete, sieve analysis of the mix).		
3	Ensure the presence of a specified water content for concrete (in case of using semi-automatic mixers).		
4	Ensure that the water used in the pouring process is potable and free of impurities.		
5	The workability of the concrete should be suitable for the element being poured, according to specifications.		
6	Ensure the availability of Abrams cones (slump tests) and their readiness.		
7	Ensure an adequate number of concrete cubes/cylinders for sampling (not less than 3 samples per 100 cubic meters or as per requirements).		
8	Ensure that the wooden formwork is wet with water before pouring.		

Table A10. (*Continued*).

Quality control checklist for pouring			
Before pouring			
Item number	**Item description**	**Pass**	**Fail**
9	Review the sequencing of pouring stages with the responsible supervisor.		
10	Review the identification of casting joints, expansion and contraction joints, and settlement joints.		
11	Ensure that spacers are placed under the bottom mesh steel of slab, under the lower rebar of beams, between the sides of the formwork for the beams and the rebars to control cover thickness.		
12	Ensure that the pouring height does not exceed 3 m (preferably less—2 m) at maximum.		
13	Ensure that weather conditions are suitable for the pouring process.		
During pouring			
1	Review and ensure the accuracy of the mix proportions, especially the water to cement ratio.		
2	Ensure that the concrete is poured to the appropriate level without excess to avoid the need for demolition later on.		
3	Precisely monitor the scaffolding and props during the pouring process to prevent any unforeseen events.		
4	Use vibration in all stages of pouring all structural elements.		
5	Ensure that column rebars are not shaken or moved during the pouring process.		
6	Make sure that each part is properly compacted after pouring, especially beams, without allowing the mechanical vibrator to touch the reinforcement steel as much as possible.		
7	Ensure that the surface of the concrete is properly leveled for the finished part using appropriate tools (such as a helicopter trowel) according to the specifications.		
8	Continuously measure the thickness of the slabs and ensure uniformity of thickness.		
9	Remove excess concrete promptly before hardening and ensure that all surfaces are level and clean after pouring is complete.		
After pouring			
1	Ensure that the concrete continues to be cured by spraying and moistening it with water for at least seven days after pouring.		
2	Ensure that the formwork is removed correctly in terms of timing, location, and type of structural element.		
3	Monitor the results of breaking concrete cubes in a structured tracking table with dates.		

Building Engineering 2024, 2(1), 509.
https://doi.org/10.59400/be.v2i1.509

Article

Practical approach for analysing and engaging stakeholders in construction megaprojects

Ayman Mashali*, Ahmed Eltantawy

Mansoura University, Mansoura 35511, Egypt
*** Corresponding author:** Ayman Mashali, ayman.mashali@yahoo.com

CITATION

Mashali A, Eltantawy A. Practical approach for analysing and engaging stakeholders in construction megaprojects. Building Engineering. 2024; 2(1): 509. https://doi.org/10.59400/be.v2i1.509

ARTICLE INFO

Received: 23 January 2024
Accepted: 27 February 2024
Available online: 10 March 2024

Abstract: Purpose: The construction industry is a complex environment, it is facing massive challenges, especially on megaprojects, due to the huge construction development and stakeholder management (SM). This paper seeks to explore, investigate, and assess the methods for analysing and engaging stakeholders on construction megaprojects to overcome stakeholder management problems and enhance performance. **Methodology:** The quantitative methodology is adopted in this research; a questionnaire survey is carried out among big construction firms in Qatar, with a 59% response rate. Quantitative data analysis was conducted using the statistical package for social science (SPSS) software. **Findings:** This paper investigated and assessed the common methods for analysing and engaging stakeholders on construction megaprojects, where they come together more integrative. Hence, this will boost their chances of reaching higher levels of success and project effectiveness. Lastly, the findings are foreseen to aid project managers in adjusting their strategies when considering future implementation plans via a broad picture and understanding of SM and their relationships in CMPs. **Practical implications:** Investigating and assessing the methods for analysing and engaging stakeholders is expected to assist project managers in improving projects' performance and completing construction within the predefined time and cost. Besides, it enhances and strengthens the present body of knowledge in SM study domains and provides a starting point for practitioners and academics. **Originality:** This study contributes significantly by investigating and assessing the methods for analysing and engaging stakeholders in MCPs. Moreover, the findings are important for all concerned project stakeholders and are considered as a roadmap for effective stakeholder management in MCPs.

Keywords: stakeholder; management; engagement; construction; megaprojects

1. Introduction

The construction industry is a complex environment where collaboration and coordination among stakeholders are necessary [1]. According to earlier studies, a lack of thorough stakeholder management processes is evident throughout the project life cycle. While stakeholder management has yet to be adopted as a promising strategy for managing construction projects [2,3]. Moreover, all of the stakeholders contributions are significant for planning and control. Even though stakeholder management has long been recognized as a means to increase the likelihood of successful construction projects' completion, the full potential of stakeholder management has yet to be realized [2]. Despite the recognized importance of SM, there is still a lack of research regarding project stakeholders. The concept of SM has developed greatly because it is important to achieve project objectives [4]. Furthermore, poor SM can lead to many serious problems in the CI, such as inadequate scope and activity definition, inappropriately assigned project resources, poor and

ineffective communication, and unexpected scope modifications; all these problems may be the root cause of delays and exceeded cost [5].

Numerous difficulties and obstacles of SM in construction projects recommended by past researchers involve improper stakeholder engagement (SE) [6].

Nonetheless, a deeper understanding of SM would allow project execution teams to value project planning stages and determine if the concerns are being handled as efficiently as possible [7]. This will boost their chances of reaching higher levels of success and, as a result, time savings, cost savings, quality assurance, and project effectiveness [8].

This research aims to present an investigation and assessment of the methods for analysing and engaging stakeholders in MCPs. This knowledge gap is bridged and handled in this paper. Moreover, the research findings serve as a roadmap for governments and clients of construction projects to achieve ultimate benefits and increase earned value in their investments. The research outcomes are anticipated to support project teams and construction organizations in implementing SM.

2. Literature review

2.1. Stakeholders' definition

From Freeman [9] to PMI [10], there are broad stakeholder definitions. In conclusion, the most common definition of project stakeholders is any individual, group, or organisation who can affect or is affected by the project and includes clients, consultants, contractors, subcontractors, suppliers, and all government authorities [2,11].

2.2. Mega-projects

Megaprojects consume enormous resources that can be afforded only by giant international contractors with robust financial capabilities. Besides, it faces a group of political and social conditions [8,12]. Construction megaprojects can be described as "large-scale, complex projects that cost about $1 billion or more, need many years to develop and build, involve multiple stakeholders, and impact millions of people" [13,14].

Furthermore, megaprojects have strong economic and social roles in societies. They are not only characterized by their high construction values but also by their complexity level in design and construction, methodology, technology, schedule, finance, governance, resources, organizational performance, environment, and workflow challenges [12,15]. Moreover, the managerial challenges in mega construction projects (MCPs) are not only purely technical but also involve the management of social, political, and cultural aspects of the project [11].

Considering size and scope, megaprojects confront significant schedule and budget challenges compared to other projects. Reasons include [13]:

- Increased risks due to complex interfaces and long planning.
- Planning processes that comprise many participants with conflicting interests.
- The scope of the project can change over time.

In megaprojects, the project team's instability for a long time through the project

life cycle weakens the ability of leadership to keep constant progress rates [13].

2.3. Stakeholder engagement & involvement

Stakeholder engagement (SE) ensures that long-distance, comprehensive, and consistent participation is required [1]. Previous research describes SE as the participation process of persons and sets that are influenced by the activities of the firm actively. Also, stakeholder activities such as dialogue are one approach to evaluating stakeholder participation [16]. Whereas engagement can be considered as the relationship among the organization and various stakeholders to reinforce the efficacy of the resolutions, strategies, and performance [17]. Furthermore, SE tries realistic stakeholder opinions on their relationship, where SE seeks to better an organization's social and ethical accountability and conduct [18].

2.4. Types of engagement

Bowen et al. [19] displayed three classifications for engagement strategies: transactional, transitional, and transformational, which depend on the nature of the engagement. If society is enough included in the goal-setting and measurement processes, shared responsibility for the engagement process can also be achieved [19].

Additionally, Bowen et al. [19] stated that there is more two-way interaction between the stakeholders and the company. Moreover, many stakeholder groups are not satisfied with simply being assigned some measure of organizational value; they want an opinion on how the organization creates this value [11]. Not all, but numerous stakeholders want some voice in organizational decision-making [20].

2.5. Analysing and engaging stakeholders

Stakeholder analyses (SA) is a crucial and important portion of successfully SM [2,21]. SA means to know the stakeholders and their concerns and to value stakeholders' impact and relations. According to Yang et al., SE is about communicating, involving, and developing connections with stakeholders. Project directors should adopt methodologies that agree with the SM process. Also, they illustrated that there is no stand-alone methodology, and other methodologies should merge most of the methodologies [16].

2.6. Effective involvement of stakeholders

Project managers should establish a stakeholder participation plan to address the needs of various stakeholder groups and improve the efficacy and efficiency of decisions made throughout the project life cycle [6]. Overall, stakeholder involvement, along with other aspects such as leadership, measurement and improvement, teamwork, and process approach, is cited by Toriola-Coker et al. [22] as the most important element influencing the effective implementation of comprehensive management systems. Also, conflicts among plans and other risks to action in the execution and operations phases are mitigated by involving multiple parties in the project planning process, all of whom have different priorities and objectives [23].

However, depending on the project's nature and requirements, only certain people may get involved in the process. According to Mok et al. [24], effective and

active engagement of project members will help to improve the overall quality of the construction and increase the project value. Stakeholder perspectives on prospective engagement in the planning process were offered by Ayodele and Kajimo-Shakantu [1]. Travaglini and Dunović [23] advocated that the project preparation and planning phase is the stage where different stakeholders with various demands and objectives have the most significant possibility to impact projects and their outcomes.

2.7. Stakeholder management and construction project success

All project stakeholders' effective and ongoing involvement has been associated with project success [22,23].

Additionally, stakeholder satisfaction has been added to the traditional criteria for project success: cost, quality, and timeline [5,25].

Moreover, previous studies have linked project failures to either a lack of or ineffective stakeholder management during the project. Therefore, it is crucial to include stakeholders effectively to complete the project successfully and under the current perception of project success in CI [3,22].

Involvement and incorporating stakeholders early on and considering their interests are critical to preventing adverse reactions to the project. Therefore, stakeholder management and involvement should continue the project's duration [2,3].

As evidenced by several problems and project failures around the world, stakeholder participation has a very significant impact on project outcomes [16].

The outcomes of SM are dependent on project managers' knowledge, judgment, relations, and skills. A vital aspect of project success is the ability of the project manager to delineate the project location and engage the local community in the planning process [22].

The construction industry includes a wide range of stakeholders, in which they introduce their interests, concerns, needs, and likely chances [11].

Therefore, effective SM necessitates robust analytical proficiency to identify the concerned stakeholders and work with them to understand their expectations and the impact they can have on project success. This increases positive stakeholder engagement and decreases any probable harmful impact [1].

3. Research methodology/approach

The research strategy can be defined as how the research aims could be investigated, and it is divided into two sorts, namely, quantitative and qualitative [26].

The quantitative methodology involves both studying the overall trends in data and adding appropriate statistical criteria [27].

This study aims to explore, investigate, and assess the methods for analysing and engaging stakeholders in MCPs. To achieve this goal, a questionnaire survey is carried out to gather information from construction practitioners in Qatar. A five-level scoring scale ranging from "1" (very low) to "5" (very high) is used. The collected data is then analyzed using the SPSS software (version 22).

The sample size is selected randomly from different stakeholders representing the licensed engineers. The targeted population is the engineers licensed and working

in Qatar, which numbered 14,000, according to the Ministry of Municipality and Environment. The sample size was determined using Slovin's formula [28] as follows:

$$n = \frac{N}{1 + N(c^2)} \quad (1)$$

c = Margin of error, taken as 10% = 0.10.

N = Total population, taken as 14,000.

n = Sample size.

"Applying the equation": $n = \frac{14{,}000}{1+14{,}000(0.10^2)} = 99.29 \approx 100$

This paper utilized a quantitative approach employing an empirical, realistic survey. The questionnaire was sent to 400 individuals working at different organizations, with 235 (59%) responses received, which is a satisfactory number of responses [25,29]. After designing the questionnaire, a pretesting and pilot study are carried out to refine. Cronbach's coefficient alpha (a) [30] is the most common measure of internal consistency (reliability) when questions are asked on a Likert scale (1 to 5). The values range between 0.0 and 1.0, with the higher values implying a higher degree of internal consistency [31]. According to Pallant [32], a value of a equals or greater than 0.7 means that the data is reliable for analysis. In this study, a equals 0.96, which implies high reliability of the whole questionnaire responses to achieve the study's objectives. The collected data is analyzed through calculation of the RII, using Equation (2) [33]:

$$RII = \frac{\Sigma Wi * ni}{N * A} \quad (2)$$

where:

W_i: the weight given to each factor by the respondents and ranges from 1 to 5;

n_i: the number of respondents gave the weight W_i;

A: the maximum weight (i.e., 5 in this case); and

N: the total number of respondents.

The higher the RII value, the more important the attribute [34].

Although respondents' opinions may be subjective depending on their experience, locations, and other factors, numerous statistical techniques are employed to reduce these biases. The research methodology stages are demonstrated in **Figure 1**.

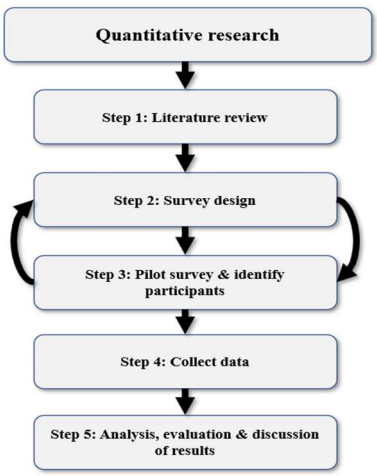

Figure 1. Research approach/methodology.

4. Analysis of results and discussions

This section describes the results of the analysis of the survey data that was obtained and discusses the findings.

4.1. Respondents' demographics

This division includes the available personal/general information about the survey participants (235 responses): in terms of their position, years of experience, nature of the organization, and the type of industry that they are involving in.

4.1.1. Category of respondents' organizations (organizational role)

In terms of the respondents' organizations, as illustrated in **Figure 2**, the plurality of respondents are consultants/designers/managers (43.40%) and contractors (33.19%), whose responses reflect the SM during the construction stage. Also, the high percentage of this class of respondents ensures information goodness.

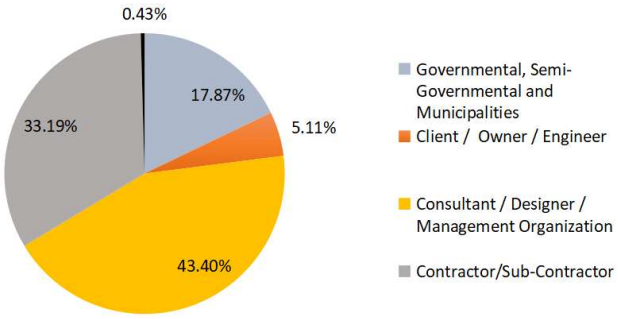

Figure 2. Category of respondents' organizations.

4.1.2. Respondents' roles/current career (respondents' job profiles)

Figure 3 indicates that (director/senior management) is 5.11%, which reflects the decision-maker of development (project manager/construction manager) and (resident engineer/client consultant) have values of 19.57% and 12.77%, respectively, with a total value of 37.45%, obtained from top management who have managerial and professional abilities, which implement the great capacity for assessment of the states. Senior engineer's level responses were 32.77%, which is good for managing and controlling. Furthermore, more than 70% of the responses were from top management and senior levels, which hold critical positions that influence the quality of the data gathered. Since this paper concentrates on SM, these findings prove that proper individuals have been approached.

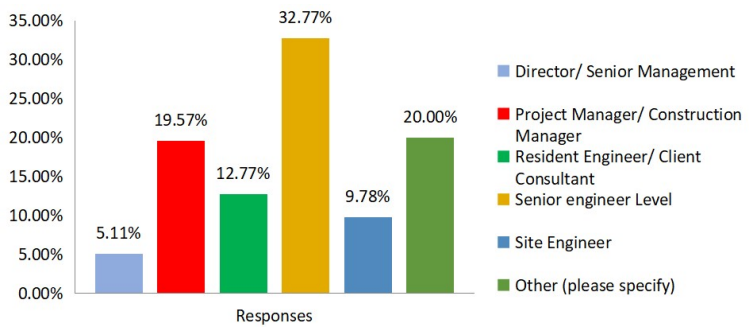

Figure 3. Respondents' job profiles (respondents' roles).

4.1.3. Respondents' years of experience in construction

In terms of years of work experience in construction, the percent of the respondents were shown in **Figure 4**; only 6.81% of participants had less than five years in the industry, and 25.11% of respondents had 11 to 15 years of work experience. Nearly about half of the participants have at least 20 years of experience. They act as leaders and decision-makers in their organizations., which indicates the importance of SM in Qatar's industry sectors.

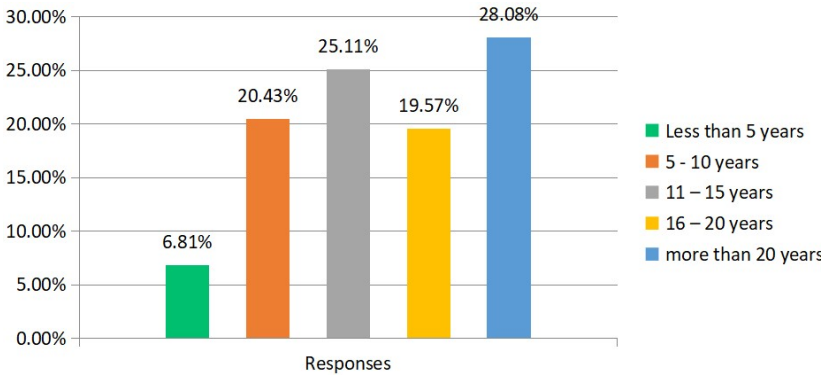

Figure 4. Respondents' "years of experience".

The highest number of extensive experiences increases the degree of assessment accuracy. Furthermore, the variety of experiences enhances the study by various information and knowledge. This is a great sign that the respondents have a minimum degree of expertise with the SM. This profile indicates a considerable experience on which the outcomes of this survey were rested.

4.1.4. Stakeholders management present in the project organization structure

Figure 5 demonstrates the percent of respondents' answers about the following: Are stakeholders management present in your project organization structure? The major answer was yes; they were more than 80.0%, which gives an excellent sign to secure quality information and reflect the current high development proceeded in Qatari construction projects.

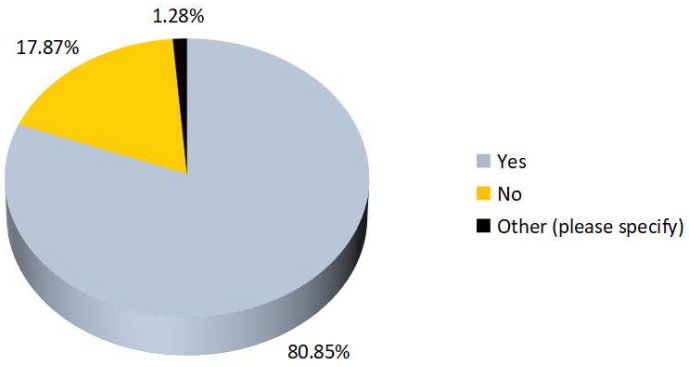

Figure 5. Distribution of respondents' percentage.

4.1.5. Respondents' "client" types

In terms of client types, the respondents indicated that more than 88.0 percent of clients were public/government organisations, as indicated in **Figure 6**. This high

percentage represents the current status of construction in Qatar and accurately reflects the current scenario in the Qatari construction market, where the government is spending and funding infrastructure development projects concerning World Cup 2022.

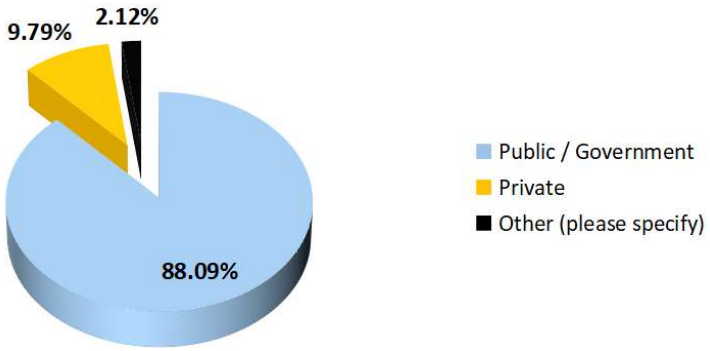

Figure 6. Respondents' "client" types.

To have a deeper understanding of how each group of respondents is involved in the construction process, descriptive statistics was adopted to determine the measures of (mean) and measures of dispersion (standard deviation and variance). The mean reflects the degree of involvement. Respondent perceptions were examined by using a five-point Likert scale: 1 = very low, 2 = low, 3 = average, 4 = high, and 5 = very high.

It is clear from the results displayed previously that the respondents had perfect experience in the construction field, as the majority had more than 20 years of experience from various organizations, and some respondents were involved in stakeholder management. Therefore, this respondents' sample is appropriate and sufficient to provide the research with a consistent view of Qatar's construction projects.

As a result, this further supports and gives more acceptance to the gathered data, later analysis, and investigation.

4.2. Discussion of survey findings

This part presents the collected outcomes of the SM practice of the chosen sample of Qatar's construction stakeholders. The main assignment in SM was stakeholder analysis and engagement. To fulfill the study aims, four questions were outlined in the survey as the following: (a) methods of analyzing stakeholders' concerns and needs; (b) methods of stakeholders' engagement according to the type of contract; (c) methods of engaging the stakeholders according to the type of project; (d) type of reply strategy to transact for the stakeholder demands.

4.2.1. Method of analysing stakeholders' concern and need

Table 1 illustrates that the *P*-value = 0.000, which is less than the significance level ($\alpha = 0.05$) for all factors, and "personal past experience" was rated first, with RII equals (86.57%). The importance of project managers' experience is highlighted in this outcome. When project managers need to gather information about stakeholder's needs and concerns before producing a proposal, they have difficulty with financial resources. Therefore, the past personal experience allows them to overcome this

obstacle because the past personal experience is cheap.

Workshops: was rated in the second position, with RII (86.29%); in this process, the project manager could obtain an opportunity to investigate and analyze the options and deal with challenging issues.

Table 1. Effective methods to analyze stakeholders' concern and need.

Notification	Mean	Std. error	Std. deviation	Variance	RII %	*P*-value (Sig.)	Rank
Personal past experience	4.3151	0.05972	0.72162	0.521	86.57	0.00	1
Interviews	4.0966	0.05899	0.71028	0.513	82.24	0.00	4
Questionnaires and surveys	3.9448	0.06476	0.77977	0.605	82.24	0.00	4
Professional services	4.1310	0.06053	0.72892	0.532	82.94	0.00	3
Workshops	4.2897	0.05529	0.66580	0.438	86.29	0.00	2
All factors of the field	4.1554		0.72127		83.44		

Professional services were ranked in the third position, with RII equals (82.94), because they afford full SM plans and economize the project manager's time.

Interview: although the interview is easy to arrange and low cost, it was ranked in fourth/last position with RII equals (82.24%). This may be related to the pressure of work and the lack of time for the concerned engineers.

Questionnaires and surveys were ranked in fourth/last position, also with RII equals (82.24%), because the project manager avoids the low response rates, which may affect the results, and the collected information may be shallow, and their point of view may not be clear.

Each method has its own power, restriction, and constraint; therefore, the most suitable method for achieving effective SM is to apply a combination of elements of every method according to the actual situation.

4.2.2. Engagement methods for the stakeholders according to type of contract

The respondents were questioned about their view concerning the efficient methods to engage stakeholders (ES) according to the type of contract in Qatar's construction project.

Lump sum contract:

Table 2 shows that "*P*-value = 0.000, which is less than the significance level (α = 0.05)" for all factors, and "meeting" was ranked first with RII (88.11%), while "interviews" with RII (75.80%) was ranked in the lowest position. This result mentions that the experience of project managers is most significant.

Table 2. Effective methods to engage stakeholders in lump sum contract.

Notification	Mean	Std. error	Std. deviation	Variance	RII %	*P*-value (Sig.)	Rank
Meetings	4.3750	0.05985	0.71815	0.516	88.11	0.00	1
Social contacts	4.0278	0.06458	0.77500	0.601	80.28	0.00	4
Negotiations	4.0833	0.07276	0.87306	0.762	81.82	0.00	2
Workshops	4.0210	0.06980	0.83471	0.697	81.40	0.00	3
Interviews	3.8028	0.07224	0.86080	0.741	75.80	0.00	5
All factors of the set					81.48		

Measurement contract:

Table 3 shown that, "*P*-value = 0.000, which is less than the significance level (α = 0.05)" for all factors. Besides, 'meeting' was ranked first, with RII equals (86.29%), while "interviews" with RII equal (75.66%) was ranked in the lowest position.

Table 3. Effective methods to engage stakeholders in measurement contract.

Notification	Mean	Std. error	Std. deviation	Variance	RII %	*P*-value (Sig.)	Rank
Meetings	4.3125	4.3125	4.3125	0.482	86.29	0.00	1
Social Contacts	3.9861	0.05660	0.67922	0.461	79.72	0.00	4
Negotiations	4.0694	0.06659	0.79906	0.639	81.40	0.00	2
Workshops	4.0210	0.06075	0.72645	0.528	80.42	0.00	3
Interviews	3.7887	0.06766	0.80628	0.650	75.66	0.00	5
All factors of the set					80.70		

Cost reimbursable contract (CRC):

Table 4 shown that, *P*-value = 0.000, which is less than the significance level (α = 0.05) for all factor as well as, 'meeting' was ranked first, with RII equals (88.41%), while "interviews" with RII equal (75.24%) was ranked in the lowest position.

Table 4. Effective methods to engage stakeholders in CRC.

Notification	Mean	Std. error	Std. deviation	Variance	RII %	*P*-value (Sig.)	Rank
Meetings	4.3889	0.05671	0.68051	0.463	87.41	0.00	1
Social contacts	4.0347	0.06187	0.74245	0.551	80.14	0.00	4
Negotiations	4.1319	0.06774	0.81289	0.661	82.80	0.00	2
Workshops	4.0559	0.05936	0.70985	0.504	80.98	0.00	3
Interviews	3.7958	0.06519	0.77678	0.603	75.24	0.00	5
All factors of the set					81.31		

It is clear from the above-mentioned tables that outcomes are similar, this means that type of contract does not affect engaging stakeholder's methods.

Design-build (D-B)/(EPC) project:

Table 5 shows that the *P*-value = 0.000, which is less than the significance level (α = 0.05) for all factors, as well as 'meeting' was ranked first, with RII equals (90.07%), but "interviews" with RII equal (78.18%) was ranked in the lowest position.

Table 5. Effective methods to engage stakeholders in D-B.

Notification	Mean	Std. Error	Std. deviation	Variance	RII %	*P*-value (Sig.)	Rank
Meetings	4.4653	0.06380	0.76564	0.586	90.07	0.00	1
Social contacts	4.1111	0.06692	0.80306	0.645	82.66	0.00	3
Negotiations	4.0903	0.07817	0.93803	0.880	83.64	0.00	2
Workshops	4.1189	0.06077	0.72665	0.528	82.66	0.00	3
Interviews	3.9085	0.06772	0.80693	0.651	78.18	0.00	5
All factors of the set					83.44		

Where design-build offers owners a single point of responsibility for both the design and construction services. The designer-builder is thus responsible for any design errors. Design-build offers owners earlier completion of their projects as a result of design and construction activities overlapping.

The previous **Tables 2–5** demonstrate that "meeting" was ranked first for all contract types, and it is the most common method for ES in the Qatari construction projects. While the meeting guarantees that attendees are aware of the subjects and information collected from their perspective, it is typically low-cost and simple to organise.

"Negotiations" was ranked in the second position for all types of contracts, and it is useful for solving the problems with the stakeholder face-to-face and disagreement settlement.

Although the "workshop" is a perfect way for discussion of the issues and analysis of the problems, it was ranked in the third position. This may be related to the individual personal skills of the project manager.

"Social contacts" was ranked in the fourth position for all types of contracts; it appears an ineffective and weak method to engage with the stakeholders.

Although the "interview" is easy to arrange and low cost, it was ranked in fifth/last position for all types of contracts. This may be related to the pressure of work and the lack of time for the concerned engineers.

Summary of effective methods to engage stakeholders according to type of contract:

Table 6 demonstrates that for all types of contracts, the "design-build/(EPC) contract" was ranked first, as well as being the most common contract type in Qatari construction projects. Since, in this project delivery method, the owner enters into one contract with a single entity responsible for delivering a complete solution to address the owner's specific needs or problems, i.e., design and construction.

Table 6. Summary of effective methods to engage stakeholders according to type of contract and procurement.

Engagement methods	Lump sum contract	Measurement contract	Cost reimbursable contract	Design build/(EPC) contract
	RII %	RII %	RII %	RII %
Meetings	88.11	86.29	87.41	90.07
Social contacts	80.28	79.72	80.14	82.66
Negotiations	81.82	81.40	82.80	83.64
Workshops	81.40	80.42	80.98	82.66
Interviews	75.80	75.66	75.24	78.18
All factors of the set	81.48	80.70	81.31	83.44

"Lump sum contract" was ranked second, "cost reimbursable contract" was ranked third, but "measurement contract" was in the last position.

4.2.3. Engagement methods for the stakeholders according to type of project

The respondents were questioned about their view concerning the efficient methods for ES according to the type of project in Qatar's construction project.

Buildings projects:

Table 7 shows that the *P*-value = 0.000, which is less than the significance level (α = 0.05), for all factors, "meeting" was ranked first with RII (87.55%), and "interviews" with RII (76.76%) was ranked in the lowest position.

Table 7. Effective methods to engage stakeholders in buildings projects.

Engagement methods	Mean	Std. error	Std. deviation	Variance	RII %	*P*-value (Sig.)	Rank
Meetings	4.3241	0.05780	0.69605	0.48448	87.55	0.00	1
Social contacts	4.0764	0.05753	0.69039	0.47664	81.68	0.00	2
Negotiations	4.069	0.0628	0.7540	0.56857	81.55	0.00	3
Workshops	3.9795	0.05870	0.70924	0.50302	80.00	0.00	4
Interviews	3.7534	0.06488	0.78399	0.61464	76.76	0.00	5
All factors of the set					81.51		

Infrastructure projects:

Table 8 shown that, "*P*-value = 0.000, which is less than the significance level (α = 0.05)", for all factor and that "meeting" was ranked first, with RII (91.80%), and "interviews" with RII (77.76%) was ranked in the lowest position.

Table 8. Effective methods to engage stakeholders in infrastructure projects.

Engagement methods	Mean	Std. error	Std. deviation	Variance	RII %	*P*-value (Sig.)	Rank
Meetings	4.5241	0.05714	0.68802	0.47337	91.809	0.00	1
Social contacts	4.2153	0.05760	0.69124	0.47781	84.34	0.00	2
Negotiations	4.1250	0.06675	0.80100	0.64161	82.80	0.00	4
Workshops	4.1575	0.06351	0.76734	0.58880	84.06	0.00	3
Interviews	3.8493	0.06250	0.75514	0.57024	77.76	0.00	5
All factors of the set					84.17		

Industrial projects:

Table 9 shows that the *P*-value = 0.000, which is less than the significance level (α = 0.05), for all factors, and that "meeting" was ranked first with RII (88.67%) and "interviews" with RII (76.08%) was ranked in the lowest position.

Table 9. Effective methods to engage stakeholders in industrial projects.

Engagement methods	Mean	Std. error	Std. deviation	Variance	RII %	*P*-value (Sig.)	Rank
Meetings	4.4207	0.05679	0.68383	0.46762	88.67	0.00	1
Social contacts	4.0764	0.05920	0.71036	0.50461	81.68	0.00	3
Negotiations	3.9514	0.06708	0.80497	0.64797	79.58	0.00	4
Workshops	4.0411	0.06365	0.76903	0.59140	81.96	0.00	2
Interviews	3.7603	0.06247	0.75480	0.56972	76.08	0.00	5
All factors of the set					81.59		

Others are combinations of two or more types of projects:

Table 10 shows that the *P*-value = 0.000, which is less than the significance level (α = 0.05), for all factors, and that "meeting" was ranked first with RII (86.62%), and "interviews" with RII (76.36%) was ranked in the lowest position.

Table 10. Others combination of two or more types projects.

Engagement methods	Mean	Std. error	Std. deviation	Variance	RII %	*P*-value (Sig.)	Rank
Meetings	4.2759	0.05911	0.71153	0.507	86.62	0.00	1
Social contacts	3.9653	0.05697	0.68361	0.467	79.86	0.00	3
Negotiations	4.0208	0.06498	0.77971	0.608	80.56	0.00	4
Workshops	3.9795	0.06334	0.76536	0.586	80.56	0.00	2
Interviews	3.7466	0.06507	0.78619	0.618	76.36	0.00	5
All factors of the set					80.79		

Tables 7–10 show that for all types of projects, "meeting" was ranked first, and it is the most engagement method type in Qatari construction projects. Whereas "interview"; although the interview is easy to arrange and low cost, it was ranked in the last position. This may be related to the pressure of work and the lack of time for the concerned engineers. Moreover, it is clear from the above-mentioned tables that outcomes are very closely related; this means that type of project does not affect engaging stakeholder's methods.

Summary of effective methods to engage stakeholders according to type of project:

Table 11 shows that, for all types of projects, "infrastructure project" was ranked first, and it is the most common project type in Qatari construction projects. These reflect the construction stage in Qatar to achieve Qatar Vision 2030.

Table 11. Summary of effective methods to engage stakeholders according to type of project.

Engagement methods	Buildings project	Infrastructure project	Industrial project	Others (combination of two or more types) project
	RII %	RII %	RII %	RII %
Meetings	87.55	91.89	88.67	86.62
Social contacts	81.68	84.34	81.68	79.86
Negotiations	81.55	82.80	79.58	80.56
Workshops	80.00	84.06	81.96	80.56
Interviews	76.76	77.76	76.08	76.36
All factors of the set	81.51	84.17	81.59	80.79

"Industrial project" was ranked in second.

"Buildings project" was ranked in third.

"Combination of two or more types of projects" was ranked in the last position.

4.2.4. Type of response strategy to deal with the stakeholder claims

The respondents were questioned about their view concerning the efficient response strategy types to deal with the stakeholder claims in the construction project.

Table 12 shows that "*P*-value = 0.000, which is less than the significance level (α = 0.05)" for all strategies, and "compromising strategy" was ranked in the first positions in this set with RII equals (83.92%). The respondents chose a compromise strategy to deal with the main stakeholder demands. This is the most preferred strategy in the construction project because the project managers use it in negotiating with the stakeholders, listening to their claims and requirements, and presenting possibilities

and areas for discussion. This strategy can be considered a win-win but is useful when finding a middle ground that satisfies all parties to some degree. Also, in this strategy, no one is truly happy with the solution; both parties must abandon something that is important to them. This is a lose-lose situation.

Table 12. Effective response strategy to deal with the stakeholder.

Strategy type	Mean	Std. error	Std. deviation	RII %	*P*-value (Sig.)	Rank
Adaptation strategy	3.9510	0.07898	0.94443	79.02	0.000	3
Avoidance strategy	3.4056	0.09936	1.18819	68.11	0.000	4
Compromising strategy	4.1958	0.06452	0.77149	83.92	0.000	1
Dismissal strategy	2.9441	0.11086	1.32567	58.46	0.000	5
Influence strategy	4.0559	0.06259	0.74848	81.26	0.000	2

"Influence strategy" was ranked in the second position in this set with RII equals (81.26%). This indicates that the project managers can use this type of strategy with the key stakeholders to seek to affect their claims in conjunction with the project aim. It requires others to undergo the point of view of one side or another. This is not recommended unless very necessary. Generally, this technique involves pushing one opinion at the expense of another. It is a win-lose situation.

An "adaptation strategy" was ranked in the third position in this set with RII equals (79.02%). This technique emphasizes agreement rather than differences of opinion. Whereas the project manager can realize that it is better to accept the demand when it is possible and does not have a major change in the project, this will be useful for achieving the project's objectives.

"Avoidance/withdrawing strategy" was ranked in the fourth position in this set with RII equals (68.11%). This strategy type could be adopted when the request of the stakeholder claim is above the projectability; furthermore, the project manager is seeking to adopt this strategy via preventing and covering himself from the claims and shifting the responsibility of the claims to another in the project. Avoiding or withdrawing from the conflict or possible conflict and allowing the concerned parties to solve the conflict on their own. This strategy is not recommended unless it is a very dangerous situation.

"Dismissal strategy" was ranked in the last position in this set with RII equals (58.46%). Most of the respondents disagreed with this strategy. This means that the project managers should transact with stakeholder's matters in a suitable and proper way.

In conclusion, previous tables clarified that the respondents considered these approaches were useful, and the project managers prefer to use a compromising strategy to deal with the main stakeholder needs. Because they can use this strategy to negotiate with the stakeholders, listening to their requirements correlated to the project, displaying likelihoods, domain for dialogue, creation satisfaction, and awarding reparations. On the other hand, the respondents are not accepting the use of the dismissal strategy.

5. Research's contributions

This study is foreseen to have multiple implications and provide a starting point for practitioners and academics by investigating and assessing the methods for analysing and engaging stakeholders on construction megaprojects.

This paper has contributed to the existing body of knowledge in SM areas, and its findings will create a solid motivation to carry out SM initiatives fully, developing more collaboration among the 'project's stakeholders and supporting the SM initiative in CMPs.

The findings are foreseen to aid project managers in adjusting their strategies when considering future implementation plans via a broad picture and understanding of SM and their relationships in CMPs.

6. Conclusion

This paper seeks to explore, investigate, and assess the methods for analysing and engaging stakeholders on construction megaprojects to overcome stakeholder management problems and enhance performance.

This paper provided the outcomes of the gathered quantitative data that have been received from responded questionnaires. The questionnaire was distributed to 400 persons from various firms, and 235 (59%) responded, which is a sufficient response, and considered a proper receiving. The survey participants have various professional disciplines and organisational backdrops, thus giving creditability to the information gathered. As this paper focuses on SM, these outcomes prove that proper people have been approached.

As a result of the study's outcomes, the conclusions have been described as the following:

- "Type of contract" does not affect engaging stakeholder's methods.
- Design-build (D & B) is the most effective approach to dealing with the stakeholder requirements and claims in MCPs.
- "Meeting" is the most effective method that should be used in engaging the stakeholders.
- "Compromising" strategy was ranked in the first position to deal with the stakeholder needs.
- Dismissal strategy not accepted.

The paper outcome will assist efficient decision-making in MCPs. Additionally, the research conclusions give a roadmap to project stakeholders that enhance SM practices. Generally, the study's outcomes contribute to and develop the goals of SM and the construction industry. However, this study provides a unique practical approach, considering deeper managing stakeholders. Thus, it results in a clear understanding of the stakeholders and their contributions, boosting project value creation.

7. Research limitations

This study, like others, has its limitations. The research was in QATAR. Hence, findings are limited to the Qatari construction projects context with an emphasis on

CMPs. Nevertheless, this research is still robust and suitable for evaluating SM in CMPs.

8. Recommendations

Based on the study outcomes, the recommendations comprise the following:

- There is an urgent necessity for crucial stakeholders to focus on staff human development and to prioritize staff development to enhance current SM practice.
- Government authority and professional organisations should work together to provide financial incentives to construction businesses to encourage them to implement SM practises.
- Government authorities and professional bodies should work toward developing relevant policies and standards within a local context.
- Organizations' senior management should prioritize evolving and installing a reliable working strategy to realize SM practices.
- Further investigation should be performed on an in-depth case study of diverse construction before and after using the outcomes of this research to validate it in practice and further enhance it to achieve more successful outcomes.

Moreover, this research recommends that construction key stakeholders adopt dynamic and positive attitudes toward SM. Owners, clients, and real estate developers are advised to be proactive in adopting efficient SM approaches in their projects to ensure project success.

Author contributions: Conceptualization, AM and AE; methodology, AM and AE; software, AM; validation, AM and AE; formal analysis, AM and AE; investigation, AM and AE; resources, AM and AE; data curation, AM and AE; writing—original draft preparation, AM and AE; writing—review and editing, AM and AE; visualization, AM and AE; supervision, AM and AE; project administration, AM and AE. All authors have read and agreed to the published version of the manuscript. All authors have read and agreed to the published version of the manuscript.

Conflict of interest: The authors declare no conflict of interest.

References

1. Ayodele TO, Kajimo-Shakantu K. Challenges and drivers to data sharing among stakeholders in the South African construction industry. Journal of Engineering, Design and Technology. 2021; 20(6): 1698-1715. doi: 10.1108/jedt-02-2021-0074
2. Mashali A, Elbeltagi E, Motawa I, Elshikh M. Stakeholder management: an insightful overview of issues. In: Proceedings of the International Conference on Civil Infrastructure and Construction (CIC 2020); 2-5 February 2020; Doha, Qatar.
3. Mashali A, Elbeltagi E, Motawa I, Elshikh M. Assessment of Stakeholders' Engagement According to Contract Type in Water Megaprojects in Qatar. In: Heggy E, Bermudez V, Vermeersch M (editors). Sustainable Energy-Water-Environment Nexus in Deserts, Proceeding of the First International Conference on Sustainable Energy-Water-Environment Nexus in Desert Climates 2019; 2-5 December 2019; Ar-Rayyan, Qatar. Springer; 2022. pp. 823-834.
4. Yang RJ, Shen GQ. Framework for stakeholder management in construction projects. Journal of Management in Engineering. 2015; 31(4).
5. Famiyeh S, Amoatey CT, Adaku E, et al. Major causes of construction time and cost overruns. Journal of Engineering, Design and Technology. 2017; 15(2): 181-198. doi: 10.1108/jedt-11-2015-0075
6. Kwofie TE, Aigbavboa CO, Thwala WD. Clusters of key barriers to life cycle assessment adoption in the South African

construction industry: perspectives of stakeholders. Journal of Engineering, Design and Technology. 2020; 19(4): 888-903. doi: 10.1108/jedt-06-2020-0223
7. Evans M, Farrell P, Mashali A. Influence of partnering on stakeholder's behaviour in construction mega-projects. The Journal of Modern Project Management. 2020; 8(1): 116-137.
8. Mashali A, Elbeltagi E, Motawa I, et al. Stakeholder management challenges in mega construction projects: critical success factors. Journal of Engineering, Design and Technology. 2022; 21(2): 358-375. doi: 10.1108/jedt-09-2021-0483
9. Freeman RE. Strategic Management: A Stakeholder Approach. Cambridge University Press; 1984.
10. Project Management Institute. A Guide to the Project Management Body of Knowledge: PMBOK® Guide, 6th ed. Project Management Institute; 2017.
11. Mashali A, Motawa I, Elshikh M. BIM-Based Stakeholder Management in Mega Construction Projects [PhD thesis]. Mansoura University; 2022.
12. El-Sabek LM, McCabe BY. Coordination Challenges of Production Planning in the Construction of International Mega-Projects in The Middle East. International Journal of Construction Education and Research. 2017; 14(2): 118-140. doi: 10.1080/15578771.2016.1276109
13. Flyvbjerg B. What you Should Know about Megaprojects and Why: An Overview. Project Management Journal. 2014; 45(2): 6-19. doi: 10.1002/pmj.21409
14. Evans M, Farrell P, Elbeltagi E, et al. Influence of Partnering Agreements Associated with BIM Adoption on Stakeholder's Behaviour in Construction Mega-Projects. International Journal of BIM and Engineering Science. 2020; 3(1): 1-17. doi: 10.54216/ijbes.030101
15. Brockmann C, Girmscheid G. Complexity of megaprojects. In: Proceedings of the CIB World Building Congress: Construction for Development; 14-17 May 2007; Cape Town International Convention Centre, South Africa. pp. 219-230.
16. Wojewnik-Filipkowska A, Dziadkiewicz A, Dryl W, et al. Obstacles and challenges in applying stakeholder analysis to infrastructure projects. Journal of Property Investment & Finance. 2019; 39(3): 199-222. doi: 10.1108/jpif-03-2019-0037
17. Yang J, Shen GQ, Bourne L, et al. A typology of operational approaches for stakeholder analysis and engagement. Construction Management and Economics. 2011; 29(2): 145-162. doi: 10.1080/01446193.2010.521759
18. Salem MA, Shawtari FA, Shamsudin MF, et al. The relation between stakeholders' integration and environmental competitiveness. Social Responsibility Journal. 2016; 12(4): 755-769. doi: 10.1108/srj-12-2015-0189
19. Bowen F, Newenham-Kahindi A, Herremans I. When Suits Meet Roots: The Antecedents and Consequences of Community Engagement Strategy. Journal of Business Ethics. 2010; 95(2): 297-318. doi: 10.1007/s10551-009-0360-1
20. Li Y, Sun H, Li D, et al. Effects of digital technology adoption on sustainability performance in construction projects: The mediating role of stakeholder collaboration. Journal of Management in Engineering. 2022; 38(3): 04022016. doi: 10.1061/(ASCE)ME.1943-5479.0001040
21. Olander S, Landin A. A comparative study of factors affecting the external stakeholder management process. Construction Management and Economics. 2008; 26(6): 553-561. doi: 10.1080/01446190701821810
22. Toriola-Coker L, Owolabi H, Alaka H, et al. Critical success factors (CSFs) for motivating end-user stakeholder's support for ensuring sustainability of PPP projects in Nigerian host communities. Journal of Engineering, Design and Technology. 2021; 21(3): 902-926. doi: 10.1108/jedt-04-2021-0202
23. Travaglini A, Dunović IB. Megaproject case studies: a stakeholder management perspective. In: Proceedings of the International Conference on Industrial Engineering and Operations Management; 8-10 March 2016; Kuala Lumpur, Malaysia.
24. Mok KY, Shen GQ, Yang J. Stakeholder management studies in mega construction projects: A review and future directions. International Journal of Project Management. 2015; 33(2): 446-457. doi: 10.1016/j.ijproman.2014.08.007
25. Heravi Torbati AH. Improving Construction Management: An Investigation into the Influences of Effective Stakeholder Involvement on Project Quality Outcomes [PhD thesis]. Queensland University of Technology; 2014.
26. Naoum S. Dissertation Research and Writing for Construction Students. Routledge; 2012. doi: 10.4324/9780080467047
27. Field A. Discovering Statistics Using IBM SPSS Statistics, 5th ed. Sage; 2018.
28. Slovin E. Slovin's Formula for Sampling Technique. Available online: https://prudencexd.weebly.com (accessed on 2 March 2024).
29. Babbie ER. The Practice of Social Research: Nelson Education, 14th ed. Cengage Learning; 2016.
30. Cronbach LJ. Coefficient alpha and the internal structure of tests. Psychometrika. 1951; 16(3): 297-334. doi:

10.1007/bf02310555
31. George D, Mallery P. IBM SPSS Statistics 26 Step by Step. Routledge; 2019. doi: 10.4324/9780429056765
32. Pallant J. SPSS Survival Manual: A Step Guide to Data Analysis Using SPSS for Windows. Allen & Unwin; 2005.
33. Halwatura RU, Ranasinghe NPNP. Causes of Variation Orders in Road Construction Projects in Sri Lanka. ISRN Construction Engineering. 2013; 2013: 1-7. doi: 10.1155/2013/381670
34. Van Tam N, Diep TN, Quoc Toan N, et al. Factors affecting adoption of building information modeling in construction projects: A case of Vietnam. Cogent Business & Management. 2021; 8(1). doi: 10.1080/23311975.2021.1918848

Building Engineering 2024, 2(1), 1190.
https://doi.org/10.59400/be.v2i1.1190

Article

Developing design response spectra for Benghazi city including soil magnification effects

Fathi M. Layas[1], Vail Karakale[2,*], Ramadan E. Suleiman[1]

[1] Department of Civil Engineering, Faculty of Engineering, University of Benghazi, Benghazi 218-61, Libya
[2] Department of Civil Engineering, Faculty of Engineering and Natural Sciences, Istanbul Medeniyet University, Istanbul 34700, Turkey
***Corresponding author:** Vail Karakale, vail.karakale@medeniyet.edu.tr

CITATION

Layas FM, Karakale V, Suleiman RE. Developing design response spectra for Benghazi city including soil magnification effects. Building Engineering. 2024; 2(1): 1190. https://doi.org/10.59400/be.v2i1.1190

ARTICLE INFO

Received: 11 January 2024
Accepted: 22 March 2024
Available online: 29 March 2024

Abstract: Earthquakes in some countries worldwide cause loss of lives and properties. In Libya, the design of structures to resist earthquake forces was based on a paper published by Mallick in 1976. In 1977, and after small changes in the earthquake zoning map of Libya, the ministry of housing, at that time, adopted it as a draft code of practice for the design of structures to resist earthquake forces. With Benghazi city undergoing significant rehabilitation and development programs, including major national projects, there is a pressing need to estimate updated probabilistic seismic hazard maps and design response spectra specific to the city. This study presented updated probabilistic seismic hazard ground motion for Benghazi city, considering different return periods and accounting for peak ground acceleration (PGA) values with various soil conditions. Proposed design response spectra for Benghazi City unveil substantial PGA amplifications in soft soil areas.

Keywords: earthquake; response spectra; soil conditions; amplifications; Benghazi; Libya

1. Introduction

In recent decades, some countries have experienced unexpected earthquakes, resulting in the loss of lives and properties. Among these countries is Turkey, where the code of practice for buildings to resist earthquakes has been developed since 1940 many times. The latest version of this code was drafted in 2018, which mainly adheres to ASCE 7-16 [1]. In light of the preliminary report by Erdik et al. [2] on the February 2023 Turkey earthquake, it was concluded that the latest version of the Turkish earthquake code, based on ASCE 7-16 [1], is considered more reliable compared to previous versions. This is attributed to its comprehensive incorporation of ductility, detailing, and capacity design principles. It was also observed by Karakale et al. [3] that a significant proportion of collapsed buildings, as shown in **Figure 1**, were constructed prior to the year 2000, when the revised earthquake-resistant design code and design-construction controls were implemented. Furthermore, in some areas, soft soil conditions and a high level of underground water table level cause amplifications of the seismic waves and liquefaction problems, as shown in **Figure 1**. Hence, design earthquake loads should take into account local site soil conditions.

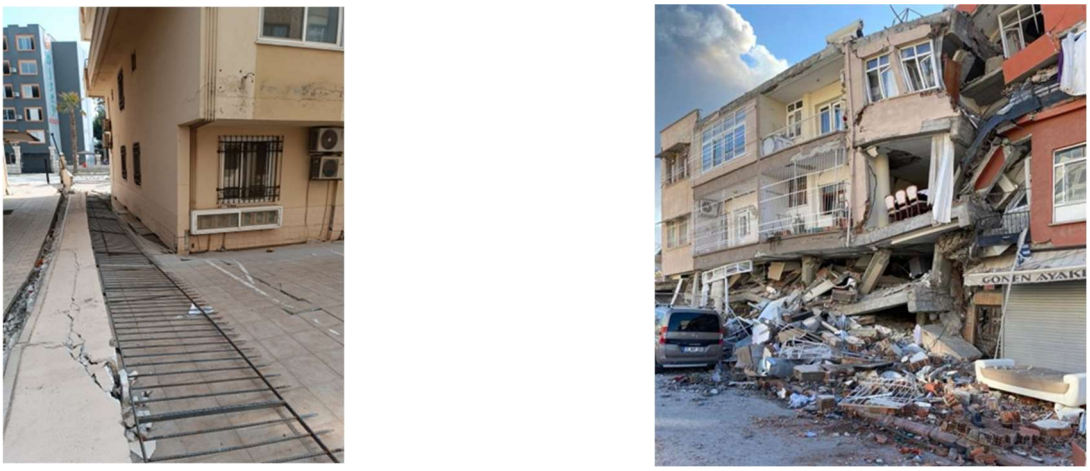

(a) **(b)**

Figure 1. Post-Kahramanmaraş earthquakes' impact on Pre-2000 constructed buildings. **(a)** Low quality concrete and poor detailing; **(b)** Soil liquefaction.

Benghazi, as the second-largest city in Libya, holds significant importance in the country's plans for rehabilitation and development. Its strategic location along the coast of the Mediterranean Sea promotes regional growth and economic activities. However, the existing seismic design code used for assessing earthquake forces in Libya, as outlined by Mallick [4], lacks the incorporation of design requirements for the response spectra method in building design. Furthermore, this code has not been updated since it was initially proposed as a local standard by the Ministry of Housing in 1978, leading to a high level of uncertainty when estimating earthquake forces during structural design. This shortfall in the seismic design code is a concern, as it can have significant implications for the safety and resilience of buildings and infrastructure in Libya. To ensure the country's preparedness for seismic events, it is crucial to update the seismic design code to incorporate the latest advancements in earthquake engineering and consider the specific response spectra requirements for building design. The results of the commonly developed, fully harmonized newly released Libyan seismic hazard model published by Lagesse et al. [5] provide a pertinent newly developed reference for seismic hazards at some major cities in Libya, including Benghazi City. The published paper showed the acceleration parameters required to construct the design spectrum curves required to design structures against earthquake forces. These values of horizontal spectra acceleration with 5% damping for peak ground acceleration are presented for 475-year and 2475-year return periods. This study is to address this issue by presenting an updated seismic design code that takes into account local site soil conditions. And developing customized design response spectra curves that engineers can utilize when designing reinforced concrete buildings in Benghazi city. These response spectra curves will be aligned with the more comprehensive ASCE 7-16 [1]. To accomplish this, it is crucial to incorporate up-to-date seismological data specific to the study area. By doing so, the study aims to enhance the seismic resilience and safety of structures in Benghazi city, considering the lessons learned from the Turkey earthquake and the advancements in earthquake-resistant design principles. Furthermore, engineers and designers in Benghazi will have access to more accurate and reliable tools for estimating earthquake forces and

designing structures that can withstand seismic events. This will contribute to enhancing the safety and resilience of the city's built environment and supporting its ongoing rehabilitation and development efforts.

Benghazi, the second-largest city in Libya, plays a crucial role in the country's plans for rehabilitation and development, thanks to its strategic location on the Mediterranean coast. However, the current seismic design code used in Libya, as outlined by Mallick, lacks the necessary provisions for incorporating the response spectra method into building design. Moreover, this code has not been updated since its initial proposal as a local standard by the Ministry of Housing in 1978, leading to significant uncertainties when estimating earthquake forces during structural design. This deficiency in the seismic design code poses a considerable risk to the safety and resilience of buildings and infrastructure in Libya [6,7].

1.1. Unveiling the seismic potential of the study area

Comprehensive seismic hazard assessments of Libya, as conducted by Kebeasy [8], Suleiman and Doser [9], Al-Heety [10], Al-Heety and Eshwehdi [11], provide detailed insights into seismicity, seismotectonics, and ground motion. These studies benefited from locally obtained ground motion data from the Libyan Digital Seismological Network (LDSN). It is worth noting that the seismically active Hün Graben may extend further north, raising concerns about the potential occurrence of larger earthquakes near densely populated coastal regions. Shaw and Jackson suggest a strong correlation between seismicity and mapped faults, indicating the possibility of extensions of known or expected faults that are currently unmapped [12].

Northeastern Libya has notable seismic potential due to its location near active fault lines and regional tectonic activity. The area sits on the northern margin of the African Plate, close to the Eurasian Plate boundary, resulting in stress accumulation and release along fault lines. The Hellenic Arc is a significant fault system in the region. Historical records and geological studies indicate past seismic events causing damage [13–15]. Assessing the seismic potential involves considering historical seismicity, active fault lines, and seismological data. Probabilistic seismic hazard analysis estimates the likelihood and intensity of future earthquakes. Ongoing research, monitoring, and updates improve understanding and accuracy to safeguard the population and infrastructure.

1.2. Peak ground motion acceleration in Benghazi city

Lagesse et al. presented a comprehensive earthquake hazard catalog for various locations in Libya, including Benghazi City [5]. Their study aimed to assess the potential risks associated with seismic activity by considering factors such as earthquake frequency, magnitude, and ground motion characteristics. They utilized extensive research, historical data, and geological features to develop probabilistic seismic hazard analysis (PSHA) models, which predict future earthquakes and their impact. The study also incorporated local geotechnical conditions and site-specific factors influencing ground shaking.

To estimate the ground motion levels, the researchers employed Ground Motion Prediction Equations (GMPEs) based on earthquake magnitude, distance from the site,

fault type, and ground conditions. Specific GMPEs were selected for each seismic source zone, including shallow-crustal, stable continental, and subduction zone GMPEs. Seismic hazard curves were calculated for different locations in Libya, indicating generally low seismic hazard levels, with slightly higher values near the Jabal al Akhdar Uplift and Hellenic Arc Subduction Zone. Interestingly, the hazard values in northeast Libya, specifically Benghazi and Derna, were found to be higher compared to northwest Libya, contradicting previous findings.

In their published paper, the authors summarized the spectra ordinates of Peak Ground Acceleration (PGA) at 0.2s, 1.0s, and 2.0s for return periods of 475 and 2475 years; this is equivalent to 10% and 2% of exceedance in 50 years, respectively. These values are specifically for sites with bedrock conditions (class B of ASCE 7-16 [1]). **Table 1** provides a summary of these values for Benghazi City.

Table 1. Spectral ordinates for PGA at 0.2 s,1.0s and 2.0s for Benghazi City.

Return period	**Period (s) and Spectral Acceleration (g)**		
	0.2	**1**	**2**
475 years	0.16	0.03	0.01
2475 years	0.39	0.09	0.04

2. Exploring the soil profile of Benghazi city

A comprehensive data collection process was conducted to assess the soil profile of Benghazi city. This involved gathering information from 65 strategically executed boreholes across the study area. The depths of these boreholes varied from 8 to 20 meters, with a significant portion reaching an approximate depth of 15 meters below ground level. **Figure 2** visually depicts the distribution and locations of the boreholes. Each borehole was utilized to collect soil properties and classifications from both undisturbed and disturbed soil samples, while also determining the groundwater table level at each location.

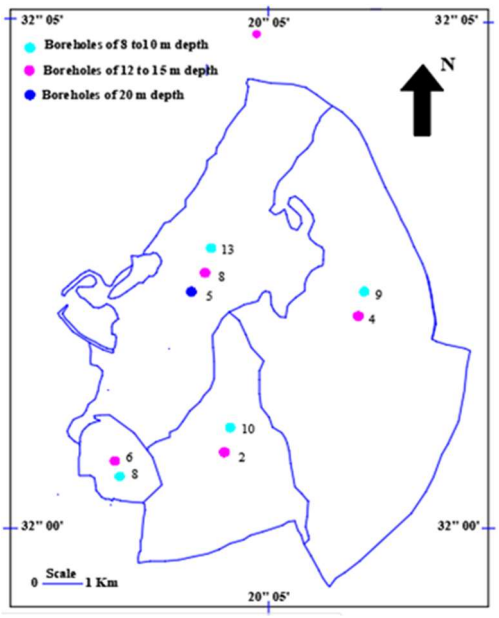

Figure 2. Borehole quantities and associated depths.

The field investigations revealed diverse soil types across the study area; the recorded Standard Penetration Test (SPT) values are corrected for split spoon configuration, borehole diameter, rod length, and energy efficiency factors. The northeast part of Benghazi city exhibited the lowest SPT blow counts, where in some instances, boreholes at a depth of 4 m displayed an overall SPT value less than 10, with certain locations even recording values below 5. However, as the depths increased, the SPT values generally increased, indicating denser soil or rock conditions. It should be noted that SPT testing is most reliable in granular soils, including silt and sand, which are prone to liquefaction and typically have lower SPT readings. At greater depths, SPT values reached 20 or more.

As we move from northeast to southwest of the city, the groundwater level gradually increases, from less than 1 m to exceeding 80 m.

The middle region of Benghazi, stretching from the northwestern and southeastern parts, comprises predominantly silty sand and marland calcarenite. As we move towards the southeast, the soil transitions to strong limestone with some shallow pockets of clay. Based on the soil profile data collected in the study area and referencing the geological information from the Benghazi sheet in Libya, the study area has been divided into different zones according to the site classification conditions specified in Table 20.3-1 of ASCE 7-16 [1].

These zones are classified from A to F, representing varying site conditions and characteristics. **Figure 3** illustrates the segmentation of the Benghazi area into these different segments, aligning with the ASCE 716 [1] site classification conditions. This categorization provides a comprehensive understanding of the site-specific considerations necessary for seismic design and assessment in the study area. By considering the specific site classification conditions, engineers and designers can make informed decisions and implement appropriate design measures to ensure the structural integrity and resilience of buildings and infrastructure in Benghazi city.

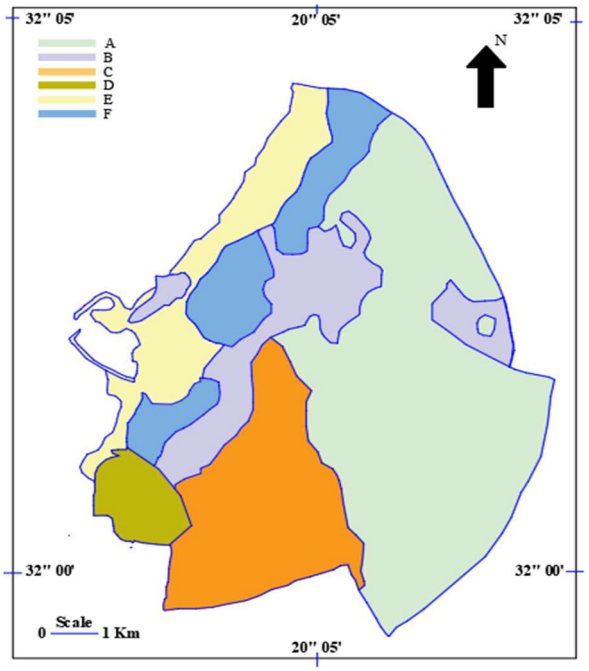

Figure 3. Alignment of Benghazi area with ASCE site classification conditions.

To gain a comprehensive understanding of the response of soil profiles in regions B, C, D, and E under the influence of six distinct earthquake events (Chi Chi, Imperial Valley, Kocaeli, Northridge, Loma Gilroy, and Parkfield earthquakes), the authors of this paper have utilized the DEEPSOIL software program developed at the University of Illinois [16]. This analysis serves the purpose of probing into the nonlinear time domain response exhibited by the soil profiles in these regions.

Additionally, the results obtained from this analysis are compared with the findings derived from the response spectra curves developed in this study, contributing to a more thorough comprehension of the soil behavior in response to seismic events.

The shear wave velocity of the soil profiles was determined using empirical formulas based on Standard Penetration Test (SPT) values, and the calculated values are presented in **Table 2**. These shear wave velocities were utilized in the DEEPSOIL analysis program.

Table 2. Shear velocity values (m/s) in Benghazi city based on SPT values for various researcher's models.

Region	SPT (Average value)	Kanai	Seed and Idriss	Hanumantharao	Uma et al	Hasançebi and Ulusay
A	-	-	-	-	-	-
B	-	-	-	-	-	-
C	45	186.50	409.20	425.51	300.79	291.80
D	25	131.07	305.00	330.48	252.01	243.34
E	12	84.38	211.31	241.03	202.06	193.96
F	5	49.90	136.40	165.42	155.25	147.99

3. Reimagining design response spectra

ASCE 7 uses the two fundamental ground motion parameters: S_S and S_1. S_S represents the "short period" spectra acceleration (T = 0.2 s), while S_1 represents the 1s (T = 1.0 s) spectra acceleration for sites on firm rock (Site Class B). which are based on the maximum considered earthquake (MCER) with a risk-based probability of approximately 10% and 2% of being exceeded within a 50-year period.

The determination of spectra response acceleration parameters for the Risk-Targeted Maximum Considered Earthquake (MCER), considering Site Class effects, is conducted using Equations (1) and (2), as outlined in ASCE 7-16 [1].

$$S_{MS} = F_a S_s \tag{1}$$

$$S_{M1} = F_v S_1 \tag{2}$$

The site coefficients F_a and F_v are obtained through interpolation from values provided in Tables 11.4-1 and 11.4-2 of ASCE 7-16 [1] respectively.

Additionally, a multiplier of 2/3 is applied to convert from the MCER basis to a slightly lower level of shaking known as the design basis earthquake (DBE).

$$S_{DS} = \frac{2}{3} S_{MS} \tag{3}$$

$$S_{D1} = \frac{2}{3} S_{M1} \tag{4}$$

The above design spectra values S_{Ds} and S_{D1} are used to construct the design spectra curves for the different site conditions through the following equations:

$$S_a = S_{DS}\left(0.4 + 0.6\frac{T}{T_o}\right) 0<T<T_0 \quad (5)$$

$$S_a = S_{DS} T_0 < T < Ts$$

$$S_a = \frac{S_{D1}}{T} \quad (6)$$

$$S_a = \frac{S_{D1}T_L}{T^2} T > T_L \quad (7)$$

where:

T: the fundamental period of the structure, s$T_o = 0.2\frac{S_{D1}}{S_{Ds}} T_s = \frac{S_{D1}}{S_{Ds}}$,

T_L: long-period transition period (s), Conservatively is taken 2 s.

The following **Figure 4a,b** illustrates the design response spectra curves corresponding to various sites classified according to ASCE 7-16 [1] from A to E. These curves represent the seismic response characteristics of the respective sites. The design response spectra curves were generated considering an importance factor (*I*) of 1 and a response modification coefficient (*R*) of 1.

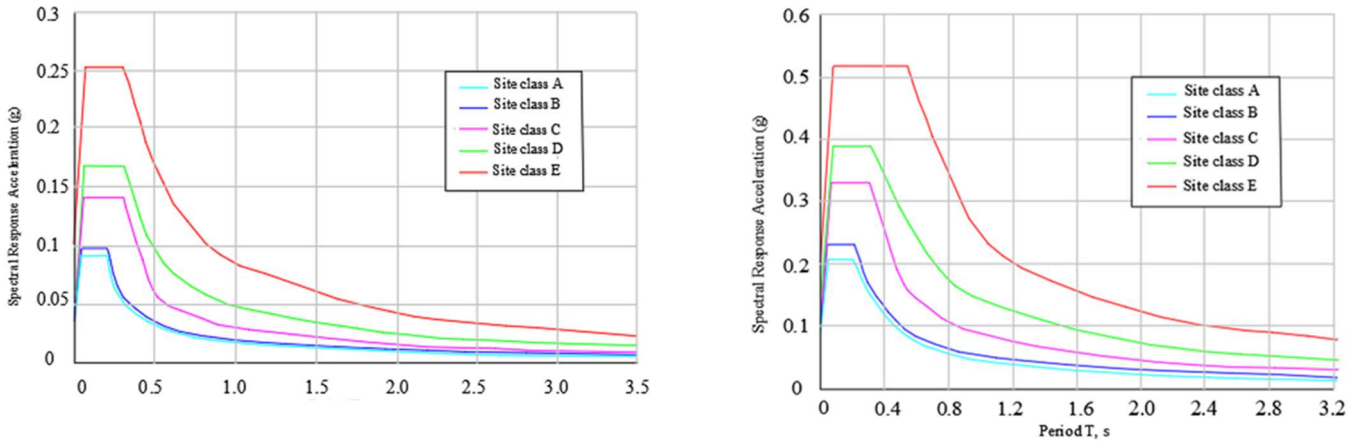

Figure 4. Design spectra curves for Benghazi city. **(a)** 475-Year Return Period; **(b)** 2745-Year Return Period.

These curves provide valuable information for engineers and designers in estimating the potential ground motion and designing structures that can effectively withstand seismic forces in accordance with ASCE guidelines. The importance factor (*I*) and response modification coefficient (*R*) are significant parameters in determining the structural response and level of seismic resistance required for different site classifications. By referring to these design response spectra curves, appropriate design measures can be implemented to ensure the safety and integrity of structures in various site conditions.

For buildings to be constructed on site type F, as defined in the ASCE 7-16 [1], several soil conditions are considered vulnerable to potential failure or collapse under seismic loading. These conditions include liquefiable soils, quick or highly sensitive clays, and collapsible or weakly cemented soils. Additionally, peat and/or highly organic clays with a depth (H) greater than 3 meters, very high plasticity clays with a depth (H) greater than 8 meters and a plasticity index (PI) greater than 75, and very thick soft to medium stiff clays with a depth (H) greater than 37 meters and an undrained shear strength (su) lower than 50 kPa fall under site type F. In these conditions, it is crucial to consider the interaction between the local site conditions and

the earthquake forces. This emphasizes the need for a thorough assessment of the specific characteristics of the site to ensure appropriate design considerations and measures are implemented to mitigate the effects of seismic activity.

4. Solution by DEEPSOIL software and comparison with response spectra curves

To capture the variations in soil shear strength with depth, each soil profile in the regions was divided into multiple layers with consistent shear wave velocity but varying shear strength. This division accounts for the well-known phenomenon of increasing soil shear strength with depth. The thickness of each layer was selected in accordance with the DEEPSOIL program's requirement, Hashash et al. [16], that the natural frequency of each layer should exceed 30 Hz. This criterion was essential for obtaining accurate results. However, specific layer thicknesses were not specified in the given information.

The analysis results for the Chi Chi earthquake time history shown in **Figure 5** are presented in **Figure 6**. The figure illustrates the amplification of peak ground acceleration (PGA) for each soil profile in response to the Chi Chi earthquake.

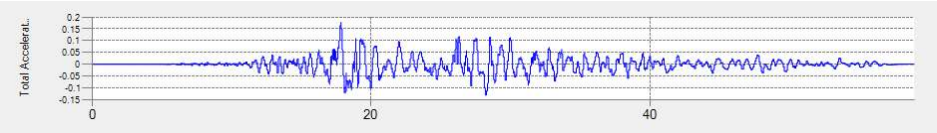

Figure 5. Time history of the chichi earthquake.

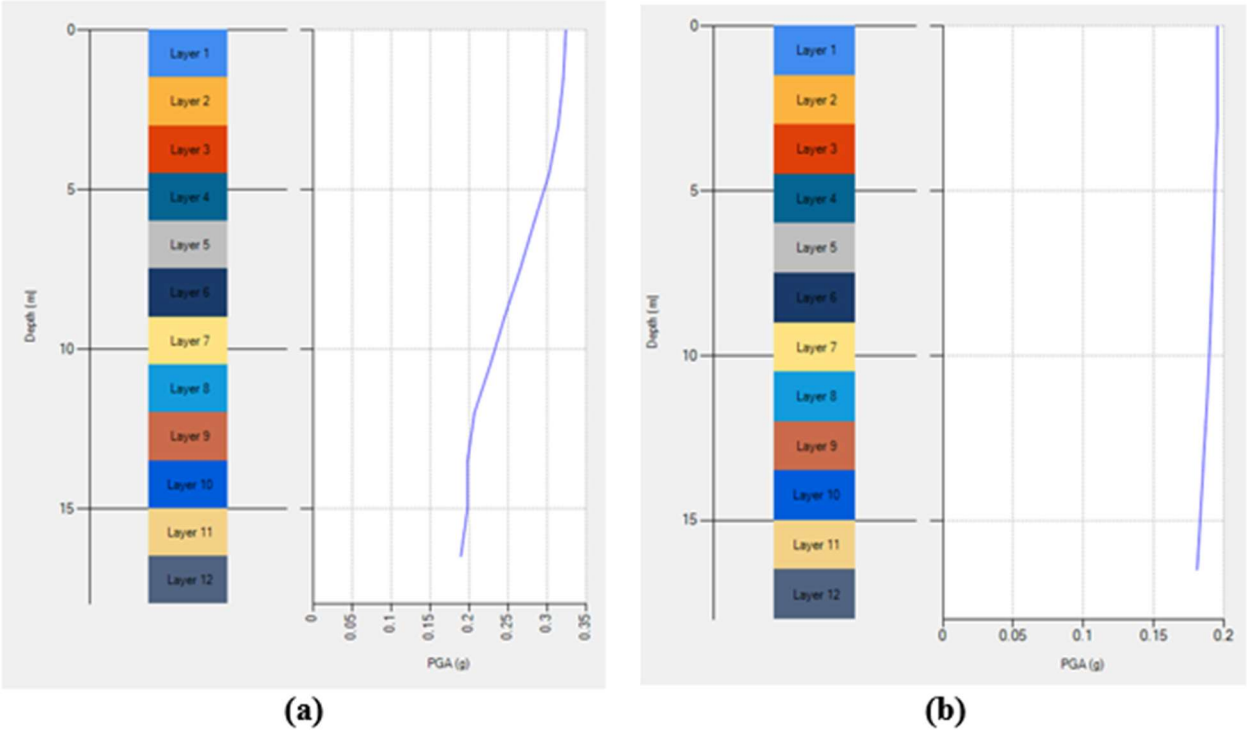

Figure 6. (*Continued*).

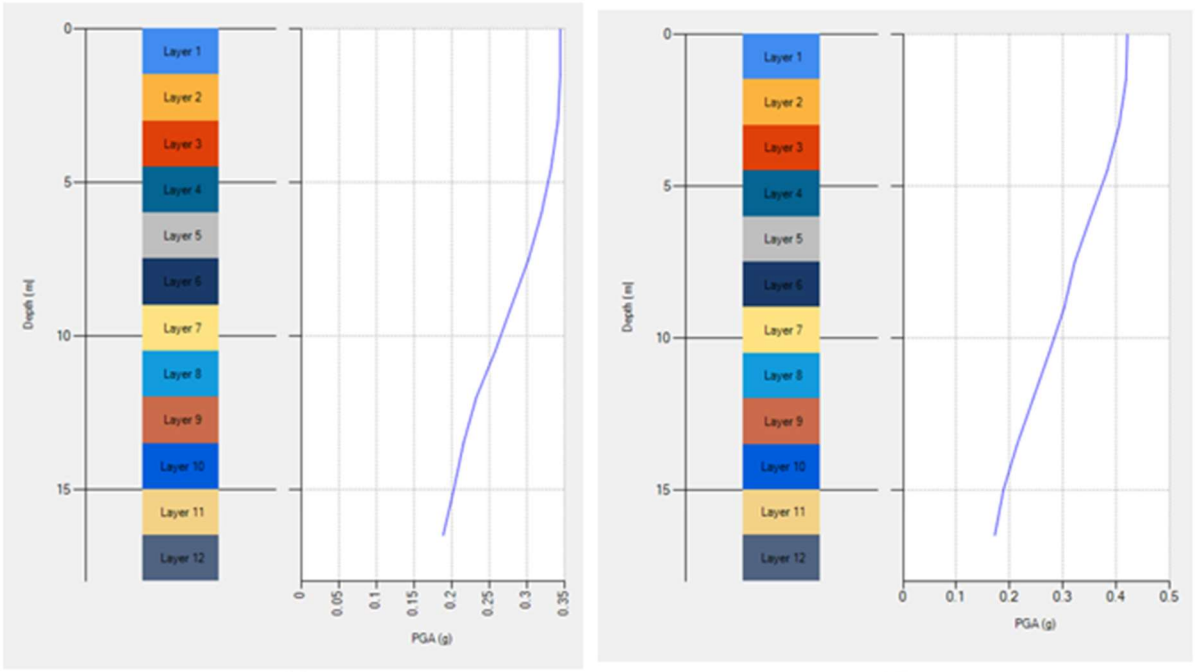

Figure 6. Soil peak ground acceleration (PGA) response during the Chi Chi Earthquake. **(a)** B region response; **(b)** C region response; **(c)** D region response; **(d)** E region response.

Table 3 provides the average PGA amplification factors for all the regions analyzed under the different earthquake events. The results indicate that as the shear wave velocity decreases, the peak ground acceleration (PGA) increases. Notably, regions C, D, and E experienced the most significant amplification, with the PGA increasing by more than two times. This implies that design earthquake loads may need to be more than doubled in regions with soft soil conditions. Therefore, it is crucial to consider soil conditions when designing earthquake loads for the Benghazi area.

Table 3. Amplification factor of all regions under various earthquakes.

Region	Imperial valley	Chi Chi	Kocaeli	Northridge	Loma Gilroy	Parkfield	Amplification factor (root mean square)
A	1.06	1.02	1.05	1.07	1.06	1.03	1.05
B	1.30	1.10	1.24	1.23	1.13	1.18	1.19
C	2.40	1.65	1.62	235	2.26	1.58	2.01
D	2.85	1.75	1.65	2.5	2.32	1.84	2.20
E	3.00	2.10	1.70	2.53	2.37	2.23	2.36

The results obtained from the DEEPSOIL software program align closely with the corresponding values derived from the developed response spectra presented in this study. This good agreement confirms the reliability of these curves for engineers and designers when considering earthquake forces in the structural design of buildings in Benghazi city.

Region F was not analyzed due to its low SPT values, indicating a potential risk of liquefaction. This exclusion highlights the need for further investigation and careful consideration of soil conditions in that particular region.

5. Conclusion

In light of the extensive rehabilitation and development programs taking place in Benghazi city, including major national projects, there is an urgent requirement to generate updated probabilistic seismic hazard maps and design response spectra specifically tailored to the city. This estimation process takes into account recent seismic activity and incorporates an enhanced earthquake design code.

The presence of soft soil conditions in regions D, E, and F within Benghazi city may result in earthquake loads that exceed twice the normal levels.

This study has presented updated probabilistic seismic hazard ground motion assessments for Benghazi city, considering different return periods and accounting for peak ground acceleration (PGA) values associated with various soil conditions. The analysis employed an extensive and current earthquake catalog as well as a customized probabilistic seismic hazard assessment (PSHA) methodology tailored to the study area.

The results obtained from the DEEPSOIL software program and the developed response spectra in this study demonstrate a strong correlation. This robust agreement confirms the reliability of the response spectra curves, providing engineers and designers with dependable information to incorporate earthquake forces into the structural design of buildings in Benghazi city.

To ensure the safety and resilience of large-scale structures and critical facilities, it is essential to conduct detailed investigations into the local site conditions at their respective locations. These investigations should encompass a comprehensive understanding of the geological and geotechnical factors that may influence seismic response.

By integrating the findings of this study into the design and construction processes, engineers and planners in Benghazi city can make well-informed decisions and implement appropriate measures to enhance the seismic performance of structures. This will contribute to the overall safety and resilience of the city's infrastructure, supporting its ongoing rehabilitation and development endeavors.

Author contributions: Conceptualization, FML and VK; methodology, VK; software, VK; validation, FML, VK and RES; formal analysis, VK; investigation, FML; resources, FML; data curation, FML; writing—original draft preparation, FML; writing—review and editing, VK; visualization, VK; supervision, FML; project administration, FML; funding acquisition, FML. All authors have read and agreed to the published version of the manuscript.

Conflict of interest: The authors declare no conflict of interest.

References

1. American Society of Civil Engineering. Minimum Design Loads and Associated Criteria for Buildings and Other Structures (7-16). American Society of Civil Engineering; 2017.

2. Erdik M, Tümsa MBD, Pınar A, et al. A preliminary report on the February 6, 2023 earthquakes in Türkiye. Available online: https://temblor.net/temblor/preliminary-report-2023-turkey-earthquakes-15027/ (accessed on 2 March 2024).
3. Karakale V, Özgür E, Ataoğlu Ş. Site Observations on Buildings' Performance in Hatay Province after Kahramanmaraş Earthquakes. El-Cezeri Journal of Science and Engineering. 2023; 10(3): 506-516. doi: 10.31202/ecjse.1253284.
4. Mallick DV. Seismic Zoning of Libya. In: Proceedings of the 6th World Conference on Earthquake Engineering; 10-14 January 1977; New Delhi, India.
5. Lagesse R, Free M, Lubkowski Z. Probabilistic Seismic Hazard Assessment for Libya. In: Proceedings of the 16th World Conference on Earthquake Engineering; 9-13 January 2017; Santiago, Chile.
6. Karakale V, Suleiman RE, Layas FM. Lateral load behavior of RC buildings exposed to fire: case study. Journal of Asian Architecture and Building Engineering. 2022; 22(1): 274-285. doi: 10.1080/13467581.2022.2026777.
7. Layas FM, Karakale V, Suleiman RE. Behavior of RC Buildings under Blast Loading: Case Study. Recent Progress in Materials. 2023; 5(3): 1-12. doi: 10.21926/rpm.2303029.
8. Kebeasy RM. Seismicity and Seismotectonics of Libya, Symposium on the Geology of Libya. Tripoli. 1978; 9: 16-21.
9. Suleiman AS, Doser DI. The seismicity, seismotectonics and earthquake hazards of Libya, with detailed analysis of the 1935 April 19, M = 7.1 earthquake sequence. Geophysical Journal International. 1995; 120(2): 312-322. doi: 10.1111/j.1365-246x.1995.tb01820.x
10. Al-Heety EA. Seismicity and seismotectonics of Libya: as an example of intraplate environment. Arabian Journal of Geosciences. 2011; 6(1). doi:10.1007/s12517-011-0347-y
11. Al-Heety EA, Eshwehdi A. Seismicity of the Northwestern Region of Libya: An Example of Continental Seismicity. Seismological Research Letters. 2006; 77(6): 691-696. doi: 10.1785/gssrl.77.6.691
12. Shaw B, Jackson J. Earthquake mechanisms and active tectonics of the Hellenic subduction zone. Geophysical Journal International. 2010; 181(2): 966-984. doi: 10.1111/j.1365-246x.2010.04551.x
13. Ambraseys NN. Material for the Investigation of the Seismicity of Libya. Libyan Studies. 1994; 25: 7-22. doi: 10.1017/s0263718900006191
14. Suleiman AB. Establishment of the Libyan National Seismological Network (LNSN): An Effort Aimed at Assessing and Mitigating Natural Disaster Risks on the National and Regional Scale. Metadata Workshop; 2009.
15. Suleiman AS, Albini P, Migliavacca P. A Short Introduction to Historical Earthquakes in Libya. Annals of Geophysics. 2004; 47: 545-554.
16. HashashYMA, Musgrove MI, Harmon JA, et al. Deepsoil 7.0, User Manual. 2020. Available online: https://www.studocu.com/id/document/institut-teknologi-sepuluh-nopember/civil-infrastructure/deepsoil-user-manual-v7/68704466 (accessed on 11 November 2023).

Building Engineering 2024, 2(1), 1226.
https://doi.org/10.24294/be.v2i1.1226

Article

Evaluation of the response of historical structures fitted with seismic-isolation

Bogdan Felix Apostol, Stefan Florin Balan*

Department of Engineering Seismology, National Institute of R-D for Earth Physics, Magurele, 077125 Ilfov, Romania
*** Corresponding author:** Stefan Florin Balan, sbalan@infp.ro

CITATION

Apostol BF, Balan SF. Evaluation of the response of historical structures fitted with seismic-isolation. Building Engineering. 2024; 2(1): 1226. https://doi.org/10.24294/be.v2i1.1226

ARTICLE INFO

Received: 2 March 2024
Accepted: 12 April 2024
Available online: 23 April 2024

Abstract: The paper highlights the performance of the seismic isolation devices installed on retrofitted buildings in reducing the seismic response when subjected to earthquakes. Two buildings from the beginning of the XXth century in Bucharest are chosen from many more, monitored over the city area. We discuss the response of these base-seismic isolated structures, relying on good quality data acquired from the recent strong earthquake (3 November 2022, M_W = 5.0). Elastic response spectra computed from recordings at two levels of each structure are used, placed under and right above the isolating layer. At one building, the existence of previous recordings and the particularity of the sensors allow a comparison with the other two relatively recent medium-intensity earthquakes. The assessment is carried out in terms of maximum acceleration $a_{max,}$ measured at certain levels in each structure, spectral acceleration amplitude SA_{max}, and spectral-peak corresponding period. We find that the base-isolation methodology is effective in reducing the response of the building right above the isolating layer, an observation valid for both structures, all components of the recordings, and spectral acceleration values. Moreover, the outcomes from the modal evaluation performed prior to rehabilitation and the seismic isolation process are presented by pointing out a higher newly acquired fundamental period of the isolated structures.

Keywords: historical retrofitted buildings; seismic isolation performance; spectral parameters; Vrancea earthquakes; medium intensity seismic activity

1. Introduction

The instrumented buildings performance over the Bucharest area has already become a continuously undergoing task with valuable results [1–3]. The level of performance enhancement and the state of damage for a large variety of structures were assessed in terms of years and type of construction, design, usage destination, and utility [4–7]. Detailed structural response data provide a potential for adjustments in the design process. The present study is focused on two old, seismically base-isolated buildings and retrofitted buildings located in the Bucharest city area. The selected buildings erected at the beginning of the XXth century are hosting administrative and educational activities.

The dynamic behavior during the earthquake of 3 November 2022, M_W = 5 [8] is analyzed. This is a continuation of a previous work, where the impact analysis of the methodology used for near-real-time response was carried out [9]. The monitoring system has proved its capabilities to ensure the data flow and make them available in a shorter time after the earthquake to the authorities, civil protection, decision makers, etc. Basically, near-real-time (i.e., right after a potentially damaging event and/or during its aftershock sequence) structure response-based status was assessed. The novelty herein consists in an evaluation of the response of a previously seismically

isolated building, now endowed with new sensors located above/under the isolating layer. A comparison is made with other old buildings' responses, already having the same type of deployment for the isolated device and sensors. The responses under another two recent earthquakes are brought into attention for the same structures, and a discussion is made from the recorded parameters and spectral-related characteristics perspective (maximum acceleration a_{max} considered at certain levels in each structure, spectral acceleration amplitude SA_{max}, spectral-peak corresponding period [3]).

2. Methodology, procedure, and building characteristics

Isolation devices are capable of sustaining dynamic strength at strong displacements induced by the ground motions. The soil particularity consisting of soft, weak-consolidated, without cohesiveness mechanical characteristics, usually included in sedimentary layering or basins, can be an issue in building design. Nonlinear phenomena in these cases add weight to the general dynamic behavior. The difficulties that have to be surpassed consist in different amplification at the ground level, a high oscillating site period, or strong variability of the involved parameters over the interest area. Therefore, a thorough seismic hazard, correct site response, and geotechnical information knowledge are compulsory for these zones. As regard the concept of isolation procedure, it must raise the flexibility and damping and withstand service loads.

The undesired response of the structures may be avoided by taking necessary measures in terms of design, as emerged from a thorough understanding of the seismicity and ground motion characteristics. The seismic isolating devices can be used in order to reduce the structure vulnerability. In this regard, among the techniques largely used in some countries, the base isolating method has been proved successful (USA, Japan, Italy, and New Zealand) in relation to the seismicity specificity and geophysical and geological characteristics of the interest areas [10–19]. In general practice of seismic isolation, the main aim is to reduce the seismic demand on the structure. The buildings considered in this study were endowed with the above-mentioned base-isolating systems. The isolation system does not absorb the earthquake energy, which is deflected through the dynamics of the system. The technique involves a certain level of damping that is helpful to avoid possible resonance. By decoupling a structure from the direct action of the horizontal components of a ground motion, it acquires a fundamental frequency that is much lower than its fixed-base frequency and the usual predominant frequencies of the ground motion. Based on the modal evaluation of the fundamental vibration period, an insight into the benefits of using base isolators in structures could be gained by considering the special case of a two degrees of freedom structure, which is separated from the ground by some type of isolating device [20–22]. The study relies either on a single degree of freedom model, with possible nonlinearities included, or, more exactly, on a system of coupled elastic oscillators [23–28].

Some buildings host costly equipment and contents that must be protected against earthquakes and be operational after a severe ground shaking; such buildings are those designated for research, health care, telecommunication, nuclear power plants, etc. Buildings constructed by following old seismic codes with conventional resistant

design approaches cannot protect the people or the valuable equipment that is contained. The constructions evaluated in this study were not randomly chosen, but taking into account their age, importance, and design. One of the chosen buildings is an administrative one, hosting the Bucharest City Hall (BCH), the other being the "Victor Slavescu" building, belonging to Bucharest University of Economic Studies (ES). For both, the isolating devices were implemented at certain elevation points in the basement, according to the design and retrofitting specifications (**Table 1**). By this procedure, the suprastructure was decoupled to some extent from its foundation, which continues to move rigidly with the soil during an earthquake.

Table 1. Seismic isolated buildings (general characteristics) [5].

No.	Name of building/monitored period	No. of floors	Year of construction	Structural system
1	General City Hall of Bucharest (BCH)/ 2017–2021, 2022-present	B + GF + 3F + Attic	1906. The building was consolidated after 2010 and was equipped with seismic insulators in the basement	Brick masonry with reinforced concrete floors with turned caissons
2	"Victor Slavescu" Building, Academy of Economic Sciences (ES) 2011-present	B + GF + 2F + Attic	1905, retrofitted in 2009, 2011 (added seismic isolators)	Brick masonry with truss roof

Legend: B–Basement; GF–Ground Floor; F–Floor.

For the modeling of the isolating system of the BCH building, some types of constitutive laws were used, such as those characterizing a linear elastic or biaxial-hysteretic behavior [29]. The preliminary analysis of the isolated building involved dynamic linear and non-linear computation of time-history type. A direct integration of the differential equations of motion based on recorded accelerograms for the 1977, 1986, and 1990 strong earthquakes was employed, imposing the input condition of 0.24 g for the scaled maximum acceleration at the ground level. The data were taken at a location that is the only one where recordings for the 1977 earthquake exist; also, it has the advantage of similar local soil features. The results show a reduction of 11–12 times for the relative displacement values on one horizontal direction and 7–8 times on another, of the seismic action at a vibration period of the isolated building of 3.3 s. As regards the stress reduction, the values are 4 and 3 times smaller for the two horizontal seismic action directions. At the same time, the relative displacements distribution at the level of each floor on the vertical shows a general solid-rigid trend of displacement, with a general displacement at isolated interface level of approximately 20–22 cm and 28–30 cm for horizontal directions of the seismic action, under the assumption of peak ground acceleration of 0.24 g, according to P100-1/2006, which was the code in force at that time [29,30].

For the ES building, the preliminary study [31] employed the same computation program (ETABS NON-LINEAR v.8.4.5.), relying on the finite element method. Modal analysis for the resistance structure has considered the first six vibration modes, as follows: three of one horizontal translational direction, two of the other horizontal direction (perpendicular to the former), and one of general torsion. All these vibration periods are in the 0.08–0.79 s range. Following the reduction of stress and displacement values, stress values diminished by 2.4 and 2.5 times for two horizontal seismic action directions, and relative displacements reduced by 3.5 at story levels and 2.5 at ground level, respectively, for both horizontal seismic action directions. The

vibration period of the isolated structure was 2.8 s. At the same time, the relative displacement distribution at each level on the vertical shows a general solid-rigid trend of displacement, with a general displacement at the isolated interface level of approximately 15 cm and 20 cm for the horizontal directions of the seismic action [31].

The comparison was made to the performance of the two buildings using the same analyses carried out by employing specific design parameters without taking into account the isolation device characteristics.

The BCH building was seismically monitored with 4 sensors located on the isolated structure from the year 2017; starting with the year 2022, one sensor was deployed above/under the isolator layer. The ES building is permanently monitored by the National Institute for Earth's Physics (NIFP) from the year 2011, with seismic accelerometers at two different levels (status at 31 December 2022) [32].

The characteristics of the most recent considered earthquake were as follows: date and triggered time 3 November 2022, 06:50:25, local time, lat. 45.4895° N, long. 26.5262° E, focal depth 148.8 km, M_W = 4.9, ROMPLUS Catalogue, 2023 [33], 122 km epicentre distance for Bucharest, and M_W = 5 according to the near-real time release of the Internal Report [8]. Herein, a magnitude 5 is considered; as for the other two earthquakes, the values in ROMPLUS are identical to those in the internal reports released in the very short aftermath of the recordings [33–35]. Moreover, the data processing and computation of the parameters are based on the mentioned references, according to the purpose of the work that involved a near-real-time evaluation of the response.

The earthquake mentioned above belongs to the intermediate-depth Vrancea seismic region and was felt with intensities about V on the MSK scale in the epicentre area and III-IV in Bucharest. For the other two seismic events, the characteristics are: date and triggered time: 28 October 2018, 03:38:11 local time, lat. 45.6079°, long. 26.4068°, focal depth 148 km, M_W = 5.5, and 31 January 2020, 04:26:48 local time, lat. 45.6937°, long. 26.6918°, focal depth 118 km, M_W = 4.8 (**Table 2**) [33]. The intensity on the Mercalli scale was VI and IV, respectively, in the epicentre zone [34,35].

Table 2. The characteristics of the three considered earthquakes [33].

Date	Time [UTC]	Depth [km]	Mw
28 October 2018	00:38:11	148	5.5
31 January 2020	01:26:47	118	4.8
3 November 2022	03:50:25	148.8	5.0

3. Response analysis

The instrumental data from the two selected structures, subjected to a medium-intensity earthquake, were processed in terms of peak recorded accelerations and spectral accelerations at two levels, below and right above the isolating devices. Recordings from three-component accelerometers, installed on these levels, consisting of acceleration time histories are pre-processed: baseline corrected and filtered using a 4th order Butterworth bandpass (0.2–25 Hz) filter. The limits were set for obtaining a good signal-to-noise ratio, and also a taper function was applied to the data to allow

the spectral-related calculation. The sensors are of the same types, and the recordings and data processing are performed according to the standard procedure by the automated Antelope seismological system, developed by Boulder Real Time Technologies [36] and installed at the National Data Centre (NDC) of the National Institute for Earth's Physics [32]. It includes program applications and module units that are run in order to ensure data acquisition, automatic seismic event detection, location, magnitudes, and other parameters computation or evaluation. The ground shaking and building seismic response parameters processing (in terms of peak ground acceleration, maximum buildings recorded acceleration, spectral acceleration, and related fundamental or oscillation period) are the tasks that are accomplished through this system.

The processing of the data releases elastic response spectra in terms of spectral pseudo-acceleration with 5% damping (**Figures 1** and **2**). The information is depicted as engineering parameters, that are maximum acceleration a_{max} recorded on three directions (two horizontal, NS, EW, and one vertical Z), maximum spectral acceleration (SA_{max}) from elastic response spectra, and corresponding oscillation periods T_{SAmax} (**Tables 3** and **4**).

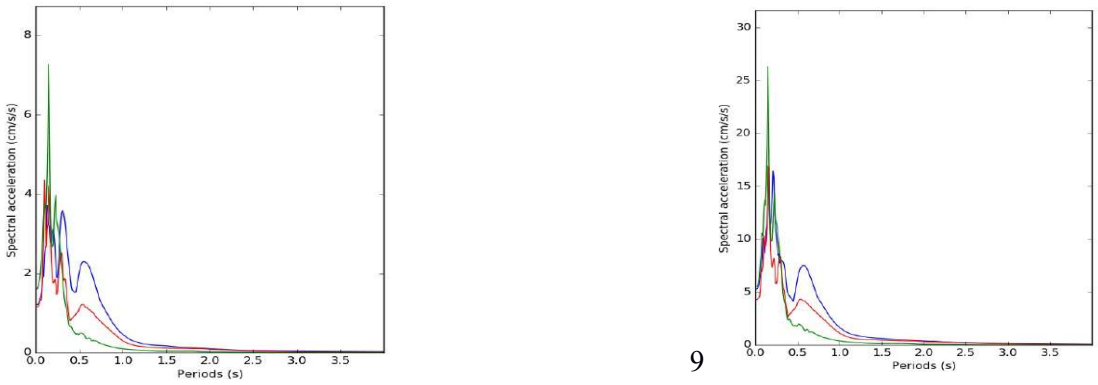

(a) **(b)**

Figure 1. Elastic response spectra for the BCH building above **(a)** and under **(b)** isolating layer from recordings of the 3 November 2022 earthquake M_W= 5 [9].

Legend: red: N-S, blue: E-W, green: Z (vertical) components of recording.

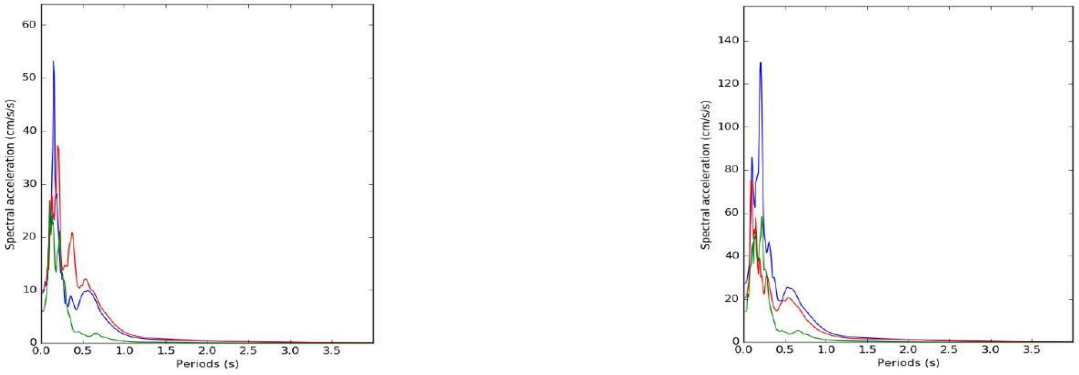

(a) **(b)**

Figure 2. Elastic response spectra for the ES building above **(a)** and under **(b)** isolating layer from recordings of the 3 November 2022 earthquake M_W= 5 [9].

Legend: red: N-S, blue: E-W, green: Z (vertical) components of recording.

Table 3. Base-isolation performance at BCH and ES buildings for 3 November 2022, M_W = 5.0 earthquake [9].

Date/ Magnitude M_W/ Depth	Station		Component								
			N-S			E-W			Z		
			a_{max} (cm/s^2)	SA_{max} (cm/s^2)	T_{SAmax} (s)	a_{max} (cm/s^2)	SA_{max} (cm/s^2)	T_{SAmax} (s)	a_{max} (cm/s^2)	SA_{max} (cm/s^2)	T_{SAmax} (s)
3 November 2022 M_W = 5, 148.8 km	ES	Above	9.83	37.29	0.2	9.48	53.24	0.15	6.04	26.85	0.1
		Under	20.59	74.95	0.09	27.45	130.08	0.21	14.25	58.28	0.22
	BCH	Above	1.16	4.35	0.1	1.21	3.72	0.13	1.62	7.28	0.15
		Under	4.32	16.95	0.15	5.33	16.45	0.21	5.54	26.36	0.15

Table 4. Response spectra parameters at the ES building for three seismic events (M_W = 5.5, 5.0, 4.8).

Station ES	Earthquake	Component								
		N-S			E-W			Z		
		a_{max} (cm/s^2)	SA_{max} (cm/s^2)	T_{SAmax} (s)	a_{max} (cm/s^2)	SA_{max} (cm/s^2)	T_{SAmax} (s)	a_{max} (cm/s^2)	SA_{max} (cm/s^2)	T_{SAmax} (s)
under	28 October 2018 M_W = 5.5	131.77	347.53	0.14	100.42	416.61	0.15	50.64	228.89	0.13
above		34.04	108.28	0.16	47.39	196.25	0.16	25.7	133.19	0.12
under	3 November 2022 M_W = 5.0	20.59	74.95	0.09	27.45	130.08	0.21	14.25	58.28	0.22
above		9.83	37.29	0.2	9.48	53.24	0.15	6.04	26.85	0.1
under	31 January 2020 M_W = 4.8	11.69	36.02	0.08	13.34	43.81	0.31	6.24	26.49	0.11
above		5.75	18.42	0.42	5.86	23.43	0.34	4.57	22.27	0.11

In **Table 3**, a clear decrease of the peak acceleration recorded by the seismic sensors above the isolating device can be seen. This is valid for all components of the recordings and at both buildings. Also, the maximum spectral accelerations, as shown in **Figures 1** and **2** and **Table 3**, display lower values above the isolator. The corresponding oscillation periods are all in a low and narrow range of 0.09–0.22 s, excluding the danger of possible resonance effects. Another observation is higher values for recordings at the ES building in comparison with the other building (BCH) at both instrumented levels. We note that this phenomenon is encountered at the ES building for other earthquakes of comparable magnitude in comparison to any other instrumented structure in Bucharest city area (**Table 4**) [2,3]. The higher recorded values at the ES building for low and medium magnitudes can be a matter of local soil conditions or due to the building dynamic characteristics themselves.

Moreover, at this building more data of good quality are available, both under and above the isolating layer; therefore, one can infer the dependence to the earthquake magnitude. From **Table 4,** it may be seen the increase of the recorded values with the earthquake's source level of strength for all measured and processed parameters.

We can also note the higher values of the oscillation period corresponding to spectral amplitude (**Figures 1** and **2**, **Table 4**) for the 31 January 2020, M_W = 4.8 earthquake, which is the lower magnitude considered in this study. These higher values are encountered for horizontal components and above the isolated layer. The other values (i.e., under isolation and both for the vertical Z component) follow the general tendency of laying in a rather low and confined range, as it is expected for these types of earthquakes. It is worth the focal depth range of ~122–149 km for these

three earthquakes, besides sharing the same focal area (Vrancea-intermediate depth) and moderate magnitude (**Table 2**).

In **Table 5**, the reduction of the seismic amplitudes is shown in terms of maximum recorded accelerations in order to have a quantitative representation for the outcome of the employed technique. For this purpose, the ES building is considered, for which more recordings exist with this type of isolating device. It is the first building to benefit from this technique and a proper sensor deployment, allowing for this type of analysis. All three earthquakes are of medium magnitude, originating in the same focal area. The reduction coefficient represents the ratio for under/above values, and the reduction percentage stands for its corresponding percent in the weight reduction. As it may be seen, the average for three relatively recent seismic events is over 50% on the two horizontal components and below this value for vertical ones. The maximum average reduction is attained for the N-S component, with 59% the higher value, corresponding to the strongest earthquake (74%, M_W = 5.5).

Table 5. Base-isolated device performance in terms of reduction coefficient and corresponding reduction percentage for the ES building for three seismic events.

Building ES, earthquake/magnitude	**Component N-S**		**Component E-W**		**Component Z**	
	Reduction coefficient	**Reduction percentage**	**Reduction coefficient**	**Reduction percentage**	**Reduction coefficient**	**Reduction percentage**
28 October 2018 M_W = 5.5	3.87	74%	2.11	52.8%	1.97	41.8%
3 November 2022 M_W = 5.0	2.09	52%	2.89	65.5%	2.35	57.9%
31 January 2020 M_W=4.8	2.03	51%	2.27	56%	1.37	26.7%
Average	2.66	59.0%	2.42	58.1%	1.89	42.13%

The consequence of the base-isolating procedure consists in raising the fundamental period for the supra-structure, or the shift of the base-supra-structure ensemble, and splitting in two values if they are considered as two coupled oscillators [23,37,38]. In some cases, this increase is considered a goal itself. However, the benefits of this outcome and its limits of applicability are discussed in correlation to various types of parameters, from the source characteristics to local effects and specific soil responses [5,37]. The structure design and dynamic features are also taken into consideration [6,7,18,19,39,40].

According to Iordachescu and Iordachescu [29], Marmureanu et al. [31] previous studies a shift towards 2.5–3 s for fundamental periods can be obtained. Given the oscillation periods of the strong and damaging earthquakes that hit Bucharest of over ~1 s, but not exceeding 1.6 s (until now!) [41–44], it can be stated that the technique has accomplished this particular point. According to the current Romanian seismic design code P100-1/2013 [45], three values of the control period T_c = 0.7, 1.0, and 1.6 s are considered in the design response spectra provided by this regulation regarding the whole Romanian territory. In this respect, for Bucharest city, a control period of T_c = 1.6 s and 0.3 g as the value for the design ground acceleration is recommended.

At the same time, the values for the soil predominant periods accepted for the city area [46,47] are in the 0.7–1.9 s domain [48]. In particular, values between 0.08–

0.79 s for the first six normal modes of vibration are suggested. It follows that the value of ~2.8 s for the ES building fulfills the objective of extracting the structure from the dangerous range of maximum amplitude of the response spectral at that site [29,31].

From **Table 4**, one may see the lower range for this parameter (oscillation period for the maximum spectral amplitude) at both buildings for all components (0.09–0.42 s). Among them, the higher values correspond to the ES building and are encountered for the less strong earthquake of 31 January 2020, for the horizontal components.

Turning back to the BCH structure, one may notice as specificity the higher values on vertical component Z in terms of maximum acceleration and spectral acceleration, in comparison with the horizontal ones, as long as, usually for this component (Z), the values are the lowest at both buildings. This situation corresponds to the two strongest earthquakes discussed here (3 November 2022, M_W = 5.0 and 28 October 2018, M_W = 5.5).

4. Discussion

During the last decade, certain types of structures were selected, according to their specificity (old buildings, retrofitted, destination and functionality, etc.), and continuously seismic monitored. Several instrumented buildings from Bucharest city and one from the epicentre area (city of Focsani, Vrancea region) have provided important data about the seismic performance of earthquake protection systems and checked out the performance goals and design issues in major earthquakes [3,6]. Out of them, two buildings, Bucharest City Hall (BCH) and "Victor Slavescu" (ES), were constructed at the beginning of the XXth century under inappropriate seismic design regulations. These structures, together with another one, a historical monument (the Arch of Triumph), have been retrofitted in order to endure the future strong earthquakes. Thereafter, the decision was taken for these buildings to be equipped with base-isolating systems (seismic isolators and viscous dampers) for reducing the lateral forces induced by strong seismic movement. One of them (BCH) has been recently endowed with a pair of seismic sensors at the basement level, above/under the isolating system. The response of the two buildings BCH and ES, subjected to medium-intensity earthquakes, was analyzed in terms of peak accelerations and spectral accelerations. Improvement in seismic response of these isolated buildings in Bucharest was evaluated.

5. Conclusions

According to our analysis, the main objective of the base isolating system is considered accomplished, as the efficiency of this type of isolation device during Vrancea-intermediate depth-originating earthquakes was proved.

The methodology has proved its aim to reduce the response of the building right above the isolating layer in comparison with values under the device. The observation is valid for both structures, all components of the recordings, and for the spectral acceleration values.

These results can be useful for quantifying the benefits and implications of seismic isolation subjected to moderate seismic events that occur in the Vrancea seismic region in terms of response spectra analysis.

The seismic monitoring of buildings has proved its capability to give a rapid damage assessment after a strong seismic event, based on the level of accelerations the buildings experienced, therefore mitigating the seismic risk for densely populated areas in Romania. Detailed structural response data provide the potential for adjustments to the design process. For the earthquake protection systems, as is the seismic base isolation case, the improvements in terms of structural response can be quantified, and the performance of the isolator devices can be assessed based on measured data.

For the specific situation of Bucharest city, including geology and corresponding site effects, the dynamic parameters must be assessed accordingly in order to estimate the proper seismic response.

The goal pursued was to take advantage of this performance while proving the potential benefits of this certain type of anti-seismic isolating technique applied to old/historical structures located in the Bucharest city downtown. The practical implications of the findings pertain to seismic risk management for this highly populated zone.

Evaluating the performance of the base-isolating technique through comparing the responses under and right above isolating devices may be useful for implementing this procedure on other structures sharing the same similarities in terms of age or design.

Data from this paper could help future practitioners and policymakers decide if using a seismic isolation system for a certain building could mitigate its vulnerability to earthquakes.

Local amplification effects and site effects are important as they determine seismic ground motion specificity and dynamic building behavior ultimately. Therefore, these retrofitting techniques should be considered and recommended for certain urban areas in tight connection to regional seismicity and seismic source specificity, considering typical seismic structural response and local effects-related parameters.

Author contributions: Conceptualization, methodology, formal analysis, BFA and SFB. All authors have read and agreed to the published version of the manuscript.

Funding: This paper was carried out within Program Nucleu SOL4RISC, contract number 24N/03.01.2023, supported by Ministry of Research, Innovation and Digitization, project no. PN23360202.

Conflict of interest: The authors declare no conflict of interest.

References

1. Aldea A, Demetriu S, Albota E, et al. Instrumental response of buildings. Studies within JICA project in Romania. In: Proceedings of the International Symposium on Seismic Risk Reduction. 26-27 April 2007; Bucharest, Romania. pp. 157-170.

2. Balan SF, Tiganescu A, Apostol BF et al. Post-earthquake warning for Vrancea seismic source based on code spectral acceleration exceedance. Earthquakes and Structures. 2019; 17(4): 365-372. doi: 10.12989/eas.2019.17.4.365.
3. Apostol BF, Balan SF, Danet A. Post-Earthquake Assessment for Seismic Risk Mitigation in Romania: Case-Studies Based on Recorded Data. Romanian Journal of Physics. 2023; 68(7-8): 804-804. doi: 10.59277/romjphys.2023.68.804
4. Demetriu S, Borcia IS, Seismic Response of Instrumented Buildings during Vrancea Earthquakes. Bulletin of the Technical University of Civil Engineering, Structural Mechanics and Structural Engineering. 2001; 2: 1-11.
5. Balan SF, Apostol BF, Tiganescu A. Soil Conditions and Structural Typologies for Seismic Isolation of Buildings, in Cities Exposed to Strong Earthquakes Hazard. Scientific Papers. Series E. Land Reclamation, Earth Observation & Surveying, Environmental Engineering. 2021; 10: 128-134.
6. Tiganescu A, Toma-Danila D, Grecu B, et al. Current status and perspectives on seismic monitoring of structures and rapid seismic loss estimation in Romania. 1st Croatian Conference on Earthquake Engineering; 22-24 March 2021; Online Conference. doi: 10.5592/co/1crocee.2021.120
7. Tiganescu A, Craifaleanu IG, Aldea A, et al. Evolution, Recent Progress and Perspectives of the Seismic Monitoring of Building Structures in Romania. Frontiers in Earth Science. 2022; 10. doi: 10.3389/feart.2022.819153
8. National Institute of Research and Development for Earth Physics. Internal Seismic Report. National Institute of Research and Development for Earth Physics; 2022.
9. Balan SF, Apostol BF, Danet A. Efficacy of the Seismic Isolating Systems for Historical Buildings under Moderate Seismic Forces. Land Reclamation, Earth Observation & Surveying, Environmental Engineering; 2024.
10. NCh 2745. Analysis and Design of Buildings with Seismic Insulation. Chilean Association of Seismology and Earthquake Engineering. National Institute for Standardization; 2013.
11. BSL. The Building Standard Law of Japan. Ministry of Land, Infrastructure, Transport and Tourism, Tokyo, Japan; 2009.
12. EN 1998-1. Eurocode 8: Design of structures for earthquake resistance-Part 1: General rules, seismic actions and rules for buildings. European Committee for Standardization; 2005.
13. AASHTO. Guide Specifications for Seismic Isolation Design. American Association of State Highway and Transportation Officials; 1999.
14. ASCE standard (American Society of Civil Engineers). ASCE/SEI 7-10. Minimum Design Loads for Buildings and Other Structures. ASCE standard (American Society of Civil Engineers); 2010. pp. 7-16.
15. NTC. Ministero Delle Infrastrutture. NTC; 2008.
16. GB 50011. National Standard of the People's Republic of China. China Architecture & Building Press; 2010.
17. Ministry of Construction and Housing and Communal Services Russian Federation. S. P. 14. Construction in Seismic Areas (Russia). Ministry of Construction and Housing and Communal Services Russian Federation; 2014.
18. Pietra D, Pampanin S, Mayes RL, et al. Design of base-isolated buildings. Bulletin of the New Zealand Society for Earthquake Engineering. 2015; 48(2): 118-135. doi: 10.5459/bnzsee.48.2.118-135
19. Yenidogan C, Erdik M. A comparative evaluation of design provisions for seismically isolated buildings. Soil Dynamics and Earthquake Engineering. 2016; 90: 265-286. doi: 10.1016/j.soildyn.2016.08.016
20. Taniguchi T, Der Kiureghian A, Melkumyan M. Effect of tuned mass damper on displacement demand of base-isolated structures. Engineering Structures. 2008; 30(12): 3478-3488. doi: 10.1016/j.engstruct.2008.05.027
21. Bratosin D, Apostol BF, and Balan SF. Avoidance strategy for soil-structure resonance by considering nonlinear behavior of the site materials. Romanian Journal of Physics. 2017; 62(808): 5-6.
22. Apostol BF. A resonant coupling of a localized harmonic oscillator to an elastic medium. Romanian Reports in Physics. 2017; 69: 116.
23. Liu T, Zordan T, Briseghella B, et al. An improved equivalent linear model of seismic isolation system with bilinear behavior. Engineering Structures. 2014; 61: 113-126. doi: 10.1016/j.engstruct.2014.01.013
24. Syed IA. Simplified design guidelines for seismic base isolation in multi-story buildings for Bangladesh National Building Code (BNBC). International Journal of the Physical Sciences. 2011; 6(23): 5467-5486. doi:10.5897/IJPS11.795
25. Ye K, Xiao Y, Hu L. A direct displacement-based design procedure for base-isolated building structures with lead rubber bearings (LRBs). Engineering Structures. 2019; 197: 109402. doi: 10.1016/j.engstruct.2019.109402
26. De Domenico D, Ricciardi G, Takewaki I. Design strategies of viscous dampers for seismic protection of building structures: A review. Soil Dynamics and Earthquake Engineering. 2019; 118: 144-165. doi: 10.1016/j.soildyn.2018.12.024

27. Bratosin D. Nonlinear restraints in seismic isolation of buildings. Proceedings of the Romanian Academy-Series A: Mathematics, Physics, Technical Sciences, Information Science. 2008; 9(3): 1-7.
28. Bratosin D, Sireteanu T. Hysteretic damping modeling by nonlinear Kelvin-Voigt model. Proceedings of the Romanian Academy, Series A: Mathematics, Physics, Technical Sciences, Information Science. 2002; 3: 99-104.
29. Iordachescu A, Iordachescu E. Rehabilitation of Town Hall Building of Bucharest through the Seismic Isolation Method. Revista Construcții. 2007; 6: 6-10.
30. Ministry of Transport, Construction and Tourism (M.T.C.T). P 100-1/2006. Seismic Design Code-Part I: Earthquake Resistant Design of Buildings. Ministry of Transport, Construction and Tourism (M.T.C.T); 2006.
31. Marmureanu GH, Iordachescu A, Iordachescu E, et al. A Study on Seismic Equipment Instrumentation of the Academy of Economic Science-Victor Slavescu (ASE) Building Retrofitted through Base-Isolating Method. Designer European Business Consult; General Designer: European Business Consult, Expertise Designer: S.C. Proescom Srl. and National Institute for Earth Physics; 2009.
32. Cristian Neagoe, Liviu Marius Manea, Constantin Ionescu. Romanian complex data center for dense seismic network. Annals of Geophysics. 2011; 54(1). doi: 10.4401/ag-4809
33. Romplus. Romanian earthquake catalogue. National Institute for Earth Physics, Magurele, Romania. 2023. Available online: www.infp.ro/romplus. (accessed on 10 January 2024).
34. National Institute of Research and Development for Earth Physics. Internal Seismic Report. National Institute of Research and Development for Earth Physics; 2018.
35. National Institute of Research and Development for Earth Physics. Internal Seismic Reports. National Institute of Research and Development for Earth Physics; 2020.
36. BRTT-Boulder Real Time Technologies. Available online: https://brtt.com/ (accessed on 2 January 2024).
37. Luco JE. Effects of soil–structure interaction on seismic base isolation. Soil Dynamics and Earthquake Engineering. 2014; 66: 167-177. doi: 10.1016/j.soildyn.2014.05.007
38. Miranda CJ. Revisiting seismic isolation from a modal energy perspective. Proceedings of the Romanian Academy. 2006; 7(1): 55-64.
39. Spyrakos CC, Koutromanos IA, Maniatakis ChA. Seismic response of base-isolated buildings including soil–structure interaction. Soil Dynamics and Earthquake Engineering. 2009; 29(4): 658-668. doi: 10.1016/j.soildyn.2008.07.002
40. Yenidogan C. Earthquake-Resilient Design of Seismically Isolated Buildings: A Review of Technology. Vibration. 2021; 4(3): 602-647. doi: 10.3390/vibration4030035
41. Pérez-Rocha LE, Avilés-López J, Tena-Colunga A. Base isolation for mid-rise buildings in presence of soil-structure interaction. Soil Dynamics and Earthquake Engineering. 2021; 151: 106980. doi: 10.1016/j.soildyn.2021.106980
42. Marmureanu G. Certainties/Uncertainties in Vrancea hazard and seismic risk evaluation. Romanian Academy Publishing House; 2016.
43. Marmureanu G, Balan FS, Marmureanu A. Larger peak ground accelerations in extra-Carpathian area than in epicenter. Available online: https://meetingorganizer.copernicus.org/EGU2020/EGU2020-7215.html?pdf (accessed on 3 January 2024).
44. Mărmureanu A, Ionescu C, Grecu B, et al. From National to Transnational Seismic Monitoring Products and Services in the Republic of Bulgaria, Republic of Moldova, Romania, and Ukraine. Seismological Research Letters. 2021; 92(3): 1685-1703. doi: 10.1785/0220200393
45. Ministry of Regional Development and Public Administration (M.D.R.A.P.). P 100-1/2013; Seismic Design Code-Part I: Earthquake Resistant Design of Buildings. Ministry of Regional Development and Public Administration (M.D.R.A.P.); 2013.
46. Mândrescu N, Radulian M, Mărmureanu Gh. Geological, geophysical and seismological criteria for local response evaluation in Bucharest urban area. Soil Dynamics and Earthquake Engineering. 2007; 27(4): 367-393. doi: 10.1016/j.soildyn.2006.06.010
47. Mandrescu N, Radulian M, and Marmureanu G. Microzonation of Bucharest: Geology of the Deep Cohesionless Deposits and Predominant Period of Motion. Revue Roumain de Geophysique. 2004; 48: 120-1.
48. Wenzel F, Lungu D, Novak O, et al. Vrancea Earthquakes: Tectonics, Hazard and Risk Mitigation. Springer Netherlands; 1999. doi: 10.1007/978-94-011-4748-4

Building Engineering 2024, 2(1), 1231.
https://doi.org/10.59400/be.v2i1.1231

Article

Net zero energy analysis and energy conversion of sustainable residential building in Muscat, Oman

Muthuraman Subbiah[1,*], Hafiz Zafar Sharif[1], Sivaraj Murugan[2], Kumar Ayyappan[3]

[1] Department of Engineering, University of Technology and Applied Sciences, Muscat 133, Oman
[2] Department of Mechanical Engineering, Rohini College of Engineering and Technology, Tamilnadu 629401, India
[3] Department of Applied Sciences, Amrita College of Engineering and Technology, Tamilnadu 629901, India
*** Corresponding author:** Muthuraman Subbiah, muthu9678@gmail.com

CITATION

Subbiah M, Sharif HZ, Murugan S, Ayyappan K. Net zero energy analysis and energy conversion of sustainable residential building in Muscat, Oman. Building Engineering. 2024; 2(1): 1231. https://doi.org/10.59400/be.v2i1.1231

ARTICLE INFO

Received: 21 March 2024
Accepted: 28 April 2024
Available online: 13 May 2024

Abstract: The building sector is the predominant consumer of primary energy globally. The building sector accounts for around 40% of global energy production. Net Zero Energy Buildings (NZEBs) are highly suggested by energy experts as an effective option to alleviate the strain on primary energy sources caused by the building sector. The disparity between energy performance predictions provided during the design phase and the actual energy performance of residential buildings is mostly attributed to a limited comprehension of the components that influence energy consumption and the constraints of whole building simulation software. The objective of this research was to perform a comparison analysis of the expected and actual energy consumption of a prototype net-zero energy house built at the University of Technology and Applied Sciences in Muscat. The Hourly Analysis Programme (HAP V4.2) was utilised to forecast the energy consumption of a Net Zero Energy Building (NZEB) at HCT, taking into account the availability of an Energy Recovery Ventilator (ERV) and the absence of an ERV. The newly built house underwent a one-month testing phase to fulfil many duties according to competition regulations. One of the main goals was to generate on-site energy through photovoltaic panels, producing an amount proportional to the energy consumed by the house. Upon comparing the actual energy consumption data with the simulated result, it was noticed that the actual energy demand of the house was around 20% lower than the prediction made by the simulation tool.

Keywords: sustainable buildings; energy conservation; ecohouse; energy demand; Net Zero energy

1. Introduction

The building sector is the foremost consumer of primary energy globally. The International Energy Agency (IEA) estimated in 2023 that the final energy consumption of the building industry reached 2794 million tonnes of oil equivalent (Mtoe), which is double the amount recorded between 1971 and 2019. The buildings sector is expected to increase its demand for primary energy supply by an additional 838 million tonnes of oil equivalent (Mtoe) by 2035, compared to the demand in 2019. This would put significant strain on the primary energy supply. The building sector accounts for 40% of global energy production [1]. However, according to the Internal Energy Agency [2], residential buildings in Oman consumed 47.5% of the energy produced in 2022, which is 7.5% higher than the average global demand for the building sector. There are four generally utilised definitions based on site energy, source energy, cost, and emission-based criteria. The building designer chooses the net-zero site energy option to meet the energy code criteria. A site zero energy building

(ZEB) is a building that produces an equal or greater amount of energy than it uses over the course of a year, when measured at the building's location [3].

Net Zero Energy Buildings (NZEBs) are highly suggested by energy experts as an effective option to alleviate the strain on primary energy sources caused by the building sector. The significance of this solution is acknowledged universally by governments, NGOs, unions, and agencies. A number of projects and orders worldwide are focused on NZEB solutions, which aim to reduce the reliance on primary sources of energy. Some notable examples include the ENERPOS French national project [4], IEA-SHC task 40 [5], IEA task 25 [6], IEA task 38 [7], IEA-SHC task 53 [8], APEC project [9], EPBD recast 2019/31/EU [10], ASHRAE vision 2020 [11], Executive Order (EO) 135 [12], Zero Energy Ready Home Programme [13], and Solar Decathlon competitions worldwide [14]. The design of a Net Zero Energy Building involves the combination of renewable energy sources and passive house principles to minimise reliance on primary energy sources and decrease CO_2 emissions. The design of Net Zero Energy Buildings consists of two primary parts. The first step focuses on enhancing energy efficiency through efficient building architecture, systems, appliances, operation, maintenance, and changes in user behaviour. The second step entails meeting the remaining energy needs with on-site renewable generation [15]. Model simplifications, discrepancies between forecast and final construction, occupant behaviour, commissioning, controls, management, and maintenance are among the main factors that negatively impact the actual energy consumption of residential buildings compared to simulated results. This report provides an energy analysis of the Eco home located at HCT in Muscat, Oman. The house was specifically built to attain net-zero energy status with the installation of a photovoltaic (PV) system on the roof, in the form of a canopy. Section 2 provides an introduction to the regulations of the Eco home competition. Section 3 explains the research technique used to design the house. Section 4 emphasises the energy efficient elements incorporated into the Eco house at HCT in Muscat, Oman, in order to decrease the house's energy use. Section 5 gives the energy analysis results obtained using HAP software. It also includes a comparison between the actual energy consumption of the Eco house, as recorded by the data acquisition system (DAS), and the energy consumption anticipated by the HAP software.

2. Research methodology

The Eco home team initiated the project by adopting an integrated building design strategy and examining the international energy conservation guidelines of 2018. The project was separated into three distinct phases: design, conceptual, and development. During the design phase, the building's conceptual energy analysis is conducted using the TAS software 'Thermal Analysis Simulation' developed by Environmental Design Solutions Limited (EDSL), available at http://www.edsl.net/main/. The Green Nest team took into account the following recommendations during the conceptual design and development stages for the building: The building has a rectangular shape that is expanded on the north-south axis. It is a two-story structure with a courtyard. The East and West facades have fewer openings. The building has a window-to-wall ratio of 20%, meaning that 20% of the

walls are made up of windows. The southern facade and roof are shaded to reduce sun exposure. Following the conceptual energy analysis, a comprehensive building energy analysis was conducted using HAP software to determine the energy consumption of the structure.

This analysis was based on the architectural building information model (BIM), which includes detailed information about the thermal properties of the walls, windows, floors, and roof construction. During the final phase of the design process, a comprehensive energy analysis of the building was conducted using HAP software. This software offered specific information on the annual energy consumption of lighting, electrical, and HVAC systems. The Greenest team utilised the PV Watts calculator to optimise the energy supply from solar panels and meet the energy demand of the house throughout the construction phase. The results of the HAP and PVWatts research assisted the team in identifying the most suitable HVAC equipment and optimal solar system size. The research methodology chosen for designing a Net Zero Energy Building is summarised in **Figure 1**.

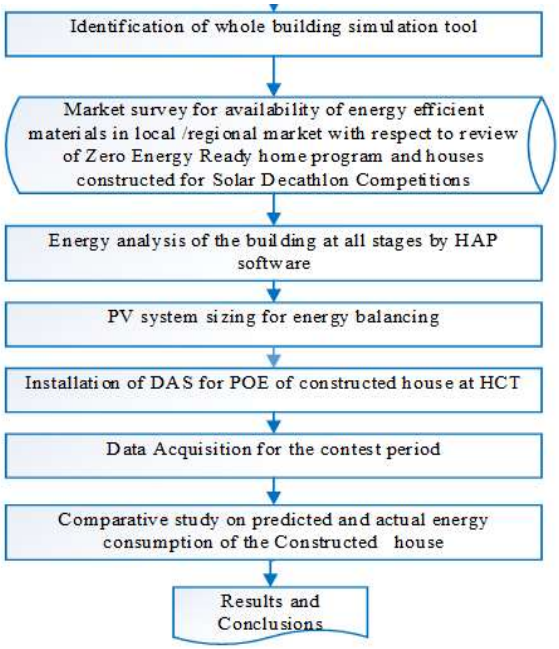

Figure 1. Research methodology.

3. Eco house at HCT, UTAS Muscat, Oman

The floor space of the two-story Eco house at Higher College of Technology (HCT), University of Technology and Applied Sciences (UTAS), Muscat, Oman, is 230.7 m^2. The ground floor of the house comprises a majlis, dining room, living room, and kitchen. The first level comprises a master bedroom, a children's bedroom, and a guest bedroom. The house is equipped with a grid-tied solar energy system with a DC rating of 22.8 kW. This system is positioned on the top of the house in the form of a canopy, facing south at a fixed angle of 5°. It is designed to maintain a temperature range of 25 °C–27 °C and a relative humidity range of 50%–70% throughout the year.

The house is built using insulated concrete forms for the walls, which have a U value of 0.233 W/m^2K. The roof is made of hollow core slabs with a U value of 0.339

W/m^{2}K, and it is also covered with solar panels. The windows are double-glazed with a shading coefficient of 0.48, and their overall U values range from 3.25 to 4.1 W/m^{2}K. The certified wooden doors have U values ranging from 3 to 3.5 W/m^{2}K. These features help to achieve the desired energy balance during the competition period.

The house is equipped with energy recovery ventilators, with one unit for each story. Additionally, there are variable refrigerant volume heat pumps, with one unit for each floor. These systems are designed to maintain comfortable conditions throughout the year. A solar hot water system with electric backup, freezer, refrigerator, clothes washer, induction oven, dishwashers, home electronics, and internal and external lighting were installed in the house to fulfil various tasks as advised by the competition organiser.

Figure 2. Eco house at University of Technology and Applied Sciences, Muscat, Oman.

The house is outfitted with a data acquisition system (DAS) that monitors and records performance and administrative measurements for various contests related to comfort zone, refrigerator, freezer, hot water, clothes washer, cooking, dishwasher, lighting, home electronics, and energy balance. This is illustrated in the accompanying **Figure 2**. The completed Eco house at the University of Technology and Applied Sciences in Muscat incorporated several sustainable elements, as outlined in **Table 1**. The Eco house team successfully achieved the goal of creating a Net Zero Energy Building for the competition duration, thanks to these groundbreaking innovations.

Table 1. Sustainable features of the house.

S/No	Sustainable feature description	S/No	Sustainable feature description
1	Appropriate sizing/ number of floors	11	Cross flow ventilation
2	North-South oriented building	12	Certified wood (FSC certified)
3	Insulation of wall (NADURA ICF), roof and floor	13	Vertical green wall (west wall)
4	Double glazed windows	14	LED lighting
5	External shading	15	5-Star energy efficient appliances
6	Food and low water plants	16	Solar hot water system
7	Eco friendly refrigerant	17	Energy generation onsite by solar panels
8	Energy recovery ventilator	18	Solar mobile charging station
9	Grey water treatment system	19	Real-time energy and water usage display
10	Rainwater collection	20	Paints with low toxicity

4. Energy analysis results

The graphic displays the mean HVAC load on the central cooling coil. The summer profile was derived using the mean data collected from May to October 2023, including the months of July and August 2023. This is illustrated in the accompanying **Figure 3**. The significant surge observed between 8:00 am and 10:00 am can be attributed to the arrival of six students who engaged in various activities such as cooking, water heating, turning on electric lights, and operating home appliances.

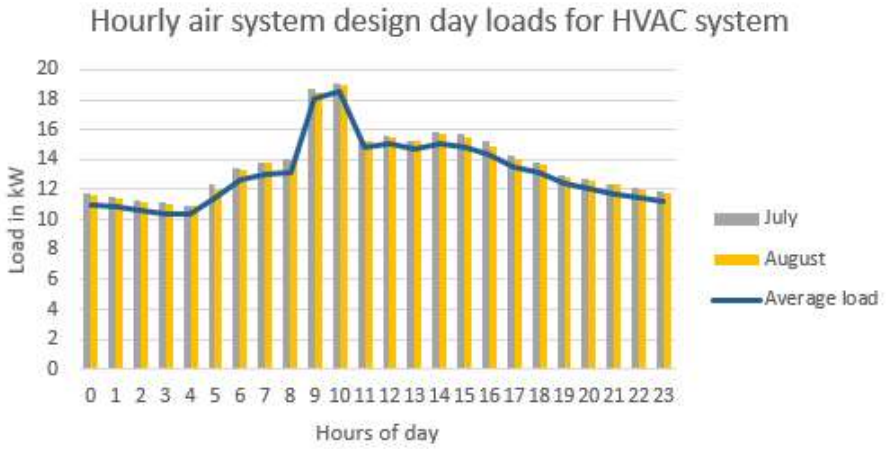

Figure 3. Hourly air system design day loads for HVAC system.

Figure 4 displays the simulation results for the zone design load of the building envelope, lighting, people, and electric equipment. The findings revealed that electric equipment contributed 30% of the overall cooling load, while windows, walls, roofs, and the lighting system collectively accounted for 7% to 14% of the load.

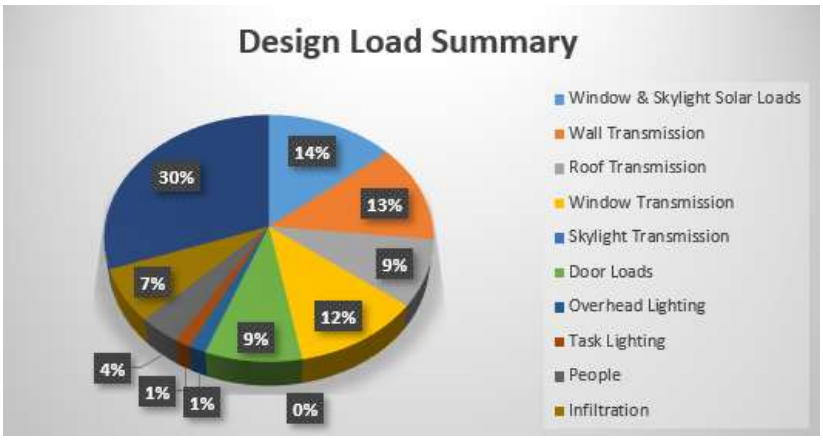

Figure 4. Zone design load summary.

The data presented in **Figure 5** demonstrate the energy requirements of a standard-sized house and an eco-friendly dwelling in Muscat. The projected findings indicate that the energy consumption of the Eco house is 61.2% lower than that of a standard house, mostly due to a reduction of 69.5% in HVAC load and 23.16% in non-HVAC load.

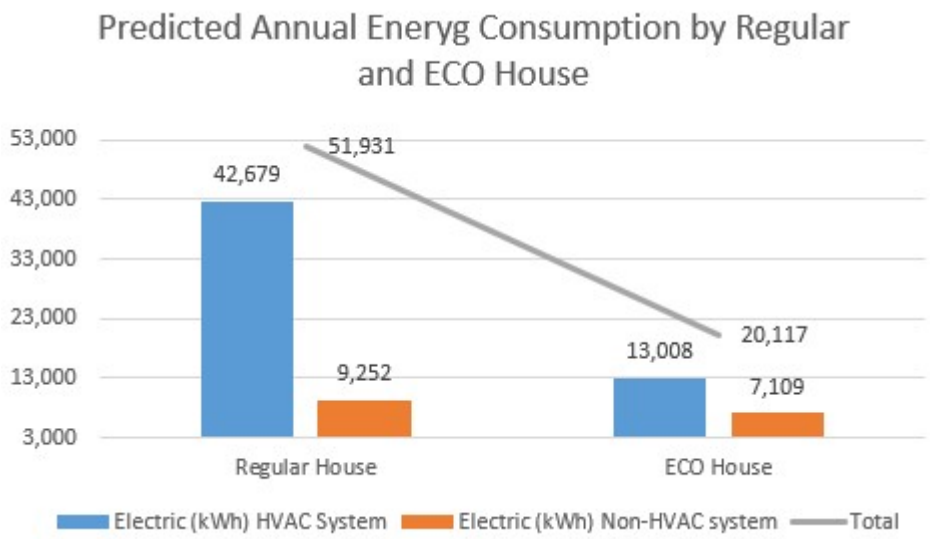

Figure 5. Annual Energy Consumption by Regular and Eco house.

The Building Energy Index is a metric that quantifies the overall energy use of a residential property over the course of one year, divided by the entire floor area of the property. In this instance, the analysis solely projected the BEI values for the regular house and Eco house while also providing the suggested BEI for green buildings (see **Figure 6**). This was due to the lack of available data on the Eco house's energy consumption for a complete year under the same operating conditions specified in the competition criteria in **Table 1**. The Building Energy Index (BEI) of the Zero Energy House at HCT is 87.20 kWh/m^2/year, which is significantly lower than the BEI of 225 kWh/m^2/year for a conventional house of the same size in Muscat. This information is based on the predictions made by the simulation tool and aligns with the suggested BEI for green buildings in Malaysia [15].

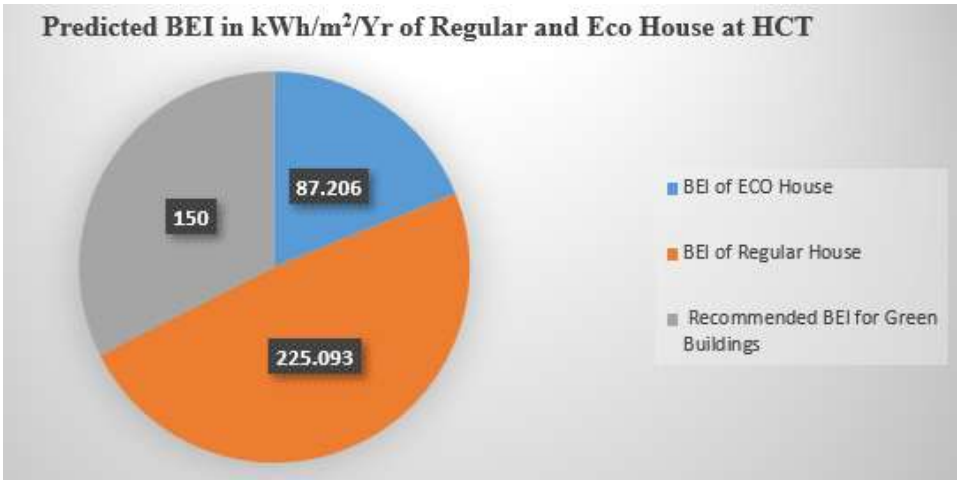

Figure 6. Building Energy Intensities of different houses.

The figure displays the energy consumption results of both HVAC and non-HVAC systems over the competition period, including both the actual and forecasted values (see **Figure 7**). A comparison of the results showed that the energy consumption predicted by the HAP software for the HVAC system was only 5%

higher than the actual energy consumed during the competition period. However, the energy consumption predicted by the HAP software for the non-HVAC system was 27.56% higher than the actual energy consumed by the house. This difference can be attributed to the non-operation of the Energy Recovery Ventilator and Grey Water Pump during the competition period. The HVAC system of the house accounted for 44% of the overall energy consumption during the contest time, while the non-HVAC system accounted for the remaining 56%.

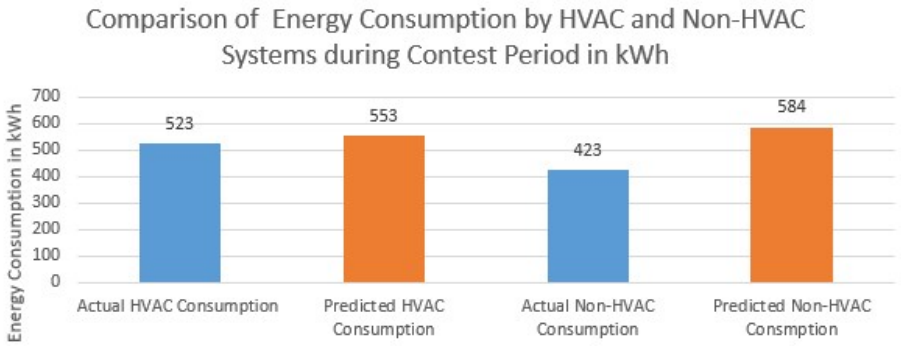

Figure 7. Comparison of energy consumption by HVAC and Non-HVAC system during contest period in kWh.

The graphic displays the real energy consumption of electrical equipment throughout the contest period. The energy consumption breakdown is as follows: HVAC system accounted for 55.26% of the total energy, lighting system for 14.95%, cook top for 6.84%, water heater for 6.31%, fridge-freezer for 3.8%, dishwasher for 2.68%, clothes washer for 0.95%, home electronics for 1.06%, DAS for 1.08%, and unmeasured electrical load for 1.57% (see **Figure 8**).

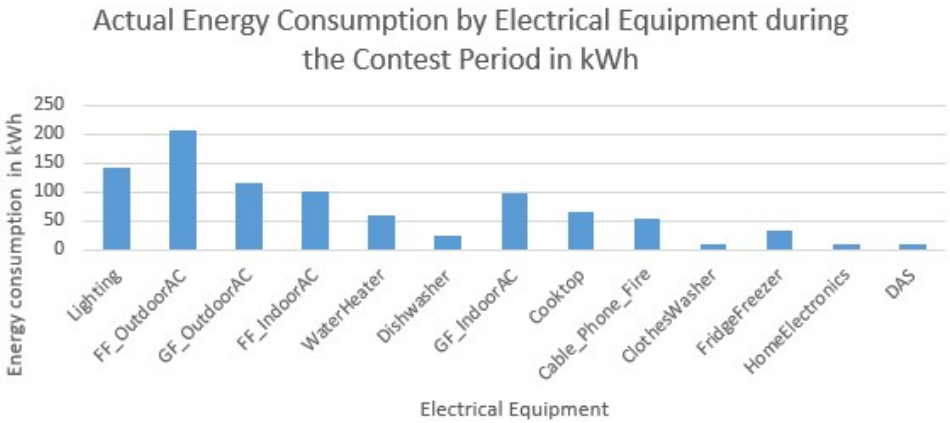

Figure 8. Actual energy consumption by electrical equipment during the contest.

The PV watt calculator estimated that the solar system installed in the Eco house would produce approximately 34,239 kWh of electricity in one year. The PV watts calculator forecasted a production of 2183.5 kWh for the competition month, from 18 September to 16 December 2023. However, the solar system installed on the roof only generated 2167.77 kWh during that period, which is a deviation of only 0.73% from the expected numbers, as depicted in **Figure 9**.

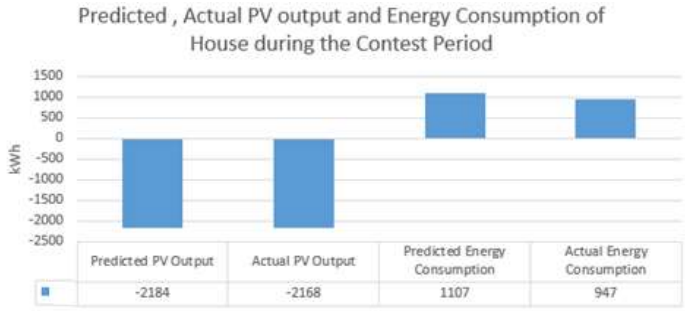

Figure 9. Predicted and actual PV output and energy consumption of house during the contest period.

The comparison of energy consumption and energy production data, as shown in **Figure 10**, indicates that the Eco house is able to consistently attain a net zero energy status on a monthly basis. The findings from **Figure 10** indicate that the Eco house is capable of generating an additional 32.7% of energy during the peak energy-demanding month of June and up to 64.5% extra energy during the month of February, which has the lowest energy demand. The findings indicated that by implementing a safety margin of 10%, a house can attain a net zero energy status on an annual basis while requiring a 40% smaller photovoltaic (PV) system for installation.

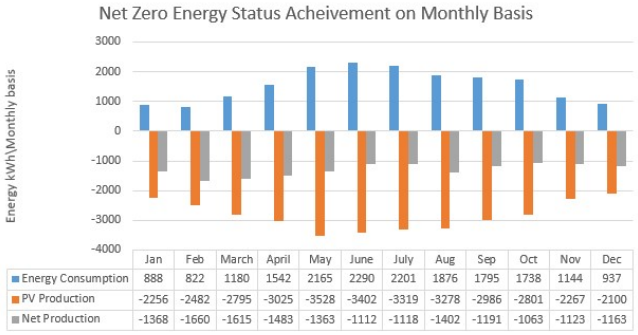

	Jan	Feb	March	April	May	June	July	Aug	Sep	Oct	Nov	Dec
Energy Consumption	888	822	1180	1542	2165	2290	2201	1876	1795	1738	1144	937
PV Production	-2256	-2482	-2795	-3025	-3528	-3402	-3319	-3278	-2986	-2801	-2267	-2100
Net Production	-1368	-1660	-1615	-1483	-1363	-1112	-1118	-1402	-1191	-1063	-1123	-1163

Figure 10. Net zero energy status achievement on monthly basis.

The data acquired from the installed data acquisition system in the Eco house, as shown in **Figure 11**, indicates that the building has successfully achieved the status of a Net Zero Energy Building during the contest time. Furthermore, it has exported a total of 1221 kWh of energy to the grid.

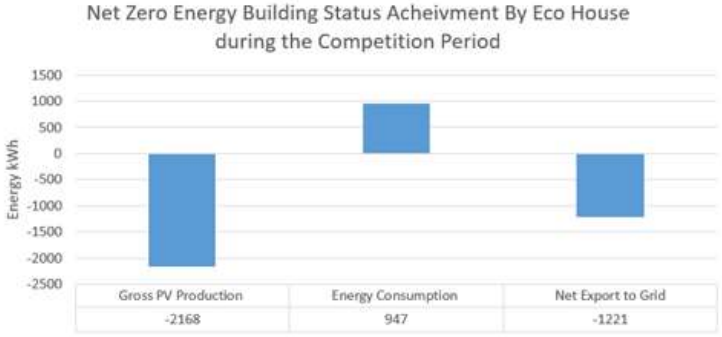

Figure 11. Net zero energy building status achievement in contest month.

5. Conclusion

The building sector is characterized by high energy consumption, and the cost of energy represents a substantial portion of its daily operational expenses. The building sector obtains energy from the grid, which is generated by thermal, hydro, nuclear, and off-site renewable energy sources, as well as on-site renewable energy sources. This study evaluated the energy consumption of a 230 m^2 Eco house and found that the HVAC system, lights, induction hob, water heater, and freezer are the primary energy consumers in the house. Identifying sustainable components in the design of an Eco house is considered a valuable strategy to attain a low Building Energy Index (BEI) of 87 kWh/m^2/year in comparison to a typical house with a BEI greater than 225 kWh/m^2/year. The analysis suggests that the amount of electricity consumed by the household was lower than the amount of electricity produced by the grid-tied solar system during the competition period. This project stands out as an early and successful endeavour to create a net-zero energy building in Muscat. The positive outcomes of this project provide strong encouragement to construct several net-zero energy buildings in the GCC region. This will help to decrease energy consumption and reduce the building sector's contribution to CO_2 emissions.

Author contributions: Conceptualization, methodology, simulation, analysis, MS; writing—original manuscript preparation, MS and HZS; introduction, HZS; review papers and method writing of the manuscript, SM; supervision, visualization, and editing of the manuscript, KA. All authors have read and agreed to the published version of the manuscript.

Acknowledgments: The University of Technology and Applied Sciences, HCT-Muscat provided support for this work through the National Level Eco house Competition, which was funded by The Research Council and Ministry of Higher Education in Oman.

Conflict of interest: The authors declare no conflict of interest.

References

1. Kamal MA. Design Concepts and Architectural Interventions. Acta Technica Napocensis: Journal of Civil Engineering & Architecture. 2022; 5(1).
2. International Energy Agency. Updating building energy codes to ensure the sustainability of our global energy future. Available online: https://www.iea.org/publications/freepublications/publication/PolicyPathwaysModernisingBuildingEnergyCodes.pdf. (accessed on 1 May 2024).
3. Torcellini P, Pless S, Deru M., et al. An Examination of the Definition of Zero Energy Buildings- A Classification System Based on Renewable Energy Supply Options. U.S. Department of Energy Office of Scientific and Technical Information; 2010. doi: 10.2172/983417
4. Garde F, Lenoir A, Scognamiglio A, et al. Design of Net Zero Energy Buildings: Feedback from International Projects. Energy Procedia. 2014; 61: 995-998. doi: 10.1016/j.egypro.2014.11.1011. hal-01153038
5. International Energy Agency. Oman's electricity and heat production data for the year 2018. Available online: htps://www.iea.org/statistics/statisticssearch/report/?country=Oman&product=electricityandheat (accessed on 1 May 2024).
6. Baldwin C, Cruickshank CA. An evaluation of solar cooling solutions for residential use in Canada. Journal Energy Procedia. 2022; 30: 495-504. doi: 10.1016/j.egypro.2022.11.059

7. DOE. Energy-efficient home that produces as much energy as it consumes, known as a Zero Energy Ready Home. Available online: https://energy.gov/eere/buildings/zero-energy-ready-home (accessed on 1 May 2024).
8. ASHRAE. The American Society of Heating, Refrigerating and Air-Conditioning Engineers. ASHRAE's Vision 2017 aims to create buildings that achieve net zero energy use. Available online: https://www.ashrae.org/file%20library/doclib/public/20170226_ashraevision2017.pdf (accessed on 1 May 2024).
9. Federal Centre. The Federal Facilities Environmental Stewardship & Compliance Assistance Centre. Available online: https://www.fedcenter.gov/programs/eo13514. (accessed on 1 May 2024).
10. Garde F, David M, Lenoir A, Ottenwelter E. Towards Net Zero Energy Buildings in Hot Climates: Part 1, New Tools and Methods. Available online: https://task40.iea-shc.org/Data/Sites/1/publications/DC-TP6-Garde-2011-11.pdf (accessed on 1 May 2024).
11. EHDC. Rules for the Oman EcoHouse Design Competition. Available online: https://ecohouse.trc.gov.om/ecohouse/about/rules (accessed on 1 May 2024).
12. EPBD. Available online: http://www.buildup.eu/sites/default/files/content/EPBD2019_31_EN.pdf. (accessed on 1 May 2024).
13. Mugnier D, Fedrizzi R, Thygesen R, et al. Underground hydrogen storage: a review. Journal Energy Procedia. 2022; 70: 470-473. doi: 10.1016/j.egypro.2022.02.149
14. A study comparing best practices and energy reduction results of almost zero energy buildings in the APEC region. Available online: https://aimp2.apec.org/sites/PDB/_layouts/APEC/print.aspx?List=4c96f8e1-0610-4a91-98c3-e5ed15907cbb&ID=1661 (accessed on 1 May 2024).
15. Khin A, Lau K, Salleh E, et al. The study investigates the impact of shading devices and glass configurations on cooling energy reduction in high-rise office buildings located in hot-humid climates, specifically focusing on the case of Malaysia. International Journal of Sustainable Built Environment. 2016; 1: 1-13.

Building Engineering 2024, 2(1), 1301.
https://doi.org/10.59400/be.v2i1.1301

Article

Architecting sustainability performances and enablers for grid-interactive efficient buildings

Riadh Habash*, Md Mahmud Hasan

School of Electrical Engineering and Computer Science, University of Ottawa, Ottawa, ON K1N 6N5, Canada
*** Corresponding author:** Riadh Habash, rhabash@uottawa.ca

CITATION

Habash R, Hasan MM. Architecting sustainability performances and enablers for grid-interactive efficient buildings. Building Engineering. 2024; 2(1): 1301. https://doi.org/10.59400/be.v2i1.1301

ARTICLE INFO

Received: 17 April 2024
Accepted: 16 May 2024
Available online: 31 May 2024

Abstract: Today, grid-interactive, efficient buildings are gaining popularity due to their potential sustainability performances through their ability to learn, adapt, and evolve at different scales to improve the quality of life of their users while optimizing resource usage and service availability. This is realized through various practices such as management and control measures enabled by smart grid technologies, interoperability, and human-cyber-physical security. However, despite their great potential, the research of those technologies still faces various challenges. These include a lack of communication and control infrastructure to address interpretability, security, cost barriers, and difficulties balancing occupant needs with grid benefits. Initially, system modelling and simulation are promising approaches to address those challenges ahead of time. It involves consideration of complex systems made up of components from various research domains. This paper addresses the above practices, highlighting the value of integrating technology and intelligence in the planning and operation of buildings, both new and old. It provides a way to educate architects and engineers about this emerging field and demonstrates how these practices can help in creating efficient, resilient, and secure buildings that contribute to occupant comfort and decarbonization.

Keywords: grid-interactive efficient building; digital twins; building information modeling; human-in-the-loop; human-cyber-physical security

1. Introduction

Buildings account for 40% of the primary energy consumption, 75% of the electricity consumption, and 35% of the greenhouse gas (GHG) emissions in the US [1], and probably a similar range worldwide. Accordingly, buildings have a major role in reducing GHG emissions and quantifying building resources such as energy efficiency and demand flexibility, which are vital to defining an optimal decarbonization route. This is enabled today by a set of new concepts coming up around smart grid technologies, such as microgrids, demand response (DR), load scheduling strategies, peer-to-peer electricity trading, energy storage services, energy hubs, energy prosumers, distributed energy resources (DER), etc. that make the functionality of the building more complex. In this new context, the energy is intermittent, distributed, mobile, and can be stored [2].

Grid-interactive efficient buildings (GEB) are networked systems consisting of hardware and software accompanied by natural, human, and machine intelligence. Several major sustainability performances underpin these buildings as a part of the urbanization system, including occupant comfort, energy efficiency and sufficiency, low carbon, controlled adaptivity, and demand flexibility. This is realized through management and control measures enabled by smart grid technologies, interoperability, and cyber-physical security [3]. Interoperability is even more

significant in the context of GEBs, which rely heavily on communication within a building and between buildings and the grid. By embracing intelligent GEBs, it is possible to speed up the journey towards a sustainability performance agenda in three ways. Firstly, alleviating bottlenecks in the energy distribution network makes the smart grid stronger and more resilient. This allows for quicker rollout of renewable energy and electric vehicles. Secondly, by enabling energy savings of around 30%–40% in the buildings themselves. Thirdly, by being part of virtual power plants, which contribute directly to DERs. **Figure 1** shows an amalgamation of the five major sustainability performances and the two technological enablers.

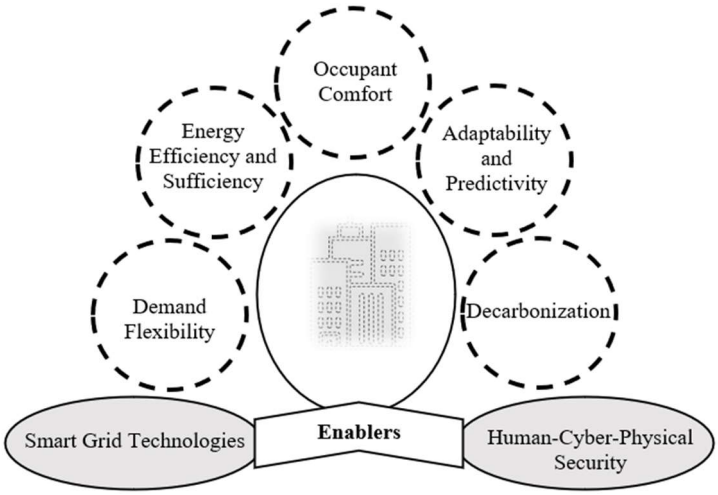

Figure 1. Sustainability performances and enablers for grid-interactive efficient buildings.

Appropriate energy-efficient design approaches, including insulation, thermal mass, orientation, tightness, shading, and space conditioning, decrease the volume of energy consumption. These are needed to manage heat loss or gain through the building envelope and to control the concentrations of airborne contaminants within the building. Controlling outdoor ventilation in buildings is important as it impacts indoor air quality (IAQ) and energy. Once building loads are reduced, the next is using energy-efficient equipment and on-site DER generation. The gain is especially true when energy efficiency and integration of DERs are selected early in the design process [4]. Using energy modeling and simulation can help eradicate human error by recognizing the least expensive factors for GEBs.

The less energy the building needs to operate, the less renewable energy it will need to produce on-site. This may be achieved by implementing efficient heating, ventilation, air conditioning (HVAC), lighting, and smart plug loads other than maintaining effective passive design approaches when possible. Energy from on-site DERs may be distributed through transmission means other than the electricity grid, such as charging electric vehicles [5].

This paper addresses several practices in designing and deploying GEBs, both new and old. It is organized as follows: Section 2 describes the proposed framework of the GEB within a microgrid and smart grid. Section 3 reviews the various system modeling and simulation techniques implemented in designing GEBs. Section 4 describes the concepts of energy efficiency and sufficiency analysis. Section 5

presents human-cyber-physical security as a major enabler of GEBs. Section 6 deals with conclusions and future directions.

2. Grid-interactive efficient buildings

The definition of GEB by the U.S. Department of Energy (DOE) Building Technologies Office involves using smart technologies that actively employ DERs to optimize energy usage for grid service and occupant needs while reducing costs consistently [5]. In addition, the American Society of Heating, Refrigerating, and Air-Conditioning Engineers (ASHRAE) further elaborates that GEBs engage proactively with the energy grid by utilizing renewable energy sources, energy storage systems, and smart technologies to optimize energy consumption and generation. This enables GEBs to respond to grid signals in real-time, lowering overall demand and GHG emissions [6]. GEB is a cutting-edge building designed to interact in both directions, meaning it can take in and give out energy. It is built or retrofitted in a way that seamlessly combines energy efficiency with DR and load flexibility (LF). By implementing DR and LF, the GEB can effectively reduce the overall electrical power consumption during peak demand periods. This ensures that the utility power grid operates stably and cost-effectively. This approach benefits the grid and consumers by lowering peak demand charges, resulting in economic advantages. **Figure 2** illustrates the architecture of a proposed GEB that contributes to the overall grid-level energy efficiency. Such a building can decrease the amount of electricity demanded and reduce utility costs without compromising the safety and health of its occupants.

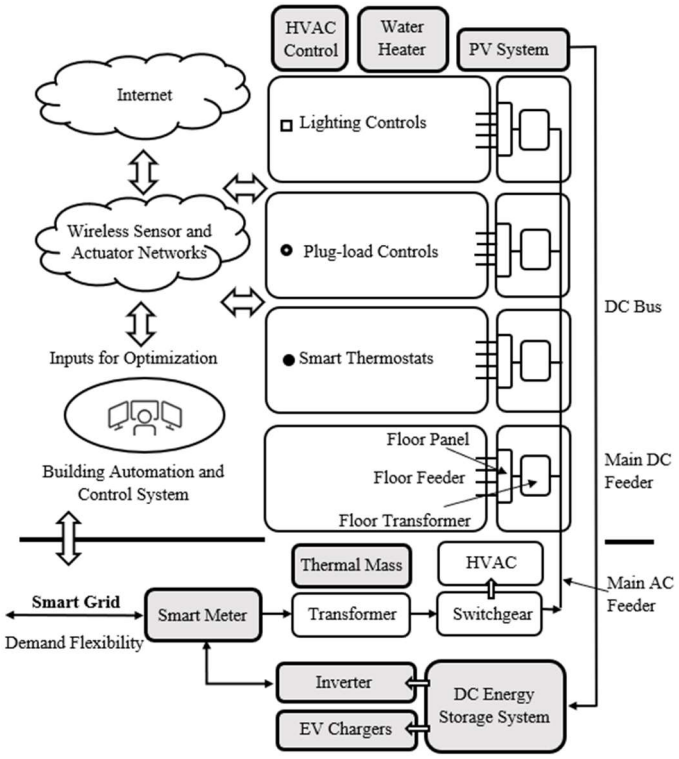

Figure 2. A proposed architecture for a grid-interactive efficient building.

DR is the modification of consumers' demand for energy consumption. It provides major services, including energy management and storage. Electric utilities

use these services to compel their users to reduce or shift energy consumption from high-cost hours to low-cost hours of the day [7]. LF, also referred to as demand flexibility, is a valuable feature offered by DERs that allows for the manipulation of electricity through reduction, shedding, shifting, or generation. This technology not only reduces energy consumption but also provides the grid with flexible building loads. As the grid becomes increasingly complex, demand flexibility is crucial in maintaining reliability, improving energy affordability, and integrating various generation sources. Advanced controls can manage electrical loads in buildings, allowing them to operate at specific times and varying output levels. For example, space conditioning is a particularly significant and distinct load use due to its size, dependence on weather, and contribution to peak demand and grid congestion. It also affects occupant comfort, productivity, and health and interacts with the building envelope [3].

Smart metering is a prerequisite and starting point for effectively implementing smart grids and GEBs. For electricity providers to deliver intelligent services to customers, bidirectional metering interfaces should be used to obtain customers' energy demand information. Data collected from smart meters, building management systems, and weather stations can be used by artificial intelligence (AI) techniques and machine learning algorithms to infer the complex relationships between energy consumption and other variables such as temperature, solar radiation, time of day, and occupancy [8]. This intelligent interaction with the grid allows for better management of both energy generation and consumption in response to grid conditions.

Wireless sensor and actuator networks (WSAN) as part of the Internet of Things (IoT) represent a rapidly expanding area of research. They can convert analog signals into digitally encoded signals for direct communication over a network for onward transmission to other intelligent devices for control and measurement purposes. They can process, analyze, and transmit this data to locations across a network for use in various applications [4]. The function of sensor intelligence can vary between "think for itself" or be part of a "think as a group" methodology in which sensors and a central data analyzer perform together. The WSAN is a part of the field level of the building automation and control system (BACS). The majority of larger (100,000 sq. ft. or above) modern buildings today have BACSs that are capable of continuously monitoring the status of the building's energy consumption through the WSAN connected to the HVAC, lighting, plug loads, ventilation, and other auxiliaries in the building like the elevator [9]. With the growing installation of photovoltaics (PV), building energy management platforms, and DR-enabled smart devices, traditional energy operation is evolving from a unidirectional utility-to-consumer model into a more distributed bi-directional power flow paradigm. Each node of the network may have several sensing units, which can measure physical variables, such as temperature, humidity, and vibration, to record and react to an event or a phenomenon.

A significant architectural resolution for a GEB is the level at which various flexibility modes are combined within a building, both for an individual grid service and across services. Devices can directly interact with the grid, market, or any other external entity. On the other hand, a building can coordinate with its resident devices and interact with the utility smart grid or external entities [3]. Additionally, co-located buildings can collaborate and provide services at different levels.

3. System modeling and simulation

Building energy estimation can proceed through information gathering, modeling, simulation, corrections, and monitoring, as shown in **Figure 3**. Studying the impact of buildings' energy consumption can be divided into three stages [10]. First, information must be gathered or assumed, and a model will be created by referencing either the planning process or a simulated building. Second, the energy attributed to the building during its construction or calibration must be re-evaluated, using actual energy data if available. Third, the actual energy consumption of the building post-construction must be evaluated.

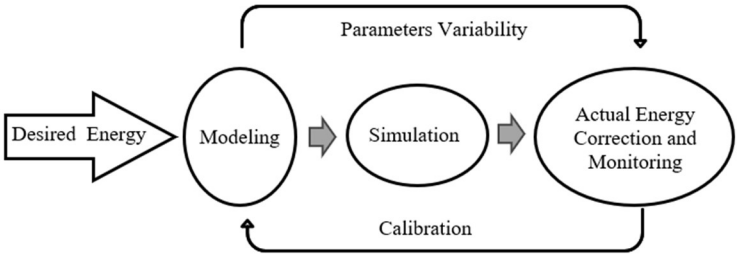

Figure 3. The process of energy estimation in a building.

3.1. Energy forecasting

The building energy model emulates the physical attributes of buildings under a given environmental condition [11] and simulates how buildings are operated to achieve indoor set points. The implementation of BACS can be explored by using models and simulations of buildings and the corresponding grid interfaces, which facilitate their potential participation in future market structures through energy forecasting. To maximize energy efficiency, accurate and consistent energy forecasts are crucial. These forecasts rely on different factors such as historical trends, weather patterns, tariff structures, and occupancy schedules. The building's thermal mass is the most promising grid service from an aggregate capacity perspective, which can help to shed and shift HVAC load. By optimizing the HVAC and lighting systems, energy forecasts can be of great help in achieving this goal.

There are three broad categories for predicting energy consumption: engineering (white-box models), AI-based (black-box models), and hybrid (grey-box models), as shown in **Figure 4**. White-box models use thermodynamic equations to estimate energy consumption, while black-box models use historical data and statistical models to predict future energy use. Grey-box models use a combination of both physical and statistical methods. In recent years, black-box models have gained popularity due to their ease of use and ability to provide optimal solutions [12].

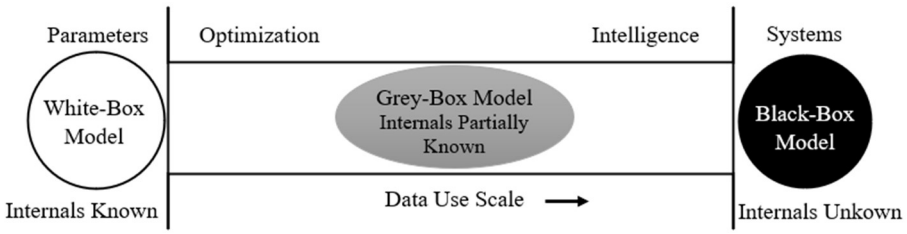

Figure 4. General categories of building energy forecasting models.

EnergyPlus™ is a popular white-box model for developing detailed physical-based building energy models [13]. Since some advanced control strategies are difficult to implement directly in EnergyPlus™, co-simulation provides a solution to conduct a two-way input/output data exchange between EnergyPlus™ and other tools for controls [14,15]. The time-series control variables are calculated by the EnergyPlus™ engine and passed to the external tools at each timestep. Then, the external tools calculate the control signal and return this to the EnergyPlus™ engine. This signal is used for the next timestep calculation. EnergyPlus™ has been commonly used in system modelling for supporting various GEBs [16,17].

Resistive-capacitive networks are one of the popular gray-box models that are considered simplified physical-based building energy models [18–20]. They may be used to model the thermal dynamics in digital twins of GEBs, which have become an emerging method for building energy modeling and simulation. In this regard, Mai and Chung [21] proposed a modelling framework for economic model predictive control that used an RC network model of a building that strongly relates to the power consumption of the HVAC system.

Data-driven models are one of the candidates for the research to support GEBs when historical data or measured data are provided using the neural network model [22]. Chellaswamy et al. [23] developed a new framework for residential building energy management systems with PV. A convolutional neural network was used to estimate the relationship between the PV array power and meteorological datasets.

3.2. Human-in-the-loop (HiL)

A comfortable indoor environment should be one of the primary services buildings provide. Nowadays, all thermal comfort standards include recommendations concerning indoor thermal conditions for both the design and operation of buildings. At its core, HiL focuses on enabling built environments that can learn, adapt, and evolve at different scales to improve the quality of life of its users while optimizing resource usage and service availability. Since these aspects are at the core of HiL, it is thus imperative to extend existing modelling tools and practices with this new emphasis [24]. A paradigm shift from ‘set-point-based’ control to ‘perception-based’ HiL control of buildings is necessary to increase comfort, reduce energy consumption, and support the transition to clean energy. However, considering these aspects in the building design phase would also be beneficial.

Indoor human comfort has been categorized into thermal, visual, and acoustic environments in addition to the IAQ. Although thermal and visual comfort are interrelated, these have been evaluated separately. Currently, the most frequently cited thermal comfort standards, namely ASHRAE 55:2020 [25], ISO 7730:2005 [26], and EN 16798-1:2019 [27], which was formerly EN 15251:2007 [28], propose requirements based on the Fanger model [29] (beyond also including other approaches), which solves the heat balance equations between the human body and its surroundings, represented as a uniform environment. Fanger defined the “predicted mean vote” (PMV) as an index that predicts the mean thermal sensation vote on a standard scale for a large group of persons exposed to a given combination of metabolic activity level, clothing insulation, and thermal environmental variables.

Based on the theory of thermal comfort, Segovia et al. [30] presented an outline of a temperature controller. It uses fuzzy logic to optimize comfort and reduce energy consumption. The controller allows multiple inputs from more than one user to set a temperature setpoint. The control logic was developed in MATLAB using the Simulink tool in the simulations. Energy use was optimized, resulting in a reduction of energy consumption between 22% and 31%.

3.3. Building Information Modeling (BIM) and digital twins

In the complex critical construction industry, buildings cannot be designed, built, and maintained without creating virtual models. This is comprised of big data, which refers to the vast quantities of information that have been stored in the past and continue to be obtained continuously. Primary sources of big data in buildings include people who are continuously generating and sharing information, information technology (IT)—enabled construction devices that gather and store data, and holistic systems such as BIM [4].

Incorporating digital technologies presents an excellent opportunity to reduce energy demand while enhancing comfort. This transformation is in line with the continuous progress in communication and information technologies as well as the advancement of interconnected and intelligent grids. Moreover, improving the energy efficiency in buildings can result in cost savings for owners and occupants and potentially better indoor comfort levels [31]. Digital twinning techniques were first used in aerospace and manufacturing, but now they are used in various applications throughout a building's life cycle (**Figure 5**). A digital twin refers to a digital or mathematical model of a physical asset that incorporates sensor readings and a data exchange mechanism between the digital model and the physical asset [32]. With the help of a building WSAN, the BIM models can be extended into digital twins, which reflect in a more precise way the behaviour and properties of the modeled building during any phase of its life cycle [33].

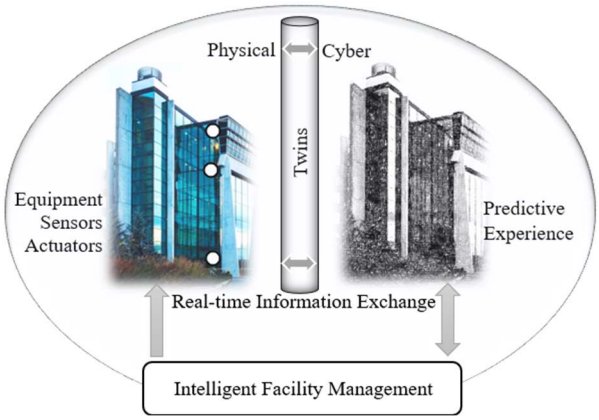

Figure 5. Digital twins for a grid-interactive efficient building.

4. Energy efficiency and sufficiency

There are two common ways to use self-generated solar energy in GEBs: on-grid and off-grid. In the off-grid option, a building has solar panels but isn't connected to the grid. In this case, the building must use all the energy panels produce through direct

consumption or storage. On the other hand, in the on-grid option, a building has solar panels that can either use or export the produced energy to the grid. This is a common option, especially in urban areas [34].

Most studies on urban PV's impact on the grid only considered rooftop PV systems, mostly because of their maturity, easy integration, and low cost. However, the strong decrease in prices of PV systems, which is likely to continue in the coming years [35], facilitates the integration of PV on vertical façades as economically viable. This opens engaging perspectives in urban environments where the available area on façades is sometimes much larger than on roofs [36].

PV systems can be distinguished based on their operational and functional requirements, their possible configurations, and the nature of equipment connection to other power sources and electrical loads [37]. To achieve the desired voltage, a series-parallel combination of PV panels is used according to the maximum voltage and current of the inverter.

For optimized PV generation, it is essential to quantify the capabilities of the GEB. PV electricity estimation helps the GEB operator determine the PV electricity that can be generated over different periods of the day. This can be estimated using solar irradiance data with PV module parameters, inverter parameters, site location, array configuration, and other weather forecast information [9] as shown in **Figure 6**. The performance of PV systems typically decreases when operating conditions deviate from the nominal operating cell temperature due to environmental factors, such as wind distribution, dust density, temperature, and humidity changes, resulting in thermal losses and open-circuit voltage drops.

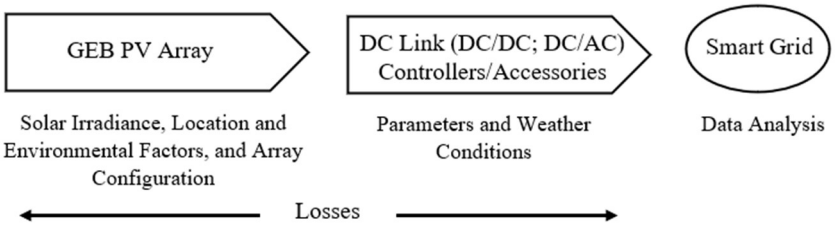

Figure 6. Components of a GEB PV electricity generation system.

Optimizing the performance of PV energy is a crucial task that requires careful planning and analysis. Optimal PV configuration is highly dependent on the local context. Differences in latitude and longitude significantly impact the integration of the façade. Computational resources are valuable assets, providing engineers and researchers with tools to model, simulate, dimension, and design PV systems.

Various tools are developed to help with the design, performance assessment, and economics of PV systems. A detailed study is necessary for the general architecture of the GEB PV system, maximum power point tracking algorithm, inverter synchronization, and grid connection [38,39]. One such tool is PVSYST, which can analyze the entire PV system, including stand-alone, grid-connected, pumping, and DC-grid PV systems. EnergyPlus™ can simulate PV production and estimate the incident solar radiation on each building surface. MATLAB/Simulink is also utilized for analyzing the performance of the PV system based on its current-voltage-power

characteristics, inverter voltage, gird voltage and current, power factor, and total harmonic distortion under different environmental conditions.

5. Human-cyber-physical security (HCPS)

The HCPS is a seamless integration of human and computational entities with the physical world and its processes [40]. This is realized as an efficient embedded application that engages physical infrastructure with cyber computation to accomplish functional security desires. In this paper, security incorporates cyber and physical real-world consequences, including safety, real-time surveillance involving structural, energy efficiency, and other human-centric values such as health and comfort. The above integration is happening within the building through WSAN to environmental data and technical services while engaging stakeholders in the process [4]. In the above scenario, human roles as a designer, operator, or occupant have changed as knowledge has evolved. The role has transformed into a smart and skilled one that leverages human skills supported by information and technology to ensure the long-term sustainability of operations and promote the occupant's well-being in various situations [41].

The rise of the WSAN and other sweeping technology initiatives is creating a huge wave of technology adoption at every system architecture level. WSAN devices, in particular, are a potential weak point for security because they do not generally have the processing power to manage increasingly complex security protocols and encryption schemes [42]. They are more vulnerable to attack than computers or mobile phones, not only because of the surge in the use of WSAN devices but also on account of the complexity, diversity, and inherent mobility of such device application scenarios [43]. At the same time, WSAN has developed rapidly but has not yet matured. Therefore, there is a need to adopt a standardized approach to IT and architecture that leverages the WSAN and enables a future path to data analytics and edge intelligence by offering secure mass deployment of WSAN technologies that also allow for continuous monitoring and control of user access [44].

In general, there are three main issues for GEBs seeking to create a secure experience for their occupants: security planning and governance; security practices that can be enhanced by embracing some safety principles; and focus on the security lessons being learned in the convergence of IT (servers, laptops, and workstations) and operational technology (OT) (HVAC, lighting, elevators, fire alarms, etc.). The security goals of a GEB, including confidentiality (privacy and authorization of access to data or information), integrity (trustworthiness of the data or information storage), availability (availability of the systems and associated functions when required), safety, and resiliency (predict, absorb, and recover from disturbances), should be grounded on both the objectives of IT as well as those of OT. This holistic approach reflects any attack on a GEB and probably on a community that can pose impacts and risks to human safety.

The HCPS concept is becoming significant in the security agenda of the GEBs. **Figure 7** displays a proposed HCPS architecture for a GEB. In-building physical components and WSAN devices are located in the field layer. These assets require monitoring tasks such as surveillance (to detect physical intrusion), environmental

(such as temperature, humidity, smoke, and fire), structural (vibration and deformation), energy efficiency, and other human-centric values. Some WSAN devices would be deployed to monitor the environment and structural integrity of the building. Other devices monitor the deployment area so that "physical intrusions" are detected. It means that the monitors also need to be monitored [45]. The WSAN gateway acts as an interface between the in-building and the outer network entities. The AI-based intrusion detection and prevention system (IDPS) monitors both ingress and egress traffic to detect cyberattacks and to protect the building from cyberattacks. At the supervisory level and other levels, there is a human-machine collaboration through knowledge and operation to implement security policies, perform maintenance, upgrade the system, and facilitate intervention. It also provides a reconfigurable interface between the cyber and physical parts of the building. The AI-based detection and analytics module gathers sensed data from the IoT sensing module and performs data preprocessing. It uses AI tools for physical event detection and prediction. The controller makes decisions based on the results obtained from the data analysis. It may generate control signals for actuators to activate the alarm system. It can also communicate with external entities (if policy allows) through the building gateway. Such entities include public safety and emergency management authorities. The alarm system is responsible for conveying alert messages to in-building occupants. The components in this architecture are assumed to be protected by standard cryptographic mechanisms [46]. GEBs or smart grid operators may also subscribe to cloud services for cyber security, energy management, data storage, and analytics [47].

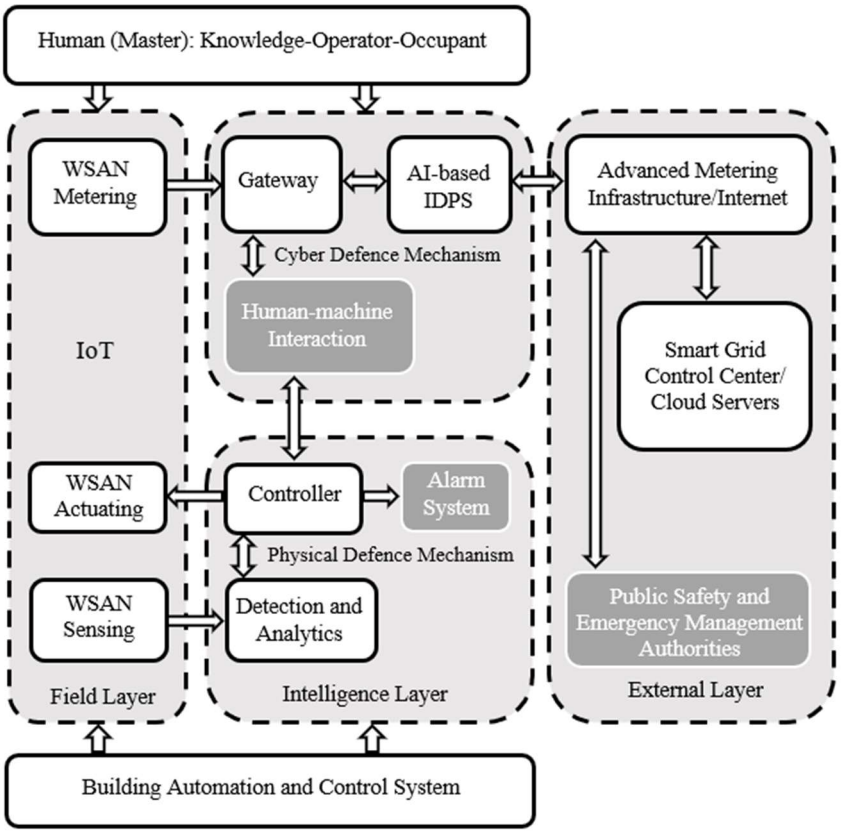

Figure 7. A proposed HCPS architecture for a GEB.

6. Conclusions: Looking ahead

Electrification provides a significant way to reduce carbon emissions and increase energy efficiency in buildings. Implementing the smart utility grid regulations and tariffs in GEBs benefits utilities, customers, and the environment. However, certain infrastructure challenges exist and must be addressed, particularly on the distribution grid. This matter requires a significant amount of funds to mitigate [48]. Additionally, new, simpler approaches to managing the proliferation of large numbers of GEBs need to be explored.

GEBs are gaining popularity due to their potential sustainability performances through their capability to learn, adapt, and evolve at different scales to improve the quality of life of their users while optimizing resource usage and service availability. Without new architecture and control techniques that move the distribution system to an open-access network, the industry will not progress toward full decarbonization quickly enough. This is achieved by implementing management and control measures enabled by smart grid technologies, interoperability, and HCPS. However, the research of these technological solutions still faces the challenge of maturity and availability of some technologies that would optimize GEB implementation. Other challenges include a lack of communication and control infrastructure, interpretability, security, cost barriers, and difficulties balancing occupant needs with grid benefits.

Finally, advancing the state of the art in GEBs can be achieved through energy efficiency, DERs, and demand flexibility. The resulting GEB developments should pave the way for cleaner, more efficient, secure, and healthy buildings. By merging grid-interactive approaches into building design and operation, it will be possible to establish a sustainable and robust future for the built environment, ensuring a smooth transition to zero-carbon buildings.

Author contributions: Writing the main text, RH; reviewing the text and adding Section 5 on HCPS, MMH. All authors have read and agreed to the published version of the manuscript.

Conflict of interest: The authors declare no conflict of interest.

References

1. NIST. Commissioning building systems for improved energy performance. Available online: https://www.nist.gov/programs-projects/commissioning-building-systems-improved-energy-performance (accessed on 20 May 2024).
2. Aguilar J, Garces-Jimenez A, R-Moreno MD, et al. A systematic literature review on the use of artificial intelligence in energy self-management in smart buildings. Renewable and Sustainable Energy Reviews. 2021; 151: 111530. doi: 10.1016/j.rser.2021.111530
3. Neukomm M, Nubbe V, Fares R. Grid-interactive efficient buildings. Available online: https://www1.eere.energy.gov/buildings/pdfs/75470.pdf (accessed on 20 May 2024).
4. Habash R. Sustainability and Health of Intelligent Buildings, 1st ed. Woodhead Publishing; 2022.
5. Peterson K, Torcellini P, Grant R, et al. A common definition for zero energy buildings. Available online: https://www.energy.gov/sites/prod/files/2015/09/f26/bto_common_definition_zero_energy_buildings_093015.pdf (accessed on 20 May 2024).

6. ASHRAE. ASHRAE releases guide on the role of grid interactivity in decarbonization. Available online: https://www.ashrae.org/about/news/2023/ashrae-releases-guide-on-the-role-of-grid-interactivity-in-decarbonization (accessed on 20 May 2024).
7. Hussain I, Ullah M, Ullah I, et al. Optimizing energy consumption in the home energy management system via a bio-inspired dragonfly algorithm and the genetic algorithm. Electronics. 2020; 9(3): 406. doi: 10.3390/electronics9030406
8. Kolokotsa D. The role of smart grids in the building sector. Energy and Buildings. 2016; 116: 703-708. doi: 10.1016/j.enbuild.2015.12.033
9. Rahman S, Haque A, Jing Z. Modeling and performance evaluation of grid-interactive efficient buildings (GEB) in a microgrid environment. IEEE Open Access Journal of Power and Energy. 2021; 8: 423-432. doi: 10.1109/oajpe.2021.3098660
10. Chang S, Yang PPJ, Yamagata Y, Tobey MB. Modeling and design of smart buildings. In: Yamagata Y, Yang PPJ (editors). Urban Systems Design: Creating Sustainable Smart Cities in the Internet of Things Era. Elsevier; 2020. pp. 59-86. doi: 10.1016/b978-0-12-816055-8.00003-8
11. Chang S, Castro-Lacouture D, Matsui K, et al. Planning and monitoring of building energy demands under uncertainties by using IoT data. In: Proceedings of the ASCE International Conference on Computing in Civil Engineering 2019; 17-19 June 2019; Atlanta, Georgia, USA. doi: 10.1061/9780784482445.027
12. Wang Z, Srinivasan RS. A review of artificial intelligence based building energy use prediction: Contrasting the capabilities of single and ensemble prediction models. Renewable and Sustainable Energy Reviews. 2017; 75: 796-808. doi: 10.1016/j.rser.2016.10.079
13. Crawley DB, Lawrie LK, Winkelmann FC, et al. EnergyPlus: Creating a new-generation building energy simulation program. Energy Building. 2001; 33(4): 319-331.
14. Qureshi FA, Lymperopoulos I, Khatir AA, et al. Economic advantages of office buildings providing ancillary services with intraday participation. IEEE Transactions on Smart Grid. 2018; 9(4): 3443-3452. doi: 10.1109/tsg.2016.2632239
15. Huang S, Wu D. Validation on aggregate flexibility from residential air conditioning systems for building-to-grid integration. Energy and Buildings. 2019; 200: 58-67. doi: 10.1016/j.enbuild.2019.07.043
16. Liu M, Heiselberg P. Energy flexibility of a nearly zero-energy building with weather predictive control on a convective building energy system and evaluated with different metrics. Applied Energy. 2019; 233-234: 764-775. doi: 10.1016/j.apenergy.2018.10.070
17. Li X, Malkawi A. Multi-objective optimization for thermal mass model predictive control in small and medium size commercial buildings under summer weather conditions. Energy. 2016; 112: 1194-1206. doi: 10.1016/j.energy.2016.07.021
18. Taha AF, Gatsis N, Dong B, et al. Buildings-to-grid integration framework. IEEE Transactions on Smart Grid. 2019; 10(2): 1237-1249. doi: 10.1109/tsg.2017.2761861
19. Joe J, Karava P. A model predictive control strategy to optimize the performance of radiant floor heating and cooling systems in office buildings. Applied Energy. 2019; 245: 65-77. doi: 10.1016/j.apenergy.2019.03.209
20. Jiang T, Ju P, Wang C, et al. Coordinated control of air-conditioning loads for systemfrequency regulation. IEEE Transactions on Smart Grid. 2021; 12(1): 548-560. doi: 10.1109/tsg.2020.3022010
21. Mai W, Chung CY. Economic MPC of aggregating commercial buildings for providing flexible power reserve. IEEE Transactions on Power Systems. 2015; 30(5): 2685-2694. doi: 10.1109/tpwrs.2014.2365615
22. Baranski M, Meyer L, Fütterer J, et al. Comparative study of neighbor communication approaches for distributed model predictive control in building energy systems. Energy. 2019; 182: 840-851. doi: 10.1016/j.energy.2019.06.037
23. Chellaswamy C, Ganesh Babu R, Vanathi A. A framework for building energy management system with residence mounted photovoltaic. Building Simulation. 2021; 14(4): 1031-1046. doi: 10.1007/s12273-020-0735-x
24. Becerik-Gerber B, Lucas G, Aryal A, et al. The field of human building interaction for convergent research and innovation for intelligent built environments. Scientific Reports. 2022; 12(1). doi: 10.1038/s41598-022-25047-y
25. ANSI/ASHRAE. Thermal Environmental Conditions for Human Occupancy. American Society of Heating, Refrigerating and Air-Conditioning Engineers (ASHRAE 55:2020); 2020.
26. ISO. Analytical Determination And Interpretation of Thermal Comfort Using Calculation of the PMV and PPD Indices and Local Thermal Comfort Criteria—Ergonomics of the Thermal Environment (ISO 7730:2005). International Organization for Standardization; 2005.
27. CEN. Energy performance of buildings—Ventilation for buildings—Part 1: Indoor environmental input parameters for

design and assessment of energy performance of buildings addressing indoor air quality, thermal environment, lighting and acoustics—Module Ml-6, European Committee for Standardization (EN 16798–1:2019). Available online: https://www.sis.se/en/produkter/construction-materials-and-building/installations-in-buildings/general/ss-en-16798-12019/ (accessed on 20 May 2024).
28. CEN. Indoor environmental input parameters for design and assessment of energy performance of buildings addressing indoor air quality, thermal environment, lighting and acoustics (EN 15251:2007). Available online: https://standards.iteh.ai/catalog/standards/cen/92485123-bf64-40e3-9387-9724a642eae8/en-15251-2007 (accessed on 20 May 2024).
29. Fanger PO. Thermal Comfort: Analysis and Applications in Environmental Engineering. Danish Technical Press; 1970.
30. Segovia E, van Schaik P, Vukovic V. Indoor thermal comfort controller integrating human interaction in the control-loop as a live component. In: Nixon JD, Al-Habaibeh A, Vukovic V, et al. (editors). Energy and Sustainable Futures: Proceedings of the 3rd ICESF. Springer Nature Switzerland; 2023. pp. 107-115. doi: 10.1007/978-3-031-30960-1
31. Volk R, Stengel J, Schultmann F. Building Information Modeling (BIM) for existing buildings—Literature review and future needs. Automation in Construction. 2014; 38: 109-127. doi: 10.1016/j.autcon.2013.10.023
32. Bortolini R, Rodrigues R, Alavi H, et al. Digital twins' applications for building energy efficiency: A Review. Energies. 2022; 15(19): 7002. doi: 10.3390/en15197002
33. Hou H, Lai JHK, Wu H, et al. Digital twin application in heritage facilities management: Systematic literature review and future development directions. Engineering, Construction and Architectural Management. 2023. doi: 10.1108/ecam-06-2022-0596
34. Thebault M, Gaillard L. Optimization of the integration of photovoltaic systems on buildings for self-consumption – Case study in France. City and Environment Interactions. 2021; 10: 100057. doi: 10.1016/j.cacint.2021.100057
35. Fath K, Stengel J, Sprenger W, et al. A method for predicting the economic potential of (building-integrated) photovoltaics in urban areas based on hourly radiance simulations. Solar Energy. 2015; 116: 357-370. doi: 10.1016/j.solener.2015.03.023
36. Redweik P, Catita C, Brito M. Solar energy potential on roofs and facades in an urban landscape. Solar Energy. 2013; 97: 332-341. doi: 10.1016/j.solener.2013.08.036
37. Allouhi A, Saadani R, Kousksou T, et al. Grid-connected PV systems installed on institutional buildings: Technology comparison, energy analysis and economic performance. Energy and Buildings. 2016; 130: 188-201. doi: 10.1016/j.enbuild.2016.08.054
38. Sahri Y, Tamalouzt S, Belaid SL, et al. Performance improvement of Hybrid System based DFIG-Wind/PV/Batteries connected to DC and AC grid by applying Intelligent Control. Energy Reports. 2023; 9: 2027-2043. doi: 10.1016/j.egyr.2023.01.021
39. Khosravi N, Baghbanzadeh R, Oubelaid A, et al. A novel control approach to improve the stability of hybrid AC/DC microgrids. Applied Energy. 2023; 344: 121261. doi: 10.1016/j.apenergy.2023.121261
40. Zhou J, Zhou Y, Wang B, et al. Human–cyber–physical systems (HCPSs) in the context of new-generation intelligent manufacturing. Engineering. 2019; 5(4): 624-636. doi: 10.1016/j.eng.2019.07.015
41. Wang B, Zheng P, Yin Y, et al. Toward human-centric smart manufacturing: A human-cyber-physical systems (HCPS) perspective. Journal of Manufacturing Systems. 2022; 63: 471-490. doi: 10.1016/j.jmsy.2022.05.005
42. Schoechle T. Re-inventing wires: the future of landlines and networks, 2018. Available online: https://electromagnetichealth.org/wp-content/uploads/2018/02/ReInventing-Wires-1-25-18.pdf (accessed on 20 May 2024).
43. Wu H, Han H, Wang X, et al. Research on artificial intelligence enhancing Internet of Things security: A survey. IEEE Access. 2020; 8: 153826-153848. doi: 10.1109/access.2020.3018170
44. O'Brien L. Cybersecurity for smart buildings, 2019. Available online: https://www.arcweb.com/blog/cybersecurity-smart-buildings (accessed on 20 May 2024).
45. Hasan MM, Mouftah HT. Cyber-physical vulnerabilities of wireless sensor networks in smart cities. In: Song H, Fink GA, Jeschke S (editors). Security and Privacy in Cyber-Physical Systems: Foundations, Principles and Applications. John Wiley & Sons; 2017. pp. 263-280. doi: 10.1002/9781119226079.ch13
46. Hasan MM, Mouftah HT. Cloud-centric collaborative security service placement for advanced metering infrastructures. IEEE Transactions on Smart Grid. 2019; 10(2): 1339-1348. doi: 10.1109/tsg.2017.2763954

47. Hasan MM, Mouftah HT. Encryption as a service for smart grid advanced metering infrastructure. In: Proceedings of the 2015 IEEE Symposium on Computers and Communication (ISCC); 6-9 July 2015; Larnaca, Cyprus. pp. 216-221. doi: 10.1109/iscc.2015.7405519
48. Aikin KE. The future of grid-interactive efficient buildings and local transactive energy markets. In: Sioshansi F (editor). The Future of Decentralized Electricity Distribution Networks. Elsevier; 2023. pp. 437-463. doi: 10.1016/b978-0-443-15591-8.00022-x

Building Engineering 2024, 2(1), 1334.
https://doi.org/10.59400/be.v2i1.1334

Article

Field and intervention study on indoor environment in professional classrooms

Yue Lyu

School of Civil Engineering, Shaoxing University, Shaoxing 312000, Zhejiang Province, China; 2014000048@usx.edu.cn

CITATION

Lyu Y. Field and intervention study on indoor environment in professional classrooms. Building Engineering. 2024; 2(1): 1334. https://doi.org/10.59400/be.v2i1.1334

ARTICLE INFO

Received: 26 April 2024
Accepted: 24 May 2024
Available online: 5 June 2024

Abstract: To study the variation of environment in the professional classroom during lecture hours, multiple field experiments and intervention experiments on indoor and outdoor temperatures were conducted in a university professional classroom in Shaoxing during the spring. Environmental data, including indoor and outdoor temperatures, relative, and CO_2 concentrations, were recorded every 5 min. Volatile organic compounds (VOC) were sampled, and indoor air quality was evaluated repeatedly. Results showed that the classroom's average indoor air temperature ranged from 17.8–29.2 ℃, the average indoor relative humidity from 34.5%–91.0%, the average CO_2 concentrations from 921.6–1805.2 ppmv, and total VOC concentrations from 330–682 ppbm. The subjective evaluation conducted during the intervention experiments indicated a significant increase in perceived odor intensity upon entering the classroom. When the CO_2 concentration reached 2000 ppmv, the satisfaction and acceptability of the air quality for the subjects and invitees decreased significantly. In the temperature range of 17–31 ℃, the CO_2 emission rate of the human body was estimated to increase by 0.78 L/h for every 1 ℃ increase in temperature. To maintain the indoor CO_2 concentration at 1000 ppmv, the required ventilation rate for each person must be increased by 0.25 ± 0.3 L/s.

Keywords: classrooms; VOC; CO_2 concentration; CO_2 emission rate; intervention measurements

1. Introduction

Classrooms are the primary locations where students acquire knowledge, with students spending more than 40% of their time in these spaces [1,2]. Indoor pollutant levels of 2–5 are several times those of outdoor pollutants [3,4]. The reasons behind this include crowded classrooms, short break times, low ventilation during breaks, inadequacy in providing fresh air, absence of mechanical ventilation, unplanned construction of ventilation systems, factors bringing pollutants from the outdoors, and the existence of impermeable windows [5,6]. Almost all students are exposed to indoor air in school buildings during their educational lives. In these institutions, pollutants from several sources have a negative impact on the health, comfort, and performance of students and employees, especially affecting memory, concentration, and learning abilities. Therefore, the air quality inside the classroom is a key indicator for measuring students' learning comfort and learning efficiency. In schools, it is important to create a favorable teaching and learning environment. The air quality inside classrooms depends on air temperature, humidity, radiation, internal lighting, air flow, activities, clothing, and climate change and has a significant impact on the physical and mental health of students.

The deterioration of indoor air quality is caused by a combination of outdoor

pollutants entering classrooms and indoor sources of pollutants [7,8]. In the research field of indoor environments, indoor CO_2 concentration, content, and concentration of volatile organic compounds (VOCs) can be regarded as a measure of indoor air quality affected by human pollutants [9].

Regarding CO_2 concentration studies, previous research has shown that the higher the CO_2 concentration, the worse the quality of brain work [10,11]. When the CO_2 concentration reaches 1000–2000 ppmv, people feel cloudy air and have difficulty breathing. When it exceeds 2000 ppmv, it may contribute to an increase in pulse rate, blood pressure, and skin temperature, causing headaches, drowsiness, fatigue, nausea, impaired concentration, and decreased mental and physical working capacity [12–14]. It is evident that there is no universally defined standard for indoor CO_2 concentration limits across countries. The US ASHRAE standard (2016) recommends a maximum daily mean indoor CO_2 concentration of 1000 ppmv and that the indoor-outdoor differential concentration should not exceed 700 ppmv. The UK BS EN 15251 standard (2008) stipulates indoor and outdoor CO_2 concentration limits for different indoor air quality levels. The German VDI 6022 Part 3 standard (2011) specifies a maximum CO_2 concentration of 1500 ppmv in classrooms. The Chinese GB/T18883 standard (2012) refers to the 1000 ppmv CO_2 concentration recommended by the ASHRAE standard.

Many previous studies have used ordinary classrooms as settings to illustrate the range of changes in indoor CO_2 concentrations. These studies encompassed various scenarios, including natural ventilation [15–18], mechanical ventilation [12,19], both ventilation modes combined [20–22] the utilization of air purifiers [23], and the implementation of a human respiratory heat model [24].

Most of these studies were conducted in summer or autumn; ordinary classrooms were selected as the study sites, and multiple classrooms were monitored simultaneously to obtain the maximum and minimum values of CO_2 concentration. Population density ranged from 0.01–0.59 (person/m^2), resulting in a wide range of CO_2 concentration fluctuations.

Regarding research on VOCs, numerous studies have shown that indoor exposure to VOCs can lead to significant adverse health effects and pathological architectural syndrome [25,26]. Particularly, pollutants emitted by building decorations, such as volatile benzene gases and aldehydes, can harm the human body for a long time. In addition, some buildings are not well ventilated, with limited pollutant dilution capacity, and long-term exposure or excessive inhalation of VOC can lead to malignant diseases, such as cancer and leukaemia, as well as obvious adverse effects on the human respiratory, cardiovascular, and nervous systems, causing irreparable damage to the human body. Apart from VOCs usually derived from indoor materials, furniture, and permeating air [27], VOCs originating from indoor spaces have also attracted new attention, especially in dense spaces, such as classrooms and lecture halls in education buildings, where human emissions may be an important source [28]. For example, VOC emissions produced by humans (from skin or breath) [29], clothing, personal possessions [30], and activities such as smoking and using personal care products [31]. In addition, the presence of humans in indoor environments reduces ozone concentration, and the reaction between ozone and human skin oil remaining on hair and clothing can contribute to indoor VOCs [32]. Many previous studies have

analyzed VOC components in ordinary classrooms. For example, in the condition of natural ventilation [26,33], in the condition of mechanical ventilation [34,35], in the above two ventilation modes [36,37], the utilization of air purifiers [38], and in the condition of heating [39]. Most of these studies were mainly conducted in summer or winter, and ordinary classrooms were selected as the study site; multiple classrooms were monitored simultaneously to obtain the components of VOCs, while the detection interval was longer, usually before and after class.

In the study of indoor ventilation, good and effective ventilation methods can not only meet people's requirements for the indoor environment but also reduce the loss of indoor energy. Simultaneously, good ventilation can remove indoor pollutants and achieve clean indoor air. Therefore, ventilation is considered an important measure for improving indoor air quality. However, there is no standardization of the limit value of classroom ventilation rates. The US ASHRAE Standard [40] and Australia [41] provide ventilation rates corresponding to different age groups with different population densities. The UK BS EN 15251 standard [42] recommends the required ventilation rate for each individual at three indoor air quality levels. The German VDI 6022 Part 3 standard [43] indicates an average ventilation rate of 30 m^3/h for each person. The Chinese GB 50736 Standard [44] is based on the US ASHRAE standard and provides the corresponding value of required ventilation rates for each individual based on different population densities.

Previous studies have examined ventilation rates [6,7,14,15,45,46]. However, most of them recommend values of ventilation rates required to eliminate anthropogenic pollution in classrooms under a single temperature condition without considering the effect of temperature on human biological emissions. This approach has some limitations.

In summary, (1) Most previous studies focused on the measurement method, with a few combining it with a questionnaire. Evaluating indoor air quality grade is closely related to the impact of environmental pollution on human health, and the influence of the environment on the subjective perception of the human body should be considered. (2) Most studies represent the internal air quality of classrooms during specific seasons; based on test results from several classes in a certain season, only a few studies have conducted continuous monitoring of indoor air quality. To avoid the risk of environmental pollution, the relevant departments can timely and effectively control and rectify the unqualified air quality to ensure a safe and healthy environment; the air quality inside the classroom should be continuously monitored; (3) Previous studies have focused on ordinary classrooms, whereas there are few studies on professional classrooms (such as architectural classrooms). The class content in ordinary classrooms is primarily taught by teachers, whereas that in professional classrooms is relatively rich (e.g., teacher lectures, group discussions, program reports, drawings, and models). The different behaviors of indoor personnel have a significant impact on indoor air quality.

Therefore, the innovative points include 1) the real-world classroom scenarios with 100 min, 2) the combination of field and intervention studies; 3) the combination of objective measures and subjective surveys; 4) the continuous monitoring for sixteen weeks; and 5) the professional classroom with relatively rich classroom content. The scientific contributions are mainly reflected in that this study conducted field

measurements in professional classrooms to investigate air quality during daily classroom lectures. Intervention experiments were also conducted to study the effects of temperature on indoor air quality in real-world classroom scenarios. The engineering application potential of this study includes: 1) This study aimed to supplement information on the environmental characteristics of professional classrooms and provide reference data for improving the relevant ventilation standards. 2) This study has certain reference value for the study of the indoor thermal environment and air quality of university professional classrooms. 3) This study will continuously promote the research and development of teaching environments and improvement countermeasures in university professional classrooms. In summary, this study's real-world classroom scenarios and comprehensive measurements will provide valuable data for improving ventilation standards and promoting research and development in professional classroom environments.

2. Experimental methodology

The study was conducted in a classroom at a university in Shaoxing, Zhejiang Province, for 16 consecutive weeks from 28th February to 20th June in 2022 (spring and summer). The classroom was naturally ventilated before each test, and all windows and doors were closed during the class. There are 16 experiments together, and they were completed in the same classroom from 8:00 a.m. to 9:40 a.m. every Monday. Indoor temperature, relative humidity, CO_2 concentration, and total volatile organic compound (TVOC) concentration were measured separately during class.

The purpose of 12 field measurements was to study the characteristics of the classroom's indoor environment and changes in the indoor air quality. The other 4 interventions (2 in spring and 2 in summer) were designed to provide a more thorough analysis of the impact of indoor air quality and students' comfort levels in the classroom. Therefore, the composition of indoor VOCs was determined, and the results of the subjective evaluation of the perceived air quality in the classroom were analyzed.

2.1. Experimental subjects

2.1.1. Experimental classroom

The classroom used in the experiment was located on the first floor of a teaching building on the Hexi Campus of Shaoxing University. As shown in **Figure 1**, the dimension of the classroom is 9.9 m × 7.2 m × 3.2 m (length × width × height). The classroom's south wall is an external wall, with three external windows of 1.80 m × 2.56 m, which were all closed during class, and the size of the inter-window wall is 1.125 m. The windowless north wall is adjacent to the corridor, and there are front and back doors with both 1.2 m wide in the north wall. The front and back doors were opened randomly during breaks. The corridor is 1.8 m wide, and the dimensions of the three windows in the corridor, the state of the window closure, and the size of the inter-window wall are the same as those on the south wall. The east and west walls are windowless interior walls. Floor-type air conditioners were placed in the southwest corner of the classroom for indoor temperature control. There were six ceiling fans in the classroom that were not opened during class, and there was no mechanical

ventilation system. The size of the desk is 0.65 m × 0.4 m × 0.76 m (length × width × height); the transverse and longitudinal spacing between the desks is 0.66 m and 0.8 m, respectively. It should be noted that the four adjacent rooms were all architecture classrooms, which were refreshed in January 2022, and furniture such as desks and chairs was also replaced in January 2022.

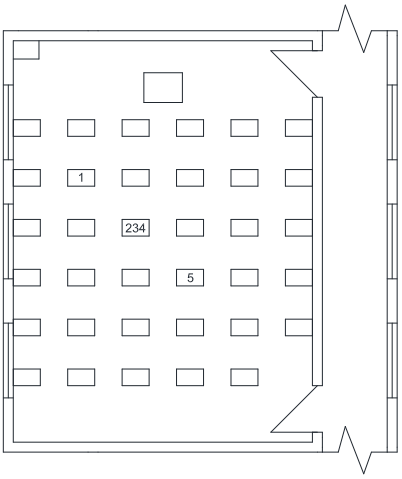

Figure 1. Classroom plan.

Note: the temperature, relative humidity and CO_2 concentration were measured in number '1, 2 and 5', TVOC was measured in number '3' and VOCs was measured in number '4'.

The front and back doors are randomly opened during recess and are all closed during class. The front and back doors are randomly opened during recess and are all closed during class. The front and back doors are randomly opened during recess and are all closed during class. There is a front door and a back door, both 1.2 m wide.

2.1.2. Characteristics of the subjects

Each lecture lasted 45 min, with a 10-min break. The classroom was exclusively for architectural students, designed specifically for architectural instruction. The course content for each class was tailored to meet the requirements of the major, as shown in **Table 1**.

Table 1. Course content for each week.

Number of weeks	Course content	
	0–45 min	55–100 min
1	TL, GD, RS, SD	TL, GD, RS, SD
2, 3, 5, 6, 7, 9, 10, 11, 13, 14, 15	TL	GD, SD
4, 8, 12, 16	GD, AF	RS

Teacher lecture (TL): When the teacher is lecturing, the teacher utilizes multimedia and a laser pointer together for teaching (the classroom is not equipped with chalk), walks back and forth at random sometimes, and talks. The students remained seated, listened to the lectures, and took notes. Random answers to questions.

Group discussion (GD): During the group discussion, the teacher walked back and forth and answered questions. Students sat in groups of 5–6, maintaining their positions while conversing.

Report on stage (RS): While reporting on stage, the teacher stood up, listened, and asked questions. Students stood on the platform, delivering presentations lasting 10 min each, with four students presenting each time. The other groups were also able to ask questions.

Student drawing designs (SD): For students drawing designs, the teacher walks back and forth randomly to answer questions. Students sit or stand to draw designs, and everyone uses a laptop to communicate with each other.

Analogue formation (AF): When creating the model, the teacher walked back and forth randomly to answer questions. Students sat or stood to create models and communicate with one another.

There were 26 students (20 males and 6 females) in this professional class in full attendance. The personal information of the 26 students is shown in **Table 2**. The students attending the class were 19 ± 1 year old, with an average skin surface area of 1.82 ± 0.17 m^2 and a body mass index of 20.77 ± 2.60 kg/m^2. All the students were in good health and did not engage in smoking and other bad habits. Furthermore, there was a female teacher and an experimenter in the classroom. Considering the absence of any students, the population density in the classroom should be 0.32–0.39 persons/m^2. However, not everyone left the classroom during the 10-minute break, and the study did not count how many students stayed in the classroom during the 10-minute break in the 16 experiments. The number of students in the classroom for each experiment is listed in **Table 3**.

Table 2. Personal information of subjects and invitees (mean value ± standard deviation).

Role	Number of persons	Height (m)	Weight (kg)	Age (years)	Average skin surface area (m^2)	Body mass index (kg/m^2)
Subjects	20 males/6 females	1.75 ± 0.16	70.7 ± 20.21	19 ± 1	1.82 ± 0.17	22.77 ± 2.60
Invitees	13 males/13 females	1.72 ± 0.07	70.1 ± 15.56	23 ± 1	1.76 ± 0.25	22.26 ± 5.50

Note. Skin surface area = $0.202 \times (\text{weight})^{0.425} \times (\text{height})^{0.725}$ [47], Body mass index = weight/height^2.

Table 3. Number of students and population density of classrooms during each measurement.

Number	Date	Total number of persons	Males	Females	population density (person/m^2)
1	28th, eb.	28	20	8	0.39
2	7th, Mar.	28	20	8	0.39
3	14th, ar.	28	20	8	0.39
4a	21st, ar.	27	20	7	0.38
5b	28th, Mar.	26	20	6	0.36
6	4th, Apr.	28	20	8	0.39
7	11th, pr.	28	20	8	0.39
8	18th, pr.	28	20	8	0.39
9	25th, pr.	27	20	7	0.38
10	9th, May.	25	19	6	0.35
11	16th, ay.	23	18	5	0.32
12	23rd, ay.	28	20	8	0.39
13	30th, ay.	27	20	7	0.38
14	6th, Jun.	28	20	8	0.39
15A	13th, un.	26	18	8	0.36
16B	20th, Jun.	28	20	8	0.39

Another group of 26 postgraduate students in a professional class were invited

for sensory assessment in the intervention measurements. Their personal information is shown in **Table 3**. The invitees were 23 ± 1 years old, with an average skin surface area of 1.76 ± 0.25 m^2 and a body mass index of 22.26 ± 5.50 kg/m^2. All students were in good health, and the male-to-female ratio was 1:1. There were no significant differences in the anthropometric data.

2.1.3. Characteristics of the vocational class studied

The architectural design course of architecture major has the following characteristics: the lecture is taught by the teacher in the first 45 min, then the students draw with a laptop, and they could communicate with others in the second 45 min. At the same time, the teacher could arrange for the students to report the drawing content irregularly in the second 45 min. The architectural design courses are taught in this form in universities in China. The architectural design is the main course for architecture major, consisting of architectural design (1) to (8), with one architectural design course per semester.

2.2. Experimental procedures

The detailed steps of the basic and interventional measurements are shown in **Figure 2**. Before the basic measurement, the students entered the classroom successively, and the environmental measurements began at 8 a.m. (i.e., 0 min for the lecture). These measurements included an unceasing monitor of the air temperature, relative humidity, and CO_2 concentration. The TVOC concentration was recorded intermittently every 5 min at 0, 20, 40, 55, 75, and 95 min during class. There was a 10-minute break between classes from 8:45 a.m. to 8:55 a.m., allowing students to enter and exit the classroom freely through the front and back doors. At other times, the classroom doors and windows were closed.

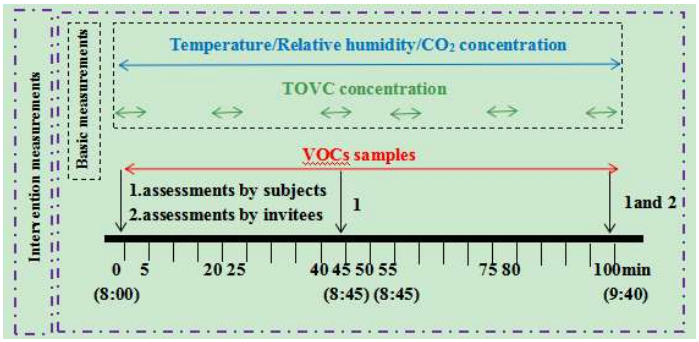

Figure 2. Procedures for basic and intervention measurements.

The intervention measurements and the basic measurement process were essentially the same, but with some differences. (1) For the intervention group (tests 5 and 16), the indoor temperature was maintained at 25 ± 1.5 °C using an air conditioner, while for the control group (tests 4 and 15), the indoor temperature changed naturally without an air conditioner. (2) Volatile organic compound sampling was conducted for 100 min before and during the class in all four intervention measurements. (3) Subjective evaluations of classroom air perception quality were collected from the subjects and invitees during the class in the four intervention measurements. The subjects were in class all the time, and they completed the questionnaires three times

at 0, 45, and 100 min; the invitees came in at 0 and 100 min, and they completed the questionnaires twice at 0 and 100 min, respectively.

2.3. Environmental element measurements

The instruments and parameters used for these 16 measurements are listed in **Table 4**. The indoor CO_2 concentration, temperature, and relative humidity were continuously recorded using a TR-76 Ui-s instrument at 1-min intervals. Prior to formal measurements, all instruments were calibrated by certified quality inspection agencies. The TVOC concentration was measured using a portable VOC detector (TSI EMV-7) calibrated with isobutylene as the standard gas before using the instrument. TVOC concentrations were recorded intermittently every 5 min at 0, 20, 40, 55, 75, and 95 min during class with data recording intervals of 1 s. Finally, the average value at 5 min was considered the indoor TVOC concentration value of the corresponding period. The three measurement points shown in **Figure 1** as 1, 2, 3, 4, and 5 were arranged on a desk along the room diagonal at equal intervals in the horizontal direction. The table is 0.76 m high. Considering that students sit in class, we can avoid blocking the sight with instrument shelves. Obtain a more complete representation of the temperature, relative humidity, and CO_2 concentration distributions in the classroom. The TVOC concentration had only one measurement point, located at the centre of the student. As shown in **Figure 1**, the temperature, relative humidity, and CO_2 concentration were measured in numbers '1, 2, and 5'; TVOC was measured in number '3'; and VOCs were measured in number '4'. It should be noted that, owing to the needs of the experiment, the three desks were empty; that is, no students were sitting there during class.

Table 4. Instrument specifications.

Measured parameters	Instruments	Manufacturers	Measurement range	Measurement accuracy	Recording interval
Temperature (℃)	TR-76 Ui-s	T&D	0–55	± 0.5	1 min
Relative humidity (%)			10–95	± 2.5%	1 min
CO_2 (ppmv)			0–9999	± (50 ppmv + 5% reading)	1 min
TVOC (ppbm)	TSI EMV-7	TSI	0–500000	± 5%	1 s

In addition to these parameters, VOCs were also sampled from the intervention measurements (Tests 4, 5, 15, and 16). An automatic sampler GSP-400FT (GASTEC) and an activated carbon tube 258A-20-20 (GASTE) were selected as the sampling devices. Samples were taken before class, when nobody was present, and during that class for a duration of 100 min. All samples were stored in a −5 ℃ reservoir and later sent to a specialized laboratory for processing and analysis. After pretreatment in the laboratory, all samples underwent gas chromatography-mass spectrometry (GC Orbitrap, Thermo Fisher Scientific). Full-scan MS acquisition was performed using an m/z range of 30–400 with a resolution of 60,000 FWHM. The outlet and inlet temperatures were set at 230 ℃ and 280 ℃, respectively, and the shunt samples were ionized by EI with a shunt ratio of 10:1. The MS transmission line temperature was 230 ℃, the temperature of the electronic ionization source was 260 ℃, and the obtained data were processed using Trace Finder 5.1 data processing software. Finally,

the detected compounds, their corresponding retention times, and chromatographic peak intensity values were determined.

It should be noted that the indoor and outdoor measurements were conducted simultaneously, which included outdoor relative humidity, outdoor temperature, and outdoor CO_2 concentration. The data were collected by the instrument TR-76Ui-s placed on the windowsill outside the classroom at a 1-min interval.

2.4. Questionnaire survey

In addition to personal information such as sex, age, height, weight, health status, and bad habits, the questionnaire survey also included information on the perception of air quality in the classroom, such as odor intensity, acceptability, and satisfaction with air quality [48]. Odor intensity was assessed using 6 points of consecutive grades, namely, no odor (0), slight odor (1), moderate odor (2), strong odor (3), very strong odor (4), and overwhelming odor (5). The air quality acceptability was two consecutive grades: from obviously unacceptable (−2) to just unacceptable (−1), from just acceptable (0) to fully acceptable (1); Air quality satisfaction was assessed by consecutive grades with two ends, with dissatisfaction (0) and satisfaction (1).

2.5. Calculation of the CO_2 emission rate of the members in the classroom

As the main source of CO_2 in the classroom were the classroom members, the mean CO_2 emission rate of the members was calculated after measuring the indoor CO_2 concentration. Each 100-min measurement was divided into two cycles with a 10-minute break, and the interval in which the concentrations of CO_2 increased steadily in every cycle was truncated for calculating. According to the indoor CO_2 mass balance equation in Equation (1), the formula for calculating the personnel CO_2 emission rate can be obtained using the integral conversion method of Equation (2).

$$\frac{d(C_i V)}{dt} = GN + C_{out}Q - C_i Q \quad (1)$$

$$G = 10^{-6} \times \frac{Q}{N} \times \left(\frac{C_1 - C_2}{e^{-\frac{Q}{V}\Delta t} - 1} + C_1 - C_{out}\right) \quad (2)$$

where C_i is the measured indoor CO_2 concentration (C_1 is the indoor CO_2 concentration which is recorded at 10 and 60 min of class, C_2 is the CO_2 concentration which is recorded at 30 and 80 min of class, ppmv), V is the classroom volume (228 m^3), t is the time of C_i (minute), G is the human CO_2 emission rate (L/h per person), N is the number of students remaining in the classroom, and C_{out} is the outdoor CO_2 concentration, with 470 ± 26 ppmv as measured by the TR-76 Ui-s instrument. Q is the ventilation rate of the classroom with all the windows and doors closed, and 26.0 L/s as measured using the tracer gas (CO_2) concentration decay method [49]. Δt is the time interval (20 min) of the calculation period.

The uncertainty of the CO_2 emission rate Equation (3) was calculated following the uncertainty analysis in JJF 1059.1–2012 ‘Evaluation and expression of measurement uncertainty’ [48].

$$U_c(y) = \sqrt{\sum_{i=1}^{n} \left[\frac{\partial f}{\partial x_i}\right]^2 u^2(x_i)} \quad (3)$$

where the derivative term $\frac{\partial f}{\partial x_i}$ is the sensitivity coefficient of the input variable x_i, and $u^2(x_i)$ is the standard uncertainty of the input variable x_i.

The uncertainty in the CO_2 emission rate includes the following variables: (1) Uncertainty in the measurement of the CO_2 concentration due to an indication error, calculated as $u(x) = \frac{a}{k}$ where a is the instrument precision specified by the manufacturer. That is, the CO_2 concentration measured by the TR-76 Ui-s instrument is 50 ppmv, and k has a confidence factor of 1.732; (2) The CO_2 concentration uncertainty is caused by multiple measurements, which are calculated by the range method. The expression is $u(x) = \frac{R}{C\sqrt{n}}$, where R is the difference range, C is the confidence factor equal to 1.64, and n is the number of measurements, which was three in this study. (3) Uncertainty in the ventilation rate gained by the CO_2 concentration decay method and (4) uncertainty in the classroom volume were considered. The change in the net classroom volume caused by the number of members in the classroom was estimated to be less than 0.12 m^3; therefore, the uncertainty caused by volume could be ignored.

3. Results

3.1. Thermal environment in the field measurement

3.1.1. Temperature

Figure 3 shows the changes in indoor and outdoor temperatures during the measurement process. (1) The change in outdoor temperature: the average outdoor temperature gradually increased from 11.4 ℃ to 30.1 ℃ due to seasonal changes from spring to summer. Additionally, the outdoor temperatures also increased by 1.5–3.3 ℃ during each 100-min measurement, especially in test 16 on 20th June with the fastest rise.

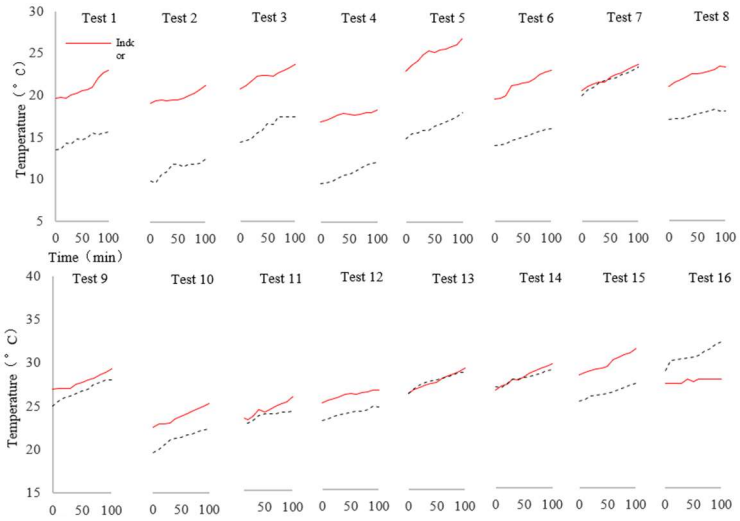

Figure 3. Indoor and outdoor air temperature in 16 tests.

(2) The change of indoor temperature: the average indoor temperature showed an upward trend from February to June, with the lowest being 17.8 ℃ and the highest being 29.2 ℃, also influencing seasonal changes. An air conditioner was used to control the indoor temperature for the intervention measurements in tests 5 and 16. The measurement results indicated that the indoor temperature was 25 ± 1.5 ℃, which showed that the indoor temperature was well controlled with the air conditioner in the classroom and could meet the conditions of the experiment. At the same time, during the 100-minute measurement period, the indoor temperature gradually increased by 1.0–4.0 ℃ because the doors and windows were closed during the class, and the indoor temperature was mainly affected by the various behaviors of the members in the classroom. In test 1, the teacher arranged four course contents, and the students were very active, resulting in an increase of 3.4 ℃ in the indoor temperature of the classroom within 100 min. In tests 2, 3, 5, 6, 7, 9, 10, 11, 13, 14, and 15, the intervention measurements were conducted during the 0–45 min and 55–100 min intervals. In test 5, which took place in spring, the classroom temperature increased by 4.0 ℃, the highest among all test groups, due to the air conditioner heating. While comparing 0–45 min and 55–100 min, the amplitude of the temperature increases also differed from the different behaviors of the members in the classroom. Overall, the magnitude of the increase in the indoor temperature within 0–45 min was less than that within 55–100 min. In tests 4, 8, 12, and 16, the intervention measurements were conducted during 0–45 min and 55–100 min intervals. In test 16, which took place in summer with the air conditioner refrigeration, the indoor temperature decreased by 1.0 ℃ within 100 min. While comparing 0–45 min and 55–100 min, test 16, the amplitude of the temperature change was not obvious under the influence of air conditioning. For Tests 4, 8, and 12, the magnitude of the indoor temperature increases within 0–45 min is greater than that within 55–100 min. In addition, there was a 10-min break for the 16 test groups; although the front and back doors were randomly opened at this time, the indoor temperature was not significantly affected by the short opening time.

(3) Comparison of the indoor and outdoor temperature: the temperature difference between indoor and outdoor was 0.9–6.4 ℃, which may be due to the influence of the building envelope making the indoor temperature higher than that of the outdoor temperature.

It is worth mentioning that the indoor and outdoor temperatures in Test 7 were essentially the same before class, and similar conditions were found in Tests 11, 13, and 14. This was because the doors and windows of the classroom were open before class in these four tests. After confirming with the logistics staff of the teaching building, the students who used the classroom the night before forgot to close the doors and windows, which led to the above results.

3.1.2. Relative humidity

Figure 4 shows the calculation results for the indoor and outdoor relative humidity. It can be seen that: (1) The change of outdoor relative humidity: the average outdoor relative humidity was 35.7%–93.6%, and the outdoor relative humidity increased with the outdoor temperature. In addition to seasonal factors, this could be because the experimental classroom is near the Fengze River, and a higher outdoor

temperature could lead to more water vapor in the air, which, in turn, increases the relative humidity outside. However, regardless of the outdoor temperature, the outdoor relative humidity exceeded 80% on rainy days, as shown in Tests 3, 4, 9, 10, 12, 13, 15, and 16. This shows that the relationship between the outdoor relative humidity and temperature on rainy days is not obvious. Meanwhile, the outdoor relative humidity remained in a relatively stable state during the 100-minute measurement, ranging from 0.0–1.5%. This may be because the outdoor temperature increased from 1.5–3.3 ℃, but did not increase enough to cause excessive changes in the outdoor relative humidity.

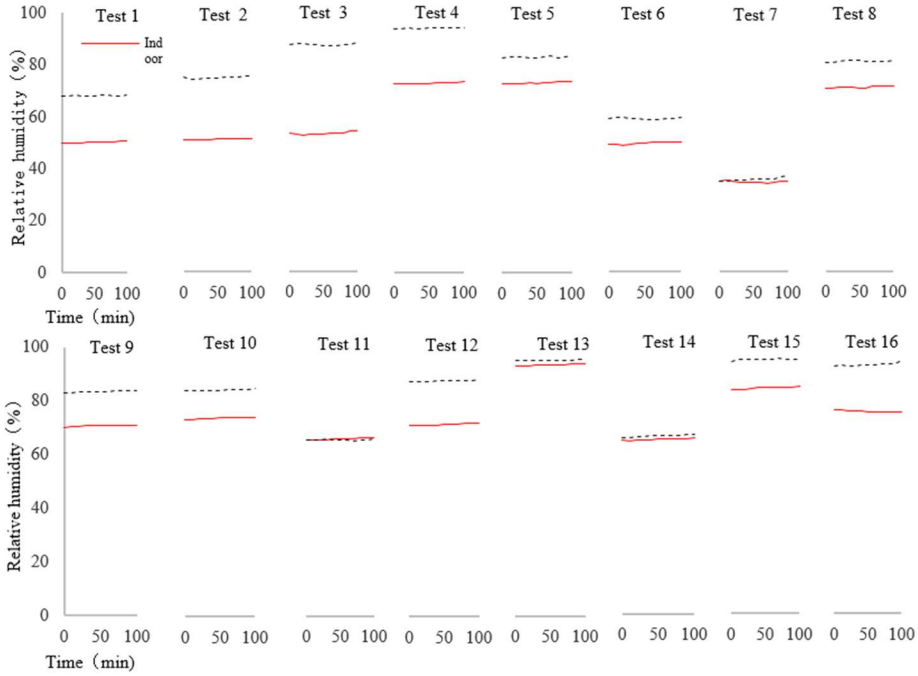

Figure 4. Indoor and outdoor relative humidity in 16 tests.

(2) Change in the indoor relative humidity: the average indoor relative humidity ranged from 34.5%–91.0%. Meanwhile, the indoor relative humidity fluctuated slightly in the range of 0.0%–1.0% during the 100-minute measurement. The doors and windows were closed during class; therefore, the indoor relative humidity was mainly affected by the indoor temperature and indoor members' breathing. However, the indoor relative humidity did not change much, which may be due to the following: first, the increase in the indoor temperature was not sufficient to cause a change in the indoor relative humidity; second, the population density of 0.32–0.39 people/m^2 in the classroom was too low to affect the indoor relative humidity. Meanwhile, the indoor relative humidity increased by 0.5% for intervention measurement 5 and decreased by 0.8% for intervention measurement 16 within 100 min, indicating that the intervention measurement did not have a significant impact on the indoor relative humidity. In addition, the indoor relative humidity was not significantly affected by the short door-opening time during a 10-min break.

(3) Comparison of indoor and outdoor relative humidity: the relative humidity difference between indoors and outdoors was 1.1%–26.0%. The indoor and outdoor relative humidities in Test 7 were basically the same before class, and similar

conditions were found in Tests 11, 13, and 14.

Except for the mean values, the measured indoor temperature and relative humidity uncertainties were calculated in this study, as listed in **Table 5**. The uncertainty for the indoor temperature and indoor relative humidity was 0.5 ± 0.1 ℃ and 1.6 ± 0.2%, respectively. The relative errors were below 3% and 4%, respectively.

Table 5. Uncertainty for the three measurement points: indoor temperature, relative humidity and CO_2 concentration.

	(Mean value ± standard deviation)	**Ranges**
Indoor temperature (℃)	0.5 ± 0.1	0.4–0.7
Indoor relative humidity (%)	1.6 ± 0.2	1.4–2.0
CO_2 concentration (ppmv)	99 ± 7	80–110

3.2. CO_2 concentration measurement

The indoor CO_2 concentration measured in the classroom was shown in **Figure 5** and was 500–887 ppmv at the beginning of the lecture. During class, the indoor CO_2 concentration gradually increased because of the accumulation of CO_2 produced by classroom members when the doors and windows were closed. The opening of the front and back doors during a 10-min break resulted in a transient decrease in the indoor CO_2 concentration. Subsequently, the CO_2 concentration continued to increase, reaching 2100–3600 ppmv by the end of the class. The average indoor CO_2 concentration was 1176.9–2031.7 ppmv during the 16 tests, and the real-time CO_2 concentration above 1000 ppmv was about 90% of the class duration. Overall, the trend in the CO_2 concentration was consistent with that of the indoor temperature. In tests 1, 2, 3, 5, 6, 7, 9, 10, 11, 13, 14, and 15, test 5 exhibited the fastest increase in CO_2 concentration within 100 min. The increase of 0–45 min in the CO_2 concentration was less than that at 55–100 min CO_2 concentration. In tests 4, 8, 12, and 16, there was no significant difference in the magnitude of the CO_2 concentration rise within 100 min for test 16. At tests 4, 8, and 12, the 0–45 min CO_2 concentration increases were greater than the 55–100 min CO_2 concentration increases.

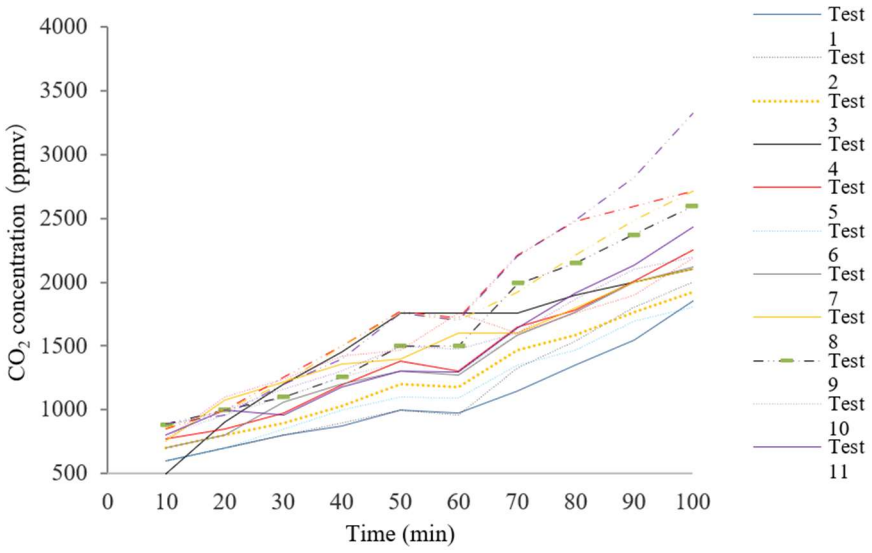

Figure 5. Measured indoor CO_2 concentration during 100-min class.

The average indoor temperature during the corresponding period was calculated in this study. **Figure 6** shows the calculated average CO_2 emission rates and indoor temperatures. The average emission rate of CO_2 was 22.76 ± 3.26 L/h for each person, with an uncertainty for the average emission rate of CO_2 of 2.6 L/h for each person approximately. The resulting relative error was less than 7%. It is evident that there is a positive correlation between human CO_2 emission rate and indoor temperature ($p < 0.05$), namely, the increased indoor temperature would cause an increase in human CO_2 emission rate. Based on the regression analysis, it can be estimated that the human CO_2 emission rate increases by 0.78 L/h for each person when the temperature increases by 1 ℃ with the range of 17 ℃–31 ℃. According to ASHRAE 62.1 [50], the CO_2 emission rate of adult males in standard sedentary and reading states was approximately 15.48 L/h. Therefore, the human CO_2 emission rate increased by approximately 4.5% for every 1 ℃ increase in temperature.

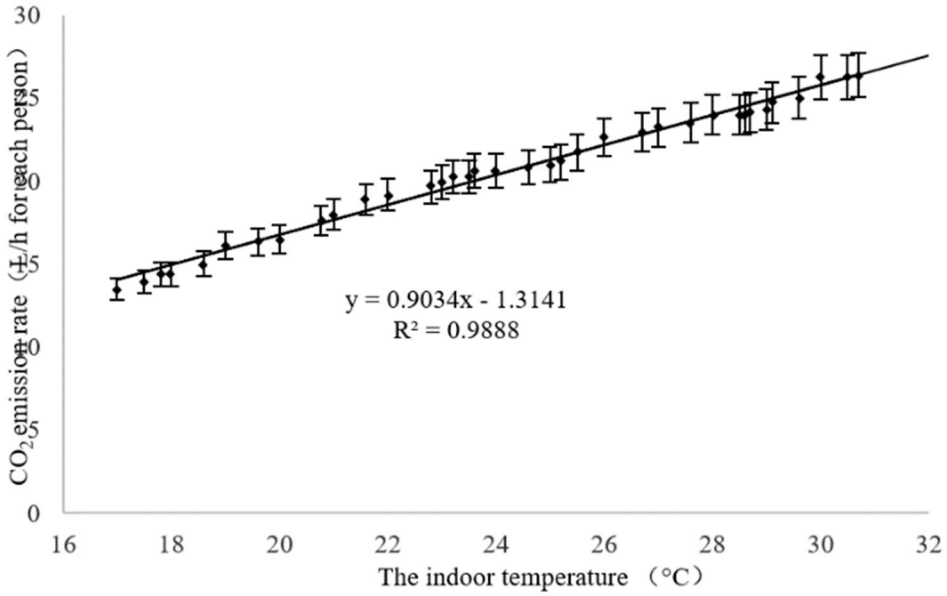

Figure 6. The CO_2 emission rate at different temperature.

3.3. TVOC concentration measurement

Figure 7 shows the results of TVOC concentration measurements conducted in the classroom. The mean TVOC concentration varied widely across 16 measurements, with the maximum and minimum values being 1026 ± 13 ppbm and 520 ± 7 ppbm, respectively. The mean TVOC concentration across the 16 measurements was 706 ± 276 ppb. Comparatively, TVOC concentrations in Tests 9 and 15 were higher from 0 min than the other test groups because of the higher indoor temperatures of the two groups from the beginning. The TVOC concentration in test 5 showed an obvious upward trend with air conditioner heating, and the indoor temperature rose rapidly, leading to a rapid rise in the TVOC concentration; however, it remained stable in test 16, also utilizing an air conditioner, alongside a consistent indoor temperature.

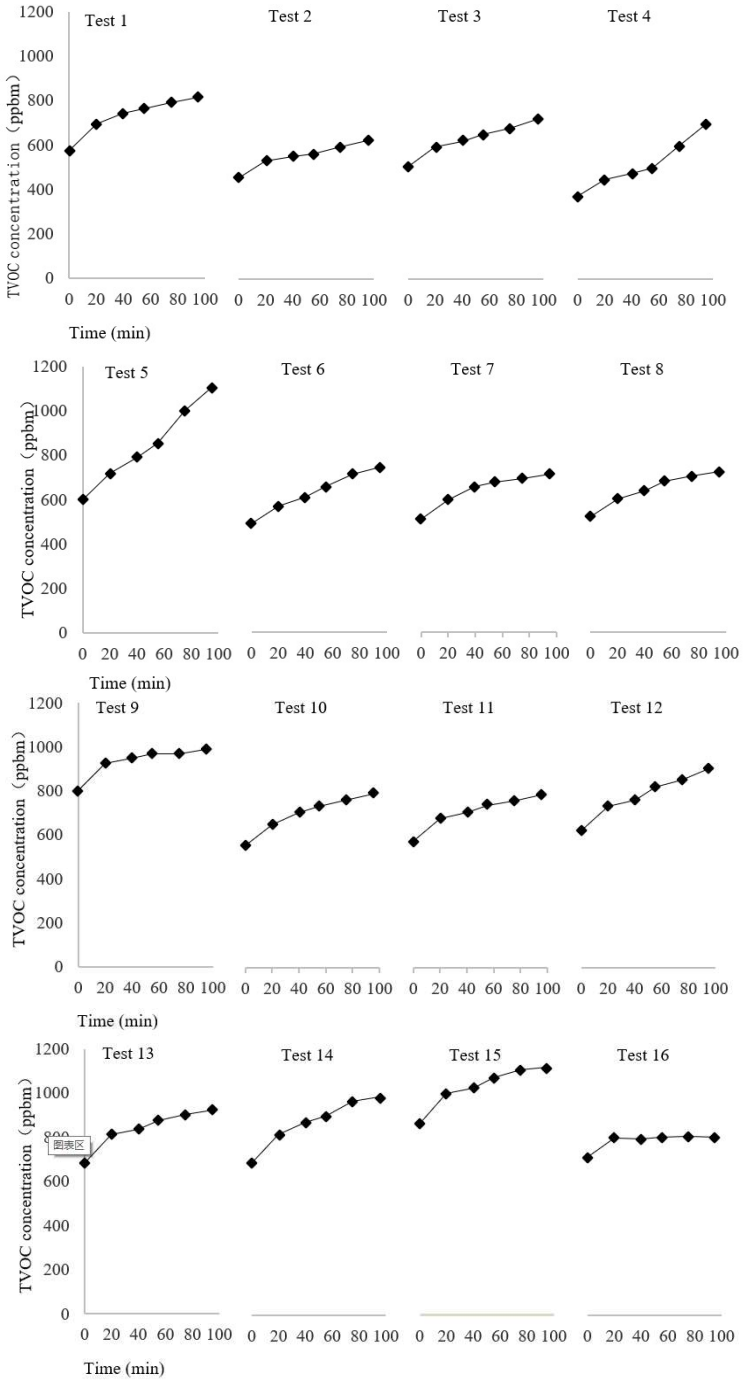

Figure 7. Measured indoor TVOC concentration during 100-min class.

Zheng et al. [51] and Jia et al. [28] showed that the indoor TVOC concentration change exhibited a trend similar to that of the CO_2 concentration, both rising slowly, which is consistent with the results of this study. However, their study also indicated that the average indoor TVOC concentration in spring and summer was 400.5 ± 26 ppbm and 296 ± 30 ppbm, respectively, which was inconsistent with the average TVOC concentration (706 ± 276 ppbm) in this study. This may be because, although the number of indoor personnel, the typical activity of personnel, the opening or closing of doors and windows, and the function of the classroom were different in spring and summer, the average indoor TVOC concentration was also different.

3.4. Indoor VOCs composition

Eight air samples were collected before and during the four intervention experiments (tests 4, 5, 15, and 16), and 40 common compounds were detected, which is shown in **Table 6**. Most of the VOCs detected were exogenous.

Table 6. The volatile organic compounds detected in the surveyed classrooms.

No.	Component name	CAS No.	No.	Component name	CAS No.
1	Benzonitrile	100-47-0	21	Benzene, 1,3-dichloro-2-isocyano-(9CI)	6697-95-6
2	2-Methylthiophene	554-14-3	22	Ethylbenzene	100-41-4
3	1-Ethyl-3-methylbenzene	620-14-4	23	Naphthalene	91-20-3
4	Mesitylene	108-67-8	24	Isoprene	78-79-5
5	Dodecane	112-40-3	25	1,3-Butanediol	107-88-0
6	Butylated Hydroxytoluene	128-37-0	26	Thiophene	110-02-1
7	Benzene	71-43-2	27	Heptanal	111-71-7
8	2,4-Dithiapentane	1618-26-4	28	Benzothiazole	95-16-9
9	2-methyl-5-(1-methylethyl) bicyclo [3.1.0] hex-2-ene	2867/5/2	29	Styrene	100-42-5
10	4-Isopropylbiphenyl	7116-95-2	30	p-Xylene	106-42-3
11	o-Xylene	95-47-6	31	1,4-Dichlorobenzene	106-46-7
12	Acetone	67-64-1	32	3,4-Dimethylbenz	5973-71-7
13	Dimethyldisulfide	624-92-0	33	Formaldehyde	50-00-0
14	Methyl propyl trisulfide	17619-36-2	34	(1-Butyloctyl) benzene	2719-63-3
15	(1-Methylethyl) benzene (Cumene)	98-82-8	35	Propylbenzene	103-65-1
16	Methyl propyl disulfide	2179-60-4	36	1-Ethyl-2-methylbenzene	611-14-3
17	Tetrachloroethylene	127-18-4	37	Toluene	108-88-3
18	1,6-Dimethyl-4-(1-methylethyl) naphthalene	483-78-3	38	Phenol	108-95-2
19	m-Xylene	108-38-3	39	1-Ethyl-4-methylbenzene	622-96-8
20	Isophyllocladene	511-85-3	40	1,1′-Biphenyl, 3,4-diethyl-	61141-66-0

For a more detailed understanding of the differences in the indoor VOC composition at different temperatures before (0 min) and during (100 min) classes, two air samples collected in each intervention experiment were analyzed in this study. The results of Tests 4 and 16 (**Figure 8**), and Tests 5 and 15 (**Figure 9**) were generally consistent. The relative concentration difference of the same component was qualitatively determined from the chromatogram.

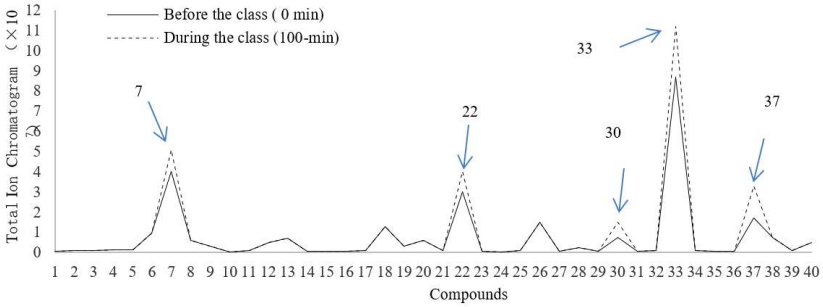

Figure 8. Chromatography comparison of sampling results before and after Class (Test 4 and 16).

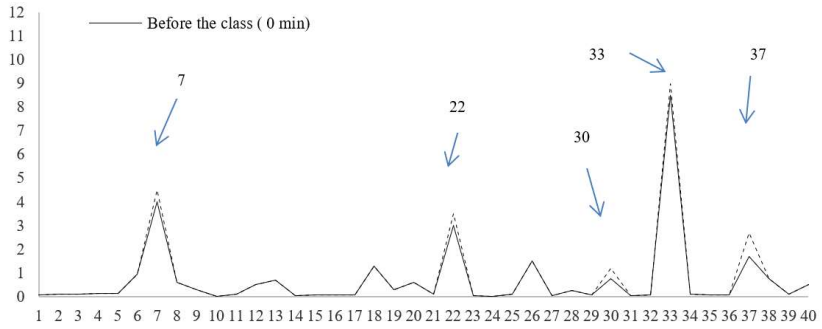

Figure 9. Chromatography comparison of sampling results before and after class (Test 5 and 15).

In tests 4 and 16, the concentrations of benzene (No. 7), ethylbenzene (No. 22), *p*-xylene (No. 30), formaldehyde (No. 33), and toluene (No. 37) increased significantly, whereas the levels of the other 35 components remained unchanged. In tests 5 and 15, the trends were similar, but the five compounds increased less than those in tests 4 and 16. This difference could possibly be attributed to the fact that in Tests 4 and 16, the building materials for the models were kept in the classroom with the doors and windows closed during classes. In Tests 5 and 15, there was no model in the class; therefore, there were no other building materials in the classroom.

3.5. Air quality assessment in the classroom in the intervention experiments

The subjective perceptions of indoor air quality by subjects experiencing adaptation in the classroom and by invitees upon entering the intervention experiment are shown in **Figure 10**. The results demonstrated that the air quality satisfaction and acceptability of Tests 5, 15, and 16 were significantly lower than those of Test 4, and the odor intensity was significantly stronger than that of Test 4. Furthermore, this difference persisted with an increase in stay time. Since the mean indoor temperature for tests 4, 5, 15, and 16 was 17.8 ℃, 25.2 ℃, 29.2 ℃ and 27.3 ℃, respectively (seen analysis in 3.1 above), it could be concluded that there was a reduced perceived air quality along with the increased temperature and stay time.

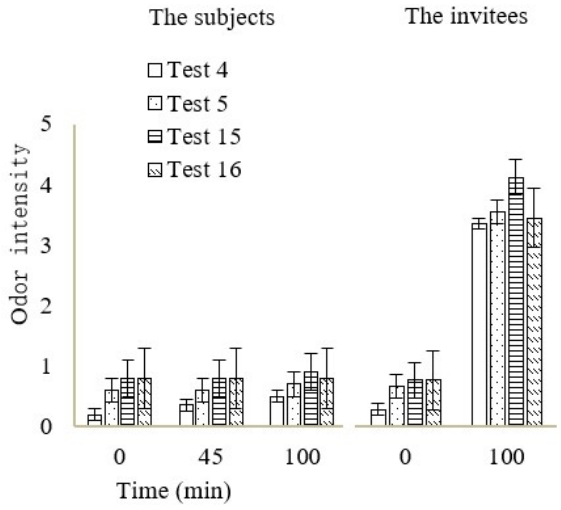

Figure 10. (*Continued*).

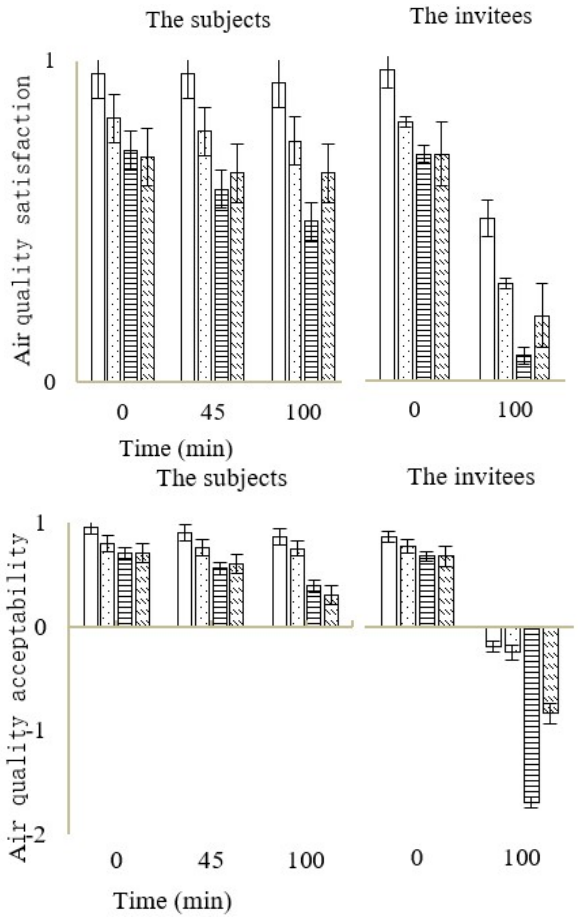

Figure 10. Air quality assessment performed by subjects and invitees in the intervention experiments.

Note: L represents the CO_2 concentration (ppmv) corresponding to the 0, 45 and 100 min of the test group. From **Figure 5**, A-D values were 500, 776, 887, 876, E-H values were 1760, 1380, 1760 and 1500, and I-L values were 2200, 2595, 3600 and 2430, respectively.

From the analysis in Section 3.2, the CO_2 concentrations in tests 4, 5, 15, and 16 were 500, 776, 887, and 876 ppmv at 0 min, 1760, 1380, 1760, and 1500 ppmv at 45 min, and 2200, 2595, 3600, and 2430 ppmv at 100 minutes, respectively. Therefore, the premise of the air quality assessment in this study was that the CO_2 concentration should be 500–3600 ppmv.

According to the odor intensity results, the evaluation of tests 4, 5, 15, and 16 at 0, 45, and 100 min was between no odor and a slight odor, and test 4 was closer to no odor. For the invitees, the evaluation of the four groups ranged between no odor and slight odor at 0 min. There was greater variation at 100 min, with a strong odor in tests 4, 5, and 16, and a very strong odor in test 15.

Based on the results of air quality satisfaction and acceptability, the evaluation of Test 4 was the highest among the four tests of the corresponding test times for both the subjects and invitees. The evaluations of the two groups were very similar at 0 min; however, when the CO_2 concentration was above 2000 ppmv at 100 minutes, the evaluation value of the invitees was lower than that of the subjects. The invitees were more dissatisfied with air quality satisfaction on tests 4, 5, 15, and 16. In tests 4, 5, and 16, the evaluation range of air quality acceptability for the invitees was between just unacceptable and just acceptable. In Test 15, the corresponding evaluation results were

almost unacceptable.

The above analysis shows that the subjects had a better perception of air quality than the interviewees, with lower perceived odor intensity and higher satisfaction and acceptability of air quality. This difference seems reasonable, considering that the subjects stayed continuously in the classroom and had strong olfactory adaptation. The results of this study were inconsistent with those of Liu et al. [9], who indicated that respondents' acceptance of indoor air quality was mainly influenced by thermal sensations, independent of the CO_2 concentration. This may be because 1) Liu's study focused on the winter semester, whereas this study focused on spring and summer. 2) Liu's study investigated students' thermal comfort and perceived air quality in naturally ventilated university classrooms while the doors and windows were closed during class.

4. Discussion

4.1. Influence of indoor temperature on the CO_2 emission rate of the human body

The average CO_2 emission rate ranged from 19.5–26.02 L/h per person, which was higher than that reported in previous studies. Qi et al. [52] showed experimentally that the CO_2 emission rate in sedentary was 13.57 L/h for Chinese males and 11.13 L/h for females at 22–24 ℃, respectively. Similarly, Wang [53] explained that the CO_2 emission rate for Chinese males and females in the sitting reading state was 16.2 L/h and 13.2 L/h, respectively, at a temperature of 26 ℃. This may be because in the 16 tests, the status of the subjects pointed out in previous studies was sedentary, whereas the status of the subjects in this study had many changes. Therefore, the average CO_2 emission rate obtained in this study was high.

Previous studies have suggested that the CO_2 emission rate depends mainly on the metabolic rate [54], which is determined by temperature [55]. Thus, an increase in temperature leads to a higher metabolic rate, subsequently resulting in higher CO_2 emission rates. Based on the results of the present study, it could be concluded that the human CO_2 emission rate increases by 0.78 L/h for each person when the temperature increases by 1 ℃ within the range of 17–31 ℃. This result is similar with that of Zhang [54], where the human thermal sensation ranged from neutral to warm between the temperatures at 26 ℃–32 ℃, resulting in a significant increase in CO_2 emissions. These results suggest that, compared to thermal neutrality, people emit more CO_2 when they feel thermal warmth. Similar findings have also been reported by Liu et al. [9], Luo et al. [56], and Kuga et al. [11], indicating a higher CO_2 emission rate occurred at higher temperatures when subjects were warm.

4.2. Modified ventilation rate corresponding to the human CO_2 emission rate

In this study, the trace gas (CO_2) concentration is used to measure the ventilation capacity in the classroom Equation (4). The trace gas method follows the principle of mass conservation and is calculated as follows:

$$\frac{dC}{dx} = \frac{Q}{V}(C_{out} - C_x)\frac{V_{co_2}}{V} \quad (4)$$

where $\frac{dC}{dx}$ is the outdoor airflow rate for each person (L/s); V is the classroom volume (228 m^3); C_x is the indoor CO_2 concentration (ppmv); C_{out} is the outdoor CO_2 concentration (470 ppmv); Q is the ventilation rate (L/S); and $V\text{co}_2$ is the human emission rate (L/s). To maintain the indoor CO_2 concentration at 1000 ppmv, the required ventilation rate per person was 6.75 L/s according to Equation (3). This result is largely consistent with ASHRAE 62.1 criteria [40]. In general, to maintain 1000 ppmv of indoor CO_2 concentration, the calculated ventilation rate for each person needs to increase by 0.25 ± 0.3 L/s to account for the increased human CO_2 emission because of the temperature rise.

4.3. Characteristics of the VOCs in the classroom

This study points out that the substances with the highest detection frequency were benzene, formaldehyde, toluene, *p*-xylene, and ethylbenzene. This result is similar to those of previous studies [15,57], which also identified benzene, *p*-xylene, ethylbenzene, and toluene as the most frequently detected in experimental classrooms. Benzene primarily originates from paint, adhesives, plates, foam plastics, etc.; formaldehyde from wood, glass glue, latex paint, paint, etc.; toluene and *p*-xylene from paint, plywood, foam filler, etc.; and ethylbenzene from paint, spray paint, adhesives, etc. Indoor concentrations of these substances are related to fatigue values [15], and excessive exposure to these substances increases the risk of cancer [57]. In conclusion, related research should focus on the pollutants released by various indoor building materials.

However, the VOC components detected in this study differed from those detected by Fu et al. [26], Kang et al. [58], and Liu et al. [59]. This may be because of different factors, including occupied conditions, season and function, classroom type, types of items inside the classroom, quality of furniture, and possible factors correlated with human-related items.

Furthermore, this study is inconsistent with the Zhang et al. [22] study, which indicated that the real-time difference of indoor VOC composition is more obvious when the indoor temperature is between 16 ℃ and 24 ℃, and there is basically no difference in real-time of indoor VOC components when the indoor temperature is between 24 ℃ and 30 ℃. Several factors contribute to these differences. First, regarding objective factors, the architecture classroom was renovated in January 2022, and furniture such as desks and chairs were also replaced. The renovations were completed in February 2022, but the windows were kept open for extended periods to ensure ventilation. Since it was winter, the effect of scattered taste was not the best. Second refers to subjective factors, that is, the content of the classroom is different. In tests 4 and 16, model-making activities were arranged, and the students brought a large quantity of building materials into the classroom; therefore, the concentration of some VOCs increased significantly over 100 min. Hence, it can be seen that the concentration of indoor VOCs is not only related to temperature but also to the above objective and subjective factors.

4.4. Deficiencies

The results of the current study contribute to the field of indoor air quality, but some shortcomings still remain. First, this experiment only covered spring and summer, and the data obtained did not reflect the actual conditions in autumn and winter. Therefore, future experiments should include at least two semesters covering all four seasons. Second, this study only performed a simple correlation analysis between the indoor air temperature and CO_2 emission rate. To further elucidate the association mechanism between air temperature and CO_2 emission rates, a wider temperature range should be investigated. Third, the experiment was conducted in a single classroom setting. If the experimental conditions permit, multiple classrooms with different orientations should be selected to conduct future experiments. Fourth, the current participants and invitees were only students from one class, and the number of students could be expanded in the future. Fifth, to ensure environmental safety, it is necessary to predict the long-term concentrations of VOCs, taking into account the effects of temperature changes. Simultaneously, source apportionment can be conducted to quantify the contribution rates of various sources of these targeted VOCs under actual conditions. Sixth, there are some difficulties encountered during data collection; a few subjects and invitees would be late. In several experiments, the teacher also delayed sometimes. As a result, the questionnaire may not be completed at a very precise time. Moreover, in the 16 experiments, students were absent some times, which cannot ensure the same number of students in each experiment.

5. Conclusion

In the spring semester of university, the average outdoor temperature ranged from 11.4 ℃–30.1 ℃, and the average outdoor relative humidity was 35.7%–93.6%. The average indoor temperature ranged from 17.8 ℃–29.2 ℃ and the average indoor relative humidity was 34.5%–91.0%. In the 100-minute period, the indoor temperature generally increased by 1.0 ℃–4.0 ℃, and the indoor relative humidity fluctuated slightly in the range of 0.0%–1.0%.

Before and after the class, the average indoor CO_2 concentration was 500–887 ppmv and 2100–3600 ppmv, respectively. Across 16 tests, the average indoor CO_2 concentration was 1176.9–2031.7 ppmv. The average minimum and maximum concentrations of indoor TVOC were 520 ± 7 ppbm and 1026 ± 13 ppbm, respectively, and the average indoor TVOC concentration across the 16 tests was 706 ± 276 ppbm. The environmental results indicated that the thermal conditions in the surveyed classrooms were acceptable, but indoor air quality required improvement.

An increase in the indoor temperature has a negative effect on the perception of air quality. When the average classroom temperature increased from 17.8 ℃ to 26.3 ℃, the subjects reported that the intensity of odors they experienced ranged between no odors and slight odors, while the invitees indicated a strong intensity. When the CO_2 concentration reached 2000 ppmv at 100 min, the air quality satisfaction and acceptability of the participants and invitees decreased significantly, and the evaluation value of the invitees was lower than that of the participants.

There was a significant positive correlation between the human CO_2 emission rate and indoor temperature. The human CO_2 emission rate was estimated to increase

by 0.78 L/h for every 1 ℃ increase in temperature in the range of 17 ℃–31 ℃. To maintain an indoor CO_2 concentration of 1000 ppmv, the required ventilation rate per person must be increased by 0.25 ± 0.3 L/s.

A total of 16 universities in China offer architecture majors; the architectural design courses are taught in this form in universities in China. The architectural design is the main course for architecture major, consisting of architectural design (1) to (8), with one architectural design course per semester. Therefore, the results can be applicable to the same vocational classes in other universities.

Future research directions should include the following aspects, for example: further exploration of VOC sources, long-term monitoring in four seasons, expanded sample size and settings, recommendations for mitigation strategies, and educational outreach and policy implications. The above research content could help advance our understanding of IAQ management.

Funding: The authors of this paper would like to express their gratitude to Historical and cultural city research center (NO:13012001009027) for their financial support.

Conflict of interest: The author declares no conflict of interest.

References

1. Gao XY. Experimental Analysis of the Effect of Natural Ventilation on the CO_2 Concentration in Campus Classroom. Chongqing University; 2016. doi: CNKI:CDMD:2.1016.732242
2. Marchetti N, Cavazzini A, Pasti L, et al. A campus sustainability initiative: Indoor air quality monitoring in classrooms. In: Proceedings of the 2015 XVIII AISEM Annual Conference; 3-5 February 2015; Trento, Italy. doi: 10.1109/aisem.2015.7066774
3. Deng SH, Lau J. Seasonal variations of indoor air quality and thermal conditions and their correlations in 220 classrooms in the Midwestern United States. Building and Environment. 2019; 157: 79-88. doi: 10.1016/j.buildenv.2019.04.038
4. Shendell DG, Barnett C, Boese S. Science-Based Recommendations to Prevent or Reduce Potential Exposure to Biological, Chemical, and Physical Agents in Schools. Journal of School Health. 2004; 74(10): 390-396. doi: 10.1111/j.1746-1561.2004.tb06603.x
5. Clausen G, Carrick L, Fanger PO, et al. A Comparative Study of Discomfort Caused by Indoor Air Pollution, Thermal Load and Noisec. Indoor Air. 1993; 3(4): 255-262. doi: 10.1111/j.1600-0668.1993.00006.x
6. Kabirikopaei A, Lau J. Uncertainty analysis of various CO_2-based tracer-gas methods for estimating seasonal ventilation rates in classrooms with different mechanical systems. Building and Environment. 2020; 179: 107003. doi: 10.1016/j.buildenv.2020.107003
7. Rajagopalan P, Andamon MM, Woo J. Year long monitoring of indoor air quality and ventilation in school classrooms in Victoria, Australia. Architectural Science Review. 2021; 65(1): 1-13. doi: 10.1080/00038628.2021.1988892
8. Yu YZ, Wang B, You SJ, et al. The Effects of Manual Airing Strategies and Architectural Factors on the Indoor Air Quality in College Classrooms: A Case Study. Air Quality, Atmosphere & Health. 2021; 15(1): 1-13. doi: 10.1007/s11869-021-01074-y
9. Liu JL, Yang X, Jiang QW, et al. Occupants' thermal comfort and perceived air quality in natural ventilated classrooms during cold days. Building and Environment. 2019; 158: 73-82. doi: 10.1016/j.buildenv.2019.05.011
10. Coley DA, Beisteiner A. Carbon Dioxide Levels and Ventilation Rates in Schools. International Journal of Ventilation. 2002; 1(1): 45-52. doi: 10.1080/14733315.2002.11683621
11. Kuga K, Ito K, Wargocki P. The effects of warmth and CO_2 concentration, with and without bioeffluents, on the emission of CO_2 by occupants and physiological responses. Indoor Air. 2021; 31(6): 2176-2187. doi: 10.1111/ina.12852
12. Haddad S, Synnefa A, Ángel Padilla Marcos M, et al. On the potential of demand-controlled ventilation system to enhance indoor air quality and thermal condition in Australian school classrooms. Energy and Buildings. 2021; 238: 110838. doi: 10.1016/j.enbuild.2021.110838
13. Haverinen-Shaughnessy U, Shaughnessy RJ, Cole EC, et al. An assessment of indoor environmental quality in schools and

its association with health and performance. Building and Environment. 2015; 93: 35-40. doi: 10.1016/j.buildenv.2015.03.006
14. Mendell MJ, Eliseeva EA, Davies MM, et al. Do classroom ventilation rates in California elementary schools influence standardized test scores? Results from a prospective study. Indoor Air. 2015; 26(4): 546-557. doi: 10.1111/ina.12241
15. Korsavi SS, Montazami A, Mumovic D. Ventilation rates in naturally ventilated primary schools in the UK; Contextual, Occupant and Building-related (COB) factors. Building and Environment. 2020; 181: 107061. doi: 10.1016/j.buildenv.2020.107061
16. Mutmainnah N, Mulyadi R, Hamzah B. Air Quality Characteristics in Junior High School Classroom with Natural Ventilation in Pangkep Regency. EPI International Journal of Engineering. 2019; 2(2): 157-161. doi: 10.25042/epi-ije.082019.11
17. Shrestha M, Rijal HB, Kayo G, et al. An investigation on CO_2 concentration based on field survey and simulation in naturally ventilated Nepalese school buildings during summer. Building and Environment. 2022; 207: 108405. doi: 10.1016/j.buildenv.2021.108405
18. Taemthong W. Selecting Ventilation Fan Capacity for University Classroom Based on Empirical Data. International Journal of Environmental Science & Sustainable Development. 2019; 4(1): 13-21. doi: 10.21625/essd.v4i1.487
19. Chan WR, Li X, Singer BC, et al. Ventilation rates in California classrooms: Why many recent HVAC retrofits are not delivering sufficient ventilation. Building and Environment. 2020; 167: 106426. doi: 10.1016/j.buildenv.2019.106426
20. Cai CR, Sun ZW, Weschler LB, et al. Indoor air quality in schools in Beijing: Field tests, problems and recommendations. Building and Environment. 2021; 205: 108179. doi: 10.1016/j.buildenv.2021.108179
21. Sahu V, Gurjar, BR. Spatial and seasonal variation of air quality in different microenvironments of a technical university in India. Building and Environment. 2020; 185: 107310. doi: 10.1016/j.buildenv.2020.107310
22. Zhang D, Ding E, Bluyssen PM. Guidance to assess ventilation performance of a classroom based on CO_2 monitoring. Indoor and Built Environment. 2022; 31(4): 1107-1126. doi: 10.1177/1420326x211058743
23. Choe Y, Shin JS, Park J, et al. Inadequacy of air purifier for indoor air quality improvement in classrooms without external ventilation. Building and Environment. 2022; 207: 108450. doi: 10.1016/j.buildenv.2021.108450
24. Kierat W, Ai Z, Melikov A, et al. Towards enabling accurate measurements of CO_2 exposure indoors. Building and Environment. 2022; 213: 108883. doi: 10.1016/j.buildenv.2022.108883
25. Chi CC, Chen WD, Guo M, et al. Law and features of TVOC and Formaldehyde pollution in urban indoor air. Atmospheric Environment. 2016; 132: 85-90. doi: 10.1016/j.atmosenv.2016.02.043
26. Fu N, Wei P, Jia YB, et al. Indoor volatile organic compounds in densely occupied education buildings of four universities: Target list, concentration levels and correlation analysis. Building and Environment. 2021; 191: 107599. doi: 10.1016/j.buildenv.2021.107599
27. Huang LH, Qian H, Deng SX, et al. Urban residential indoor volatile organic compounds in summer, Beijing: Profile, concentration and source characterization. Atmospheric Environment. 2018; 188: 1-11. doi: 10.1016/j.atmosenv.2018.06.009
28. Jia YB, Zheng X, Guan J, et al. Investigation of indoor total volatile organic compound concentrations in densely occupied university buildings under natural ventilation: Temporal variation, correlation and source contribution. Indoor and Built Environment. 2020; 30(6): 838-850. doi: 10.1177/1420326x20914000
29. Sun X, He J, Yang X. Human breath as a source of VOCs in the built environment, Part I: A method for sampling and detection species. Building and Environment. 2017; 125: 565-573. doi: 10.1016/j.buildenv.2017.06.038
30. He J, Sun X, Yang X. Human respiratory system as sink for volatile organic compounds: Evidence from field measurements. Indoor Air. 2019; 29(6): 968-978. doi: 10.1111/ina.12602
31. Yang T, Xiong J, Tang X, et al. Predicting Indoor Emissions of Cyclic Volatile Methylsiloxanes from the Use of Personal Care Products by University Students. Environmental Science & Technology. 2018; 52(24): 14208-14215. doi: 10.1021/acs.est.8b00443
32. Xiong JY, He ZC, Tang XC, et al. Modeling the Time-Dependent Concentrations of Primary and Secondary Reaction Products of Ozone with Squalene in a University Classroom. Environmental Science & Technology. 2019; 53(14): 8262-8270. doi: 10.1021/acs.est.9b02302
33. Duan JH, Wang LX, Zhuo SH, et al. Seasonal variation of airborne phthalates in classroom and dormitory, and its exposure assessment in college students. Energy and Buildings. 2022; 265: 112078. doi: 10.1016/j.enbuild.2022.112078
34. Vallecillos L, Borrull A, Marcé RM, et al. Passive sampling to control air quality in schools: Uptake rate determination and

application. Indoor Air. 2020; 30(5): 1005-1017. doi: 10.1111/ina.12684
35. Vornanen-Winqvist C, Alapieti T, Mikkola R, et al. Volatile organic compounds in school buildings with indoor air quality problems. In: Proceedings of Joint annual meeting of the International Society of Exposure Science and the International Society for Environmental Epidemiology; 2019.
36. Fong ML, Lin Z, Fong KF, et al. Evaluation of thermal comfort conditions in a classroom with three ventilation methods. Indoor Air. 2011; 21(3): 231-239. doi: 10.1111/j.1600-0668.2010.00693.x
37. Gohara T, Iwashita G. Field study on the indoor air quality in elementary schllos in Kagoshima city: Part 1 VOCs concentrations in elementary schools. Journal of Architecture & Planning. 2002; 67(553): 63-70. doi: 10.3130/aija.67.63_2
38. Zhou JQ, Deng BQ, Kim CN. Numerical Simulation of VOCs Distribution with an Air Cleaner in a Classroom. International Symposium on Heating, Ventilating and Air Conditioning; 2009.
39. Can E, Özden Üzmez Ö, Döğeroğlu T, et al. Indoor air quality assessment in painting and printmaking department of a fine arts faculty building. Atmospheric Pollution Research. 2015; 6(6): 1035-1045. doi: 10.1016/j.apr.2015.05.008
40. ASHRAE. Standard 62.1., 2016. Ventilation for Acceptable Indoor Air Quality. American Society of Heating, Refrigerating and Air-Conditioning Engineers, Inc.; 2016.
41. Committee ME-062, Ventilation and Air conditioning. Australian Standard, AS 1668.2-2012. The Use of Ventilation and Air Conditioning in Buildings, Part 2: Mechanical Ventilation in Buildings. Committee ME-062, Ventilation and Air Conditioning; 2012.
42. British Standards Institute. S. EN15251., 2008. Indoor Environmental Input Parameters for Design and Assessment of Energy Performance of Buildings Addressing Indoor Air Quality, Thermal Environment Lighting and Acoustics. British Standards Institute; 2008.
43. Verein Deutscher Ingenieure. VDI 6022 Part 3., 2011. Ventilation and Indoor Air Quality-Assessment of Indoor Air Quality. Verein Deutscher Ingenieure; 2011.
44. Ministry of Housing and Urban-Rural Development of the People's Republic of China. GB, GB 50736. Design Code for Heating Ventilation and Air Conditioning of Civil Buildings. China Architecture & Building Press; 2012.
45. Park S, Park H, Seo J. Analysis on the Exhaust Air Recirculation of the Ventilation System in Multi-Story Building. Applied Sciences. 2021; 11(10): 4441. doi: 10.3390/app11104441
46. Rastogi K, Lohani D, Acharya D. Context-Aware Monitoring and Control of Ventilation Rate in Indoor Environments Using Internet of Things. IEEE Internet of Things Journal. 2021; 8(11): 9257-9267. doi: 10.1109/jiot.2021.3057919
47. Zhang XJ, Zhao CX, Zhang TY, et al. Association of indoor temperature and air quality in classrooms based on field and intervention measurements. Building and Environment. 2023; 229: 109925. doi: 10.1016/j.buildenv.2022.109925
48. The state bureau of quality and technical supervision of the People's Republic of China. B/T, GB/T 18204.18-2000., 2000. Method for Determination of Air Change Flow of Indoor Air in Public Places. The State Bureau of Quality and Technical Supervision of the People's Republic of China; 2000.
49. Jindal A. Investigation and analysis of thermal comfort in naturally ventilated secondary school classrooms in the composite climate of India. Architectural Science Review. 2019; 62(6): 466-484. doi: 10.1080/00038628.2019.1653818
50. Persily AK, Jonge LD. Carbon Dioxide Generation and Building Occupants. ASHRAE Journal. 2017; 59(7): 64-66.
51. Zheng X, Jia YB, Guan J, et al. Impact analysis of human emission on total volatile organic compound concentration in university classrooms: A field study. Heating Ventilating & Air Conditioning. 2020; 50(1): 115-121.
52. Qi MW, Li XF, Weschler LB, et al. CO_2 generation rate in Chinese people. Indoor Air. 2014; 24(6): 559-566. doi: 10.1111/ina.12110
53. Wang XN. Experimental Study of Human Carbon Dioxide Generaton Rate at Different Activity Levels. Xi'an University of Architecture and Technology; 2021.
54. Zhang YJ. The Experimental Research into the Influence of Temperature and Carbon Dioxide to Human Comfort in Small Space. Chongqing University; 2018.
55. Robinson WR, Peters RH, Zimmermann J. The effects of body size and temperature on metabolic rate of organisms. Canadian Journal of Zoology. 1983; 61(2): 281-288. doi: 10.1139/z83-037
56. Luo MH, Zhou X, Zhu YX, et al. Revisiting an overlooked parameter in thermal comfort studies, the metabolic rate. Energy and Buildings. 2016; 118: 152-159. doi: 10.1016/j.enbuild.2016.02.041
57. Li KW, Shen JD, Zhang X, et al. Variations and characteristics of particulate matter, black carbon and volatile organic compounds in primary school classrooms. Journal of Cleaner Production. 2020; 252: 119804. doi:

10.1016/j.jclepro.2019.119804
58. Kang J, Liu JJ, Pei JJ. The indoor volatile organic compound (VOC) characteristics and source identification in a new university campus in Tianjin, China. Journal of the Air & Waste Management Association. 2017; 67(6): 725-737. doi: 10.1080/10962247.2017.1280561
59. Liu S, Li R, Wild RJ, et al. Contribution of human-related sources to indoor volatile organic compounds in a university classroom. Indoor Air. 2015; 26(6): 925-938. doi: 10.1111/ina.12272

Building Engineering 2024, 2(1), 1348.
https://doi.org/10.59400/be.v2i1.1348

Article

Potential of low-value plastic waste (LVPW) in concrete through latrine ring manufacturing

Mushtaq Ahmed[1], Muhammad Azizul Hoque[1], H. M. A. Mahzuz[1,*], Nazmul Islam Rafi[1], Md. Jubayer Hossan Salman[1], Khadijatul Kubra Mim[1], Krisha Rana[2], Md. Abdullah Al Ahad[2], Md. Ariful Islam[2], Ratan Kumar Roy[2]

[1] Department of Civil and Environmental Engineering (CEE), Shahjalal University of Science and Technology (SUST), Sylhet 3114, Bangladesh
[2] iDE, Sylhet 3100, Bangladesh
*** Corresponding author:** H. M. A. Mahzuz, mahzuz_211@yahoo.com

CITATION

Ahmed M, Hoque MA, Mahzuz HMA, et al. Potential of low-value plastic waste (LVPW) in concrete through latrine ring manufacturing. Building Engineering. 2024; 2(1): 1348. https://doi.org/10.59400/be.v2i1.1348

ARTICLE INFO

Received: 30 April 2024
Accepted: 7 June 2024
Available online: 19 June 2024

Abstract: In this research, low-value plastic waste (LVPW) is used in concrete as a potential solution for sustainable waste management in the construction industry. In concrete, LVPW is utilized to produce Eco-Ring (Eco-conscious Latrine Ring). The use of a mix ratio of 1:2:3 and 1:2:4 in concrete mixes is studied. The impact of the percentage of recycled plastic on the mechanical properties of the final product is analyzed. The results show that the use of LVPW reduces both strength and unit weight but ensures its solidification. Sufficient strength for latrine rings is maintained, ensuring a balance between structural integrity and waste reduction. LVPW incorporation offers cost savings, with reductions of aggregate use up to 10%–15% in the present analysis. Justified consideration of the impact on mechanical properties, along with potential adjustments to optimize compatibility and address workability/aesthetics, can help maximize the benefits of this technology.

Keywords: concrete; latrine ring; mix ratio; solidification; waste management

1. Introduction

Plastics are synthetic organic polymers that are widely used in different applications ranging from water bottles, clothing, food packaging, medical supplies, electronic goods, construction materials, etc. [1]. In the last six decades, plastics have become an indispensable and versatile product with a wide range of properties, chemical compositions, and applications. Environmental pollution by plastic wastes is now recognized widely to be a major environmental burden [2], especially in the aquatic environment where there is prolonged biophysical breakdown of plastics [3], detrimental negative effects on wildlife [4], and limited plastic removal options [5].

Generally, waste plastic has a 'recycle' value. A good number of business policies are carried out in the total recycling process (**Figure 1**). For example, plastic waste from polyethylene terephthalate (PET) bottles, High-Density Polyethylene (HDPE) containers, Polypropylene (PP) packaging, including yogurt containers and food containers, Low-Density Polyethylene (LDPE) films, Flexible plastic packaging, including wraps and pouches, Expanded Polystyrene (EPS) foam, electronic devices with plastic components, end-of-life automotive plastics, including bumpers and interior components, etc. have certain economical values. A scenario of plastic reuse in Sylhet City, Bangladesh, is shown in **Figure 2** [6]. Since these plastics have economic value, they are not included as components of the research.

(a) **(b)** **(c)** **(d)**

Figure 1. Wastes from **(a)** PET bottles; **(b)** HDPE waste; **(c)** expanded Polystyrene (EPS) foam; **(d)** electronic devices with plastic components.

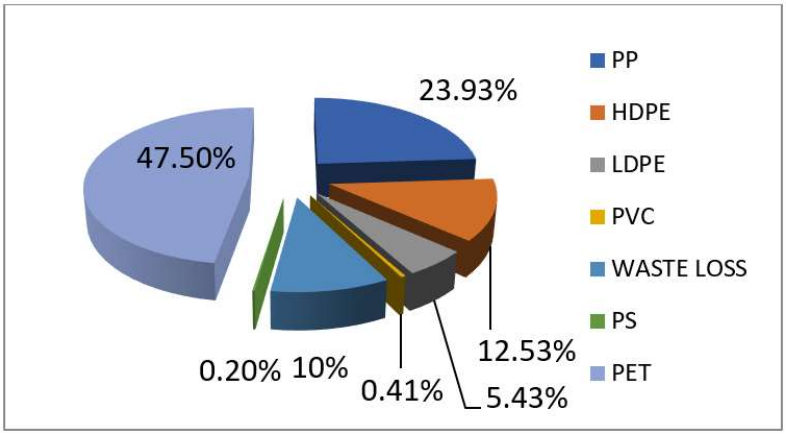

Figure 2. Present recycled plastic composition in Sylhet.

But some plastics have very low value for recycling or even have no value. These are termed as Low-Value Plastic Waste (LVPW). LVPW (**Figure 3**) has limited economic value in the recycling market due to various factors, like difficulties in collecting and processing, difficulties in recycling due to its low-grade or complex compositions, low demand for the recycled products, contamination probabilities etc. These are the plastics where the costs of collecting and processing are higher than the revenue generated from sales of the recovered plastic. Here are some examples of LVPW:

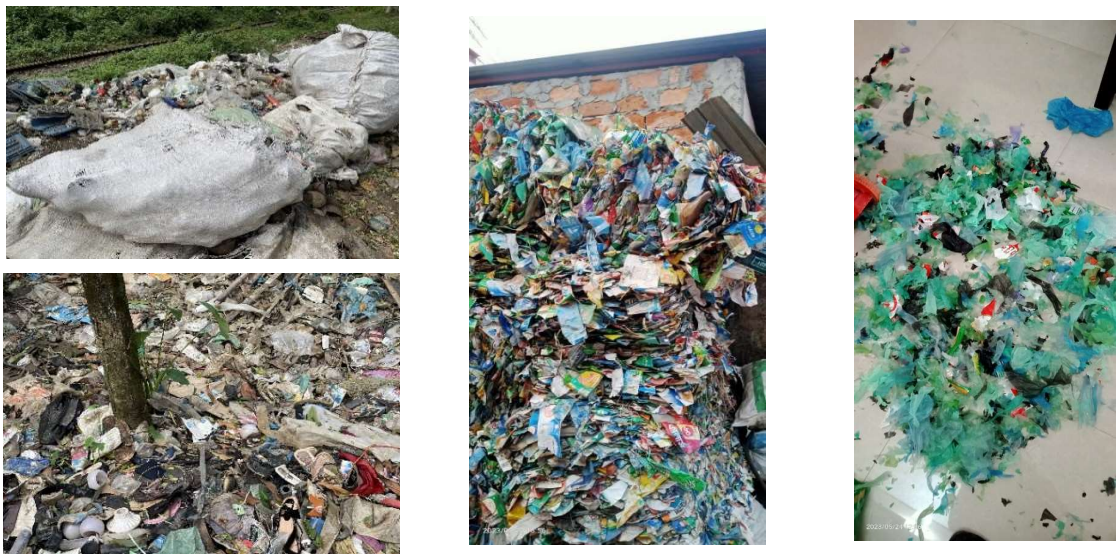

Figure 3. Some examples of low-value plastic wastes.

1) Mixed Plastic Waste: Plastic waste that is mixed with various materials, making it difficult to separate and recycle efficiently, may have little to no economic value.
2) Single-Use, Multi-Layered Packaging: Single-use packaging, especially those with multiple layers of different materials (e.g., Tetra Packs), can be challenging to recycle economically. Separating and processing the layers can be technically demanding and expensive.
3) Small Plastic Items and Fragments: These are microplastics, bottle caps, and plastic film scraps, which may have limited economic value.
4) Contaminated Plastics: Plastic waste contaminated with non-recyclable materials, such as food residues, oils, or hazardous substances, may have little to no economic value.
5) Low-grade Plastics or Plastics with Complex Compositions: Some specific types of plastics may be challenging to recycle economically due to their chemical composition or lack of demand in the recycling market.
6) Low-Quality Plastic Films: Thin, low-quality plastic films, such as those used in packaging for single-use items, may have limited economic value in recycling. These are often difficult to process due to their lightweight nature and do not meet the standards for recycling.

However, mismanagement of LVPW can cause water clogging in drains and canals, odor problems, land-water-air pollution, human-wildlife hazards, visual discomfort, lowering of soil fertility and so on. Since LVPW has little or no economic value, solidification in a concrete environment can ensure a management strategy for this issue. By this, not only the consumption of natural resources i.e., sand, brick and stone can be reduced but also environmental protection can be enhanced. Therefore, in this study, such an attempt is taken where use of Low-Value Plastic Waste in Concrete is going to be studied to produce Eco-Ring (Eco-conscious Latrine Ring), where very high strength of concrete may not be an issue.

2. Existing scientific knowledge on the subject

From 1964 to 2014, plastics production increased from 15 million metric tons to 311 million metric tons [7]. If this trend continues, it is expected that plastic production will double in 20 years and almost quadruple by 2050. In landfills, between 22% and 43% of plastics are disposed of, and at least 8 million tons of plastics are disposed of in the ocean [8]. Dhaka, the capital of Bangladesh—among the total solid waste, plastic was 4.15% in 2005 and 5.46% in 2014 [9]. Waste plastic can turn into a potential resource if it can be used in concrete, which can solidify this waste. Several studies have been conducted to evaluate the applicability of different types of plastics for such purposes. Hasan et al. [9] evaluated the properties of concrete with recycled plastic as coarse aggregate by 5%, 10%, 15%, and 20% replacement of stone. They used HDPE plastic and prepared a total of 90 cylinders and 5 beams. The maximum reduction in compressive strength was 44% for the 20% replacement of stone by recycled plastic. They concluded that up to 15% replacement of stone by recycled plastic is applicable for structural application. Another experiment was conducted by Subramani and Pugal [10] on partial replacement of coarse aggregate with

polyhydroxybutyrate (PHB). 5% to 15% of coarse aggregate was replaced by plastic. It was observed that 20% of aggregate can be replaced with acceptable strength. Ghernouti et al. [11] studied the applicability of plastic bags as fine aggregate in concrete. 10%, 20%, 30%, and 40% fine aggregate was replaced with plastic fine aggregate. The conclusion was drawn by remarking that plastic bags can be used successfully to replace conventional fine aggregates in concrete. In another study, after thorough mixing, the hot molten paste was poured with standard brick dimensions. The brick was subjected to compressive and water absorption tests. The results showed that the plastic composite brick was more efficient than the clay brick and cement brick [12]. Similar results were achieved by Singhal and Netula [13] and Shah et al. [14]. Merbouh et al. [15] used low-density polyethylene (LDPE) to replace aggregate. They replaced 0% to 1.0% of the aggregate by LDPE. Noticeable ductility in fracture was recorded with a significant reduction in density. It was proposed to use LDPE in concrete where less compressive strength and tensile strength are required. In a few other studies, nine technologies [16,17] were assessed for processing low-value plastic (LVP) waste (recycling, plastic to product, plastic to lumber, pyrolysis, solvolysis, mixing with asphalt, mixing with construction materials, waste processing, and technology ranking).

In a couple of studies [18,19], compressive strength and unit weight of concrete were sorted out where plastic was used as a partial replacement (25% and 50%) of coarse aggregate. It was tried to find out the mix ratios that can be used as per the Local Government of Engineering Department of Bangladesh (LGED) and Bangladesh Standard (BDS) 208:2002 [20,21]. As the addition of plastic decreases the unit weight of concrete, it can be used to produce lightweight concrete. However, the strength of concrete using 25% and 50% plastic as coarse aggregate is not sufficient for structural purposes. So, this concrete can be used for non-load-bearing purposes as per LGED and BDS. Hasan [22,23] found that 25%–50% replacement of plastic waste with coarse aggregate in the concrete of the different mix ratios (1:3:6, 1:3:4, and 1:3:2) can ensure a compressive strength of solid concrete blocks 5.0 MPa (IS 2185-1) [24].

3. Relevance of the study to national or regional priorities

From the above-mentioned review of scientific findings, it can be concluded that the use of plastic waste reduces compressive strength and unit weight but ensures its solidification, thus protecting the environment from harmful effects. Also, it can be concluded that it is better to use such concrete for non-load-bearing structures only. In most of the studies, plastic wastes are replaced with coarse aggregates with a replacement from 5%–75%, while the best result is achieved between 5%–25%.

A “latrine ring” typically refers to a concrete ring used in the construction of latrines or pit toilets (**Figure 4**). In the context of sanitation and the construction of basic toilet facilities, these rings play a crucial role. Latrine rings are commonly made of concrete but can also be manufactured from other durable materials. They are designed to fit together, forming a circular structure that is placed over the pit or excavation. The rings provide structural support for the superstructure of the latrine, which includes the seat and any covering structure. They also help prevent the collapse

of the pit walls. Therefore, the strength of the rings should be such that they will be able to withstand the side-soil pressure and overburden pressure. It is important to note that the specific design and use of latrine rings may vary based on local construction practices, available materials, and the type of sanitation facility being built. In regions without access to advanced sanitation infrastructure, these simple yet effective structures contribute significantly to public health and hygiene.

Figure 4. Typical latrine ring (diameter 30″, thickness 1.5″, height 12″).

Based on this logical reason in this study, LVPW is going to be used in concrete targeting the strength of latrine rings, and if plastic waste can be used here successfully, then let's also designate them as 'Eco-rings.'. If the expected outcome of the research is achieved, and if it is then practiced in construction, it will certainly reduce the present concerns about plastic waste in a quantified manner and will save the natural resources of Bangladesh.

4. Objectives of the study

1) To evaluate the effects on concrete if the aggregate is partially replaced by LVWP.
2) To identify its optimum percentage of replacement for the production of latrine rings.
3) To compare the cost of latrine rings with the traditional rings available in the market.

5. Materials and methodology

This experimental study approaches the utilization of Low-Value Plastic Waste in constructing Eco-conscious Latrine Ring. The required methodology is presented in **Figure 5**. Also, the properties of materials used are described in the following sections.

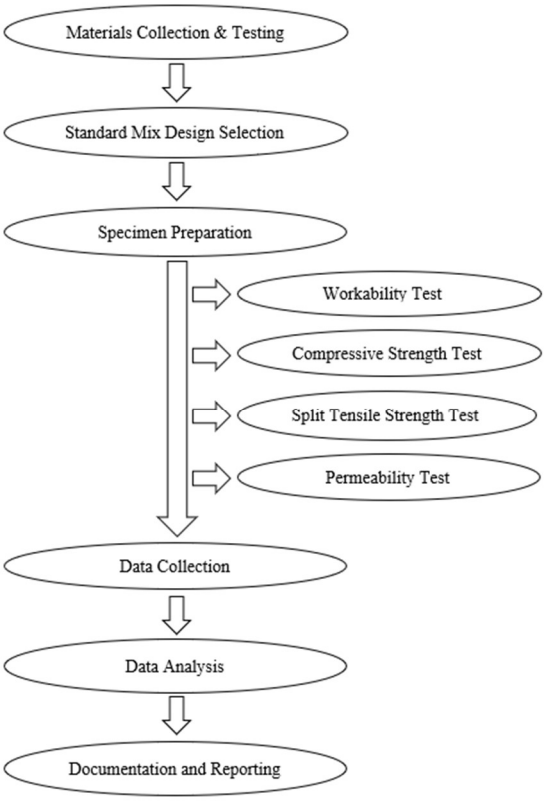

Figure 5. Experimental procedure.

In this study, cement (as a binding material), river sand (as fine aggregate), brick chips (as coarse aggregate), and LVPW (as fine and coarse aggregate) were used as the ingredients of concrete. Several tests were conducted to identify their properties and perform efficient mix proportions for concrete.

5.1. Experimental setups

The cement used in this study, Supercrete, is Portland Limestone Cement (PLC) and complies with BDS EN 197-1:2003, CEM II/ B-L, 42.5N standard. It has a composition of clinker 65% to 79%, limestone 21% to 35%, and slag/fly ash/gypsum 0% to 5%. For normal consistency of cement, ASTM designation C187 and for initial and final setting times of cement, ASTM designation C191 were followed. All data are presented in **Table 1**.

Table 1. Physical properties of cement.

Normal consistency	**28%**
Initial setting time	115 min
Final setting time	300 min

5.2. Low-value plastic waste (LVPW)

Low-value plastic waste (LVPW) refers to a mixture of different wastes (such as Styrofoam, PET, Polyethene bags, multilayer packaging, rubber, electronic, and

medical waste, etc.). Here it is used as the replacement of both fine and coarse aggregate in concrete. Few studies [25, 26] have shown improved sorting of low-value recyclable waste, but in current studies LVPW is sorted manually from dumping sites. The particle size range varies from 0.075 mm to 12.5 mm. The shredded plastic waste was collected from a nearby recycling plant. Previously, they were collected from different sources and shredded into sizes in that plant. Examining the physical properties of the LVPW that were used was a challenge as it had a mixture of different types of plastics, each having different properties. Still, sieve analysis and tests for unit weight calculation were conducted on them. In sieve analysis, for proper sieving, both mechanical and manual sieving were done (**Figure 6**). The unit weight was obtained by compacting the wastes using a piston that was self-constructed, as shown in **Figure 7**. It was done by rodding procedure and followed by ASTM standard C29. Having a mixture of different types of plastic, including Styrofoam and polyethylene bags, made it unsuitable for oven drying. Furthermore, for this very reason, it was floating in water (**Figure 8**), which means it has less unit weight. The gradation curve for LVPW is presented in **Figure 9a**, and the physical properties results are summarized in **Table 2**.

(a) **(b)** **(c)**

Figure 6. Sieving **(a)** Mechanically **(b)** and **(c)** Manually.

Figure 7. Compaction of LVPW.

Figure 8. LVPW, sand & brick chips placed in water tank.

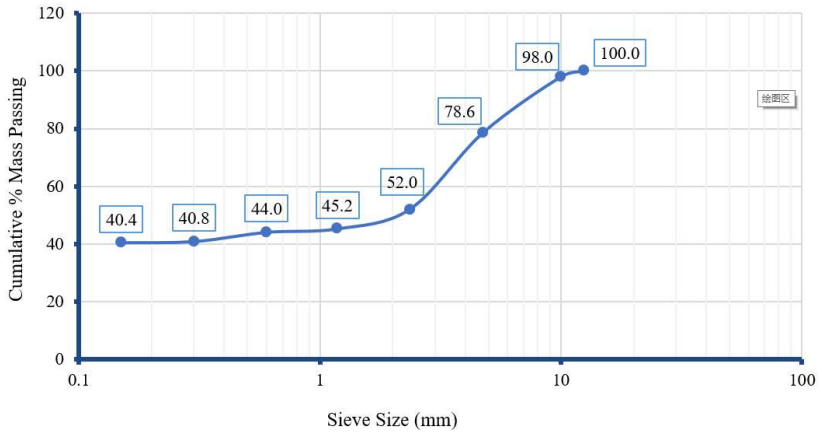

(a)

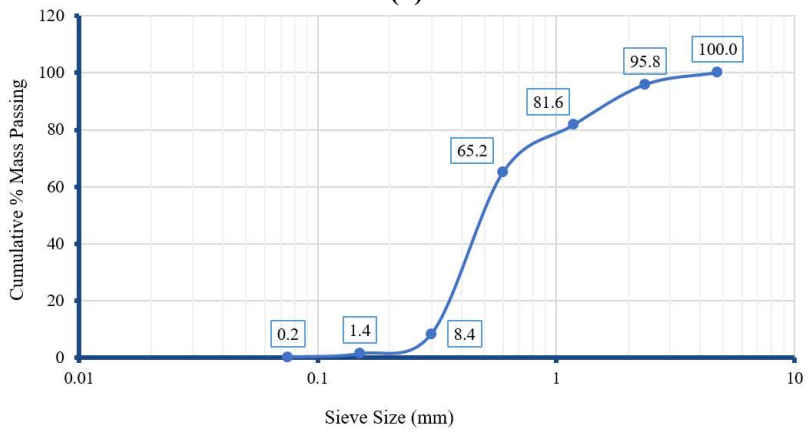

(b)

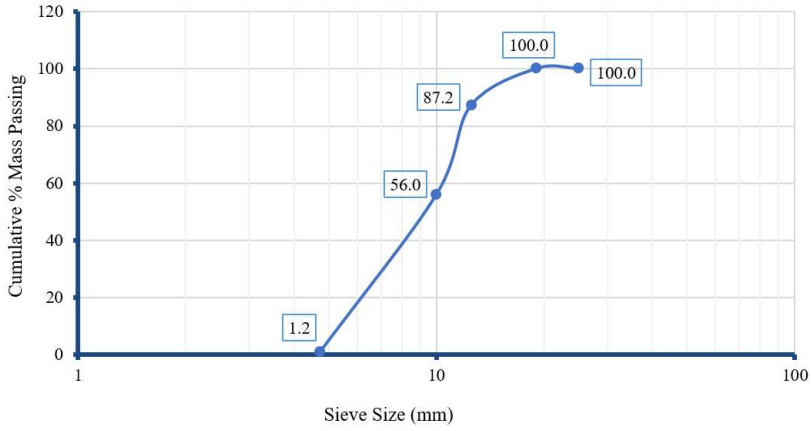

(c)

Figure 9. Particle size distribution of **(a)** LVPW; **(b)** sand; **(c)** brick chips.

Table 2. Physical properties of fine and coarse aggregates.

Properties	Standard	LVPW	Sand	Brick Chips
Maximum aggregate size (mm)	ASTM C136	12.5	4.75	14
Fineness modulus	ASTM C136	5.02	2.48	6.56
Unit weight (kg/m^3)	ASTM C29	473	1603.51	1007.65
Specific gravity (OD)	ASTM C128 & ASTM C127	-	2.59	1.92
Specific gravity (SSD)	ASTM C128 & ASTM C127	-	2.63	2.13
Water absorption capacity (%)	ASTM C128 & ASTM C127	-	1.63	10.93

5.3. Fine aggregate

The reddish-brown river sand collected from the local source was used as the fine aggregate in concrete. Gradation of sand was performed as per the ASTM standard requirements of specification C136. The particle size distribution of fine aggregate is presented in **Figure 9b**. Unit weight determination was done by rodding procedure that conformed to the ASTM standard requirements of specification C29. Water absorption capacity and specific gravity of the sand were measured following the ASTM standard requirements of specification C128. All the physical properties of sand are summarized in **Table 2**.

5.4. Coarse aggregates

As the latrine ring doesn't require higher strength, brick chips were used as coarse aggregate. It was collected from the local market and then crushed into the required size. The compressive strength of the bricks was 13.7 MPa. The thickness of the ring generally is very low (40–80 mm), so the highest size of brick chips is chosen between 14 and 12.5 mm. Gradation of brick chips was performed as per the ASTM standard requirements of specification C136, presented in **Figure 9c**. Also, unit weight determination was done by rodding procedure that conformed to the ASTM standard requirements of specification C29. Water absorption capacity and specific gravity of the sand were measured following the ASTM standard requirements of specification C127. All the physical properties of brick chips are summarized in **Table 2**.

5.5. Concrete mix proportions

During the test, two different mix ratios were used, which are 1:2:3 and 1:2:4. Here LVPW was replaced by the total aggregate in five different percentages (0%, 5%, 10%, 15%, 20%). All the aggregates, coarse and fine, used in the concrete mixture were in saturated surface dry (SSD) condition. No water-reducing admixture was used here. The mix proportion of various ingredients required for the 1:2:3 ratio was calculated and presented in **Table 3,** and for the 1:2:4 ratio, the same was calculated and presented in **Table 4**. Each mix design is designated with a unique name for ease in referencing within the text. As the ratio of coarse aggregate is the only variable here, for 1:2:3 it was named prototype 3P and for 1:2:4 named 4P. Then the said percentages of LVPW are added. For example, 3P10 means the prototype has a mix ratio of 1:2:3, where 10% total aggregate is replaced by LVPW. And the w/c ratio is fixed at 0.60 by the trial-and-error method, considering the convenient slump value.

Table 3. Materials quantities for 1:2:3 mix ratio.

Prototype Sample ID	Percent of LVPW	Cement (kg)	Sand (kg)	Brick chips (kg)	LVPW (kg)
3P00	0%	9.403	20.941	19.739	0.000
3P05	5%	9.403	19.894	18.752	0.772
3P10	10%	9.403	18.847	17.765	1.544
3P15	15%	9.403	17.800	16.778	2.316
3P20	20%	9.403	16.753	15.791	3.089

Table 4. Materials quantities for 1:2:4 mix ratio.

Prototype Sample ID	Percent of LVPW	Cement (kg)	Sand (kg)	Brick chips (kg)	LVPW (kg)
3P00	0%	8.060	17.949	22.559	0.000
3P05	5%	8.060	17.052	21.431	0.794
3P10	10%	8.060	16.155	20.303	1.588
3P15	15%	8.060	15.257	19.175	2.383
3P20	20%	8.060	14.360	18.047	3.177

5.6. Preparation of concrete specimens

Total 90 concrete cylinders were prepared in two different sizes following ASTM C 192-15 at room temperature of 25 ℃. For each prototype, 6 cylinders were prepared for the compression and tensile strength tests, having a 100 mm inner diameter and a 200 mm height, and 3 cylinders for the permeability test, having an inner diameter of 175 mm and a height of 175 mm. So, for 5 different prototypes, 45 cylindrical molds at each mix ratio were prepared. Specimens were placed in a curing tank for 28 days, as shown in **Figure 10**. **Figure 11** shows the major tests of eco-ring concrete through a flowchart.

Figure 10. Concrete setup for curing.

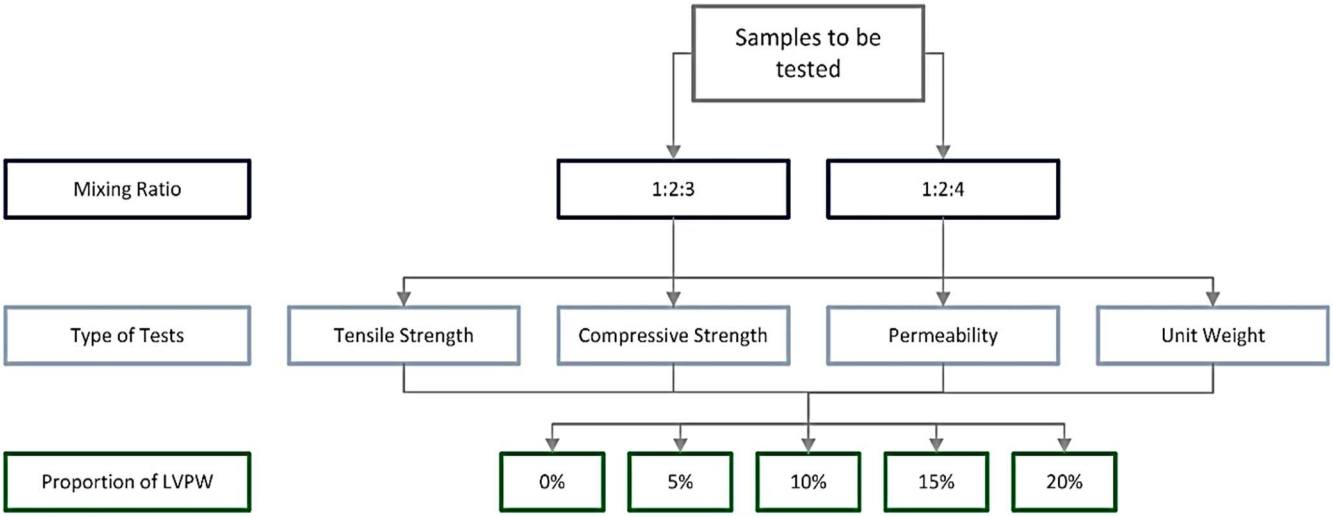

Figure 11. Tests of eco-ring concrete.

A process of testing the tensile strength of concrete involves splitting a cylinder across its vertical diameter. It is a method of evaluating the tensile strength of concrete that is done in an indirect manner. The splitting tensile strength of the concrete samples was determined using ASTM 496-17 after 28 days of curing.

According to ASTM, the splitting tensile strength is $\frac{2P}{\pi LD}$, where P = Applied highest load; D = Diameter of the specimen = 100 mm; L = Length of the specimen = 200 mm.

Latrine ring concrete is required to possess a good degree of impermeability to prevent subsoil water pressure. That's why the permeability of the LVPW concrete at 28 days was tested in this study. The relative permeability coefficient (Kr) of the concrete can be determined $K_r = a \times \frac{D_m^2}{2TH}$, where, K_r is the relative permeability coefficient, mm/s; a is the absorption ratio of the concrete, which was at a constant value of 0.03; T is the duration of the permeability test; D_m is the water-seepage height, which was 177.8 mm in this study; H is the water head (mm) of corresponding constant *pressure* $\left(H = \frac{\text{Pressure (MPa)} \times 10^6}{9.81}\right)$.

6. Results and discussions

Based on **Tables 5** and **6** as well as **Figures 12** and **13**, the results are consistent with the expectation. As the amount of LVPW increases, a decrease in:

Table 5. Mechanical properties for mix ratio 1:2:3.

LVPW	Slump Value (mm)	Splitting Tensile Strength (MPa)	Compressive Strength (MPa)	Unit Weight (Kg/m^3)
0%	57.2	2.99	20.25	22.47
5%	45.2	2.49	15.53	21.58
10%	30.2	2.27	13.97	21.35
15%	27.4	2.18	11.43	20.77
20%	21.6	1.74	8.64	20.46

Table 6. Mechanical properties for mix ratio 1:2:4.

LVPW	Slump Value (mm)	Splitting Tensile Strength (MPa)	Compressive Strength (MPa)	Unit Weight (Kg/m^3)
0%	25.4	2.37	14.90	22.52
5%	12.7	2.15	14.15	21.62
10%	9.5	1.22	10.25	21.14
15%	7.9	1.17	7.68	20.90
20%	9.5	1.14	6.39	20.44

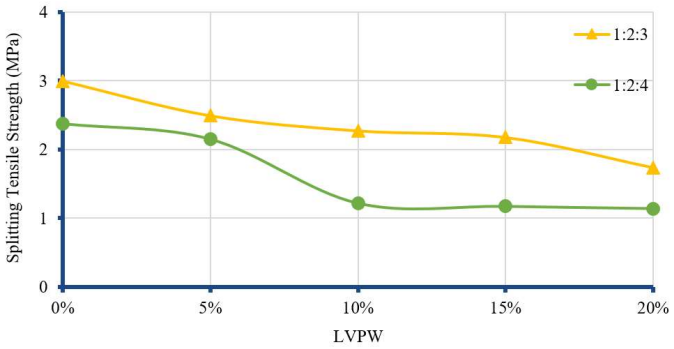

Figure 12. Impact of LVPW on split tensile strength.

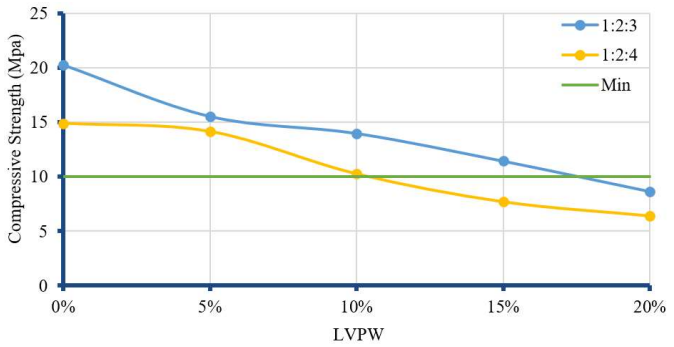

Figure 13. Impact of LVPW on compressive strength.

- Compressive strength: Similar to tensile strength, the concrete seems less resistant to compression with higher LVPW content. For instance, at 0% LVPW for a concrete mix ratio of 1:2:3, the compressive strength is 20.25 MPa, whereas at 20% LVPW, the compressive strength is 8.64 MPa.
- Tensile strength: The table shows that concrete specimens tend to withstand less tension before breaking as the LVPW content goes up. As per ACI code, the range of tensile strengths of normal weight concrete is $6\sqrt{f_c'} - 8\sqrt{f_c'}$ whereas $4\sqrt{f_c'} - 6\sqrt{f_c'}$ for lightweight concrete. For instance, at 0% LVPW for a concrete mix ratio of 1:2:3, the tensile strength is 2.99 MPa which is greater than both 2.98 MPa and 2.25 MPa determined from the above formulas. Again, at 20% LVPW, the tensile strength is 1.74 MPa which is greater than both 1.95 MPa and 1.46 MPa obtained from the above formulas. This indicates that the tensile strength of this concrete is in between an acceptable range.
- Unit weight: As LVPW is a lightweight material added to the concrete mix, it would naturally bring down the overall weight per unit volume of the concrete.

For instance, at 0% LVPW for concrete mix ratio 1:2:3, the unit weight is 22.47 Kg/m^3, whereas at 20% LVPW, the unit weight is 20.46 Kg/m^3.

The incorporation of LVPW into concrete mixes presents a potential solution for waste management, but it can have a significant impact on the mechanical properties of the final product. This phenomenon can be attributed to several factors related to the inherent properties of LVPW and its interaction with the concrete matrix. Here is a breakdown of the potential mechanisms:

a) Unlike traditional aggregates, LVPW particles, due to their smooth and often hydrophobic (water-repelling) nature, struggle to form strong bonds with the cement paste that binds the concrete together. This weak interface between plastic and cement hinders the effective transfer of stress throughout the concrete structure, leading to reduced overall strength.

b) The presence of LVPW particles within the concrete matrix can act as internal voids, separators, or points of weakness. These microscopic cracks can initiate and propagate under stress, compromising the structural integrity of the concrete and ultimately reducing its ability to withstand compressive and tensile forces.

c) LVPW is typically less dense than the natural aggregates it replaces. This lowers the overall density of the concrete, which can indirectly impact its strength. Denser concrete generally exhibits higher compressive and tensile strengths.

While LVPW offers a potential avenue for sustainable waste management in the construction industry, its inclusion requires careful consideration of its impact on the mechanical properties of concrete. Addressing the issues of weak bonding and internal cracking through surface treatment or compatible additives might be necessary to achieve a balance between waste reduction and structural performance.

However, the reduced density of LVPW concrete presents a significant advantage for low-cost toilet rings, slabs, and pillar projects for the following reasons:

1) Lighter weight, easier handling: LVPW concrete's lighter weight makes it easier to transport and maneuver during construction, reducing labor costs associated with handling heavier traditional concrete materials for these non-load-bearing applications.

2) Cost-effective alternative: LVPW can potentially offer a more cost-effective solution compared to virgin materials for toilet rings, slabs, and pillars. This aligns well with keeping costs low in these projects.

6.1. Selecting minimum compressive strength requirements

When constructing a latrine ring, selecting the appropriate concrete compressive strength is crucial for ensuring its durability and functionality. Standard codes provide guidelines for minimum compressive strength based on the intended use of the concrete. However, in the case of latrine rings, the specific application falls outside the typical categories. Considerations and the rationale for choosing a suitable strength can be as follows:

1) Minimum compressive strength for non-structural use: Indian code IS 2185-1 (2005) specifies a minimum compressive strength of 5 MPa for non-structural applications. Minimum compressive strength for structural use: The American Concrete Institute (ACI-318) code sets a range of 10–15 MPa.

2) Latrine Ring Classification: While a latrine ring experiences some load, it wouldn't be categorized as purely structural. It primarily supports the user's weight, a little lateral earth pressure, and doesn't carry significant building loads. On the other hand, it's not entirely non-structural, like decorative elements.
3) Earth Pressure Impact: Since the latrine ring's depth is limited to a maximum of 7 ft (approximately 2.1 meters) from the ground surface, the maximum potential earth pressure it encounters is estimated to be around 3 MPa.
4) Wired Reinforcement: The inclusion of minimal wired reinforcement in the latrine ring can further enhance its load-bearing capacity and provide additional crack resistance.

By considering standard building codes and the unique application, a benchmark of 10 MPa for compressive strength is a reasonable compromise, meaning it can withstand more pressure than it's likely to experience in this application. This falls between the minimums for non-structural and structural uses.

At 0% LVPW, the compressive strength is highest, and it declines steadily as the LVPW content goes up to 20%. However, **Figure 13** suggests that a maximum of 17.5% LVPW can be incorporated into a 1:2:3 concrete mix, while a maximum of 11% LVPW can be incorporated into a 1:2:4 concrete mix and still achieve a compressive strength above 10 MPa. Finally, maintaining a safe range, 15% LVPW can be recommended for a 1:2:3 mix ratio, and 10% LVPW can be recommended for a 1:2:4 mix ratio.

6.2. Water permeability test results

The permeability test results at 28 days, including the water head (*H*) corresponding to constant water pressure, the duration of water penetration into the concrete until creating a visible droplet on the surface, and the relative permeability coefficient (*Kr*), are presented in **Figure 14**. From **Figure 14**, it can be seen that the LVPW mixing percentage had a significant influence on the permeability of the concrete. As % of LVPW increases, permeability of concrete also increases. 1:2:4 mix concrete is more permeable than 1:2:3 mix concrete. For 1:2:4, permeability is high when LVPW is greater than 10%, which may not be acceptable for latrine rings.

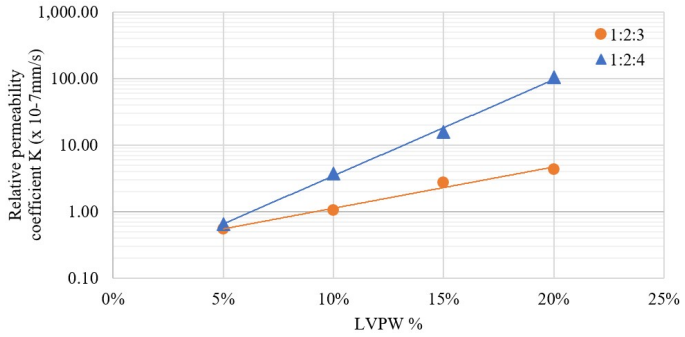

Figure 14. Impact of LVPW on permeability.

6.3. Comparative analysis for non-mechanical properties of LVPW in concrete mixes

The workability, appearance, and surface smoothness decrease with the addition

of LVPW, whereas permeability increases (**Table 7**). With a water-cement ratio of 0.6, for sample 3P15 (15% LVPW), workability is rated as "Medium". This might require moderate effort to achieve proper handling and pouring during construction compared to mixes with higher workability. But, for sample 3P10, workability is rated as "Good" which implies that it requires much less effort. On the other hand, for sample 4P10 (10% LVPW), workability is rated as "Fair". This might require much more effort than normal concrete. But, in comparison to other percentages of LVPW for the same mixing ratio, it has a better form of workability. Surface smoothness and appearance are described as "LVPW is slightly/moderately/clearly visible on the surface" for both samples (**Table 7**). This might affect the aesthetic appeal of exposed concrete elements. Although surface roughness for 4P10 and 3P15 is comparatively much higher than the control mix (LVPW is moderately visible on the surface), it can be acceptable by giving a finishing with extra mortar. As the percentage of LVPW increases, the permeability increases as it produces smaller micro-cracks inside and makes paths for water seepage. However, medium permeability may be accepted for proposed eco-rings.

Table 7. Qualitative result of prototyping phase.

Prototype Sample ID	Mix Ratio	LVPW	Is Strength within Permissible Limit?	Workability	Appearance & Surface Smoothness	Permeability	Remarks
3P00	1:2:3	0%	Yes	Very Good	Smooth finish	Very Low	Passed
3P05		5%	Yes	Very Good	Smooth finish	Low	Passed
3P10		10%	Yes	Good	LVPW is slightly visible on the surface	Low	Passed
3P15		15%	Yes	Average	LVPW is moderately visible on the surface	Medium	Passed
3P20		20%	No	Fair	LVPW is clearly visible on the surface, rough finish	Medium	Failed
4P00	1:2:4	0%	Yes	Average	Smooth finish	Very Low	Passed
4P05		5%	Yes	Fair	LVPW is slightly visible on the surface	Low	Passed
4P10		10%	Yes	Fair	LVPW is moderately visible on the surface, slightly rough finish	Medium	Passed
4P15		15%	No	Poor	LVPW is clearly visible on the surface, rough finish	High	Failed
4P20		20%	No	Poor	LVPW is clearly visible on the surface, rough finish	Very High	Failed

Appearance & Surface Smoothness Classification

Smooth finish

LVPW is slightly visible on the surface

LVPW is moderately visible on surface

LVPW is clearly visible on surface, rough finish

Containing LVPW of a maximum of 15% for 1:2:3 and 10% for 1:2:4 mix ratio, both samples achieve a compressive strength exceeding the 10 MPa benchmark required for non-load-bearing applications like latrine rings, slabs, and pillars. This translates to a certain amount of cost savings compared to conventional concrete. While both offer a balance between maximizing LVPW for environmental and economic benefits and maintaining sufficient strength and workability, the slightly rough surface texture might be acceptable for unexposed elements or those receiving a thin grout finish.

6.4. Comparative analysis for cost-effectiveness of LVPW in concrete mixes

Few insightful studies [27–30] are made for in-depth management of the cost of the recycling sector for plastic packaging in a developing country context. In the current study, it can be seen from **Figure 15**, **Tables 8** and **9**, that the case for incorporating LVPW into concrete mixes is a highly cost-effective and sustainable solution. For the 1:2:3 mix with 15% LVPW (Sample ID: 3P15), the cost reduction is 3.37% for one latrine ring compared to the control mix (3P00). For the 1:2:4 mix with 10% LVPW (Sample ID: 4P10), the cost reduction is 2.74% for one latrine ring compared to the control mix (4P00). Both samples demonstrate cost savings when using LVPW. The minimal acquisition cost of LVPW further amplifies the cost-effectiveness of LVPW concrete. In most cases, the savings on aggregate costs are likely to outweigh any minor expenses associated with LVPW collection or processing. Beyond cost savings, LVPW utilization offers a significant environmental benefit. It provides a sustainable solution for managing low-value plastic waste by diverting it from landfills and promoting circular economy practices in the construction industry.

Table 8. Cost comparison (for mix ratio 1:2:3, per Latrine ring, height—12″, Dia—30″, Thickness—1.5″).

Raw materials	Cost/unit	With 0% LVPW (3P00)	With 15% LVPW (3P15)	Saving (%) Per Latrine ring
		Cost (TK)		
Cement	550 TK/bag	110	110	3.37*
Sand	40 TK/cft	20	17	
Bricks chips	160 TK/cft	120	102	
LVPW	5 TK/Kg	0	13	
Total cost		249	241	

*In cost calculation the cost of GI wire is not considered since it is common in all cases.

Table 9. Cost comparison (for mix ratio 1:2:3, per Latrine ring, height—12″, Dia—30″, Thickness—1.5″).

Raw materials	Cost/unit	With 0% LVPW (4P00)	With 10% LVPW (4P10)	Saving (%) Per Latrine ring
		Cost (TK)		
Cement	550 TK/bag	94	94	2.74*
Sand	40 TK/cft	17	15	
Bricks chips	160 TK/cft	137	123	
LVPW	5 TK/Kg	0	9	
Total cost		248	241	

*In cost calculation the cost of GI wire is not considered since it is common in all cases.

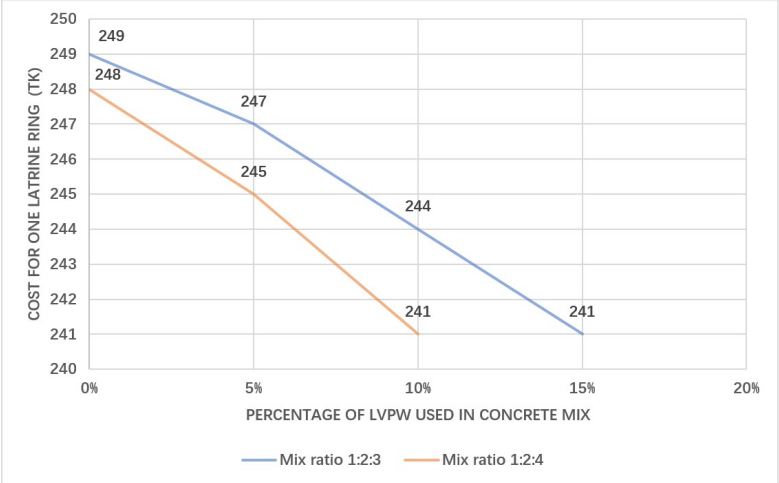

Figure 15. Cost comparison for one latrine ring (height—12″, Dia—30″, Thickness—1.5″).

7. Conclusion

Considering all tests done in this study, i.e., strength, appearance, cost, and seepage, the 1:2:3 ratio of concrete with 10% LVPW (3P10) can be considered the optimum choice. However, from an economic point of view, both 1:2:3 ratio concrete with 15% LVPW (3P15) and 1:2:4 ratio concrete with 10% LVPW (4P10) are good options. But, comparing these two cost-effective options, 1:2:3 ratio concrete with 15% LVPW (3P15) is a better option as it gives more strength and consumes more plastic waste. In conclusion it can be said that:

1) Increasing LVPW content leads to a decrease in tensile strength, compressive strength, and unit weight of concrete. This is weak bonding between LVPW and cement, internal cracking, and the lower density of LVPW compared to natural aggregates. Despite strength reductions, LVPW concrete remains a viable option for specific applications.
2) For non-load-bearing elements like latrine rings, the reduced weight of LVPW concrete offers advantages in handling and potentially lower labor costs associated with transporting and maneuvring the material during construction. This translates to cost savings alongside the reduced material costs of LVPW itself.
3) While the study suggests maximum LVPW contents for achieving 10 MPa strength (15% for 1:2:3 mix and 10% for 1:2:4 mix), further research might explore methods to improve the compatibility of LVPW with concrete, potentially allowing for higher LVPW incorporation rates.
4) LVPW concrete offers cost savings compared to conventional concrete, with a reduction of aggregate use of 15% for the 1:2:3 mix and 10% for the 1:2:4 mix. The minimal acquisition cost of LVPW further strengthens its economic advantage. From the optimized point of view, 1:2:3 ratio concrete with 15% LVPW is a better option as it gives more strength and consumes more plastic waste.
5) While workability is slightly reduced with LVPW, it remains within acceptable limits for construction. The slight decrease in surface smoothness might be

mitigated by using grouting or other finishing techniques.

In a nutshell, LVPW concrete presents a compelling solution for sustainable and potentially cost-effective construction in specific applications. Careful consideration of the impact on mechanical properties, along with potential adjustments to optimize LVPW compatibility and address workability/aesthetics, can help maximize the benefits of this promising technology. This solidification ensures waste management is expected to contribute significantly to the environment as well as to society.

Author contributions: Conceptualization, MA, HMAM and MAH; methodology, HMAM and NIR; software, MJHS; validation, KKM; formal analysis, HMAM, MJHS and KKM; investigation, MA, HMAM; resources, KR, MAAA; data curation, MAI and RKR; writing—original draft preparation, HMAM, MA, NIR; writing—review and editing, HMAM, MA, MAH; visualization, MJHS and KKM; supervision, MA; project administration, MA; funding acquisition, KR, MAAA, MAI and RKR. All authors have read and agreed to the published version of the manuscript.

Acknowledgments: The authors are expressing their gratitude to iDE-Bangladesh for providing the necessary financial support and also to the Department of Civil and Environmental Engineering (CEE), Shahjalal University of Science and Technology (SUST), Sylhet, Bangladesh for providing the very important Lab-support.

Conflict of interest: The authors declare no conflict of interest.

References

1. Proshad R, Kormoker T, Islam MDS, et al. Toxic effects of plastic on human health and environment: A consequences of health risk assessment in Bangladesh. International Journal of Health. 2017; 6(1): 1-5. doi: 10.14419/ijh.v6i1.8655
2. Rochman CM, Browne MA, Halpern BS, et al. Classify plastic waste as hazardous. Nature. 2013; 494(7436): 169-171. doi: 10.1038/494169a
3. Derraik JG. The pollution of the marine environment by plastic debris: A review. Marine Pollution Bulletin. 2002; 44(9): 842-852. doi: 10.1016/S0025-326X(02)00220-5
4. Thompson RC, Olsen Y, Mitchell RP, et al. Lost at Sea: Where Is All the Plastic? Science. 2004; 304(5672): 838. doi: 10.1126/science.1094559
5. Kaiser J. The Dirt on Ocean Garbage Patches. Science. 2010; 328(5985): 1506-1506. doi: 10.1126/science.328.5985.1506
6. Sakib AN, Salma AI, Ahmed M. Plastic waste management and feasibility of fuel production—A case study in Sylhet. Journal of Environmental Technology and Construction Management. 2012; 1(1): 66-78.
7. Len N. The New Plastics Economy Rethinking the Future of Plastics. World Economic Forum; 2016.
8. Gourmelon G. Global Plastic Production Rises, Recycling Lags. Vital Signs, Worldwatch Institute; 2015.
9. Hasan MA, Hoque MA, Ahmed M. Application of Plastic Waste as an Alternative to Coarse Aggregate for Concrete Block Construction. In: Proceedings of the 7th International Conference on Engineering Research, Innovation and Education; 12-14 January 2023; Sylhet, Bangladesh.
10. Subramani T, Pugal VK. Experimental Study on Plastic Waste as a Coarse Aggregate for Structural Concrete. International Journal of Application or Innovation in Engineering & Management. 2015; 4(5).
11. Ghernouti Y, Rabehi B, Safi B, et al. Use of recycled plastic bag waste in the concrete. Journal of International Scientific Publications: Materials, Methods and Technologies. 2014; 8.
12. Kamble SA, Karad DM. Plastic Bricks. International Journal of Advance Research in Science and Engineering. 2017; 6.
13. Singhal A, Netula O. Utilization of Plastic Waste in Manufacturing of Sand Bricks. In: Proceedings of the 3rd International Conference on New Frontiers of Engineering, Science, Management and Humanities (ICNFESMH-2018); Pune.
14. Shah R, Garg H, Gandhi P, et al. Study of Plastic Dust Brick Made from Waste Plastic. International Journal of Mechanical and Production Engineering. 2017; 5(10).

15. Merbouh M, Glaoui B, Mazouz A, et al. Use Plastic Bag Waste in Cement Concrete. Waste Management Symposium EURASIA; 2014.
16. Soemadijo P, Anindita F, Akib R, et al. A Study of Available Technology for Recycling Low Value Plastic in Indonesia. Journal of Environmental Science and Sustainable Development. 2022; 5(2). doi: 10.7454/jessd.v5i2.1128
17. Shi Y, Chai J, Xu T, et al. Microplastics contamination associated with low-value domestic source organic solid waste: A review. Science of The Total Environment. 2023; 857: 159679. doi: 10.1016/j.scitotenv.2022.159679
18. Mahzuz HMA, Tahsin A. Use of Plastic as a Partial Replacement of Coarse Aggregate in Concrete for Brick Classifications. International Journal of Scientific & Technology Research. 2019; 8(8): 883-886.
19. Darwin D, Charles WDP, Nilson AH. Design of concrete structures. McGraw-Hill Education; 2015.
20. Mathew P, Ambika KP, Pavitra P, et al. Comparative Study on Waste Plastic Incorporated Concrete Blocks with Ordinary Concrete Blocks. International Research Journal of Engineering and Technology. 2016; 3(5).
21. Bangladesh Standards and Testing Institution. BDS 208: (2002), Bangladesh Standard. Bangladesh Standards and Testing Institution; 2002.
22. Local Government Engineering Department of Bangladesh. Local Government Engineering Department of Bangladesh (LGED); 2005.
23. Hasan A, Islam MN, Karim MR, et al. Properties of Concrete Containing Recycled Plastic as Coarse Aggregate. In: Proceedings of the International Conference on Recent Innovation in Civil Engineering for Sustainable Development (IICSD-2015); DUET, Gazipur.
24. Hollow and Solid Concrete Blocks. IS (2005). IS 2185-1. In IS Concrete masonry unit: Part-1. Hollow and Solid Concrete Blocks; 2005.
25. Ji T, Fang H, Zhang R, et al. Automatic sorting of low-value recyclable waste: a comparative experimental study. Clean Technologies and Environmental Policy. 2022; 25(3): 949-961. doi: 10.1007/s10098-022-02418-7
26. Fu S, Qian Y, Yuan H, et al. Effect of cone angles of a hydrocyclone for the separation of waste plastics with low value of density difference. Waste Management. 2022; 140: 183-192. doi: 10.1016/j.wasman.2021.11.028
27. Tianchen J, Huaiying F, Rencheng Z, et al. Low-value recyclable waste identification based on NIR feature analysis and RGB-NIR fusion. Infrared Physics & Technology. 2023; 131: 104693. doi: 10.1016/j.infrared.2023.104693
28. Nizamuddin S, Jamal M, Santos J, et al. Recycling of low-value packaging films in bitumen blends: A grey-based multi criteria decision making approach considering a set of laboratory performance and environmental impact indicators. Science of The Total Environment. 2021; 778: 146187. doi: 10.1016/j.scitotenv.2021.146187
29. Bening CR, Kahlert S, Asiedu E. The true cost of solving the plastic waste challenge in developing countries: The case of Ghana. Journal of Cleaner Production. 2022; 330: 129649. doi: 10.1016/j.jclepro.2021.129649
30. Gall M, Wiener M, Chagas de Oliveira C, et al. Building a circular plastics economy with informal waste pickers: Recyclate quality, business model, and societal impacts. Resources, Conservation and Recycling. 2020; 156: 104685. doi: 10.1016/j.resconrec.2020.104685

Building Engineering 2024, 2(1), 544.
https://doi.org/10.59400/be.v2i1.544

Review

Machine learning algorithms for safer construction sites: Critical review

Yin Junjia*, Aidi Hizami Alias, Nuzul Azam Haron, Nabilah Abu Bakar

Department of Civil Engineering, Faculty of Engineering, Universiti Putra Malaysia, Serdang 43400, Malaysia
*** Corresponding author:** Yin Junjia, gs64764@student.upm.edu.my

CITATION

Junjia Y, Alias AH, Haron NA, Abu Bakar N. Machine learning algorithms for safer construction sites: Critical review. Building Engineering. 2024; 2(1): 544. https://doi.org/10.59400/be.v2i1.544

ARTICLE INFO

Received: 18 February 2024
Accepted: 6 April 2024
Available online: 26 April 2024

Abstract: Machine learning, a key thruster of Construction 4.0, has seen exponential publication growth in the last ten years. Many studies have identified ML as the future, but few have critically examined the applications and limitations of various algorithms in construction management. Therefore, this article comprehensively reviewed the top 100 articles from 2018 to 2023 about ML algorithms applied in construction risk management, provided their strengths and limitations, and identified areas for improvement. The study found that integrating various data sources, including historical project data, environmental factors, and stakeholder information, has become a common trend in construction risk. However, the challenges associated with the need for extensive and high-quality datasets, models' interpretability, and construction projects' dynamic nature pose significant barriers. The recommendations presented in this paper can facilitate interdisciplinary collaboration between traditional construction and machine learning, thereby enhancing the development of specialized algorithms for real-world projects.

Keywords: machine learning (ML); construction; risk management; critical review; Litmaps®; Open knowledge maps®

1. Introduction

Occupational safety has always been a headache for many workers in high-risk industries, such as high-voltage electricians, tower crane drivers, and deep-well miners, to name a few [1,2]. Accidents, whether artificial or not, can cause significant loss of life and property, as well as immense psychological grief for families. According to the latest data (11 January 2024) from the International Labor Organization (ILO), many countries such as Costa Rica, Argentina, Chile, France, and Denmark had at least 9421, 3587, 3142, 3043, and 2814 injuries per 100,000 workers, respectively [3]. This has also led to a focus on research around risk. Construction risk is complex and dynamic, arising from inherent uncertainties and variability [4]. Given the involvement of many stakeholders in large construction projects, including owners, financial institutions, project managers, designers, construction crews, manufacturers, suppliers, labor, insurance agencies, legal counsel, and public and regulatory agencies [5,6]. Effective risk management is crucial for their successful execution. Risk assessment is a cornerstone of construction management, involving identifying, analyzing, and mitigating potential risks that may arise during various project phases [7,8]. Historically, construction risk management was regarded as a static process at the project initiation stage [9,10]. However, constant changes in construction methods, coupled with a growing recognition of risk volatility, have led to a paradigm shift in risk management approaches [11]. The contemporary perspective acknowledges that risks are not fixed but evolve over the project lifecycle [12]. Therefore, it is imperative to adopt a dynamic and proactive approach to risk

management that accounts for the evolving nature of risks and adapts to changing project circumstances.

Fuzzy set theory (FST) was introduced by scholars in 1989 as a means of linguistic risk assessment for construction [13,14]. This approach enabled analysts to communicate the level of risk associated with individual project elements to stakeholders in easily understandable linguistic terms [15]. On the other hand, OSHA employs the risk matrix, a standard methodology for risk assessment. However, subjective approaches to risk assessment, such as those based on historical accidents, rely heavily on personal knowledge, experience, intuitive judgment, and rules of thumb. Many risk models are still based on expert opinion and emphasize linear causality, making it challenging to incorporate non-linear relationships such as security commitments and organizational culture [16,17]. Recent studies have highlighted the power of ML. As shown in **Figure 1**, according to the most recent data from the Scopus database, articles on ML grew exponentially from 2014 to 2023, reaching 131,489 from 11,264. Many scholars have also recognized that the rapidly changing algorithms have led to the need to regularly review research about the application of ML in construction risk. However, few studies critically examined the ML algorithm in this niche. The collective wisdom of the domain should be continuously constructed and updated, as knowledge is dynamically changing and growing and is contributed by multiple domain experts [18].

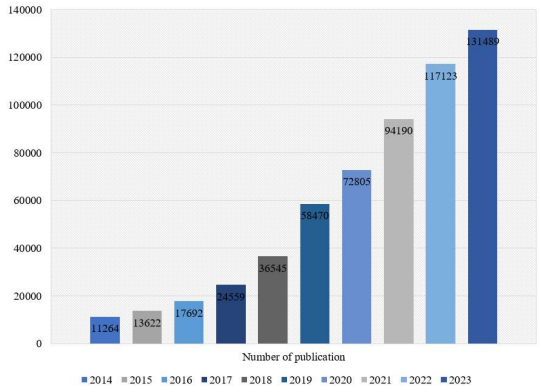

Figure 1. Machine learning annual publications (2014–2023).

Therefore, this article enriches the knowledge system in the following ways: 1) provides scientific and researched empirical evidence for engineers in chaotic working environments by reviewing existing algorithms' purpose, background, and limitations; 2) promotes the iteration of machine learning knowledge in construction risk by critically reviewing previous research; and 3) helps practitioners choose appropriate computational methods to formalize complex engineering knowledge. This study sheds light on the current main ML algorithms in construction risk by selecting 100 powerfully relevant and high-level research articles published between 2018 and 2023. The rest of the paper is structured as follows: Section 2 provides an overview of machine learning. Section 3 introduces the research methodology, and Section 4 introduces each algorithm's application, advantages, and disadvantages in construction risk assessment. Section 5 discusses future improvements in ML. Section 6 summarizes the research findings of this article and gives recommendations.

2. Background

Machine learning (ML) intersects several disciplines, including computer science, statistics, and artificial intelligence developments [19]. It addresses the problem of constructing computer algorithms and models that enable computer systems to improve automatically based on experience and increase performance on specific tasks [20,21]. Fundamentally, the beauty of ML is the ability to analyze, predict, and make decisions based on known data with increasing accuracy if the data sample expands [22]. As a result, it is popular in many data-intensive industries, such as the chemical industry, where active ML has been used to optimize the performance of CO_2 electrocatalysts [23]. In the medical field, Warnat-Herresthal et al. [24] used ML to identify patients with leukemia based on their blood transcriptome.

ML encompasses three fundamental types: supervised, unsupervised, and reinforcement learning [25]. One of the significant challenges that ML models face is overfitting and underfitting. Overfitting occurs when a model matches too closely to the training data, leading to inadequate performance on new and unseen data. On the other hand, underfitting occurs when a model is too simple to capture the underlying data patterns [26]. Supervised learning algorithms are designed to learn from labeled datasets, where each input data point is associated with a corresponding label [27]. The algorithm then learns to map input data to the correct output by adjusting its parameters based on the error between the prediction and the actual label [28]. Where features are the input variables, and labels are the outputs or predictions that the model is trying to learn. For example, algorithms make decisions based on historical data on contractor bidding opportunities, and the individual representations of project characteristics that enable the system to make decisions are called features. Unsupervised learning involves training on unlabeled datasets where the system automatically explores patterns in the data without guidance, such as clustering and lowering dimensionality. Reinforcement learning, on the other hand, trains a model and makes it make decisions by interacting in a scenario. The model is continually modified based on feedback from decisions such as rewards and penalties, aiming to maximize cumulative rewards over time.

3. Methods and materials

Compared to the traditional retrieval methods (from Scopus or WoS), we try to adopt a two-stage meta-analytic paper retrieval method to provide a new reference for future literature retrieval. In the first step, our approach used Open knowledge maps® to sift through the top hundred papers on “construction risk management” and “machine learning” efficiently [29]. By grouping these documents based on their metadata, including title, abstract, author, journal, and subject keywords, we can create a word co-occurrence matrix to determine the relevance of each article. As shown in **Figure 2**, the resulting map represents the textual similarity between each article and the search query. The proximity of circular regions on the map indicates how closely related their subjects are, with more central areas indicating more remarkable similarity to the overall topic. Using this method, we can effectively manage the number of documents to review while exploring a wide range of content.

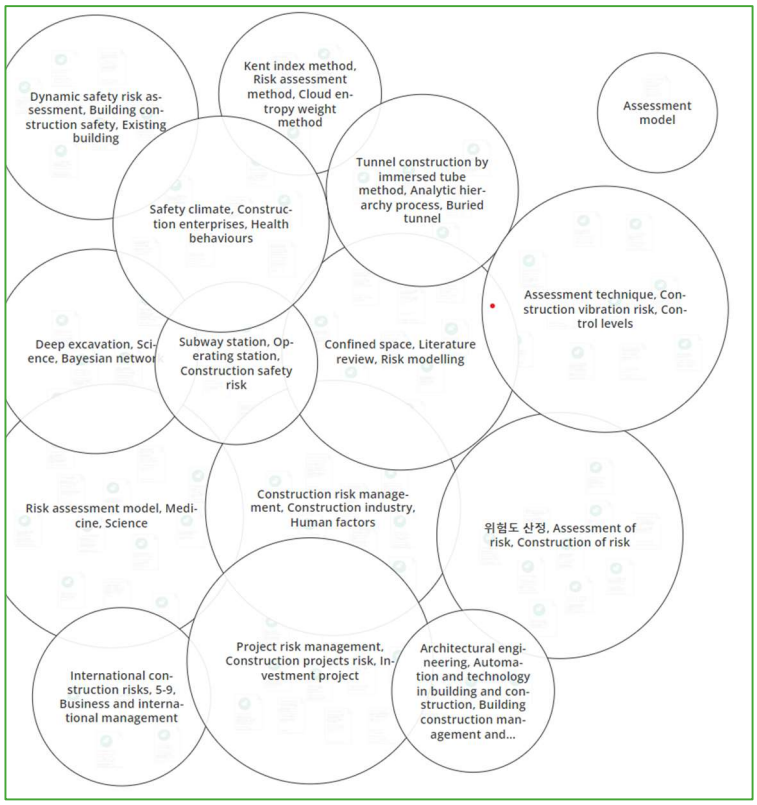

Figure 2. Top 100 Strong-related articles about ML in construction risk.

In the second step, **Figure 3** comprehensively showed the top 20 citations and references associated with the subject matter using Litmaps®. The inner circle of the map represents the input, namely "Construction Risk Assessment" and "Machine Learning," and its corresponding combination of citations and references. The outer circle demonstrates the articles' findings that are most pertinent to the domain. After completing the literature search, we collected data from the selected literature, including key findings, methods, applications of ML techniques, challenges addressed, and innovations introduced [30]. This information was then systematically organized and cataloged for analysis. Identify patterns, trends, and common themes in the selected literature by analyzing the collected data. Finally, we will compare ML algorithms and their effectiveness in construction risk management.

Figure 3. Top 20 high-cited articles about ML in construction risk.

4. Results

The keyword cloud in **Figure 4** is generated based on the frequency statistics of documents. It is intended to facilitate the reader's understanding of the current state of ML in the field. Standard algorithms include SVM, logistic regression, and ANN. They are utilized in almost every risk management process, including risk identification, classification, assessment, diagnosis, and prevention. The study summarizes the main ML algorithms in construction risk, as illustrated in **Table 1**. Since the author's past research has discussed artificial neural networks and Bayesian networks, this article will not discuss them.

Table 1. ML in construction risk management.

Algorithm	Application	Source
Regression	Mapping landslide sensitivity; project delay risk prediction; predicting construction duration; Credit risk assessment models for financial institutions; Analysis of ground settlement during tunnel construction; Predicting variance in construction productivity; Determination of poor compliance with OSH rules of construction workers; long-term probabilistic prediction of rock burst hazard.	Tessema et al. [31]; Zhu et al. [32]; Gariazzo et al. [33]; Hemasinghe et al. [34]; Li and Jimenez [35].
RF	Integrated land carrying capacity assessment; multi-objective optimization of shield construction parameters; Constructing a monitoring model for dam safety; Predicting BIM labor cost; Detecting corporate misconduct; Activity recognition of construction equipment; concrete dam deformation monitoring; Analyzing and adjusting EPB shield steering in real-time; hybrid optimization of seismic performance of mountain buildings.	Xie et al. [36]; Hu et al. [37]; Wang et al. [38]; Wu et al. [39]; Wen et al. [40].
SVM	Predicting project outcomes; Rapid building fire risk assessment; projects delay risk prediction; Hypertension risk assessment for steelworkers in deep foundation pits; Estimation of construction waste generation; Seismic hazard safety evaluation of existing buildings; Early cost estimates of bridges; Estimation of construction waste generation.	Hu et al. [41]; Chen and Lin [42]; Tserng et al. [43]; Fan and Sharma [44]; Fu et al. [45].
GCN	Boring machinery load prediction in tunnel excavation; Interaction Behaviors Identification of Construction Workers; Identification of accident-injury type and body part factors; Action recognition of construction workers under occlusion; Determining construction method patterns to automate and optimize scheduling; Monitoring and prediction of landslide-related deformation.	Mostofi et al. [46]; Khalili et al. [47]; Mostofi et al. [48]; Fu et al. [49]; Li et al. [50]; Zhang et al. [51]
KNN	Projects delay risk prediction; Safety risk evaluations of deep foundation construction schemes; Estimation of management reserve; Assessing worker perceived risk; Analysis of factors influencing rockfall runout distance; Short-term rockburst risk prediction for profound underground works;	Chen et al. [52]; Pandey and Bandhu [53]; Jaber et al. [54]; Lee et al. [55].
Apriori	Analysis of deformation response to landslide disaster; Mining geological disaster sensitivity evaluation indicators; Mining Construction Cross-Operation Risk Association Rules.	Linwei et al. [56]; Chen et al. [57]; Chen et al. [58]
PCA	Extraction of construction accident characteristics; Analysis of crucial behavioral risk factors for construction practitioners; Explore construction settlement data; Identify and remove outliers.	Shao et al. [59]; Xiang et al. [60]; Siddiqui et al. [61]
XGBoost	Handling large datasets; Predicting enterprise financial management risks; Investment Estimates for Assembled Concrete Buildings; Predict construction cost overruns; Investment estimation of prefabricated concrete buildings.	Yan et al. [62]; Cherif and Kortebi [63]; Coffie and Cudjoe [64]; Liu et al. [65]
K-Means	Identifying clusters of projects with similar risk profiles; Early warning of risks in government investment and construction projects; Supplier risk assessment; Risk assessment of integrated pipeline corridor construction projects; BIM performance assessment system; Identifying high frequency-low severity construction safety risks.	Liu and Li [66]; Wang et al. [67]; Ayhan and Tokdemir [68]
ARIMA	Predicting construction cost index; Predicting construction material prices; Forecasting the ratio of a low bid to owner's estimate for highway construction; Effect of dam construction on the lake; Structural health monitoring and identification; Predicting perceived fatigue levels.	Kim et al. [69]; Moon et al. [70]; Ghashghaie and Nozari [71]; Kaloop et al. [72]; Hajifar et al. [73]

Figure 4. Keyword cloud of the documents.

4.1. Linear and logistic regression

Linear regression (LiR) is a statistical technique that models the connection between a dependent variable and one or more independent variables [74]. It aims to create a linear equation that predicts the dependent variable based on the independent variable values [75]. Equation (1) shows that multiple regression analysis integrates numerous independent variables throughout the dataset without considering shared variance, and R^2 assesses reliability. LiR helps analyze the impact of various factors (independent variables) on a specific risk outcome (dependent variable). Huang & Hsieh [76] employed LiR to forecast BIM labor costs. It produces a simple and understandable model that explains each independent variable's influence on predicting risk outcomes. Secondly, LiR is computationally efficient and straightforward, suitable for swift analysis and evaluation. Thirdly, LiR equation coefficients measure the strength and direction of the relationship between the independent and dependent variables. Still, it is unsuitable for capturing complex, variable relationships or interactions. Additionally, linear regression is sensitive to outliers, which can significantly affect model parameters and predictions [77]. Therefore, LiR is not ideal for nonlinear relationships.

$$Y = a + b_1x_1 + b_2x_2 + \cdots + b_nx_n \pm e \quad (1)$$

here Y could be the risk factor variable, a is a constant, b_1 through b_n are estimated regression coefficients, x_1 through x_n are predictor or independent variable values, and e is the closure error.

Logistic regression (LoR) is a statistical technique that predicts the probability of a binary outcome (0 or 1) based on one or more predictor variables, as demonstrated in Equation (2). LoR can be utilized to model and predict the probability of a specific risk event happening or not [78]. Levy and Baha [79] employed LoR models to anticipate borrower solvency. Akboğa and Baradan [80] employed LoR modeling to identify factors contributing to construction injury severity. Bhattacharjee et al. [81] used an interval based LoR and FMEA to assess potential failures. Both regression coefficients are interpretable, making it easy to understand how each predictor variable impacts the probability of a risk event occurring. LoR is restricted to binary outcomes, designed for binary outcomes, and needs to be modified or expanded for multi-category outcomes [82].

$$y = \frac{1}{1 + e^{-z}} = \frac{1}{1 + e^{-(w^T x + b)}} \tag{2}$$

where z is a real number, w is a column vector, x is a row vector, and b is a real number. $w^T x$ denotes the inner product of w and x. e is the base of the natural logarithm. The function y has a range of (0,1). When y is greater than 0.5, we consider the input data belong to the positive category; otherwise, we consider the input data to belong to the negative category. In addition, the loss function of logistic regression is the cross-entropy loss function.

4.2. Principal component analysis

Principal Component Analysis (PCA) is a statistical technique used for dimensionality reduction in multivariate data analysis. Its primary purpose is to transform the original variables into a new set of uncorrelated variables, known as principal components, which capture the maximum variance in the data. PCA can identify the data set's most influential patterns or features by arranging these components in descending order of variance. This dimensionality reduction method simplifies the data while preserving its essential features, making it valuable in various fields such as image processing, pattern recognition, and data compression. The specific formula is as follows:

$$x = \frac{1}{n} \sum_{i=1}^{N} x_i \tag{3}$$

$$S^2 = \frac{1}{n-1} \sum_{i=1}^{n} (x_i - \bar{x})^2 \tag{4}$$

$$\mathrm{Cov}(X, Y) = \frac{1}{n-1} \sum_{i=1}^{n} (x_i - x)(y_i - y) \tag{5}$$

here, x is mean, S^2 isvariance, $\mathrm{Cov}(X, Y)$ is covariance.

Zhang et al. [83] proposed the weight calculation method of Group Analytic Hierarchy Process-Principal Component Analysis to rank the critical construction risk factors. Most studies use PCA as a data preprocessing tool [84,85]. Nevertheless, it also has some disadvantages. First, it is often difficult to directly interpret the specific meaning of the principal components obtained by PCA. Although it can map high-dimensional data to a low-dimensional space, the meaning of the comprehensive evaluation function is unclear when the sign of the factor loading of each principal component is positive or negative. Secondly, PCA is sensitive to outliers, which may cause the extracted principal components to deviate from the actual situation. Finally, PCA assumes that the data follows a Gaussian distribution. If the data distribution does not conform to this assumption, it may result in inaccurate analysis.

4.3. Support vector machines

The Support Vector Machine (SVM) is a powerful binary classification model that utilizes a linear classifier to optimize the feature space [86]. SVM's primary learning strategy involves interval maximization, which can be formulated as a convex quadratic programming problem [87]. This is also equivalent to minimizing a regularized hinge loss function. It is also an optimization algorithm used to solve

convex quadratic programming. The fundamental idea behind SVM is to locate a separating hyperplane that accurately separates the training dataset while maximizing the geometric intervals [88]. The basic idea is to solve for a separating hyperplane that correctly divides the training dataset and maximizes the geometric separation [89]. As shown in Equation (6), $w \cdot x_i + b = 0$ is the separating hyperplane, and there are infinitely many such hyperplanes (i.e., perceptual machines) for a linearly divisible dataset. Still, the geometrically maximally spaced separating hyperplane is unique. The algorithmic formulation of the SVM is as follows [90]:

$$\begin{gathered} \min w, b \frac{1}{2} \| w \|^2 \\ \text{s.t. } y_i(w \cdot x_i + b) \geq 1, i = 1,2, \ldots, n \end{gathered} \tag{6}$$

here x_i is the feature vector of the ith sample; y_I is the category labeling of the ith sample, taking the value of +1 or −1.

It can be applied to classify risks such as credit into different categories based on input features [91,92]. Gong et al. [93] used a binary particle swarm optimization algorithm to reduce the redundancy of information in the dataset. Then, they modified the classification algorithm using an Adaboost-enhanced support vector machine classifier, which overcame the difficulties of correctly classifying a small number of samples in an unbalanced dataset. SVM has gained popularity in recent years due to its effectiveness in high-dimensional feature space and its ability to handle complex patterns in data. It is well-suited for scenarios where a clear margin of separation exists between different classes or categories, making it a valuable tool for risk classification tasks such as credit risk assessment.

Several studies have explored the use of SVM in various risk assessment applications. For example, Liu et al. [94] developed an SVM model based on particle swarm optimization to predict the safety risk of metro construction, achieving an average accuracy of 85.26%. Wei et al. [95] proposed a new rapid-fire risk assessment method based on fuzzy mathematics and an SVM algorithm. Additionally, researchers have attempted to enhance the performance of SVM by integrating it with other algorithms, such as the firefly algorithm and Gradient Boosting Decision Tree [96–98]. While SVM has several advantages, it also has some limitations that should be carefully considered. For instance, SVM is computationally intensive, especially for large data sets or complex kernel functions, which may affect scalability. It is also sensitive to noisy data, outliers, and mislabeled instances, which can significantly impact model performance and generalization [99]. Finding the optimal set of hyperparameters for SVM requires careful tuning, which can be challenging.

4.4. Random forest

Random Forest (RF) is an ensemble ML algorithm that has become increasingly popular in various ML applications, including classification and regression tasks [100]. As shown in **Figure 5**, the algorithm constructs many decision trees during training and outputs pattern (classification) or mean (regression) predictions for individual decision trees [101]. In construction risk, RF has been used to predict and classify different types of risks based on relevant input features, such as falls from heights [102,103]. Studies have shown that RF models can effectively estimate the relationship between monitoring values and pit safety risk and predict and prevent

occupational accidents [104,105]. RF has also been used to develop risk indicators with high accuracy in various fields, such as supply chain finance risk [106], flood risk [107], and landslide risk assessment [108]. These studies have demonstrated that RF is a robust algorithm that can handle missing data efficiently, including incomplete data sets in the assessment process [109–111]. Scholars have also proposed a fractional RF method with low dependency on a comprehensive training dataset that can predict extensive device activities using a small amount of training data [112,113].

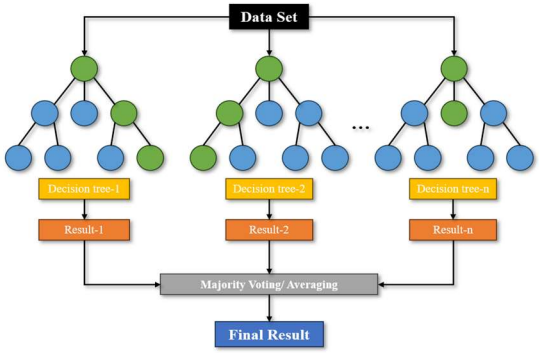

Figure 5. Random forest model.

Furthermore, RF provides a measure of feature importance that can help identify the most influential risk factors [114]. It is also robust to noisy data and outliers, and aggregating predictions from multiple trees eliminates individual errors and outliers [115]. Additionally, training individual trees in an RF can be done in parallel, making it computationally more efficient, especially for large data sets [116]. However, it is essential to note that RF may be biased toward the dominant class in the training data, leading to imbalanced predictions if the class distribution is imbalanced [117]. Moreover, while individual trees can be trained in parallel, the overall construction of an RF can be computationally expensive, particularly for large numbers of trees [118]. The diversity measure between the decision trees improves the model's generalization, but it is still necessary to minimize the number of trees to find the optimal subset [119].

4.5. K-nearest neighbor

The K-nearest neighbor (KNN) algorithm is a powerful instance-based learning method that can be utilized for both classification and regression problems. The fundamental concept behind the KNN algorithm is to locate the k closest instances to a new input instance in the training set and subsequently predict the instance's class based on the classes of these k instances. The Equation (4) of the KNN algorithm is as follows [120]:

$$y = \underset{c_j}{\operatorname{argmax}} \sum_{i=1}^{k} w(i) \cdot I(y_i = c_j) \tag{7}$$

here y denotes the predicted category, c_j denotes the jth category, $w(i)$ denotes the weight of the distance $d(x, I)$ from the input instance x, and $I(y_i = c_j)$ is the indicator function, when $y_i = c_j$, $I(y_i = c_j) = 1$, otherwise $I(y_i = c_j) = 0$.

In KNN, an object is classified by the majority class of its k nearest neighbors, where "k" is a user-defined parameter. Construction risk can be applied to categorize

risks or predict risk outcomes based on the characteristics of similar historical cases. Lee et al. [121] used it to retrieve similar projects and a genetic algorithm to optimize the retrieved cases with an error rate of less than 5%. Kamran et al. [122] reduced the magnification of the original database using the state-of-the-art method of the Isometric Mapping (ISOMAP) algorithm; it then used the Fuzzy c-Mean (FCM) algorithm to classify the datasets obtained from ISOMAP, and thirdly, employed it to predict the short-term rock burst datasets at different levels of accuracy, with an accuracy of 96%. Liu et al. [123] constructed an improved fusion KNN model to evaluate the posture state of workers.

KNN is a straightforward and practical method for quickly assessing risk, mainly when interpretability is crucial. Moreover, it is suitable for analyzing data with an unknown or complicated distribution since it does not rely on making assumptions about the underlying data [124]. KNN can also detect local patterns, making it an effective tool for identifying risks with spatial or temporal clustering. However, it is computationally demanding, mainly when applied to large datasets, as it requires computing the distance between the query and all training instances. KNN is also sensitive to outliers, as extreme values in the dataset can affect the nearest neighbors. In addition, irrelevant or redundant features can introduce noise into distance calculations and compromise the performance of KNN [125,126]. In high-dimensional space, the distance between instances tends to become more uniform, which may reduce the effectiveness of KNN. Finally, the choice of parameter "k" (number of neighbors) can impact KNN's performance and may need to be adjusted based on the data's specific characteristics [127]. For instance, Zhang et al. [128] used a weighted k-value to plan deep foundation pits.

4.6. XGBoost

XGBoost is a refined algorithm rooted in GBDT. While sharing the basic concept of GBDT, it incorporates several enhancements, including second-order derivatives for greater loss function accuracy, regularization terms to address tree overfitting, and block storage for parallel computation [129]. Its objective function comprises a loss function and a regularization term. The loss function can be the mean square error (MSE) for regression problems or cross-entropy for classification problems. Qin [130] predicted corporate financial risk and found that the model's errors were all within 3%, with the maximum prediction error of only 2.68%. In another study, Liu et al. [131] assessed pipeline safety using it and achieved an accuracy of 91.8%. The algorithm analyzes the feature's importance, which helps prioritize risk factors in decision-making. Including regularization terms in the objective function helps prevent overfitting and improves the model's generalization [132]. It is designed for parallel and distributed computing, efficiently handling large building datasets [133]. However, it faces the challenge of interpretability, and data preprocessing is necessary to handle missing values and outliers for optimal performance.

In the future, it may be possible to use more superficial ensemble structures to enhance the interpretability of XGBoost models. The development of automatic hyperparameter tuning methods can simplify the model development process and improve the algorithm's ease of use [134]. Construction projects involve data that

changes over time, and improving XGBoost's ability to process time series data directly could enhance its applicability to construction risk management. However, the complexity and dynamic interrelationships of the studied attributes make it difficult for the XGBoost model to predict residual values [135].

4.7. *K*-means

The *k*-means algorithm is a distance-based clustering algorithm. Its steps include [136]: 1) randomly initialize *k* centers of mass, i.e., the centroids of the *k* clusters; 2) for each sample, calculate its distance from the k centers of mass and assign it to the cluster with the closest distance; 3) for each cluster, recalculate its center of mass; 4) repeat steps 2 and 3 until the center of mass no longer changes or a preset number of iterations is reached. Distance can be used as Euclidean distance, Manhattan distance, etc. *K*-means can group construction projects based on shared risk characteristics, which allows risk profiles to be created for different projects and can also help identify geographic or project-specific "hot spots" where specific risks are more prevalent [137]. This information is valuable for resource allocation. Many academics use *K*-mean clustering to identify similarities between different construction projects based on risk factors, which can help with benchmarking. Evolving risk patterns are uncovered by regularly updating clusters and reassessing risks.

K-means is computationally efficient and relatively simple to implement, making it suitable for quick analyses and real-time applications. The algorithm scales to large datasets, making it ideal for large-scale complex projects [138]. Being an unsupervised learning algorithm means it does not require labeled data, making it adaptable to situations where comprehensive risk labeling is not readily available. Each item is assigned to a cluster, providing precise categorization and simplifying the interpretation of results. However, the results of *K*-means are sensitive to the initial position of the centroids. Different initializations may lead to other solutions and finding the optimal centroids can be challenging. The algorithm assumes that the clusters are spherical and of equal size, making it difficult to identify irregularly shaped clusters or clusters with different densities, which are common in construction risk datasets [139]. Improvements have also been made to the *K*-means method to deal with non-spherical or irregularly shaped clusters, improving its applicability in various construction risk situations. For example, developing strategies to automatically determine the optimal number of clusters (*K*) could alleviate the sensitivity to the initial choice of centroids and improve the usability of the algorithm.

4.8. ARIMA

ARIMA (Autoregressive Integrated Moving Average) is a time-series forecasting algorithm that can make time-series forecasts of construction-related variables such as project cost, completion time, or other performance indicators [140]. Equation (8) of the ARIMA model is given below:

$$Y_t = c + \phi_1 Y_{t-1} + \cdots + \phi_p Y_{t-p} + \theta_1 \epsilon_{t-1} + \cdots + \theta_q \epsilon_{t-q} + \epsilon_t \quad (8)$$

here, Y_t denotes the observed value at time t and c is a constant; $\phi_1, \cdots, \phi_p$ is the autoregressive coefficient; ϵ_t is white noise; $\theta_1, \cdots, \theta_q$ is the moving average

coefficient. The parameters p, d, q of the ARIMA model denote the number of autoregressive terms, difference order and moving average terms, respectively.

ARIMA provides a quantitative basis for assessing the likelihood of delays, cost overruns, or other adverse events. It can assist in resource planning by predicting the demand for construction materials, labor, and equipment based on historical usage patterns [141]. ARIMA explicitly accounts for the time dependence of the data and is, therefore, well-suited to modeling construction-related variables that evolve [142]. Secondly, ARIMA is very robust when dealing with noisy time series data and is, therefore, suitable for situations where construction project data may be subject to variability and uncertainty [143]. The parameters and results of the model can usually be interpreted to give an understanding of the impact of past observations on future projections. It is very effective for univariate time series data, which is common in construction risk analysis, where univariate variables (e.g., project duration or cost) are often the focus of the study. However, ARIMA assumes that the underlying data patterns are linear and require the time series data to be static, which is challenging in dynamic yet complex construction systems. In addition, because it focuses primarily on internal time-series patterns, it is easy to overlook external factors or unexpected shocks to a construction project. Therefore, incorporating suitable exogenous variables is a topic worth considering.

4.9. Graph convolutional network

Graph Convolutional Network (GCN) is a deep learning algorithm that operates on graph-structured data. Equation (9) demonstrates the algorithm of GCN [144]:

$$H^{(l+1)} = \sigma\left(\widetilde{D}^{-\frac{1}{2}}\tilde{A}\widetilde{D}^{-\frac{1}{2}}H^{(l)}W^{(l)}\right) \tag{9}$$

here $H^{(l)}$ is the node feature matrix of the lth layer, $W^{(l)}$ is the weight matrix of the lth layer, $\tilde{A} = A + I$, I is the unit matrix, and $\widetilde{D}$ is the degree matrix of $\widetilde{A}$.

It can model the complex relationships and dependencies between various risk factors in a construction project and represent them as a graph [145]. Nodes can represent project risk components, while edges represent their relationships [146]. It can help identify critical nodes in a construction project, such as unsafe interactions between people, machines, and materials [147]. Temporal information can be integrated to enable dynamic risk assessment by considering the evolution of risk factors at different stages in the construction. Mostofi and Toğan [148] combined a GCN to account for the dependency information between accidents and predicted the severity outcome of each construction activity with 94% accuracy.

GCN can improve the efficiency of risk assessment by using transfer learning to train models on one construction project that apply to new projects with similar risk structures. However, GCNs require large amounts of labeled data to learn effectively, which may not always be readily available. The raw recorded data may contain noise, which reduces the prediction accuracy of the GCN deep learning model [149]. Integrating external data sources such as weather patterns, economic indicators, or regulatory changes into GCN can enhance its ability to capture external influences on building risk [150].

4.10. Apriori

Apriori algorithm is a classical association rule mining technique used in data mining and machine learning. It aims to discover frequent item sets in transaction databases and extract meaningful associations between items. The algorithm uses a bottom-up approach, starting with a single item and progressively identifying larger item sets through iterative concatenation and pruning based on a predefined support threshold. Support measures how often the itemset appears in the dataset. The strength of association rules can be measured by their support and confidence, as shown in Equations (10) and (11).

$$\text{Support}(X,Y) = \frac{\text{num}(XY)}{\text{num(allsamples)}} \tag{10}$$

$$\text{Confidence}(XY) = \frac{P(X \mid Y)}{P(Y)} \tag{11}$$

Xie et al. [151] used it to mine disaster information and prevent incorrect reference management. Deng et al. [152] analyzed subway operation accident cause association rules based on the Apriori algorithm and network method. This algorithm needs to scan the data set multiple times and calculate frequent item sets, so the calculation complexity is high and the speed is slow. On large data sets, the efficiency may not be high enough. Secondly, it must store many intermediate results, requiring ample memory space. Finally, it can only handle discrete data and is powerless for continuous data.

5. Discussion

Construction projects often involve heterogeneous and incomplete data, leading to inaccurate model predictions. Much of the quantitative data is difficult to collect without the full assistance of site managers and workers, especially in China, where disruptions to the construction schedule can hinder researchers [153]. It has become the norm to model multiple ML tools simultaneously, compare their associated fit parameters, such as F1 and RSMEA, recall rate, and then select the "best performing" tool [154]. Accurately capturing and modeling this complexity is a significant challenge for traditional algorithms. Taking safety risks as an example, the construction industry lacks standardized incident text data formats and reporting practices [155]. Different data sources and formats make integrating information effectively difficult for many ML models. Construction projects change over time, with changing conditions, requirements, and stakeholders, and the many human decisions involved are not so easily quantifiable [156]. However, computer vision attempts to understand human behavior and incorporate it into ML models. Many state-of-the-art ML algorithms lack transparency, interpretability, and complex deep learning models. In risk management, stakeholders often require explanations of predictions, which can hinder adopting specific algorithms. In addition, limited computer literacy and a lack of awareness of potential advantages among construction industry practitioners in most developing countries can similarly hinder the widespread adoption of ML technologies. Data for many projects is subject to confidential contractual terms and regulatory norms, and complying with these

regulations while implementing ML models can be challenging, especially if the models are seen as "black box" systems [157].

Improving the use of ML in construction risk management requires a combination of data-driven approaches, advanced algorithms, and integration with existing processes. First, there is data collection and integration. Consider collecting comprehensive, high-quality data from various sources, including project management systems, sensor data, historical project data, weather conditions, etc. Then, data from different departments and systems will be integrated to create a holistic view of the project and its associated risks. Next, fostering collaboration between building technicians and machine learning experts requires promoting mutual understanding of expertise and goals. Launching an interdisciplinary training program can help bridge the knowledge gap, enabling building technicians to grasp basic machine learning concepts and machine learning experts to understand the intricacies of building processes. In addition, joint project planning sessions and interdisciplinary teams can facilitate a holistic approach, allowing building technicians to provide real-world insights and machine learning experts to deliver tailored solutions. Construction companies need to adjust their corporate structure and set up AI represented by ML as a specialized function, which not only creates sustainable returns for the company but is also an inevitable choice not to be eliminated by the times. Besides ML, other methods also made sustained contributions, as shown in **Table 2**. It is also an excellent option to integrate ML with these techniques to form a new approach.

Table 2. Other methods in construction risk evaluation.

Source	Method	Contribution
Zhu et al. [158]	4D simulation	The methodology provides a 4D simulation environment for modeling drone interactions on a dynamic construction site.
Zhong et al. [159]	Finite Element Model (FEM)	The methodology can assess the seismic risk of bridges throughout their life cycle, including construction and use.
Nguyen et al. [160]	Hierarchical regression	The methodology provides a comprehensive list of GB risks, categorized and assessed according to the project life cycle.
Sohrabi and Noorzai [161]	PLS-SEM	The methodology is based on a project life-cycle perspective that considers the link between the risks leading to claims and the main parties involved.
Hatamleh et al. [162]	Factor analysis	The methodology identifies the risks developing countries face and emphasizes how risks can benefit industry practitioners.
Al-Mhdawi et al. [163]	Deductive and inductive reasoning	The methodology proposes new risk models for analyzing the risks associated with extreme situations such as pandemics.
Gashaw and Jilcha [164]	Fuzzy Synthesis Evaluation (FSE) and System Dynamics (SD)	The methodology considers the overall dynamics, interrelationships, and uncertainties of risks to inform the assessment of the impact of project objectives.
Do et al. [165]	Expert scoring	The methodology simultaneously examines the chain of risk factors, the sources of risk, and the scope of influence of risk factors.
He et al. [166]	AHP and Fuzzy Comprehensive Evaluation (FCE)	The method quantitatively evaluates the risk level of pyrotechnic operations and rationally ranks the importance of various risk factors.
Mohandes et al. [167]	AHP	The methodology is based on a fuzzy hybrid multidimensional model that considers the context of construction-related activities that lead to accidents and provides a comprehensive ranking system for project risk.
Badi et al. [168]	Grey Theory	The methodology identifies the risks of construction projects through preliminary research, extensive interviews with construction experts, and site visits.
Zhang and Li [169]	Projection Pursuit Method and Improved Set Pair Analysis	The method is based on the risk decomposition structure matrix, which considers the risk dynamics and establishes the deep foundation pit risk evaluation index system.
Ju et al. [170]	Best worst method (BWM) and game theory and extension cloud	The methodology considers disaster-causing factors when assessing building safety risks.
Sadeghi et al. [171]	Trapezoidal fuzzy ordinal priority approach (OPA-F)	The methodology constructs a new OPA-F using trapezoidal fuzzy numbers, assesses the blockchain risks faced by construction organizations, and develops a framework.

6. Conclusion

The number of machine learning papers is growing exponentially, and regular review is essential to promote the dissemination of interdisciplinary knowledge in the industry. This study's significance is critically reviewing ten machine learning algorithms that have been popular in construction risk over the last five years to inform new researchers. Machine learning has great potential in construction risk management but requires combining technology, data, and domain knowledge to achieve better results. Linear regression is suitable for predicting continuous numerical outcomes, such as project cost or completion time. However, it is assumed that there is a linear relationship between the variables, which may not always be accurate in complex construction projects. Logistic regression is suitable for binary classification problems, such as predicting whether a project will be completed on time or delayed. However, assuming linear decision boundaries may not capture more complex relationships in the data. SVMs are adequate for regression and classification tasks, especially when working with nonlinear and high-dimensional data. However, the choice of kernel and parameters can be sensitive, and different kernel functions, such as the triangular kernel function and the Gaussian kernel function, may perform differently or poorly on large data sets. RF is suitable for classification and regression tasks, robust enough to overfit, and can handle large datasets with many features. However, it lacks interpretability, and the training time for extensive forests can be extended. KNN is simple and effective for classification and regression tasks, especially when dealing with localized patterns. However, it is sensitive to irrelevant or redundant features and computationally expensive to predict for large datasets. PCA in construction risk analysis offers the advantage of reducing dimensionality and aiding in identifying key risk factors and patterns; however, it may oversimplify complex interactions and might not capture non-linear relationships in the data. On the other hand, the Apriori algorithm enables the discovery of association rules among construction risk factors, enhancing understanding; nevertheless, it may face challenges with large datasets and requires careful parameter tuning. XGBoost is very effective for classification and regression tasks and is often used in competitions due to its high predictive performance. However, it is computationally expensive and is easy to overfit if not correctly adjusted. K-Means is suitable for clustering similar construction projects based on characteristics such as project size, location, or complexity. However, it must be assumed that the clusters are spherical, sensitive to the initial cluster center, and may not work well for clusters of uneven size. ARIMA is suitable for time series forecasting in construction risk analysis, such as predicting future project delays or cost overruns. However, it requires assumptions of linearity and stationarity and may not capture complex nonlinear trends in time series data.

The study recommends using a combination of these algorithms to address construction risks. The choice of algorithm should depend on the specific characteristics of the data and the nature of the risk being analyzed. Proper data preprocessing, feature engineering, and hyperparameter tuning are critical to achieving optimal model performance. In addition, there is a distinct lack of standardization across the industry, leading to challenges in actual data collection. Therefore, future

research should prioritize standardization efforts and seek consensus on best practices to meet project-specific needs, such as tight deadlines and confidentiality agreements.

Conflict of interest: The authors declare no conflict of interest.

References

1. Liu R, Liu HC, Shi H, et al. Occupational health and safety risk assessment: A systematic literature review of models, methods, and applications. Safety Science. 2023; 160: 106050. doi: 10.1016/j.ssci.2022.106050
2. Pinto A, Nunes IL, Ribeiro RA. Occupational risk assessment in construction industry - Overview and reflection. Safety Science. 2011; 49(5): 616-624. doi: 10.1016/j.ssci.2011.01.003
3. ILOSTAT. ILOSTAT data tools to find and download labor statistics. Available online: https://ilostat.ilo.org/data (accessed on 15 April 2024).
4. Hastak M, Shaked A. ICRAM-1: Model for International Construction Risk Assessment. Journal of Management in Engineering. 2020; 16(1): 59-69.
5. Lee HS, Kim H, Park M, Ai Lin Teo E, Lee KP. Construction Risk Assessment Using Site Influence Factors. Journal of Computing in Civil Engineering. 2012; 26(3): 319-330.
6. Mulholland B, Christian J. Risk Assessment in Construction Schedules. Journal of Construction Engineering and Management. 1999; 125(1): 8-15.
7. Ashtari MA, Ansari R, Hassannayebi E, et al. Cost Overrun Risk Assessment and Prediction in Construction Projects: A Bayesian Network Classifier Approach. Buildings. 2022; 12(10): 1660. doi: 10.3390/buildings12101660
8. Mudiyanselage SE, Nguyen PHD, Rajabi MS, et al. Automated Workers' Ergonomic Risk Assessment in Manual Material Handling Using sEMG Wearable Sensors and Machine Learning. Electronics. 2021; 10(20): 2558. doi: 10.3390/electronics10202558
9. Gondia A, Siam A, El-Dakhakhni W, Nassar AH. Machine Learning Algorithms for Construction Projects Delay Risk Prediction. Journal of Construction Engineering and Management. 2020; 146(1): 04019085.
10. Huang J, Zeng X, Fu J, et al. Safety Risk Assessment Using a BP Neural Network of High Cutting Slope Construction in High-Speed Railway. Buildings. 2022; 12(5): 598. doi: 10.3390/buildings12050598
11. Ni G, Fang Y, Niu M, et al. Spatial differences, dynamic evolution and influencing factors of China's construction industry carbon emission efficiency. Journal of Cleaner Production. 2024; 448: 141593. doi: 10.1016/j.jclepro.2024.141593
12. Verma A, Prakash S, Kumar A. AI-based Building Management and Information System with Multi-agent Topology for an Energy-efficient Building: Towards Occupants Comfort. IETE Journal of Research. 2020; 69(2): 1033-1044. doi: 10.1080/03772063.2020.1847701
13. Kangari R, Riggs LS. Construction risk assessment by linguistics. IEEE Transactions on Engineering Management. 1989; 36(2): 126-131. doi: 10.1109/17.18829
14. Lin SS, Shen SL, Zhou A, et al. Risk assessment and management of excavation system based on fuzzy set theory and machine learning methods. Automation in Construction. 2021; 122: 103490. doi: 10.1016/j.autcon.2020.103490
15. Taroun A. Towards a better modelling and assessment of construction risk: Insights from a literature review. International Journal of Project Management. 2014; 32(1): 101-115. doi: 10.1016/j.ijproman.2013.03.004
16. KarimiAzari A, Mousavi N, Mousavi SF, et al. Risk assessment model selection in construction industry. Expert Systems with Applications. 2011; 38(8): 9105-9111. doi: 10.1016/j.eswa.2010.12.110
17. Subramanyan H, Sawant PH, Bhatt V. Construction Project Risk Assessment: Development of Model Based on Investigation of Opinion of Construction Project Experts from India. Journal of Construction Engineering and Management. 2012; 138(3): 409-421.
18. Hartmann T, Trappey A. Advanced Engineering Informatics - Philosophical and methodological foundations with examples from civil and construction engineering. Developments in the Built Environment. 2020; 4: 100020. doi: 10.1016/j.dibe.2020.100020
19. Sun H, Burton HV, Huang H. Machine learning applications for building structural design and performance assessment: State-of-the-art review. Journal of Building Engineering. 2021; 33: 101816. doi: 10.1016/j.jobe.2020.101816

20. Wang X, Mazumder RK, Salarieh B, et al. Machine Learning for Risk and Resilience Assessment in Structural Engineering: Progress and Future Trends. Journal of Structural Engineering. 2022; 148(8).
21. Zhang J, Zi L, Hou Y, et al. A C-BiLSTM Approach to Classify Construction Accident Reports. Applied Sciences. 2020; 10(17): 5754. doi: 10.3390/app10175754
22. Butler KT, Davies DW, Cartwright H, et al. Machine learning for molecular and materials science. Nature. 2018; 559(7715): 547-555. doi: 10.1038/s41586-018-0337-2
23. Zhong M, Tran K, Min Y, et al. Accelerated discovery of CO_2 electrocatalysts using active machine learning. Nature. 2020; 581(7807): 178-183. doi: 10.1038/s41586-020-2242-8
24. Warnat-Herresthal S, Schultze H, Shastry KL, et al. Swarm Learning for decentralized and confidential clinical machine learning. Nature. 2021; 594(7862): 265-270. doi: 10.1038/s41586-021-03583-3
25. Sun D, Wen H, Wang D, et al. A random forest model of landslide susceptibility mapping based on hyperparameter optimization using Bayes algorithm. Geomorphology. 2020; 362: 107201. doi: 10.1016/j.geomorph.2020.107201
26. Akinosho TD, Oyedele LO, Bilal M, et al. Deep learning in the construction industry: A review of present status and future innovations. Journal of Building Engineering. 2020; 32: 101827. doi: 10.1016/j.jobe.2020.101827
27. Alpaydın E. Machine Learning. Mit Press; 2021.
28. Hegde J, Rokseth B. Applications of machine learning methods for engineering risk assessment - A review. Safety Science. 2020; 122: 104492. doi: 10.1016/j.ssci.2019.09.015
29. Maps OK. Open Knowledge Maps—A visual interface to the world's scientific knowledge. Open Knowledge Maps; 2023.
30. Litmaps. app.litmaps.com. Available online: https://app.litmaps.com/seed (accessed on 15 April 2024).
31. Tessema AT, Alene GA, Wolelaw NM. Assessment of risk factors on construction projects in gondar city, Ethiopia. Heliyon. 2022; 8(11): e11726. doi: 10.1016/j.heliyon.2022.e11726
32. Zhu Z, Sun J, Li X. An construction method of scorecard using machine learning and logical regression. Procedia Computer Science. 2022; 214: 1541-1545. doi: 10.1016/j.procs.2022.11.341
33. Gariazzo C, Taiano L, Bonafede M, et al. Association between extreme temperature exposure and occupational injuries among construction workers in Italy: An analysis of risk factors. Environment International. 2023; 171: 107677. doi: 10.1016/j.envint.2022.107677
34. Hemasinghe H, Rangali RSS, Deshapriya NL, et al. Landslide susceptibility mapping using logistic regression model (a case study in Badulla District, Sri Lanka). Procedia Engineering. 2018; 212: 1046-1053. doi: 10.1016/j.proeng.2018.01.135
35. Li N, Jimenez R. A logistic regression classifier for long-term probabilistic prediction of rock burst hazard. Natural Hazards. 2017; 90(1): 197-215. doi: 10.1007/s11069-017-3044-7
36. Xie P, Zhang R, Zheng J, et al. Probabilistic analysis of subway station excavation based on BIM-RF integrated technology. Automation in Construction. 2022; 135: 104114. doi: 10.1016/j.autcon.2021.104114
37. Hu W, Zhang S, Fu Y, et al. Objective diagnosis of machine learning method applicability to land comprehensive carrying capacity evaluation: A case study based on integrated RF and DPSIR models. Ecological Indicators. 2023; 151: 110338. doi: 10.1016/j.ecolind.2023.110338
38. Wang R, Asghari V, Hsu SC, et al. Detecting corporate misconduct through random forest in China's construction industry. Journal of Cleaner Production. 2020; 268: 122266. doi: 10.1016/j.jclepro.2020.122266
39. Wu X, Wang L, Chen B, et al. Multi-objective optimization of shield construction parameters based on random forests and NSGA-II. Advanced Engineering Informatics. 2022; 54: 101751. doi: 10.1016/j.aei.2022.101751
40. Wen H, Wu J, Zhang C, et al. Hybrid optimized RF model of seismic resilience of buildings in mountainous region based on hyperparameter tuning and SMOTE. Journal of Building Engineering. 2023; 71: 106488. doi: 10.1016/j.jobe.2023.106488
41. Hu R, Chen K, Chen W, et al. Estimation of construction waste generation based on an improved on-site measurement and SVM-based prediction model: A case of commercial buildings in China. Waste Management. 2021; 126: 791-799. doi: 10.1016/j.wasman.2021.04.012
42. Chen JH, Lin JZ. Developing an SVM based risk hedging prediction model for construction material suppliers. Automation in Construction. 2010; 19(6): 702-708. doi: 10.1016/j.autcon.2010.02.014
43. Tserng H P, Lin G F, Tsai L K, et al. An enforced support vector machine model for construction contractor default prediction. Automation in Construction, 2011; 20(8): 1242-1249. doi: 10.1016/j.autcon.2011.05.007

44. Fan M, Sharma A. Design and implementation of construction cost prediction model based on SVM and LSSVM in industries 4.0. International Journal of Intelligent Computing and Cybernetics. 2021; 14(2): 145-157. doi: 10.1108/ijicc-10-2020-0142
45. Fu W, Zhang H, Huang F. Internet-based supply chain financing-oriented risk assessment using BP neural network and SVM. PLOS ONE. 2022; 17(1): e0262222. doi: 10.1371/journal.pone.0262222
46. Mostofi F, Toğan V, Ayözen YE, et al. Construction Safety Risk Model with Construction Accident Network: A Graph Convolutional Network Approach. Sustainability. 2022; 14(23): 15906. doi: 10.3390/su142315906
47. Khalili M A, Guerriero L, Pouralizadeh M, et al. Monitoring and prediction of landslide-related deformation based on the GCN-LSTM algorithm and SAR imagery. Natural Hazards; 2023; 119(1): 39-68. doi: 10.1007/s11069-023-06121-8
48. Mostofi F, Toğan V. Predicting Construction Accident Outcomes Using Graph Convolutional and Dual-Edge Safety Networks. Arabian Journal for Science and Engineering. 2023; 49: 13315-13312. doi: 10.1007/s13369-023-08609-8
49. Fu X, Pan Y, Zhang L. A causal-temporal graphic convolutional network (CT-GCN) approach for TBM load prediction in tunnel excavation. Expert Systems with Applications. 2024; 238: 121977. doi: 10.1016/j.eswa.2023.121977
50. Li P, Wu F, Xue S, et al. Study on the Interaction Behaviors Identification of Construction Workers Based on ST-GCN and YOLO. Sensors. 2023; 23(14): 6318. doi: 10.3390/s23146318
51. Zhang Y, Du Z, Hu L. A construction method of urban road risky vehicles based on dynamic knowledge graph. Electronic Research Archive. 2023; 31(7): 3776-3790. doi: 10.3934/era.2023192
52. Chen JH, Hsu SC, Luo YH, Skibniewski MJ. Knowledge Management for Risk Hedging by Construction Material Suppliers." Journal of Management in Engineering. 2012; 28(3): 273-280.
53. Pandey P, Bandhu KC. A credit risk assessment on borrowers classification using optimized decision tree and KNN with bayesian optimization. International Journal of Information Technology. 2022; 14(7): 3679-3689. doi: 10.1007/s41870-022-00974-1
54. Jaber F K, Al-Zwainy F M S, Hachem S W. Optimizing of predictive performance for construction projects utilizing support vector machine technique. Cogent Engineering, 2019; 6(1): 1685860. doi: 10.1080/23311916.2019.1685860
55. Chenzhong R, Wenliang K, Taihua Z, et al. Intelligent Generation and Analysis of the Municipal Road Construction Scheme Based on the KNN Algorithm. Mathematical Problems in Engineering. 2022; 10: 1-15. doi: 10.1155/2022/8752870
56. Li L, Wu Y, Huang Y, et al. Optimized Apriori algorithm for deformation response analysis of landslide hazards. Computers & Geosciences. 2023; 170: 105261. doi: 10.1016/j.cageo.2022.105261
57. Chen B, Wei N, Qu T, et al. Research on weighting method of geological hazard susceptibility evaluation index based on Apriori Algorithm. Frontiers in Earth Science. 2023; 11. doi: 10.3389/feart.2023.1127889
58. Chen Q, Tian Z, Lei T, et al. An association rule mining model for evaluating the potential correlation of construction cross operation risk. Engineering, Construction and Architectural Management. 2022; 30(10): 5109-5132. doi: 10.1108/ecam-09-2021-0792
59. Shao B, Hu Z, Liu D. Using Improved Principal Component Analysis to Explore Construction Accident Situations from the Multi-Dimensional Perspective: A Chinese Study. International Journal of Environmental Research and Public Health. 2019; 16(18): 3476-3476.
60. Xiang P, Jia F, Li X. Critical Behavioral Risk Factors among Principal Participants in the Chinese Construction Industry. Sustainability. 2018; 10(9): 3158. doi: 10.3390/su10093158
61. Siddiqui F, Sargent P, Montague G. The use of PCA and signal processing techniques for processing time-based construction settlement data of road embankments. Advanced Engineering Informatics. 2020; 46: 101181. doi: 10.1016/j.aei.2020.101181
62. Yan H, He Z, Gao C, et al. Investment estimation of prefabricated concrete buildings based on XGBoost machine learning algorithm. Advanced Engineering Informatics. 2022; 54: 101789. doi: 10.1016/j.aei.2022.101789
63. Cherif IL, Kortebi A. On using Extreme Gradient Boosting (XGBoost) Machine Learning Algorithm for Home Network Traffic Classification. IEEE Xplore; 2019.
64. Coffie GH, Cudjoe SKF. Using extreme gradient boosting (XGBoost) machine learning to predict construction cost overruns. International Journal of Construction Management. 2023.
65. Liang W, Luo S, Zhao G, et al. Predicting hard rock pillar stability using GBDT, XGBoost, and LightGBM algorithms. Mathematics, 2020; 8(5): 765. doi: 10.3390/math8050765
66. Liu P, Li Y. An improved failure mode and effect analysis method for multi-criteria group decision-making in green logistics risk assessment. Reliability Engineering & System Safety. 2021; 215: 107826. doi: 10.1016/j.ress.2021.107826

67. Wang G, Liu M, Cao D, et al. Identifying high-frequency-low-severity construction safety risks: an empirical study based on official supervision reports in Shanghai. Engineering, Construction and Architectural Management. 2021; 29(2): 940-960. doi: 10.1108/ecam-07-2020-0581
68. Ayhan BU, Tokdemir OB. Accident Analysis for Construction Safety Using Latent Class Clustering and Artificial Neural Networks. Journal of Construction Engineering and Management. 2020; 146(3): 04019114.
69. Kim S, Choi CY, Shahandashti M, Rok Ryu K. Improving Accuracy in Predicting City-Level Construction Cost Indices by Combining Linear ARIMA and Nonlinear ANNs. Journal of Management in Engineering. 2022; 38(2).
70. Moon S, Chi S, Kim DY. Predicting Construction Cost Index Using the Autoregressive Fractionally Integrated Moving Average Model. Journal of Management in Engineering. 2018; 34(2): 04017063.
71. Ghashghaie M, Nozari H. Effect of Dam Construction on Lake Urmia: Time Series Analysis of Water Level via ARIMA. Journal of Agricultural Science and Technology. 2018; 20(7): 1541-1553.
72. Kaloop MR, Eldiasty M, Hu JW. Safety and reliability evaluations of bridge behaviors under ambient truck loads through structural health monitoring and identification model approaches. Measurement. 2022; 187: 110234. doi: 10.1016/j.measurement.2021.110234
73. Hajifar S, Sun H, Megahed FM, et al. A forecasting framework for predicting perceived fatigue: Using time series methods to forecast ratings of perceived exertion with features from wearable sensors. Applied Ergonomics. 2021; 90: 103262. doi: 10.1016/j.apergo.2020.103262
74. Lam TYM, Siwingwa N. Risk management and contingency sum of construction projects. Journal of Financial Management of Property and Construction. 2017; 22(3): 237-251. doi: 10.1108/jfmpc-10-2016-0047
75. Montgomery DC, Peck EA, Vining GG. Introduction to Linear Regression Analysis. John Wiley & Sons; 2021.
76. Huang CH, Hsieh SH. Predicting BIM labor cost with random forest and simple linear regression. Automation in Construction. 2020; 118: 103280. doi: 10.1016/j.autcon.2020.103280
77. Esmaeili B, Hallowell MR, Rajagopalan B. Attribute-Based Safety Risk Assessment. II: Predicting Safety Outcomes Using Generalized Linear Models. Journal of Construction Engineering and Management. 2015; 141(8): 04015022.
78. Lyu J. Construction of Enterprise Financial Early Warning Model Based on Logistic Regression and BP Neural Network. Computational Intelligence and Neuroscience. 2022; 2022: 1-7. doi: 10.1155/2022/2614226
79. Levy A, Baha R. Credit risk assessment: a comparison of the performances of the linear discriminant analysis and the logistic regression. International Journal of Entrepreneurship and Small Business. 2021; 42(1/2): 169. doi: 10.1504/ijesb.2021.112265
80. Akboğa Kale Ö, Baradan S. Identifying Factors that Contribute to Severity of Construction Injuries using Logistic Regression Model. Teknik Dergi. 2020; 31(2): 9919-9940. doi: 10.18400/tekderg.470633
81. Bhattacharjee P, Dey V, Mandal UK. Risk assessment by failure mode and effects analysis (FMEA) using an interval number based logistic regression model. Safety Science. 2020; 132: 104967. doi: 10.1016/j.ssci.2020.104967
82. Wong CH. Contractor Performance Prediction Model for the United Kingdom Construction Contractor: Study of Logistic Regression Approach. Journal of Construction Engineering and Management. 2004; 130(5): 691-698.
83. Zhang X, Huang S, Yang S, et al. Safety Assessment in Road Construction Work System Based on Group AHP-PCA. Mathematical Problems in Engineering. 2020; 2020: 1-12. doi: 10.1155/2020/6210569
84. Bai L, Song C, Zhou X, et al. Assessing project portfolio risk via an enhanced GA-BPNN combined with PCA. Engineering Applications of Artificial Intelligence. 2023; 126: 106779. doi: 10.1016/j.engappai.2023.106779
85. Shi H, Li W, Deng Y. Applying Principal Component Analysis and Unascertained Method for the Analysis of Construction Accident Risk. Journal of Computers. 2010; 5(8): 1273-1280. doi: 10.4304/jcp.5.8.1273-1280
86. Wang G, Ma J. A hybrid ensemble approach for enterprise credit risk assessment based on Support Vector Machine. Expert Systems with Applications. 2012; 39(5): 5325-5331. 10.1016/j.eswa.2011.11.003
87. Khemakhem S, Ben Said F, Boujelbene Y. Credit risk assessment for unbalanced datasets based on data mining, artificial neural network and support vector machines. Journal of Modelling in Management. 2018; 13(4): 932-951. doi: 10.1108/jm2-01-2017-0002
88. Mangeli M, Shahraki A, Saljooghi FH. Improvement of risk assessment in the FMEA using nonlinear model, revised fuzzy TOPSIS, and support vector machine. International Journal of Industrial Ergonomics. 2019; 69: 209-216. doi: 10.1016/j.ergon.2018.11.004
89. Steinwart I. Support Vector Machines. Springer; 2014.

90. Noble W S. What is a support vector machine?. Nature Biotechnology. 2006; 24(12): 1565-1567. doi: 10.1038/nbt1206-1565
91. Yang R, Feng J, Sun Y. Construction and classification prediction of risk assessment lindicators for water environment treatment PPP projects. Available online: https://www.researchsquare.com/article/rs-2845690/v1 (accessed on 15 April 2024).
92. Zhang L, Hu H, Zhang D. A credit risk assessment model based on SVM for small and medium enterprises in supply chain finance. Financial Innovation. 2015; 1(1). doi: 10.1186/s40854-015-0014-5
93. Gong P, Guo H, Huang Y, et al. Safety risk evaluations of deep foundation construction schemes based on imbalanced data sets. Journal of civil engineering and management. 2020; 26(4): 380-395.
94. Liu P, Xie M, Bian J, et al. A Hybrid PSO-SVM Model Based on Safety Risk Prediction for the Design Process in Metro Station Construction. International Journal of Environmental Research and Public Health. 2020; 17(5): 1714. doi: 10.3390/ijerph17051714
95. Wei Y, Zhang J, Wang J. Research on Building Fire Risk Fast Assessment Method Based on Fuzzy comprehensive evaluation and SVM. Procedia Engineering. 2018; 211: 1141-1150. doi: 10.1016/j.proeng.2017.12.121
96. Chang YC, Chang KH, Wu GJ. Application of Extreme gradient boosting trees in the construction of credit risk assessment models for financial institutions. Applied Soft Computing. 2018; 73: 914-920. doi: 10.1016/j.asoc.2018.09.029
97. Li Z. GBDT-SVM Credit Risk Assessment Model and Empirical Analysis of Peer-to-Peer Borrowers under Consideration of Audit Information. Open Journal of Business and Management. 2018; 6(2): 362-372. doi: 10.4236/ojbm.2018.62026
98. Zhang H, Shi Y, Yang X, et al. A firefly algorithm modified support vector machine for the credit risk assessment of supply chain finance. Research in International Business and Finance. 2021; 58: 101482. doi: 10.1016/j.ribaf.2021.101482
99. Yin Q, Zhou J, Zhou Y, et al. Construction safety risk assessment method of construction engineering based on improved SVM. International Journal of Sustainable Development, 2023; 26(3-4): 329-343. doi: 10.1504/IJSD.2023.10058663155
100. Chen J, Liu L, Pei J, et al. An ensemble risk assessment model for urban rainstorm disasters based on random forest and deep belief nets: a case study of Nanjing, China. Natural Hazards. 2021; 107(3): 2671-2692. doi: 10.1007/s11069-021-04630-y
101. Tang L, Cai F, Ouyang Y. Applying a nonparametric random forest algorithm to assess the credit risk of the energy industry in China. Technological Forecasting and Social Change. 2019; 144: 563-572. doi: 10.1016/j.techfore.2018.03.007
102. Liu W, Zhang Y, Liang Y, et al. Landslide Risk Assessment Using a Combined Approach Based on InSAR and Random Forest. Remote Sensing. 2022; 14(9): 2131. doi: 10.3390/rs14092131
103. Zermane A, Mohd Tohir MZ, Zermane H, et al. Predicting fatal fall from heights accidents using random forest classification machine learning model. Safety Science. 2023; 159: 106023. doi: 10.1016/j.ssci.2022.106023
104. Kang K, Ryu H. Predicting types of occupational accidents at construction sites in Korea using random forest model. Safety Science. 2019; 120: 226-236. doi: 10.1016/j.ssci.2019.06.034
105. Zhou Y, Li S, Zhou C, Luo H. Intelligent Approach Based on Random Forest for Safety Risk Prediction of Deep Foundation Pit in Subway Stations. Journal of Computing in Civil Engineering. 2019; 33(1).
106. Zhang H, Shi Y, Tong J. Online supply chain financial risk assessment based on improved random forest. Journal of Data, Information and Management. 2021; 3(1): 41-48. doi: 10.1007/s42488-021-00042-6
107. Zhu Z, Zhang Y. Flood disaster risk assessment based on random forest algorithm. Neural Computing and Applications. 2021; 34(5): 3443-3455. doi: 10.1007/s00521-021-05757-6
108. Wang Y, Wen H, Sun D, et al. Quantitative Assessment of Landslide Risk Based on Susceptibility Mapping Using Random Forest and GeoDetector. Remote Sensing. 2021; 13(13): 2625. doi: 10.3390/rs13132625
109. Aprillia H, Yang HT, Huang CM. Statistical Load Forecasting Using Optimal Quantile Regression Random Forest and Risk Assessment Index. IEEE Transactions on Smart Grid. 2021; 12(2): 1467-1480. doi: 10.1109/tsg.2020.3034194
110. Armaghani DJ, Mahdiyar A, Hasanipanah M, et al. Risk Assessment and Prediction of Flyrock Distance by Combined Multiple Regression Analysis and Monte Carlo Simulation of Quarry Blasting. Rock Mechanics and Rock Engineering. 2016; 49(9): 3631-3641. doi: 10.1007/s00603-016-1015-z
111. Liu Y, Chen H, Zhang L, et al. Risk prediction and diagnosis of water seepage in operational shield tunnels based on random forest. Journal of civil engineering and management. 2021; 27(7): 539-552.
112. Ghosh S, Das A. Wetland conversion risk assessment of East Kolkata Wetland: A Ramsar site using random forest and support vector machine model. Journal of Cleaner Production. 2020; 275: 123475. doi: 10.1016/j.jclepro.2020.123475
113. Langroodi AK, Vahdatikhaki F, Doree A. Activity recognition of construction equipment using fractional random forest. Automation in Construction. 2021; 122: 103465. doi: 10.1016/j.autcon.2020.103465

114. Junjia Y, Alias AH, Haron NA, et al. A Bibliometrics-Based Systematic Review of Safety Risk Assessment for IBS Hoisting Construction. Buildings. 2023; 13(7): 1853. doi: 10.3390/buildings13071853
115. Han J, Kim J, Park S, et al. Seismic Vulnerability Assessment and Mapping of Gyeongju, South Korea Using Frequency Ratio, Decision Tree, and Random Forest. Sustainability. 2020; 12(18): 7787. doi: 10.3390/su12187787
116. Lee YYR, Samad H, Miang Goh Y. Perceived Importance of Authentic Learning Factors in Designing Construction Safety Simulation Game-Based Assignment: Random Forest Approach. Journal of Construction Engineering and Management. 2020; 146(3): 04020002.
117. Shoar S, Chileshe N, Edwards JD. Machine learning-aided engineering services' cost overruns prediction in high-rise residential building projects: Application of random forest regression. Journal of Building Engineering. 2022; 50: 104102. doi: 10.1016/j.jobe.2022.104102
118. Chen J, Li Q, Wang H, et al. A Machine Learning Ensemble Approach Based on Random Forest and Radial Basis Function Neural Network for Risk Evaluation of Regional Flood Disaster: A Case Study of the Yangtze River Delta, China. International Journal of Environmental Research and Public Health. 2019; 17(1): 49. doi: 10.3390/ijerph17010049
119. Karabadji NEI, Amara Korba A, Assi A, et al. Accuracy and diversity-aware multi-objective approach for random forest construction. Expert Systems with Applications. 2023; 225: 120138. doi: 10.1016/j.eswa.2023.120138
120. Sabry F. K Nearest Neighbor Algorithm. One Billion Knowledgeable; 2023.
121. Lee KP, Lee HS, Park M, Kim DY, Jung M. Management-Reserve Estimation for International Construction Projects Based on Risk-Informed k-NN. Journal of Management in Engineering. 2017; 33(4): 04017002.
122. Kamran M, Ullah B, Ahmad M, et al. Application of KNN-based Isometric Mapping and Fuzzy C-Means Algorithm to Predict Short-term Rockburst Risk in Deep Underground Projects. Frontiers in Public Health. 2022; 10. doi: 10.21203/rs.3.rs-2128698/v1
123. Liu X, Xu F, Zhang Z, et al. Fall-portent detection for construction sites based on computer vision and machine learning. Engineering, Construction and Architectural Management. 2023. doi: 10.1108/ecam-05-2023-0458
124. Sanni-Anibire MO, Zin RM, Olatunji SO. Machine learning model for delay risk assessment in tall building projects. International Journal of Construction Management, 2022; 22(11): 2134-2143. doi: 10.1080/15623599.2020.1768326
125. Burns JJR, Shealy BT, Greer MS, et al. Addressing noise in co-expression network construction. Briefings in Bioinformatics. 2021; 23(1). doi: 10.1093/bib/bbab495
126. Zhong G, Lu G, Liu M, Cui M. A novel risk assessment system for port state control inspection. In: Proceedings of the 2008 IEEE International Conference on Intelligence and Security Informatics; 17-20 June 2008; Taipei. pp. 242-244. doi: 10.1109/ISI.2008.4565068
127. Arabiat A, Al-Bdour H, Bisharah M. Predicting the construction projects time and cost overruns using K-nearest neighbor and artificial neural network: a case study from Jordan. Asian Journal of Civil Engineering. 2023; 24(7): 2405-2414. doi: 10.1007/s42107-023-00649-7
128. Zhang Y, Ding L, Peter ED. Planning of Deep Foundation Construction Technical Specifications Using Improved Case-Based Reasoning with Weighted k-Nearest Neighbors. American Society of Civil Engineers. 2017; 31(5).
129. Brownlee J. XGBoost with Python. Machine Learning Mastery; 2016.
130. Qin R. The Construction of Corporate Financial Management Risk Model Based on XGBoost Algorithm. Chen M, ed. Journal of Mathematics. 2022; 2022: 1-8. doi: 10.1155/2022/2043369
131. Liu W, Chen Z, Hu Y. XGBoost algorithm-based prediction of safety assessment for pipelines. International Journal of Pressure Vessels and Piping. 2022; 197: 104655. doi: 10.1016/j.ijpvp.2022.104655
132. Wang Y, Ni XS. A XGBoost risk model via feature selection and Bayesian hyper-parameter optimization. Available online: https://arxiv.org/abs/1901.08433 (accessed on 15 April 2024).
133. Shi L, Qian C, Guo F. Real-time driving risk assessment using deep learning with XGBoost. Accident Analysis & Prevention. 2022; 178: 106836. doi: 10.1016/j.aap.2022.106836
134. Luo H, Yang Q, Wang W, et al. XGBoost-based assessment method for fire risk levels of transmission lines. Journal of Electric Power Science and Technology. 2024; 38(6): 132-141. doi: 10.19781/j.issn.1673-9140.2023.06.014
135. Shehadeh A, Alshboul O, Al Mamlook RE, et al. Machine learning models for predicting the residual value of heavy construction equipment: An evaluation of modified decision tree, LightGBM, and XGBoost regression. Automation in Construction. 2021; 129: 103827. doi: 10.1016/j.autcon.2021.103827

136. Hamerly G, Elkan C. Learning the k in k-means. Available online: https://proceedings.neurips.cc/paper/2003/hash/234833147b97bb6aed53a8f4f1c7a7d8-Abstract.html (accessed on 15 April 2024).
137. Er Kara M, Oktay Fırat S. Supplier Risk Assessment Based on Best-Worst Method and K-Means Clustering: A Case Study. Sustainability. 2018; 10(4): 1066. doi: 10.3390/su10041066
138. Chattapadhyay DB, Putta J, Rao RMP. Risk Identification, Assessments, and Prediction for Mega Construction Projects: A Risk Prediction Paradigm Based on Cross Analytical-Machine Learning Model. Buildings. 2021; 11(4): 172.
139. Tao Y, Yong X, Yang J, et al. Risk Early-Warning Framework for Government-Invested Construction Project Based on Fuzzy Theory, Improved BPNN, and K-Means. Mathematical Problems in Engineering. 2022; 2022: 1-19. doi: 10.1155/2022/5958472
140. Shumway RH, Stoffer DS, Shumway RH, et al. ARIMA models. Time series analysis and its applications: With R examples, 2017; 75-163. doi: 10.1007/978-3-319-52452-8_3
141. Cao H, Goh YM. Analyzing construction safety through time series methods. Frontiers of Engineering Management. 2019; 6(2): 262-274. doi: 10.1007/s42524-019-0015-6
142. Li M, Baek M, Ashuri B. Forecasting Ratio of Low Bid to Owner's Estimate for Highway Construction. Journal of Construction Engineering and Management. 2021; 147(1).
143. Yi F, Zeng H, Liu T, Wu Y. Research on cement price fluctuation prediction based on EEMD-ARIMA. In: Li J, Lu W, Peng Y, et al. (editors). Proceedings of the 27th International Symposium on Advancement of Construction Management and Real Estate. Springer; 2023.
144. Liu Z, Zhou J. Introduction to Graph Neural Networks. Springer International Publishing; 2020. doi: 10.1007/978-3-031-01587-8
145. Fu X, Wu M, Ponnarasu S, et al. A hybrid deep learning approach for dynamic attitude and position prediction in tunnel construction considering spatio-temporal patterns. Expert Systems with Applications. 2023; 212: 118721. doi: 10.1016/j.eswa.2022.118721
146. Pan X, Zhong B, Wang Y, et al. Identification of accident-injury type and bodypart factors from construction accident reports: A graph-based deep learning framework. Advanced Engineering Informatics. 2022; 54: 101752. doi: 10.1016/j.aei.2022.101752
147. Junjia Y, Alias A H, Haron N A, et al. Identification and analysis of hoisting safety risk factors for IBS construction based on the AcciMap and cases study. Heliyon. 2024; 10(1). doi: 10.1016/j.heliyon.2023.e23587
148. Mostofi F, Toğan V. Construction safety predictions with multi-head attention graph and sparse accident networks. Automation in Construction. 2023; 156: 105102. doi: 10.1016/j.autcon.2023.105102
149. Xue G, Liu S, Ren L, et al. Risk assessment of utility tunnels through risk interaction-based deep learning. Reliability Engineering & System Safety. 2024; 241: 109626. doi: 10.1016/j.ress.2023.109626
150. Zhu W, Shi D, Cheng R, et al. Human risky behaviour recognition during ladder climbing based on multi-modal feature fusion and adaptive graph convolutional network. Signal, Image and Video Processing. 2024; 18: 2473-2483. doi: 10.1007/s11760-023-02923-2
151. Xie X, Fu G, Xue Y, et al. Risk prediction and factors risk analysis based on IFOA-GRNN and apriori algorithms: Application of artificial intelligence in accident prevention. Process Safety and Environmental Protection. 2019; 122: 169-184. doi: 10.1016/j.psep.2018.11.019
152. Deng Y, Zhang Y, Yuan Z, et al. Analyzing Subway Operation Accidents Causations: Apriori Algorithm and Network Approaches. International Journal of Environmental Research and Public Health. 2023; 20(4): 3386. doi: 10.3390/ijerph20043386
153. Junjia Y, Alias A H, Haron N A, et al. A Bibliometric Review on Safety Risk Assessment of Construction Based on CiteSpace Software and WoS Database. Sustainability, 2023; 15(15): 11803. doi: 10.3390/su151511803
154. Sarkar S, Ejaz N, Maiti J, et al. An integrated approach using growing self-organizing map-based genetic K-means clustering and tolerance rough set in occupational risk analysis. Neural Computing and Applications. 2022; 34(12): 9661-9687. doi: 10.1007/s00521-022-06956-5
155. Junjia Y, Alias A H, Haron N A, et al. Trend Analysis of Marine Construction Disaster Prevention Based on Text Mining: Evidence from China. Sustainable Marine Structures, 2024; 6(1): 20-32. doi: 10.36956/sms.v6i1.1026

156. Verma A, Prakash S, Srivastava V, et al. Sensing, Controlling, and IoT Infrastructure in Smart Building: A Review. IEEE Sensors Journal. 2019; 19(20): 9036-9046. doi: 10.1109/jsen.2019.2922409
157. Feng S, He X, Xu H, Armaghani DJ, Sheng D. Applications of Machine Learning in Mechanised Tunnel Construction: A Systematic Review. Eng. 2023; 4(2): 1516-1535.
158. Zhu Z, Jeelani I, Gheisari M. Physical risk assessment of drone integration in construction using 4D simulation. Automation in Construction. 2023; 156: 105099. doi: 10.1016/j.autcon.2023.105099
159. Zhong J, Mao Y, Yuan X. Lifetime seismic risk assessment of bridges with construction and aging considerations. Structures. 2023; 47: 2259-2272. doi: 10.1016/j.istruc.2022.12.035
160. Nguyen HD, Do QNH, Macchion L. Influence of practitioners' characteristics on risk assessment in Green Building projects in emerging economies: a case of Vietnam. Engineering, Construction and Architectural Management. 2021; 30(2): 833-852. doi: 10.1108/ecam-05-2021-0436
161. Sohrabi H, Noorzai E. Risk assessment in Iranian oil and gas construction industry: a process approach. International Journal of Quality & Reliability Management. 2021; 40(1): 124-147. doi: 10.1108/ijqrm-03-2021-0069
162. Hatamleh MT, Moynihan GP, Batson RG, et al. Risk assessment and ranking in the developing countries' construction industry: the case of Jordan. Engineering, Construction and Architectural Management. 2021; 30(4): 1344-1364. doi: 10.1108/ecam-06-2021-0489
163. Al-Mhdawi MKS, Brito M, Onggo BS, et al. COVID-19 emerging risk assessment for the construction industry of developing countries: evidence from Iraq. International Journal of Construction Management. 2024; 24(7): 693-706. doi: 10.1080/15623599.2023.2169301
164. Gashaw T, Jilcha K. Design risk modeling and analysis for railway construction projects. International Journal of Construction Management. 2022; 23(14): 2488-2498. doi: 10.1080/15623599.2022.2070344
165. Do ST, Nguyen VT, Likhitruangsilp V. RSIAM risk profile for managing risk factors of international construction joint ventures. International Journal of Construction Management. 2021; 23(7): 1148-1162. doi: 10.1080/15623599.2021.1957753
166. He S, Xu H, Zhang J, et al. Risk assessment of oil and gas pipelines hot work based on AHP-FCE. Petroleum. 2023; 9(1): 94-100. doi: 10.1016/j.petlm.2022.03.006
167. Mohandes SR, Durdyev S, Sadeghi H, et al. Towards enhancement in reliability and safety of construction projects: developing a hybrid multi-dimensional fuzzy-based approach. Engineering, Construction and Architectural Management. 2022; 30(6): 2255-2279. doi: 10.1108/ecam-09-2021-0817
168. Badi I, Bouraima MB, Jibril ML. Risk Assessment in Construction Projects Using the Grey Theory. Journal of Engineering Management and Systems Engineering. 2022; 1(2): 58-66. doi: 10.56578/jemse010203
169. Zhang L, Li H. Construction Risk Assessment of Deep Foundation Pit Projects Based on the Projection Pursuit Method and Improved Set Pair Analysis. Applied Sciences. 2022; 12(4): 1922. doi: 10.3390/app12041922
170. Ju W, Wu J, Kang Q, et al. A method based on the theories of game and extension cloud for risk assessment of construction safety: A case study considering disaster-inducing factors in the construction process. Journal of Building Engineering. 2022; 62: 105317. doi: 10.1016/j.jobe.2022.105317
171. Sadeghi M, Mahmoudi A, Deng X. Blockchain technology in construction organizations: risk assessment using trapezoidal fuzzy ordinal priority approach. Engineering, Construction and Architectural Management. 2022; 30(7): 2767-2793. doi: 10.1108/ecam-01-2022-0014

Academic Publishing Pte. Ltd.

Add: 73 Upper Paya Lebar Road #07-02B-01 Centro Bianco Singapore 534818

Tel: +65 83184869

E-mail: editorial_office@acad-pub.com

Web: http://ojs.acad-pub.com/